

AN IRVING-CLOUD PUBLICATION

Oil Cooler: A Solution to the Liquid Fuel Dilemma



Editorial

**Stephen J. Spornick, Arthur W. Bertolini,
and William Spornick**

Oil Shale: A Solution to the Liquid Fuel Dilemma

ACS SYMPOSIUM SERIES **1032**

Oil Shale: A Solution to the Liquid Fuel Dilemma

Olayinka I. Ogunsola, Ph.D., Editor
United States Department of Energy

Arthur M. Hartstein, Ph.D., Editor
United States Department of Energy, Retired

Olubunmi Ogunsola, Ph.D., Editor
Tryby Energy, Mineral and Environmental Corporation (TEMEC)

**Sponsored by the
ACS Division of Fuel Chemistry**



American Chemical Society, Washington, DC

In *Oil Shale: A Solution to the Liquid Fuel Dilemma*; Ogunsola, O., et al.; ACS Symposium Series; American Chemical Society: Washington, DC, 2010.



Library of Congress Cataloging-in-Publication Data

Oil shale : a solution to the liquid fuel dilemma / [edited by] Olayinka I. Ogunsola, Arthur M. Hartstein, Olunmi Ogunsola ; sponsored by the ACS Division of Fuel Chemistry.

p. cm. -- (ACS symposium series ; 1032)

Includes bibliographical references and index.

ISBN 978-0-8412-2539-8 (alk. paper)

1. Oil-shales--Congresses. 2. Liquid fuels--Congresses. I. Ogunsola, Olayinka I., 1950-II. Hartstein, Arthur M. III. Ogunsola, Olunmi. IV. American Chemical Society. Division of Fuel Chemistry.

TN858.O354 2009

665.5--dc22

2009050037

The paper used in this publication meets the minimum requirements of American National Standard for Information Sciences—Permanence of Paper for Printed Library Materials, ANSI Z39.48n1984.

Copyright © 2010 American Chemical Society

Distributed by Oxford University Press

All Rights Reserved. Reprographic copying beyond that permitted by Sections 107 or 108 of the U.S. Copyright Act is allowed for internal use only, provided that a per-chapter fee of \$40.25 plus \$0.75 per page is paid to the Copyright Clearance Center, Inc., 222 Rosewood Drive, Danvers, MA 01923, USA. Reproduction or reproduction for sale of pages in this book is permitted only under license from ACS. Direct these and other permission requests to ACS Copyright Office, Publications Division, 1155 16th Street, N.W., Washington, DC 20036.

The citation of trade names and/or names of manufacturers in this publication is not to be construed as an endorsement or as approval by ACS of the commercial products or services referenced herein; nor should the mere reference herein to any drawing, specification, chemical process, or other data be regarded as a license or as a conveyance of any right or permission to the holder, reader, or any other person or corporation, to manufacture, reproduce, use, or sell any patented invention or copyrighted work that may in any way be related thereto. Registered names, trademarks, etc., used in this publication, even without specific indication thereof, are not to be considered unprotected by law.

PRINTED IN THE UNITED STATES OF AMERICA

Foreword

The ACS Symposium Series was first published in 1974 to provide a mechanism for publishing symposia quickly in book form. The purpose of the series is to publish timely, comprehensive books developed from the ACS sponsored symposia based on current scientific research. Occasionally, books are developed from symposia sponsored by other organizations when the topic is of keen interest to the chemistry audience.

Before agreeing to publish a book, the proposed table of contents is reviewed for appropriate and comprehensive coverage and for interest to the audience. Some papers may be excluded to better focus the book; others may be added to provide comprehensiveness. When appropriate, overview or introductory chapters are added. Drafts of chapters are peer-reviewed prior to final acceptance or rejection, and manuscripts are prepared in camera-ready format.

As a rule, only original research papers and original review papers are included in the volumes. Verbatim reproductions of previous published papers are not accepted.

ACS Books Department

Preface

This book is the result of a symposium on oil shale presented at the Fall 2008 and National Meetings of the American Chemical Society. Thirteen papers were presented in two sessions at the Meeting. For a more comprehensive product, other people working on oil shale were invited to submit manuscripts for consideration for publication in the book. All manuscripts were peer reviewed.

The United States of America is endowed with abundant oil shale deposits from which about one trillion barrels of oil can be recovered. These huge domestic oil resources are currently untapped. Interest in developing the oil shale resources of the United States of America's has increased in the last few years as a result of high prices of conventional crude oil and concerns about reliable and secure energy supplies to meet our nation's growing demand. The technology to cleanly develop affordable fuels from oil shale requires advances in research, development and demonstration (RD&D).

In recent years, research and development activities on oil shale have significantly increased to accelerate oil shale technology while minimizing the environmental impact in an effort to enhance its commercial development. This symposium series book describes recent research and developments of various aspects (characteristics, production, processing, upgrading, utilization, environmental, economics, policy, and legal) of oil shale development.

The form of this book is organized in the following six parts:

- General overview of oil shale and oil shale technology
- Resource assessment and geology,
- Chemistry and process modeling,
- Industrial oil shale processes,
- Environmental issues affecting oil shale development, and
- Economics, legal, policy, and social issues related to oil shale development.

The authors of each chapter are sharing their timely research and their expert insights in this book. The diversity of their experiences is taking oil shale advancement forward.

August 2009

Olayinka I. Ogunsola, Ph.D.

Office of Oil and Natural Gas
U.S. Department of Energy
1000 Independence Avenue, SW
Washington, DC 20585
202-586-6743 (telephone)
202-586-6221 (fax)
Olayinka.ogunsola@hq.doe.gov (email)

Arthur M. Hartstein, Ph.D.

1615 North Queen St., #507
Arlington, VA 22209
301 807-6685 (telephone)
arthartstein@gmail.com (email)

Olubunmi Ogunsola, Ph.D.

Tryby Energy, Mineral and Environmental Corporation (TEMEC)
P.O. Box 1072
Woodbridge, VA 22195
703 583-5647 (telephone)
president@temec5.com (email)

Chapter 1

An Overview of Oil Shale Resources

Emily Knaus,¹ James Killen,² Khosrow Biglarbigi,¹
and Peter Crawford¹

¹INTEK, Inc., Arlington, VA 22201

²U.S. Department of Energy, Washington, DC 20585

There are vast quantities of oil shale around the world in deposits located in 27 countries. The quality, quantity, and origins of these shale deposits vary greatly. The United States has the largest known resource of oil shale in the world - an estimated 6 trillion barrels (*1*). Other significant deposits of oil shale can be found in Russia, Brazil, Estonia, and China. The world's oil shale resources are largely untapped and may represent considerable oil reserves with suitable economic conditions and advances in extraction technology.

Oil Shale Background Information

What Is Oil Shale?

Oil Shale is a sedimentary rock embedded with organic material called kerogen. It is essentially a geologically immature form of petroleum. The rock has not been under the necessary heat, pressure, and/or depth for the right length of time required to form crude oil. However, this immature form of petroleum can be converted to fuel feedstock (syncrude) through the process of heating and hydrogenation.

Formation and Deposition

Oil shale is formed from organic material which may have several different origins. It is often categorized according to the origin of the organic material into three major categories: terrestrial, lacustrine, and marine (*2*).

© 2010 American Chemical Society

In Oil Shale: A Solution to the Liquid Fuel Dilemma; Ogunsola, O., et al.;
ACS Symposium Series; American Chemical Society: Washington, DC, 2010.

- Terrestrial oil shale is formed from organic material, plant and animal matter that once lived on land, similar to the material that produces coal.
- Lacustrine oil shale descends from fresh or brackish water algae remains.
- Marine oil shale deposits are the result of salt water algae, acritarchs, and dinoflagellates.

The origin of the oil shale may impact its quality and/or the other minerals that are found within the deposit.

Distribution

Deposits of oil shale may be found at varying depths below the surface. Oil shale occurs in nearly 100 major deposits in 27 countries worldwide (3). It is generally found at shallow depths of less than 900 meters, whereas deeper, warmer geologic zones are required to form conventional oil. Some deposits are close to the surface in relatively thin beds of shale. Other deposits may be found deeper beneath the surface (greater than 300 meters) in very thick beds (300 meters or more in thickness).

Lithology

Oil shale is found in different host rock types, but most deposits are either carbonate or silica based. The type of rock that comprises the shale body affects the mining and heating approaches, moisture content, and air and carbon emissions released during processing. Silica and clay based oil shales tend to have higher moisture contents. Carbonate rock may crumble in mining, crushing, and handling creating small particles called fines. Fines require different retorting approaches than lump shale. Fines can also contaminate shale oil with particulates that are difficult to remove. Carbonate rock also decomposes when subjected to high temperatures causing the creation and release of carbon dioxide emissions.

Composition

The composition of oil shale may vary according to the depositional mechanism and setting. The composition of the original organic matter may impact the chemical composition of the embedded kerogen.

Quality Factors

The quality of oil shale is important in determining its suitability for production. Some of the important determinants of quality include:

- Richness/Grade (litres per ton l/t),
- Organic material content (as a percentage of weight),
- Hydrogen content,

- Moisture content, and
- Concentrations of contaminants including:
 - Nitrogen and
 - Sulfur and metals.

Richness/Grade

The commercial desirability of any oil shale deposit is dependent on the richness of the shale. Commercially attractive grades of oil shale contain 100 l/t or more. There are some deposits of oil shale that contain 300 l/t (4). The richness may in fact result in greater yields than determined by Fischer Assay due to efficiencies in processing.

Oil shales vary considerably in terms of richness or grade, which is determined by the percentage of organic carbon in the ore. Yield is an expression of the volume of shale oil that can be extracted from the oil shale. Richness of oil shale may be assessed by methodologies including Fischer Assay which is the traditional method but may not provide the total potential volume of oil that can be produced from the shale. A newer method, known as Rock-Evaluation, may provide a better measure of true potential yield (5).

Recoverability

The volume of oil shale is often expressed as the oil shale in place. This is an estimate of the total volume of oil shale contained in the ore taking into account the quality of the resource. Some deposits also have estimates of the recoverable resource which takes into consideration additional factors to determine the volume of shale that may actually be extracted from the ore. There is variation in the degree that individual deposits around the world have been evaluated or characterized; thus, the volume of shale oil is not fully known.

Global Oil Shale Resources

It is estimated that there are at least 8 trillion barrels of oil shale resource around the world (6). Countries are ranked according to the respective volumes of oil shale resource in place. The United States' oil shale resources surpass all other countries with an estimated 6 trillion barrels of resource in place. Russia, the Democratic Republic of Congo, and Brazil are the next highest ranked countries with volumes ranging from 80 billion barrels to almost 250 billion barrels of resource. Figure 1 displays the world oil shale resources estimated in each country and also provides the country's rank (7).

Of the twenty-seven countries around the world with known deposits of oil shale, Table I presents the top ten with the most abundant resource (8, 9). Following the chart, there are descriptions of eight of the top ten countries and

some additional deposits around the world. Based on available data, the origin, characteristics, and other details about deposits will be discussed.

United States

The United States (U.S.) is endowed with the largest oil shale resource in the world. The resource is located in 3 concentrated areas as displayed in Figure 2. The largest and most concentrated deposit of oil shale in the world is located in the western U.S. in the states of Colorado, Wyoming, and Utah. This large deposit is known as the Green River Formation. A second, less concentrated and lower quality deposit is located in the eastern U.S., stretching across Kentucky, Ohio, Tennessee, and Indiana. There are also smaller deposits located in the states of Alaska and Texas.

Total U.S. resource is estimated to approach six trillion barrels of oil shale in place. Of this large resource, two trillion barrels are considered high quality resource; 1.2 trillion barrels may ultimately be recoverable; and at prices in the range of 50 to 130 U.S. dollars per barrel of crude, potential shale oil reserves are estimated at 600 to 800 billion barrels (10). Figure 3 below provides this categorization of the resource.

The U.S. resources have been extensively characterized in terms of their quality and grade. Thousands of cores have been drilled and analyzed and numerous assessments have been made by industry and the government. Most often, U.S. resources are considered as three distinct oil shale regions (the western, eastern, and Alaska) due to differences in the oil shale in each location. Table II displays the quality of the oil shale in each of the three regions (11).

Table III highlights the major characteristics of oil shale resources in the U.S. including the origin of the shale, the areal extent of the deposit, and the geologic period of its formation for the two most significant oil shale regions in the U.S. (12). Following the table is a detailed description of the U.S.'s western and eastern resources of oil shale.

Western Resources

The most abundant resource is located in the western U.S. in the states of Colorado, Utah, and Wyoming in a geologic setting known as the Green River Formation. These deposits occur across 40,200 square kilometers (16 million acres) of land. It is estimated that the deposits contain approximately 1.2 trillion barrels of oil equivalent. Of the 1.2 trillion barrels, the majority are located on federally owned land managed by the U.S. Department of the Interior. Access to these resources for commercial development has been restricted by the federal government pursuant to regulations.

More than a quarter million assays have been conducted on core and outcrop samples for the Green River oil shale. Results have shown that the richest zone, known as the Mahogany zone, is located in the Parachute Creek, Colorado member of the Green River Formation. This zone can be found throughout the formation

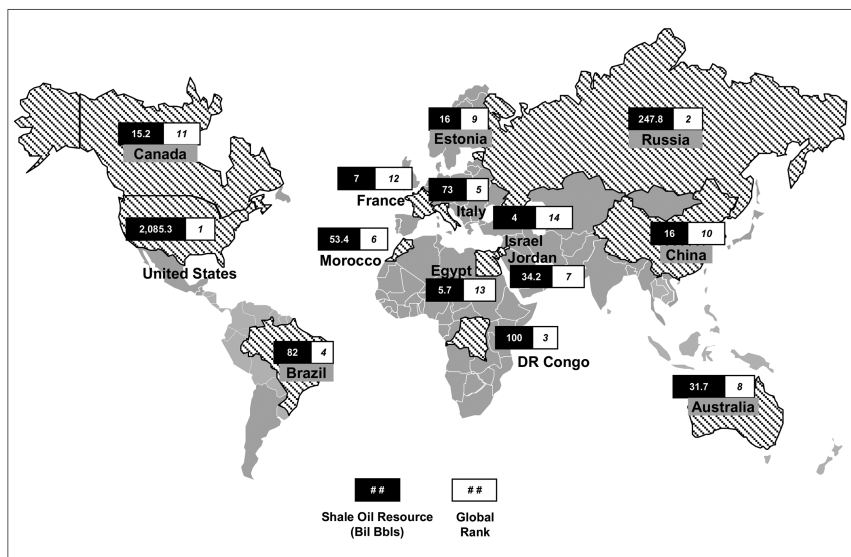


Figure 1. Map of World Resources

Table I. Top Ten Ranked Countries by Oil Shale Resource Volume

<i>Rank</i>	<i>Deposit Location</i>	<i>Resource in Place (Billions Bbls)</i>
1	United States	6,000
2	Russia	248
3	Democratic Republic of the Congo	100
4	Brazil	82
5	Italy	73
6	Morocco	53
7	Jordan	34
8	Australia	32
9	Estonia	16
10	China	10

and is easily identifiable. A layer of volcanic ash several centimeters thick, known as the Mahogany marker, lies on top of the Mahogany zone. Because of their relatively shallow nature and consistent bedding, the resource richness is well known, leading to a high degree of certainty relating to resource quality. By Fisher Assay, yields are estimated from 42 to 209 l/t and, for a few meters in the Mahogany zone, up to about 271 l/t.

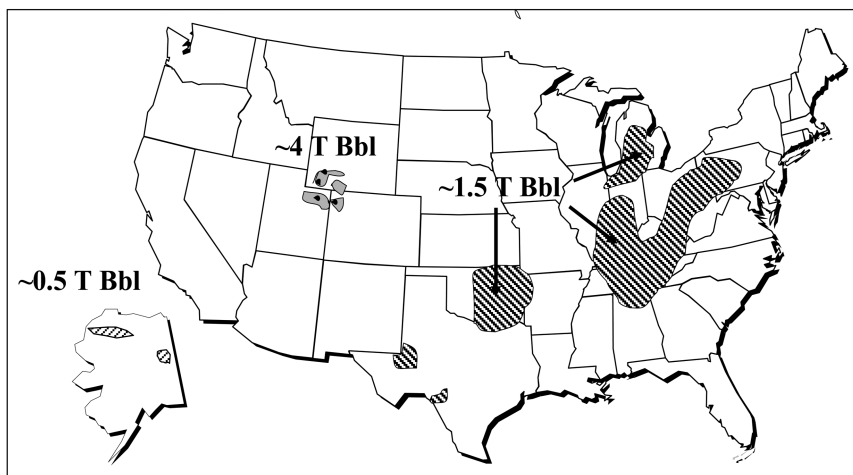


Figure 2. U.S. Oil Shale Resources

Eastern Resources

The U.S. has large oil shale deposits located in the eastern portion of the country that have also been well characterized. Much is known about the location, depth, and carbon content of the eastern resource. In comparison to the western U.S. oil shale resource, eastern shale is not as concentrated, but rather spread across a number of states. Eastern shale also has a different organic content than that of western oil shale. Conventional retorting of eastern shale yields less shale oil and a higher carbon residue.

Ninety-eight percent of these accessible deposits are in the states of Kentucky, Ohio, Tennessee, and Indiana. The Kentucky Knobs region has resources of 16 billion barrels, at a minimum grade of 100 l/t. Near-surface mineable resources are estimated at 423 billion barrels (13).

Russia

Russia has the second largest known resources of oil shale in the world. Russia contains at least 80 deposits of oil shale. Mined shale from the Kukersite deposit in the Leningrad district is burned as fuel in the Slansky electric power plant near St. Petersburg. In addition to the Leningrad deposit, the best deposits for exploitation are those in the Volga-Pechersk oil-shale province, including the Perelyub-Blagodatovsk, Kotsebinsk, and the Rubezhinsk deposits. These deposits contain beds of oil shale ranging from 0.8 to 2.6 meters in thickness but are also high in sulfur (4–6 percent, dry basis) (14).

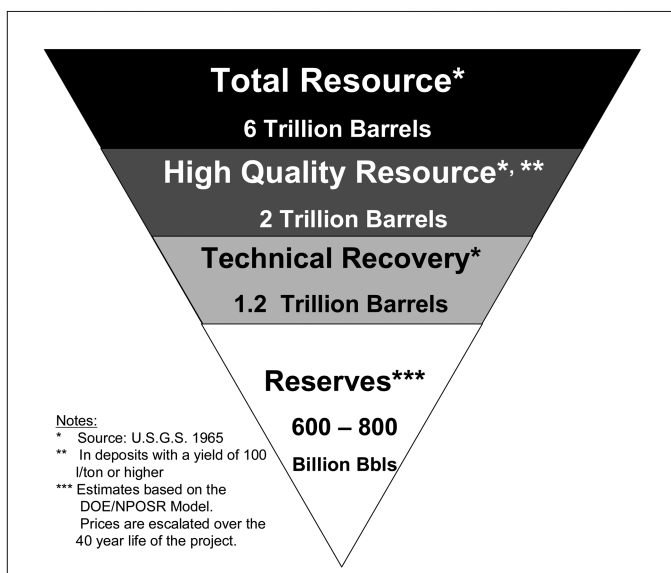


Figure 3. U.S. Oil Shale Resource Characterization

Table II. U.S. Oil Shale Quality by Region (Billions of Barrels)

Deposit Location	Quality		
	20–40 (l/t)	40–100 (l/t)	100–400 (l/t)
Western (Green River)	4,000	2,800	1,200
Eastern (& Central)	2,000	1,000	N/A
Alaska	Large	200	250
Total	6,000+	4,000	2,000+

Table III. U.S. Oil Shale Characteristics by Region

Deposit Location	Origin	Area (km ²)	Geologic Period
Western	Lacustrine	65,000	Eocene
Eastern	Marine	725,000	Devonian/Mississippian

Brazil

Brazil is ranked fourth in terms of oil shale resources. The country contains at least nine deposits of oil shale (15) as displayed in Figure 4. Two of these deposits have been well characterized, the Paraíba Valley deposit and the Iratí Formation.

The Paraíba Valley deposit is located in the state of São Paulo, northeast of the city of São Paulo. The region is estimated to contain approximately 2 billion barrels of oil shale with as much as 840 million barrels that may be ultimately recoverable.



Figure 4. Map of Brazil's Oil Shale Resources (16)

The Iratí Formation is located in the southern part of Brazil cropping out in the northeastern part of the state of São Paulo, extending southward for 1,700 kilometers to the southern border of Rio Grande do Sul. The total area of the Iratí Formation is unknown because the western part of the deposit is covered by lava flows. Table IV highlights the major characteristics of oil shale resources for the Paraíba Valley and Iratí deposits (17).

The oil shale in the Iratí Formation is characterized in further detail. In the State of Rio Grande do Sul, it is known that the oil shale is in two beds separated by 12 meters of shale and limestone. The beds are thickest in the vicinity of São Gabriel, where the upper bed is 9 meters thick and thins to the south and east, and the lower bed is 4.5 meters thick and also thins to the south. In the State of Paraná, in the vicinity of São Mateus do Sul-Iratí, the upper and lower oil shale beds are 6.5 and 3.2 meters thick, respectively. In the State of São Paulo and part of Santa Catarina, there are as many as 80 beds of oil shale, each ranging from a few millimeters to several meters in thickness, which are distributed irregularly through a sequence of limestone and dolomite. Some resources are being actively mined and converted to oil and gas by Petrobras Brazil in commercial quantities (18).

Table IV. Brazil Oil Shale Characteristics by Deposit

<i>Deposit Location</i>	<i>Origin</i>	<i>Area (km²)</i>	<i>Geologic Period</i>
Paraíba Valley	Lacustrine	86	Tertiary
Irati	Marine	unknown	Permian

Morocco

The Kingdom of Morocco is endowed with a large resource of oil shale and at least 10 distinct oil shale deposits (Figure 5).

The two deposits that have been explored most extensively are the Timahdit and the Tarfaya deposits. The Timahdit deposit is located about 250 kilometers southeast of Rabat. It underlies an area about 70 kilometers long and 4 to 10 kilometers wide. The thickness of the oil shale ranges from 80 to 170 meters. The moisture content ranges from 6 to 11 percent, and the sulfur content averages 2 percent. Total oil shale resources in the Timahdit deposit are estimated at 18 billion tons. Oil yields are expected to average 70 l/t.

The Tarfaya deposit is located in the southwestern most part of Morocco, near the border with Western Sahara. The oil shale averages 22 meters in thickness and its grade averages 62 l/t. The total oil shale resource is estimated at 86 billion tons. The moisture content of the Tarfaya oil shale averages 20 percent and the sulfur content averages about 2 percent. Table V provides the highlights of the characteristics of the Timahdit and Tarfaya deposits.

Jordan

The Hashemite Kingdom of Jordan ranks seventh in world oil shale resources. Within Jordan, 24 oil shale deposits have been identified. Of the 24 major oil shale deposits, five have been identified by the Natural Resources Authority (NRA) of Jordan as having near term development potential and were further characterized by geologic and engineering analyses. These deposits are all located in central Jordan south of the capital city, Amman. Oil shale deposits outside of central Jordan tend to be more deeply buried. Figure 6 displays all of the oil shale deposits in Jordan.

The five deposits that are well characterized in Jordan are: El-Lajjun, Sultani, Jurf Ed-Darawish, Attarat Um Ghudran, and Wadi Maghar. Characteristics of these deposits are displayed in Table VI and more detailed descriptions follow.

The El-Lajjun deposit is located about 110 kilometers south of Amman. The deposit is approximately 30 meters thick with an average oil yield of about 121 l/t. Overburden, material deposited above the oil shale, is about 30 meters. The deposit is estimated to contain a total of 1.6 billion barrels of oil shale with potentially 800 million barrels being ultimately recoverable.

The Sultani deposit is located 130 kilometers south of Amman and in close proximity to the El-Lajjun oil shale deposit. This deposit is estimated to contain

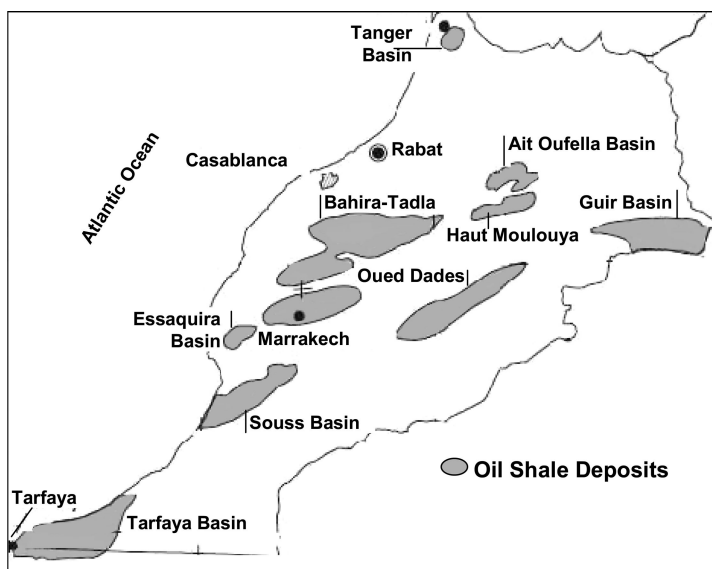


Figure 5. Map of Moroccan Resources

Table V. Moroccan Oil Shale Characteristics by Deposit

Deposit Location	Origin	Area (km ²)	Geologic Period
Timahdit	Marine	196	Cretaceous
Tarfaya	Marine	2,000	Cretaceous

1.1 billion barrels of oil shale. At 88 l/t, the oil content is somewhat lower than the El-Lajjun deposit and the overburden is greater than 60 meters thick.

The Jurf Ed-Darawish deposit is located 115 kilometers south of Amman. This deposit is larger than the nearby Sultani deposit and its oil shale thickness is greater at 60 meters. Average overburden thickness is about 45 meters. Oil content is relatively low at 67 l/t. The Jurf Ed-Darawish deposit is estimated to contain total resources of 3 billion barrels.

Two additional large deposits in Jordan are Attarat Um Ghudran and Wadi Maghar. The oil shale resource in these deposits is relatively thick at about 43 meters, overburden has a similar thickness, and oil content is approximately 80 l/t. Total resources may reach 27 billion barrels; however, the deposits have not been fully analyzed.

A sixth deposit lies to the north and east of Amman. These resources are deeper and thicker than the central Jordanian deposits and are all targets for potential in-situ development.

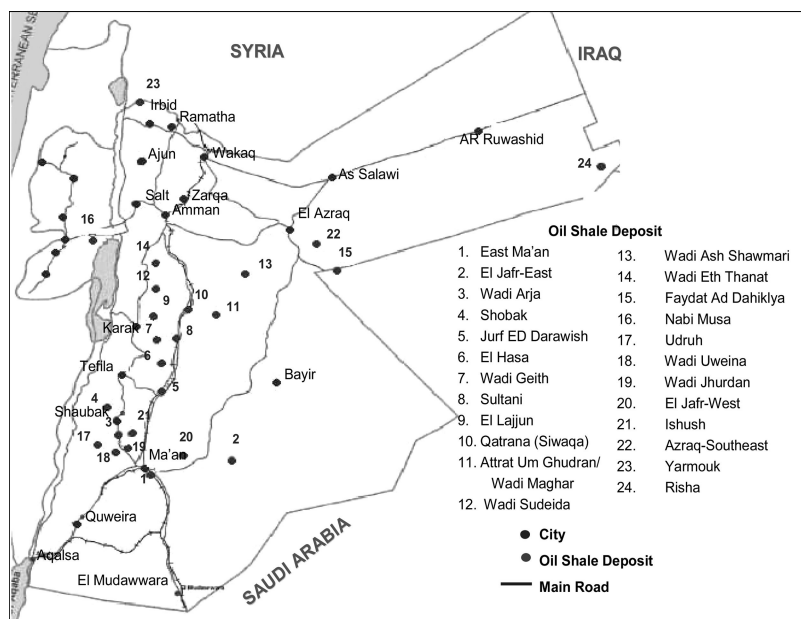


Figure 6. Jordanian Oil Shale Resources

Table VI. Jordanian Oil Shale Characteristics by Deposit

Deposit Location	Origin	Area (km ²)	Geologic Period
El-Lajjun	Marine	13	Cretaceous
Sultani	Marine	14	Cretaceous
Jurf Ed-Darawish	Marine	56	Cretaceous
Attarat Um Ghudran/Wadi Maghar	Marine	480	Cretaceous

Australia

Australia ranks eighth among the largest oil shale resource holdings in the world. It is estimated that Australia contains approximately 58 billion tons of oil shale from which 24 billion barrels of shale oil may ultimately be recoverable (19). The oil shale is located in the eastern portion of the country in the states of Queensland, New South Wales, South Australia, Victoria, and Tasmania. Figure 7 provides a map of the country's deposits.

The deposits having the best potential for economic development are those located in Queensland and include the Rundle, Stuart, and Condor deposits. Queensland contains both toolebuc and torbanite deposits (21). Table VII displays characteristics of some of the major oil shale deposits in Australia.

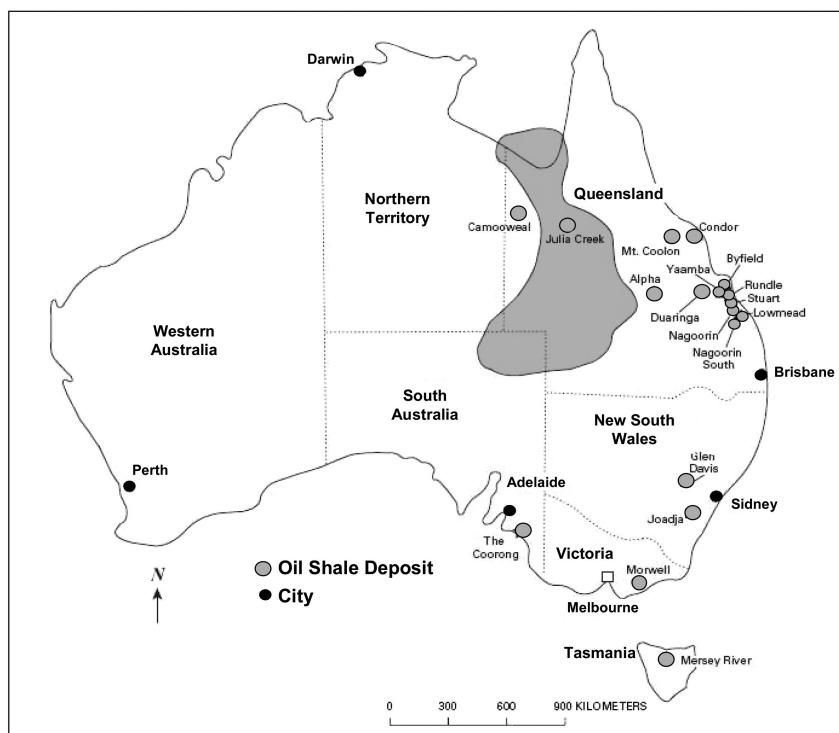


Figure 7. Australian Oil Shale Deposits (20)

New South Wales contains a large volume of oil shale resources. There are as many as 30 individual deposits in this region. The quality of the shale there ranges from 220 to 250 l/t, but may be as high as 480 to 600 l/t. There are two small deposits of torbanite (lacustrine) oil shale in Queensland, one of which may represent 19 million barrels of oil in place (22).

Australia also contains toolebuc (marine) deposits of oil shale. There are toolebuc deposits in parts of the Eromanga and Carpenteria basins located in Queensland and adjacent states. The oil shale zone ranges from 6.5 to 7.5 meters in thickness with an average yield of about 37 l/t, making it a low-grade resource. The Toolebuc Formation may contain as much as 1.7 trillion barrels of oil shale in-place. Much of this resource is close to the surface. Estimates for recoverable resource total 1.5 billion U.S. barrels; however, the oil shale is too low grade for development thus far (23).

Eastern Queensland has nine oil shale deposits that have been extensively characterized including: Byfield, Condor, Duaringa, Lowmead, Nagoorin, Nagoorin South, Rundle, Stuart, and Yaamba. These deposits were found to contain quartz and clay minerals with lesser amounts of siderite, carbonate minerals, and pyrite along with oil shale. The sizes of the deposits range from 1 to 17.4 billion tons of shale oil with grades of around 50 l/t. Three of the largest deposits are Condor with an estimated 17.4 billion tons, Nagoorin with 6.3 billion

Table VII. Australian Oil Shale Characteristics by Deposit

<i>Deposit Location</i>	<i>Origin</i>	<i>Area (km²)</i>	<i>Geologic Period</i>
New South Wales	Lacustrine	-	Permian
Queensland (torbanite)	Lacustrine	-	Permian
Queensland (toolebuc)	Marine	484,000	Cretaceous
Eastern Queensland	-	-	Tertiary

tons, and Rundle with 5.0 billion tons (24). The Stuart deposit is the largest and is estimated to contain 3 billion barrels of oil shale in-place. The Stuart deposit has been considered for commercial development in the past.

Estonia

Estonian oil shale deposits are known as Kukersite (marine). The deposits have been known since the 1700s. The deposits underlay northern Estonia and extend eastward into Russia toward St. Petersburg where it is known as the Leningrad deposit. In Estonia, a somewhat younger deposit, the Tapa deposit, overlies the Estonia Kukersite deposit. The locations of the Estonian oil shale resources, the ninth largest in the world, are displayed in Figure 8.

As many as 50 beds of Kukersite oil shale are in the Kõrgekallas and Viivikonna Formations. These beds form a 20 to 30 meter thick sequence in the middle of the Estonia field. Individual beds are commonly 10 to 40 centimeters thick and reach as much as 2.4 meters. The organic content of the richest resource reaches 40 – 45 weight percent (25). Rock-Evaluation analyses of the richest-grade oil shale in Estonia show oil yields as high as 320 to 500 l/t.

Matrix minerals in Estonian Kukersite are low-Mg calcite (>50 percent), dolomite (<10–15 percent), and siliciclastic minerals including quartz, feldspars, illite, chlorite, and pyrite (<10–15 percent). It is estimated that Estonian Kukersite oil shale resources are 5.94 billion tons (26). Table VIII shows additional characteristics of the Estonian Kukersite oil shale deposit.

Another older oil-shale deposit, the Dictyonema Shale, underlies most of northern Estonia. This deposit ranges from less than 0.5 to more than 5 meters in thickness.

China

China has a large volume of oil shale resources estimated to be as much as 16 million barrels in-place (27) and is ranked 10th in terms of oil shale resources. China has two principal deposits located at Fushun and Maoming.

The Fushun deposit is in northeastern China just south of the town of Fushun in the Liaoning Province in the Jijuntun Formation. The Formation ranges from 48 to 190 meters in thickness with the lower 15 meters consisting of low-grade

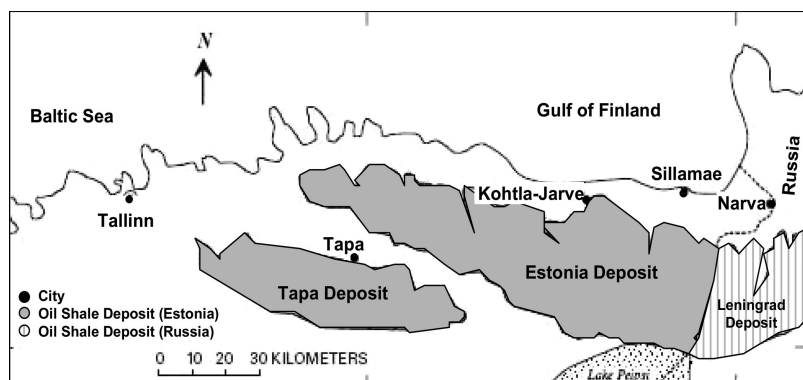


Figure 8. Map of Estonia Oil Shale Resources

Table VIII. Estonian Oil Shale Characteristics by Deposit

Deposit Location	Origin	Area (km ²)	Geologic Period
Estonia	Marine	50,000	Ordovician

oil shale and the upper 100 meters being richer grade in beds of thin to medium thickness. The oil shale is estimated to be approximately 78–89 l/t of shale oil. The total resource of oil shale at Fushun is estimated at 3,600 million tons.

The Maoming oil shale deposit is 50 kilometers long, 10 kilometers wide, and 20 to 25 meters thick. In this deposit, the resource is estimated at 5 billion tons, of which 860 million are in the Jintang mine. The Fischer assay yield of the oil shale is 4 to 12 percent and averages 6.5 percent. Table IX provides more details about the characteristics of the deposits.

Other Significant Oil Shale Deposits

Canada

Canada has as many as 19 deposits of oil shale of both marine and lacustrine origin (28). The oil shales of the New Brunswick Albert Formation have the greatest potential for development. The Albert oil shale averages 100 l/t of shale oil. The Devonian Kettle Point Formation and the Ordovician Collingwood shale of southern Ontario yield relatively small amounts of shale oil (about 40 l/t). The Boyne and Favel deposits form large resources of low-grade oil shale in the Prairie Provinces of Manitoba, Saskatchewan, and Alberta. Outcrops of lacustrine oil shale on Grinnell Peninsula, Devon Island, in the Canadian Arctic Archipelago, are as much as 100 meters thick and samples yield up to 406 l/t.

Table IX. Chinese Oil Shale Characteristics by Deposit

<i>Deposit Location</i>	<i>Origin</i>	<i>Area (km²)</i>	<i>Geologic Period</i>
Fushun	Lacustrine	-	Eocene
Maoming	Lacustrine	-	Tertiary

Israel

Israel has twenty deposits of oil shale with marine origin. The total estimated resource is 12 billion tons of oil shale. Israeli oil shale deposits range in thickness from 5 to 200 meters. The deposits have approximately 60 to 70 l/t and the shale has a high moisture content (~20 percent), high carbonate content (45 to 70 percent calcite) and high sulfur content (5 to 7 weight percent) (29).

Syria

Syrian oil shale resources are located in the Wadi Yarmouk Basin at the southern border of Syria and presumably part of the Yarmouk deposit located in northern Jordan (30). The deposit's origin is marine and contains minerals such as small amounts of quartz (1 to 9 percent), clay minerals (1 to 9 percent), and apatite (2 to 19 percent). The sulfur content of this deposit is 0.7 to 2.9 percent. Oil yields by Fischer Assay are 7 to 12 percent.

Sweden

Sweden contains an oil shale deposit known as Alum shale of marine origin. The Alum Shale is about 20 – 60 meters thick. It has been known for more than 350 years. The Alum Shale has a very high content of metals including uranium, vanadium, nickel, and molybdenum. The organic content of Alum Shale ranges from a few percent to more than 20 percent, being highest in the upper part of the shale sequence (31).

Thailand

Thailand contains lacustrine oil shale deposits near Mae Sot, Tak Province, and at Li, Lampoon Province. The Thai Department of Mineral Resources has explored the Mae Sot deposit with the drilling of many core holes. The Mae Sot deposit underlies about 53 square kilometers in the Mae Sot Basin in northwestern Thailand near the Myanmar (Burma) border. It contains an estimated 18.7 billion tons of oil shale, which is estimated to have a yield of 6.4 billion barrels of shale oil. The oil shale has a moisture content ranging from 1 to 13 percent and the sulfur content is about 1 percent. The deposit at Li has estimated resources of 15 million tons of oil shale with a potential yield of 50–171 l/t (32).

Turkey

Turkey contains lacustrine oil shale deposits which are widely distributed in middle and western Anatolia in western Turkey. The host rocks are marlstone and claystone in which the organic matter is finely dispersed. On the basis of available data, total resources of in-place shale oil for eight Turkish deposits are estimated at 284 million tons (about 2 billion barrels).

Summary of World Oil Shale Resources

World oil shale resources are characterized to varying degrees. The largest resource, the United States deposits, contain approximately 75 percent of the world's oil shale resources and a great deal is known about the quality and extent of these resources. However, there are many deposits around the world in which little is known about the quality and extent of the resource.

References

1. Duncan, D. C.; Swanson, V. E. *Organic-Rich Shales of the United States and World Land Areas*; U.S. Geological Survey: 1965.
2. Dyni, J. R. *Geology and Resources of Some World Oil-Shale Deposits*; Scientific Investigations Report 2005–5294; U.S. Geological Survey: 2006.
3. Dyni, J. R. *Oil Shale*; U.S. Geological Survey: Washington, D.C., 2003.
4. *Fact Sheet: U.S. Oil Shale Resources*; U.S. Department of Energy, Office of Petroleum Reserves, Office of Naval Petroleum and Oil Shale Reserves: 2005.
5. Dyni, J. R. *Geology and Resources of Some World Oil-Shale Deposits*; Scientific Investigations Report 2005–5294; U.S. Geological Survey: 2006.
6. Duncan, D. C.; Swanson, V. E. *Organic-Rich Shales of the United States and World Land Areas*; U.S. Geological Survey: 1965.
7. *2007 Survey of Energy Resources*; World Energy Council: 2007; p 102.
8. Duncan, D. C.; Swanson, V.E. *Organic-Rich Shales of the United States and World Land Areas*. U.S Geological Survey: 1965; U.S. resource data.
9. *2007 Survey of Energy Resources*; World Energy Council: 2007; p 102.
10. *National Oil Shale Model, A Decision Support System*; U.S. Department of Energy, Office of Petroleum Reserves, Office of Naval Petroleum and Oil Shale Reserves: 2005.
11. Duncan, D. C.; Swanson, V. E. *Organic-Rich Shales of the United States and World Land Areas*; U.S. Geological Survey: 1965.
12. Dyni, J. R. *Geology and Resources of Some World Oil-Shale Deposits*; Scientific Investigations Report 2005–5294; U.S. Geological Survey: 2006.
13. Dyni, J. R. *Geology and Resources of Some World Oil-Shale Deposits*; Scientific Investigations Report 2005–5294; U.S. Geological Survey: 2006.

14. Dyni, J. R. *Geology and Resources of Some World Oil-Shale Deposits*; Scientific Investigations Report 2005–5294; U.S. Geological Survey: 2006.
15. Padula, V. T. Oil Shale of Permian Irati Formation, Brazil. *Bull. Am. Assoc. Pet. Geol.* **1969**, *53*, 591–602.
16. Padula, V. T. Oil Shale of Permian Irati Formation, Brazil. *Bull. Am. Assoc. Pet. Geol.* **1969**, *53*, 591–602.
17. Dyni, J. R. *Geology and Resources of Some World Oil-Shale Deposits*; Scientific Investigations Report 2005–5294; U.S. Geological Survey: 2006.
18. Dyni, J. R. *Geology and Resources of Some World Oil-Shale Deposits*; Scientific Investigations Report 2005–5294; U.S. Geological Survey: 2006.
19. Dyni, J. R.; *Geology and Resources of Some World Oil-Shale Deposits*; Scientific Investigations Report 2005–5294; U.S. Geological Survey: 2006.
20. Crisp, P. T.; Ellis, J.; Hutton, A. C.; Korth, J.; Martin, F. A.; Saxby, J. D. *Australian Oil Shales – A Compendium of Geological and Chemical Data*; CSIRO Institute of Energy and Earth Sciences, Division of Fossil Fuels: 1987.
21. Alfredson, P. G. Review of Oil Shale Research in Australia. *Eighteenth Oil Shale Symposium Proceedings*; Colorado School of Mines Press: Golden, CO, 1985; pp 162–175.
22. Dyni, J. R. *Geology and Resources of Some World Oil-Shale Deposits*; Scientific Investigations Report 2005–5294; U.S. Geological Survey: 2006.
23. Noon, T. A. Oil Shale Resources in Queensland. *Proceedings of the Second Australian Workshop on Oil Shale*; CSIRO Division of Energy Chemistry: Sutherland, NSW, Australia, 1984; pp 3–8.
24. Crisp, P. T.; Ellis, J.; Hutton, A. C.; Korth, J.; Martin, F. A.; Saxby, J. D. *Australian Oil Shales – A Compendium of Geological and Chemical Data*; CSIRO Institute of Energy and Earth Sciences, Division of Fossil Fuels: 1987.
25. Bauert, H. The Baltic Oil Shale Basin—An Overview; *Proceedings of the 1993 Eastern Oil Shale Symposium*; University of Kentucky Institute for Mining and Minerals Research; 1994; pp 411–421.
26. Kattai, V.; Lökk, U. Historical review of the kukersite oil shale exploration in Estonia. *Oil Shale* **1998**, *15* (2), 102–110.
27. Dyni, J. R. *Geology and Resources of Some World Oil-Shale Deposits*; Scientific Investigations Report 2005–5294; U.S. Geological Survey: 2006.
28. Macauley, G. *Geology of the Oil Shale Deposits of Canada*; Geological Survey of Canada Open-File Report 754; 1981; p 155.
29. Minster, T. The role of oil shale in the Israeli Energy balance. *Energia* **1994**, *5* (5), 1, 4–6 (University of Kentucky Center for Applied Energy Research).
30. Puura, V.; Martins, A.; Baalbaki, K.; Al-Khatib, K. Occurrence of oil shales in the south of Syrian Arab Republic (SAR). *Oil Shale* **1984**, *1*, 333–340.
31. Andersson, A.; Dahlman, B.; Gee, D. G.; Snäll, S. *The Scandinavian Alum Shales*; Sveriges Geologiska Undersökning, Serie Ca: Avhandlingar och Uppsatser I A4; 1985; pp 50, 56.
32. Vanichseni, S.; Silapabunleng, K.; Chongvisal, V.; Prasertdham, P. Fluidized Bed Combustion of Thai Oil Shale. *Proceedings International Conference*

on Oil Shale and Shale Oil; Chemical Industry Press: Beijing, 1988; pp 514–526.

Downloaded by 89.163.35.42 on June 22, 2012 | <http://pubs.acs.org>
Publication Date (Web): February 23, 2010 | doi: 10.1021/bk-2010-1032.ch001

Chapter 2

New Challenges and Directions in Oil Shale Development Technologies

Peter M. Crawford^{1,*} and James C. Killen²

¹INTEK Inc., Arlington, VA 22201

²U.S. Department of Energy, Washington, DC 20585

*pcrawford@inteki.com

Economic, energy supply, and environmental challenges require new technologies to support diversification of global liquid fuels resources and markets. Higher oil prices make global oil shale resources more attractive. Mining and upgrading technologies for oil shale are proven at commercial scale. Retorting technologies to convert kerogen from shale ore into hydrocarbon liquids and gases continue to evolve to improve efficiency and reliability and address environmental, technical and regulatory challenges that constrain commercial development. Research and development activities in private industry, academia, and government-sponsored laboratories and research facilities continue to move oil shale technologies toward demonstration and commercialization. This chapter describes the major technical approaches for oil shale mining and processing and conversion of kerogen to refinery-quality feedstocks, current retorting technologies, and technology innovations that address technical challenges to commercial oil shale development.

Introduction

Oil shale is a sedimentary rock (carbonate or silica-based) that contains organic kerogen – a solid, immature form of petroleum. The solid does not melt and is insoluble. Conversion of the solid kerogen to hydrocarbon liquids and gases requires heating the raw ore to pyrolysis temperatures. Pyrolysis produces

hydrocarbon gases and vapors that when condensed would become liquid shale oil (1).

Natural conversion of kerogen to crude oil occurs subsurface in the oil temperature “window” of up to ~200°C over a period of millions of years. However, this reaction can be accelerated in surface and in-situ processes by increasing the temperature. Surface reactors can convert kerogen to hydrocarbon liquids in about one hour at temperatures of ~500°C. However, heating at ~500°C leads to significant hydrocarbon degradation and requires the end-product to be upgraded by hydrotreating before refining into fuels. In-situ processes heat the kerogen at a lower temperature (350°C) for a period of months, resulting in high quality products that require less upgrading.

Raw kerogen liquids may be lower in hydrogen content and higher in nitrogen and sulfur than conventional crude oil, thus requiring hydrotreating and upgrading to meet refinery feedstock standards. These upgraded feedstocks can then be used to produce high quality, ultra low sulfur diesel, jet, and naphtha based fuels as well as other high-value specialty chemicals.

Although a variety of approaches are available for accessing oil shale, converting the kerogen to hydrocarbon liquids and gases, and upgrading kerogen oil, ore access and conversion technologies fall under two general approaches (Figure 1):

- Surface retorting of mined (surface or underground) shale or
- In-situ (underground) retorting of kerogen still embedded in its natural depositional setting

Numerous technologies and variations have been conceived, developed, and tested under each approach. All have demonstrated the fundamental technical feasibility of applying heat to achieve pyrolysis and produce liquids and gases, with various levels of technical and economic success.

While mining and upgrading technologies are considered commercially proven, uncertainty remains about the commercial viability of retorting technologies that convert the kerogen-content of oil shale into valuable refinery feedstocks. Despite more than 65 years of public and private research, development and demonstration effort, and the continuous operation of small-scale oil shale plants in several countries, uncertainties remain about the commercial-scale viability of both surface and in-situ retorting technologies.

Technology Selection Criteria

Technology choice is primarily determined by the characteristics of the target resource, principally lithology and ore composition, depositional setting, and kerogen-richness, and heavily influenced by the environmental setting.

- Near-surface resources with economically viable stripping ratios (overburden to net pay ratio of ~1:1) tend to be candidates for surface mining (strip or open pit) and surface retorting.
- Deeper oil shale resources, and those accessible through outcrops, are candidates for underground mining with surface retorting.

- Some surface retorting technologies are better suited to processing lump shale (<15 millimeters diameter), while others are better suited to retorting smaller “fines” or particulates.
- Where shale deposits are deep, and the beds are very thick, in-situ heating techniques may be more effective from both technical and economic perspectives.
- Recent evidence suggests that new in-situ and surface-retorting approaches that heat shale at lower temperatures for longer periods may yield higher quality products that require little or no upgrading.
- Upgrading technology selection is largely dependent on the quality of the raw kerogen oil produced as determined by API gravity, sulfur, and nitrogen content.

Oil Shale Technology Maturation

Major oil shale technology development can require thousands of person-hours of effort and billions of dollars of investment over a period of decades to evolve from concept to successful demonstration at a commercially-representative scale. Development typically occurs in three major phases:

- **Laboratory:** Basic research, applied research, and bench-scale plants
- **Field Testing:** Field pilot plants and semi-works scale up
- **Commercial:** Scale-up from semi-works to commercially-representative scale demonstration plants, leading to full commercial-scale operating plants

As discussed more fully in the sections that follow, both the mining and upgrading technologies for oil shale are well developed and demonstrated at commercial scale. Conversion technologies are not as far along in the technology maturation process.

Technical confidence increases at each progressive phase, as does the level of project risk and the required capital investment. Failure at any point in the process can require stepping back, revising the approach or the design, or starting over again. Figure 2 depicts the path of energy technology evolution and commercialization.

By the early 1990s, more than 20 modern technologies for oil shale processing had been conceived and tested. Some encountered design or technology problems associated with scale-up. However, many others had advanced well beyond proof of concept in the lab to engineering, design, and field-testing at pilot or semi-works scale and produced significant volumes of shale oil.

Although most U.S. oil shale development efforts were terminated in the mid-1980s due to rising estimates of project costs and low global oil price and demand outlooks, several conversion technologies have been successfully demonstrated at commercially-representative scale or put into commercial operation. At least four surface technologies are currently in use, producing small commercial volumes of shale oil:

- Fushun (China)
- Petrosix (Brazil), and

- Kiviter and Galoter (Estonia)

The body of scientific and technical knowledge and understanding established by past efforts provides the foundation for new global research and technology development efforts that seek to advance oil shale mining, retort, and processing technology. New approaches and technologies are emerging and new challenges being addressed.

New Challenges

Today's oil shale technology and products must compete with conventional petroleum, as well as with emerging alternative liquid fuels, on the basis of cost, quality, and environmental impact.

In order to be commercially viable, current oil shale technology development efforts seek to economically address a new set of challenges posed by changing market conditions and stricter societal requirements and expectations. These new requirements pose technical challenges that impact the full scope of oil shale development activity, including resource access and recovery, conversion of kerogen to liquids and gases, disposition of production wastes, and collection and upgrading of produced hydrocarbons to refinery quality.

The global research community – including private companies, government supported laboratories, public and private universities, and other organizations – is actively pursuing development of new oil shale conversion technologies to meet both new and expected future economic, technical, environmental, and market imperatives. Major focal points of current oil shale RD&D include the following topic areas:

- Improving understanding of shale characteristics and depositional factors that may affect in-situ technology design and performance
- Improving recovery efficiency
- Improving process energy efficiency / net energy balances
- Reducing external energy requirements
- Reducing surface impacts affecting land use and habitats
- Reducing net water requirements
- Reducing generation or emissions of criteria air pollutants
- Achieving lifecycle carbon emissions equal to or less than conventional petroleum
- Protecting groundwater quality from in-situ processes
- Protecting ground water from surface operations
- Integrating oil shale development with other energy and economic development activity

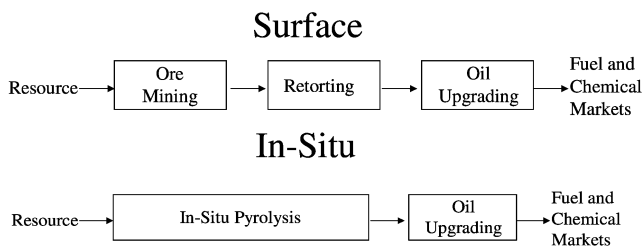


Figure 1. Conversion of Oil Shale to Products (2)

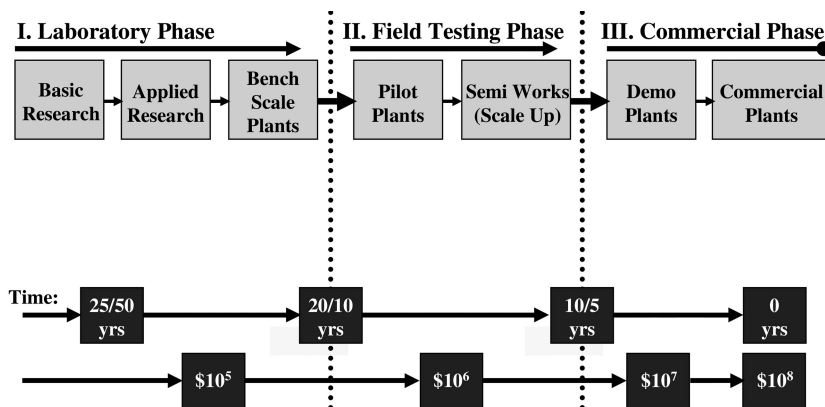


Figure 2. Evolution of Major Oil Shale Technologies (3)

Oil Shale Technologies and Trends

Oil Shale Mining Techniques

Despite the cyclical nature of U.S. and global efforts to develop oil shale resources and viable retort technologies, the technologies for surface and underground mining of coal and other mineral resources have advanced steadily.

State-of-the-art technologies have improved mine planning and design, excavation, materials handling, ore crushing and sizing, waste disposal, reclamation, restoration, and mine-safety technologies and practices. They are well demonstrated and commercially proven. Their application to oil shale will not differ fundamentally in design or practices from demonstrated commercial-scale applications for coal or other minerals. Continued advances in mining technologies can be expected to be largely transferable to surface and underground oil shale mining applications.

The major mining challenge for large-scale surface retorting operations will be the size of the surface or underground mines required to supply the large daily volumes of ore required to support continuous production at commercial scale. Surface plants producing 50,000 barrels per day could require mine outputs on the

order of 25 million tons/year. However, some U.S. mines, such as the Bingham Canyon Copper mine in Utah, produce 450,000 tons of material per day.

Surface Mining

Where the resource deposit is relatively shallow (<150 feet of overburden) or in deeper deposits with acceptable stripping ratios (overburden to net pay thickness ratio (< ~1:1), surface mining may be applicable. Surface mining approaches include both open-pit and strip mining.

Surface mining techniques offer the combined benefits of lower costs and higher productivity than other mining techniques over the life of the project. Productivity advantages include not only the rate of production but also recovery efficiency, maximizing the economic recovery of kerogen-bearing shale from the deposit. In strip mining, the excavated and mined area may be used to store overburden or spent shale, facilitating timely mine reclamation and surface restoration. Open-pit mines have generally been deemed inappropriate for spent shale disposal (Figure 3) (4).

However, despite the economical and technical advantages of various surface mining approaches, they have been generally dismissed for oil shale activities in sensitive areas due to associated environmental impacts that may include:

- Surface area disturbance and associated habitats at mine and storage sites;
- Overburden and spent shale management requirements and costs (transport, handling, storage, and disposal);
- Risks to surface and groundwater quality associated with potential run-off, leachates, and altered drainage patterns;
- Air quality impacts from fugitive dust and equipment emissions, and
- Habitat disturbance due to noise from mining and transport equipment, crushing, and blasting operations (4).

Underground Mining

Underground mining is applicable for use in deeper resources or deep resources accessible by outcrop. Room and pillar mining is the favored approach for oil shale, rather than long-wall. This method, successfully demonstrated economically and technically in coal mining operations, excavates chambers, leaving pillars to provide vertical support. This approach is viable in seams up to 100 feet thick (6). Once excavated, the chambers may provide future storage for most -- but not all -- of the spent shale, due to volumetric expansion properties of crushed and heated shale.

A disadvantage of room and pillar approaches is lower resource recovery. Only approximately 60% of the target resources can be recovered due to the required size of the pillars (7). Rock strength, fracturing, and other shale properties may also limit the applicability of underground mining in some depositional settings (8). Another limiting factor in selection of underground mining is the

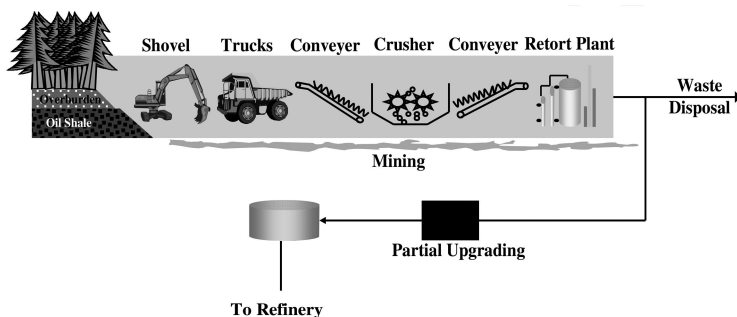


Figure 3. Surface Mining Example (5)

extensive up-front capital costs for mine facilities, pumping stations, ventilation, mine-accesses, and other underground mine safety systems and requirements.

Mining for Modified in-Situ Approaches

Where resource characteristics and depositional settings allow, the costs and challenges of ore mining and subsequent spent-shale disposal may be averted in favor of in-situ processes that heat kerogen-bearing ore in-place with limited or no excavation. Modified In-Situ (MIS) approaches require mining of a portion of the resource -- on the order of 10 percent -- to facilitate air-flow and create void space for in-situ combustion. Conventional underground mining techniques, including deep shafts, can be used to access the shale formation, rubblelize the shale, and transport it to the surface. The mined shale is then processed in surface retorts. However, new state-of-the-art in-situ processes, discussed later in this chapter, require no mining.

Oil Shale Retorting and Pyrolysis Technologies

Raw kerogen must be heated to pyrolysis temperatures to separate the organic content from the mineral content of the ore and to convert it from a solid to liquids and gases. The heating process is referred to as “retorting.” Where mined ore is to be processed on the surface, the physical ore heating facility is generally referred to as a “retort.” The thermal and chemical reaction by which the kerogen is converted from a solid to gases and liquids is referred to as “pyrolysis.”

Surface retorting processes are essentially materials handling and manufacturing operations. They require large volumes of materials to be mined and crushed and large vessels to contain and heat the mined shale to retort temperatures. The vessels must be sized to efficiently handle and heat large volumes of shale in a short period of time. In carbonate shale, such as those common to the western United States, higher temperatures employed to heat shale faster and reduce shale “residence time” in the retort, can cause the non-kerogen

shale material to breakdown, increasing carbon dioxide production. Equilibrium between temperature and residence time must be achieved.

The most efficient surface retorts process the shale in an oxygen-free environment to maximize production of high quality shale oils. Produced shale oil and gases must then be cleaned of impurities such as sulfur and nitrogen and upgraded to refinery standards. Emissions of criteria pollutants from mining, retorting, and upgrading operations must be managed to within public standards. Significant volumes of spent shale must be cooled, managed, and disposed of and mined areas must be reclaimed and restored. While retorting processes themselves may use little water, significant volumes may be required for mining, dust control, reclamation, and product upgrading. Surface and groundwater quality may be impacted by runoff from stored shale, overburden material, or spent shales, requiring diligent management.

Conversely, while in-situ processes may avert many of the costs, challenges, and potential environmental impacts associated with surface processes, they give rise to other significant challenges. They require drilling holes or shafts to access the resource and apply heat. They require efficient downhole heating technologies that can withstand harsh subsurface conditions. They also require effective methods to fracture the shale to allow consistent and effective heating of the entrained kerogen as well as to enable the produced fluids to travel from the shale body to producing wells.

Importantly, in-situ technologies require effective and reliable approaches to protect the heating area from groundwater intrusion and to protect surrounding groundwater from potential contamination by produced hydrocarbons or other toxins that may be present in the heating area after the shale oil and gases have been produced. Significant energy inputs from external sources may be required for some in-situ heating processes. Depending on the source of these energy inputs, they may contribute to significantly increasing the life-cycle carbon emissions of the overall in-situ process.

The general approaches, challenges, and current and emerging technologies and innovations associated with surface and in-situ oil shale processes are discussed below. Surface retorting processes including indirect, direct, and other heating variations will be discussed first. A discussion of in-situ processes challenges and innovations, will follow.

Surface Retorting Approaches and Technology

Generally, surface processing consists of three major steps: (1) oil shale mining and ore preparation, (2) pyrolysis of oil shale to produce kerogen oil, and (3) upgrading kerogen oil to produce refinery feedstock and high-value chemicals. This sequence is illustrated in Figure 4.

Conceptually, surface oil shale retorting seems to be a very simple process. Mined shale ore is cleaned of impurities, crushed and sized to retort specifications, dried to remove excess moisture, and heated in a surface vessel to retort temperatures, producing oil and gases that are captured as liquids gases and vapors for further processing. The residual mineral material is collected, cooled,

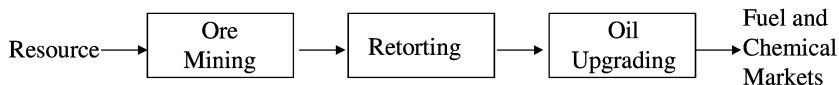


Figure 4. Conversion of Oil Shale to Products (Surface Process) (2)

and disposed. But in reality, what may appear very simple in concept becomes very complex in design and execution.

Most surface processing technologies seek to heat oil shale ore to retort temperatures as quickly as possible. This can be achieved by reducing the size of the mined ore by crushing and sizing techniques – increasing preparation costs – or by increasing the temperature in the retort vessel – increasing energy cost. The principal objectives of the retort process are:

- High product yields (production volume, recovery efficiency, and product quality)
- High thermal efficiency
- Short “residence” time in the retort – less than one hour
- High process / operational reliability
- Low environmental impact

Retort technology viability is determined by a combination of factors, including thermal efficiency, resource recovery efficiency, production rate, product quality and purity, and mechanical reliability or “up-time.” Increasingly, environmental factors are also a major determinant of efficacy, including water use and conservation, energy sources and heating methods, emissions of criteria air pollutants, spent shale composition and disposal, and carbon emissions. While addressing these challenges, retort technology development and demonstration requires lab- and pilot-scale processes to be economically and technically scalable to commercial size operations to be viable.

Table I provides a classification and overview of the surface retorting process that will be discussed in the following section.

Indirect Heating Methods

Early approaches for oil shale retorting involved indirect heating of the resource by transferring heat through the wall of a retort vessel to the ore. The low heat-conductivity coefficient of indirect heating limits the heat absorption rate of lump oil shale to several degrees per minute, requiring several hours to achieve retort temperature. This characteristic limits the size of the shale ore that can be efficiently heated, limits the capacity of the heating vessel, and limits the production rate and volume of the retort. Past technologies that applied indirect processes produced shale oil, but were characterized by poor scalability, high heating costs, and low thermal efficiency, making them inappropriate for commercial scale use.

Table I. Classification and Status of Some Surface Oil Shale Retorting Technologies (3, 9)

<i>Surface Retorting Processes</i>			
<i>Heating Method</i>	<i>Process</i>	<i>Last Status</i>	
Indirect Heating	CRE C-SOS	Pilot Planned ^b	
	EcoShale Incapsule	Field Pilot ^b	
Direct Heating			
Gas Heat Carrier	Bureau of Mines GCR (USA)	Demonstration	
	Paraho I & II (USA)	Pilot/Semi-Works	
	Petrosix (Brazil)	Commercial ^a	
	Union B (USA)	Demonstration	
	Kiviter (Estonia)	Commercial ^a	
	Fushun (China)	Commercial ^a	
	Chattanooga PFBC (USA)	Pilot ^b	
	Rotary Kiln w/ Sweep Gas (USA)	Lab ^b	
	Solid Heat Carrier	TOSCO II - Ceramic Ball (USA)	Semi-Works
		Lurgi-Ruhrgas (Multiple)	Pilot
Galoter (Estonia)		Commercial ^a	
	ATP (Canada, Australia)	Semi-Works ^b	

^a Currently in operation. ^b Currently in development.

At least two technologies are currently in development, however, that seek to overcome indirect heating limitations with new innovations.

CRE Energy, Inc.

The CRE Clean Shale Oil Surface Process (C-SOS), under development in Utah, uses an indirect-fired rotary kiln to heat crushed and sized oil ore up to 3/8 inch in diameter. The kiln may be fired by hydrogen – produced from an integrated coal gasification plant – to eliminate carbon dioxide emissions (Figure 5). By holding the retort temperature low (< 500°C) shale oil quality is maximized and degradation of the mineral component of the carbonate shale is minimize, avoiding generation of additional carbon dioxide emissions from the rotary kiln. A lab scale pilot is currently planned (3).

The EcoShale In-Capsule™ Process, under development by Red Leaf Resources in Utah, integrates surface mining with a lower-temperature, slow “roasting” method that occurs in an impoundment that is constructed in the void space created by the shale mining excavation (Figure 6). A system of piping is erected in the impoundment which is then filled with the mined lump shale, sealed, and heated indirectly with hot gases circulated through the piping. Slow heating at lower temperatures is expected to facilitate uniform heating, and yield very high grade kerogen oils and hydrocarbon gases. The produced hydrocarbon gases can be circulated back to the heaters, and used for site power generation, making the process largely energy self sufficient. Residual heat in the spent shale is used to preheat shale in subsequent capsules, resulting in higher net thermal efficiency. The impoundment avoids the expense and limitations of constructing a steel retort vessel.

It protects the heating zone from groundwater intrusion and provides a permanent impoundment for the spent shale once retorting operations are complete, thus protecting the subsurface. Overburden can be restored quickly, allowing for quick reclamation and restoration of surface conditions. The first field-scale pilot test was conducted in 2009 (10).

Direct Heating Method

Many contemporary surface retorting approaches now favor direct heating, using either hot gas as the heat carrier for larger sized “lump” ores (>10 millimeters size) or solid heat carriers for smaller fines or particulates (0 - 25 millimeters in size). With the exception of limited volumes of external fuel that are required for initial start-up heating, many of these processes obtain most or all of the energy required for heating shale from combustion or circulation of hydrocarbon gases that are produced in the retorting processes, combustion of residual carbon coke remaining on the residual “spent” shale, and / or the capture and use of residual heat in the spent shale to pre-heat fresh shale entering the retort.

Extensive research and testing has been conducted with a variety of gas and solid heat carrier technologies for surface retorts since the 1940s. Gas heat carrier retorts are typically vertical retorts, fed from the top, with two chambers. An upper retort chamber heats the shale to pyrolysis temperatures. Shale oil vapors and hydrocarbon gases are recovered. Some of the cooled gases are combusted to provide heated gases for the retort chamber. Some of the cooled gases are also circulated to the lower chamber to help cool the coked shale. The lower chamber cools the coked shale, transferring heat from the coked shale to the circulating gases which is then used to heat fresh shale.

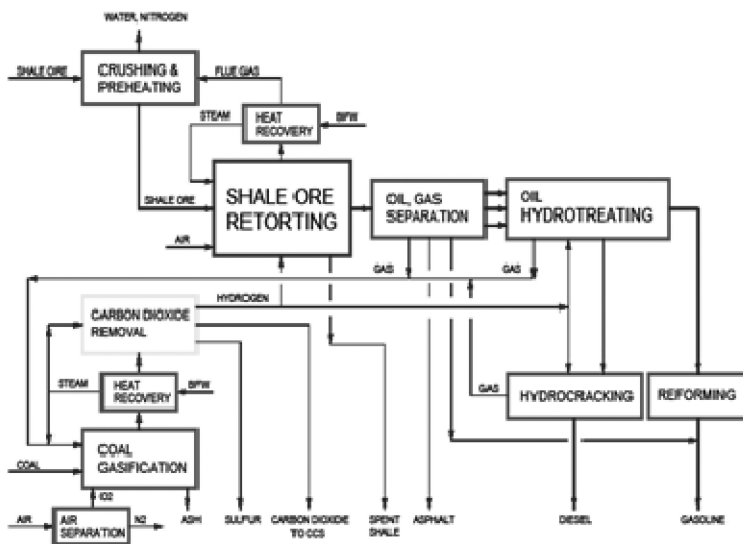


Figure 5. CRE C-SOS Process (3)

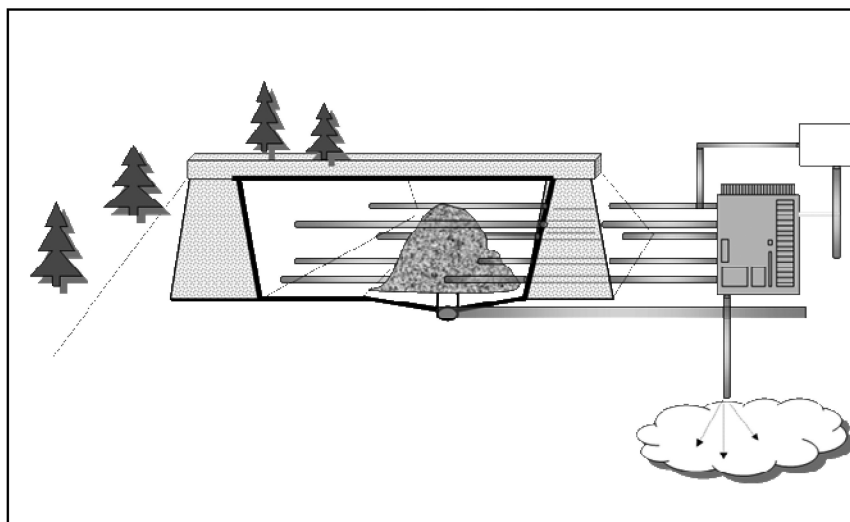


Figure 6. EcoShale's In-Capsule Process (10)

Bureau of Mines Retort

Several variations of the Gas Combustion Retort (GCR) developed for the U.S. Bureau of Mines by Cameron Engineers are currently in use for testing or shale oil production (Figure 7).

Between 1949 and 1955, three above ground gas combustion retorts were developed and operated by the U.S. Bureau of Mines, proving the technology.

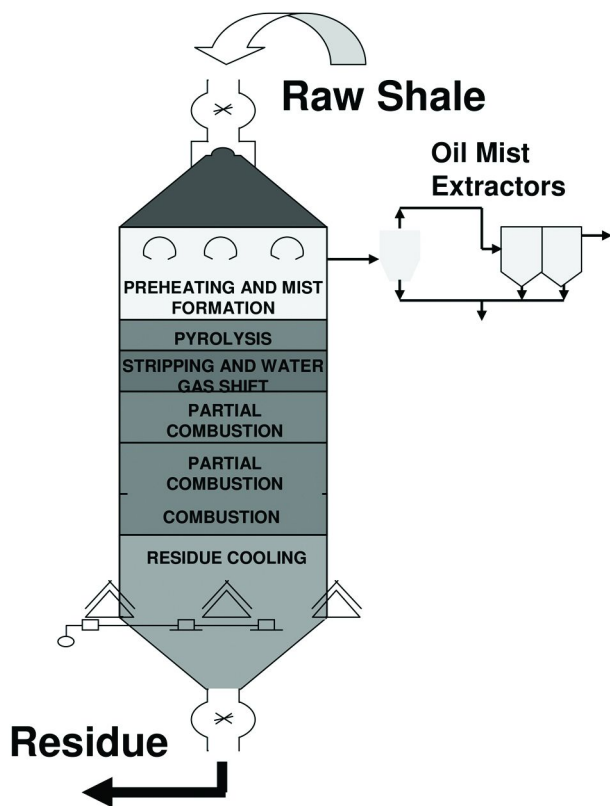


Figure 7. Gas Combustion Retort (2)

The original version of this two chamber vertical retort ignited the residual carbon coke on spent shale in the lower chamber to provide retort heat for fresh shale in the upper chamber.

Paraho Development Corporation

Subsequently, beginning in 1972, Paraho Development Corporation, a consortium of 17 private companies, produced approximately 110,000 barrels of shale oil using a modification of the Bureau of Mines GCR technology that was developed by Development Engineering Inc. The enhancements embodied in the Paraho technology allow the retort to be configured in either the original direct combustion mode or by circulating heated gases back to the retort to heat fresh shale (11).

Most of the fuel produced by Paraho was delivered to the U.S. Navy for fuels development and testing. The semi-works scale plant used for this effort was later decommissioned, but the pilot-scale test plant facility in Rifle, Colorado, has recently been refurbished for testing and design purposes by the successors of

Paraho, now known as Shale Tech International. A next generation of the Paraho technology is under development by ShaleTech (Figure 8).

Petrosix

Another variation of the GCR technology, the Petrosix retort, has been in continuous commercial use in Brazil by Petrobras since approximately 1981. An initial 5.5 M diameter plant with a daily throughput capacity of 1,600 tonnes of shale ore was built in 1981. A larger 11m diameter GCR with 6,200 tonnes per day capacity was built in 199. Combined, the two Petrosix reactors currently process approximately 7,800 tonnes of shale per day to generate a slate of products that includes: 3,870 barrels of shale oil, 120 tonnes of fuel gas, 45 tonnes of liquefied petroleum gas and 75 tonnes of sulfur (12).

The failure to make use of the fixed carbon on the coked shale reduces the thermal efficiency of the Petrosix version of the GCR technology. It also affects the residual carbon content of the spent shale which must be disposed of, potentially affecting its environmental acceptability. However, the oil yield averages 85 to 90 percent of Fisher assay and the produced hydrocarbon gases have high calorific values. The technology has also demonstrated high operational efficiency, achieving up-time in excess of 94 percent over several years in operation.

The Petrosix GCR technology is currently being evaluated for use by the Oil Shale Exploration Company (OSEC) as part of a research and development (R&D) project on a BLM RD&D lease awarded to OSEC by the U.S. Department of the Interior, Bureau of Land Management in 2007. The Petrosix is also being considered for application in other oil shale deposits around the world.

Union B

The Union B Retort was developed by Union Oil Company of California and operated at various demonstration scales for over 6 years at the Long Ridge Project on Parachute, CO, before being shut down for economic and technical reasons in 1991. Designed to produce 9,000 Bbls/day, the maximum production never exceeded about 50 percent of that intended level. The Union B process employs a rock pump to move crushed shale upwards against a counter-flow of hot recycle gases (510 -538°C) that heats the shale and pyrolyzes the kerogen into vapors and gases. Heat for the gases is supplied by combustion of the residual carbon coked on the spent shale, making the process essentially energy self-sufficient. The process requires no cooling water – gases, solids, and produced liquids are cooled by the fresh shale entering the lower section of the retort. Importantly, “the reducing atmosphere maintained in the retort results in the removal of sulfur and nitrogen compounds through the formation of H₂S and NH₃ gas” which are captured and treated. This reduces the presence of these compounds in the produced shale oil, resulting in a higher quality shale oil that requires less upgrading. The produced

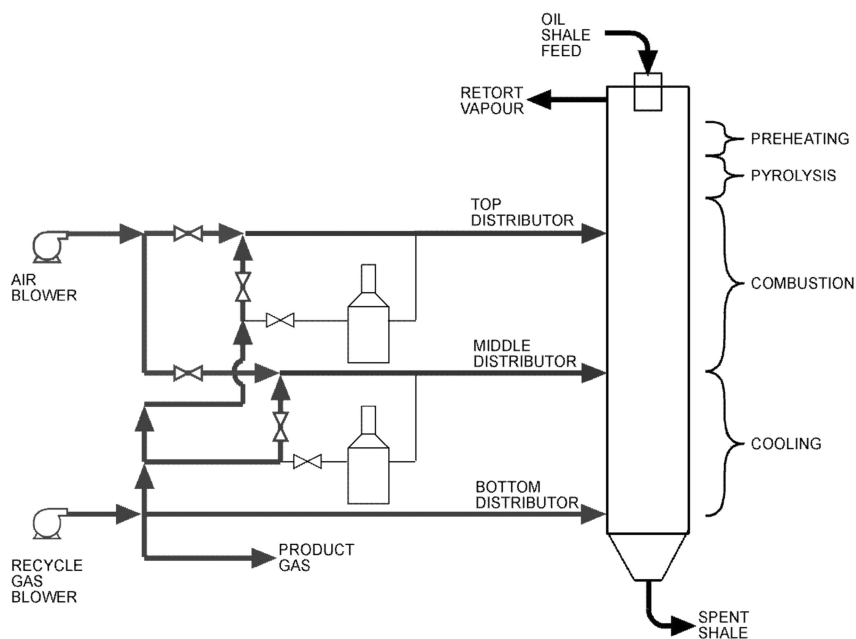


Figure 8. Paraho Process (3)

kerogen oil from Unocal's operations was usable as a low-sulfur fuel or as a very high quality feedstock for refining (13).

Other Variations

Other variations of the direct gas-heat carrier technology for lump shale include the small scale (3 meter diameter, 100-200 tons per day (tpd) throughput) Fushun lump shale retort that has been in use in China for more than 70 years, and the larger (1,000 tpd) Kiviter lump shale retorts employed by the Viru Keemia Group in Estonia.

The Fushun retort takes advantage of the fixed carbon residue on the coked shale by gasifying it, and using the resulting hot gas to heat fresh shale entering the top of the retort (Figure 9). This improves the thermal efficiency of the retort. However, the admission of air to the retort post-combustion introduces nitrogen, reducing the quality of the produced hydrocarbon gases, and the introduction of oxygen in the retort chamber causes some of the produced kerogen oil to be combusted, thus significantly reducing the shale oil yield to about 65 percent of Fisher assay. Due to the small scale of the technology, multiple retorts are typically arrayed with as many as 20 Fushun retorts sharing a single gas collection and condensation system. More than 120 of these retorts were in operation as of 2005 (14).

The Kiviter technology uses multiple internal pyrolysis chambers in the upper part of the retort, through which air and hot gases are circulated to achieve a thin-

layer pyrolysis (Figure 10). As with the Petrosix GCR, there is no use of the fixed carbon on the remaining coked shale, thus reducing thermal efficiency to about 70 percent. Nitrogen content in the produced hydrocarbon gases reduces their calorific value, and the presence of oxygen in the retort reduces yield to about 75 to 80 percent of Fisher Assay. Nonetheless, two Kiviter retorts are effectively operated to produce shale oil and products at Yarve in Estonia (15).

Recent Innovations

More recent direct gas heat carrier approaches include a fluidized-bed heating process, injection of syn-gas from a coal gasifier, and a hydrogen-donor solvent technology, as follows:

Fluidized Bed Reactor with Fired Hydrogen Heater

Fluidized bed combustion technology was developed in the 1970s to combust coal for steam and power generation in the presence of carbonate materials that would capture sulfur and reduce emissions of Sulfur Dioxide (SO₂). This technology has recently been adapted and applied for use in oil shale retorting.

The Chattanooga Process, currently under development, introduces fresh crushed shale in to a non-combustion pressurized fluidized bed reactor. Heated hydrogen is injected from the bottom of the reactor, raising the temperature of the suspended shale particles to a processing temperature of ~500°C, and converting the kerogen to hydrocarbon vapors and gases, via thermal cracking and hydrogenation (Figure 11). In this unique approach, heated hydrogen is used as the heat conveyor, the fluidizing gas for the reactor bed, and as a reactant. Reactor overhead gases are cleaned of particulate solids in a hot gas filter and cooled. Hydrocarbon products are condensed and separated from the gas stream. Liquids can be lightly hydro treated to produce very low sulfur high grade synthetic oil.

In the Chattanooga Process, hydrogen is heated in an adjacent fired heater fueled by process off-gases and either supplemental gas or product oil, depending upon economic conditions, minimizing or eliminating external natural gas requirements. Use of hydrogen in the initial process phases enhances product quality and reduces the need for extreme hydrotreating.

Recovery of waste heat, power co-generation, and use of produced light hydrocarbon gases as hydrogen plant feedstock make the process virtually self sufficient by obtaining its energy requirements from the primary plant feedstock.

Dry processing of resource material eliminates water pollution and greatly reduces water usage. Greenhouse gas emissions are substantially reduced. The majority of the CO₂ is produced in the hydrogen reformer and can be captured through amine separation and sequestered. Decomposition of Western carbonate shale and formation of CO₂ are minimized due to the operating temperature range. Spent shale or sand is immediately available for land reclamation. This process has the ability to remove 99.8% of all sulfur.

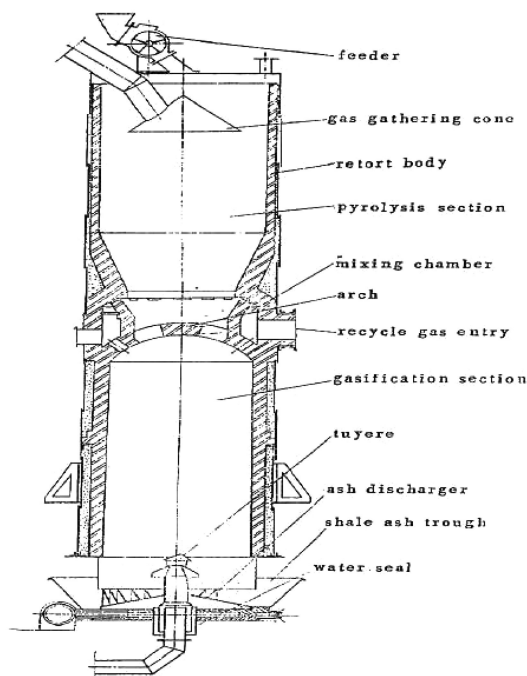


Figure 9. Fushun Retort (15)

According to the developers, high extraction yields are achieved due to the addition of hydrogen in the initial phase of processing. Pilot plant tests yielded 51.5 gals/ton from Colorado carbonate shale (with a Fischer Assay of 28.4 gal/ton). Two separate pilot plant tests on Kentucky shale also produced yields nearly double the Fischer Assay predictions. Based on pilot plant test results and with some hydrotreating, the product from oil shale would be in the range of 36°API Chattanooga Corp is preparing to design, construct and operate a demonstration facility as the next step in the commercialization process (17).

Rotary Kiln with Sweep Gas Injection from Integrated Gasifier

At least three U.S. companies, Syntec, EnShale, and Western Energy Partners, are working to develop and test an approach that injects heated synthetic gas created by a coal gasifier into a rotating kiln to directly heat and process crushed shale. The synthetic gas provides a hot, hydrogen-rich, sweep gas that interacts with the kerogen to produce energy rich hydrocarbon vapors and gases. The vapors are condensed to produce high-quality kerogen oil. The gases are stripped to remove sulfur. Residual heat from the gasifier is used to preheat the shale, improving thermal efficiency of the integrated process. Water reclamation from the gasifier also provides water required for hydrotreating and upgrading. This process has been studied and tested and proven at bench scale at the University of

Utah. One of the developers has announced plans for a 50 Bbl/d field pilot plant (18).

Rendall Hydrogen-Donor Solvent Process

A hydrogen-donor solvent approach is being developed for oil shale in Australia (Figure 12). The Rendall Process feeds crushed run-of-the-mine shale to a conditioning unit to be slurried with a recycled stream from the distillation section of the plant that includes a middle-distillate fraction. That fraction, upon hydrogenation, becomes a hydrogen-donor solvent. The hydrogen-shale slurry is heated to retort temperatures (~450°C) and then fed to a kerogen conversion / hydrogenation reactor. The release of additional hydrogen from the hydrogen-donor solvent interacts with kerogen from the shale to result in a lighter fraction oil product. The hydrogen also reduces the organic sulfur content to hydrogen sulfide (which is later converted to elemental sulfur) and scavenges oxygen and nitrogen from the kerogen, improving product quality.

The process is estimated to yield approximately 95 percent light oil and 5 percent high-value hydrocarbon gases. Emissions are estimated to be equal to approximately 5 percent of the organic carbon in the shale feedstock. Solid wastes, principally spent shale, are free of hydrocarbons and insoluble. The process has been lab tested at bench scale. Blue Ensign, an Australia firm, is planning a 1 tonne/hour pilot plant in Townsville, Australia using Australian, silica-based, Julia Creek shale. The process has also been tested using Colorado carbonate-based Green River oil shale (19).

Solid Heat Carrier Technologies

Several technologies have been devised and evaluated for processing more finely crushed shale ore and making use of the fines produced in mining and ore sizing operations that are not suitable for “lump” shale processes.

In the 1970s, TOSCO conducted extensive development and testing of the TOSCO II retort technology which employed heated ceramic balls to capture and transfer residual heat from the retorted shale to help dry and pre-heat fresh shale entering the retort. This technology was to have been demonstrated at commercially-representative scale in Exxon’s planned 47,000 Bbl/d Colony Project which was terminated during construction in 1982 due to rising costs and a low price outlook for crude oil.

The Lurgi approach uses a mixture of heated sand and hot shale for solid-to-solid heat transfer.

More recent approaches include a horizontal rotating kiln that recirculates hot shale ash (ATP), and more complex rotary drum with cyclone separation and hot solids recycle for shale heating and drying (Galoter). The Galoter process is being employed in commercial operations in Estonia.

Lurgi

The Lurgi-Ruhrgas process was developed in Germany for the devolatilization of coal fines. The application of the Lurgi-Ruhrgas process to oil shale was intended to integrate kerogen retorting with hydrocarbon refining in a single plant. The heating approach mixes fresh crushed shale (<0.25 inch diameter) with a mixture of six times as much heated spent shale and sand (heat carriers) to raise the average temperature above retort temperature, causing the fresh shale to release kerogen vapors and hydrocarbon gases. Sand and processed shale are returned to the bottom of the process, reheated with combustion gases, and recycled back through a lift pipe to process more fresh shale. Small particle sizes require a variety of mechanisms including sedimentation, centrifuging, cyclones, and electrostatic precipitators to remove fines from produced kerogen oil liquids (Figure 13) (20).

Galoter

The newer Galoter retort design, Figure 14, is a horizontal fluidized bed retort with a throughput capacity of about 3,000 ton per day (roughly half the capacity of the Petrosix 11 meter retort and three times the capacity of the Kiviter). Using shale ash as a solid heat carrier, the process is more thermally efficient, reducing energy inputs, and achieves a higher yield on the order of 85 to 90 percent of Fisher Assay. The design also delivers a higher quality of produced gases. Although the process is far more complex than the Kiviter, plant availability has steadily improved, recently achieving a very high level of operating “up-time.”

Alberta Taciuk Process (ATP) – Horizontal Rotating Kiln

The Alberta Taciuk Process is a horizontal rotating kiln design with very high thermal efficiency and high production efficiency, achieving shale oil production of 90 percent of Fisher assay or greater (Figure 15). The ATP Process was developed in 1976 for treating Alberta oil sands and later refined for use in oil shale and contaminated waste treatment options. The process was subsequently scaled up and demonstrated at commercially-representative scale in the Stewart deposit in Queensland Australia.

The ATP process combines gas recirculation and direct and indirect heat transfer from circulated hot solids in a rotating kiln. As with other surface retorts, the process is largely energy self-sufficient. Some of the hot processed shale is re-circulated in the retort with fresh shale to provide pyrolysis heat by direct, solid-to-solid heat transfer. The ATP Process has successfully produced over 1.5 million barrels of shale oil from a 4500 Bbl/d reactor at the Stuart Shale Oil Project in Queensland, Australia. Until recently, however, ATP had not been tested or demonstrated using carbonate-based U.S. oil shale. OSEC recently shipped over 300 tons of shale from the White River Mine site for testing in the

ATP in Alberta. The technology was judged a technical success, but the project was suspended in 2004.

Oil Shale Exploration Company is the recipient of a federal Oil Shale RD&D lease at the White River site in Utah. The ATP process is also being considered for use in several other projects including oil shale development efforts in China and in the Kingdom of Jordan.

In-Situ Technologies

In-situ oil shale processes introduce heat to the kerogen bearing ore while it is still embedded in its natural geological formation.

There are both advantages and disadvantages related to operations, requirements, products and quality, and environmental impacts associated with applying in-situ technologies versus surface retorting approaches.

- Materials handling is greatly reduced as only to organic content of the shale, not the entire ore body, is contacted and produced to the surface. There is no overburden to be mined, little or no subsurface mining, and no spent shale to be disposed.
- In deep and thick deposits, where in-situ approaches are most applicable, more of the resource can be contacted and heated, although less of the products will be recovered.
- Water requirements for mining, reclamation, dust control, and spent shale disposal are largely eliminated.
- Net energy efficiencies for the integrated process – from resource access and recovery, through retorting and upgrading – to waste disposal can be improved relative to some surface-based mining and retorting processes.
- Emissions of criteria air pollutants can be significantly reduced.
- Depending on the source of heating energy, lifecycle carbon emissions could also be reduced.
- Surface impacts on wildlife habitats, including those from noise, would be reduced, due to the lack of mining activity, or requirements for storage of overburden, shale, and spent shale.
- Potential surface and groundwater impacts of leachates from overburden, shale, and spent shale would be avoided.

In-situ processes also pose some significant disadvantages relative to surface approaches:

- Early approaches experienced difficulty controlling both the temperature and the directional mobility of heat in the shale formation. Excess heat can reduce shale oil quality, recovery efficiency, and yield and increase subsurface environmental impacts and emissions.
- Subsurface processes face challenges associated with heating efficiency. Shale is a slow heat absorber and not a good heat conductor. Fracturing by natural or induced methods is typically needed to achieve even and effective heat distribution through the formation and increase the surface area for heating.

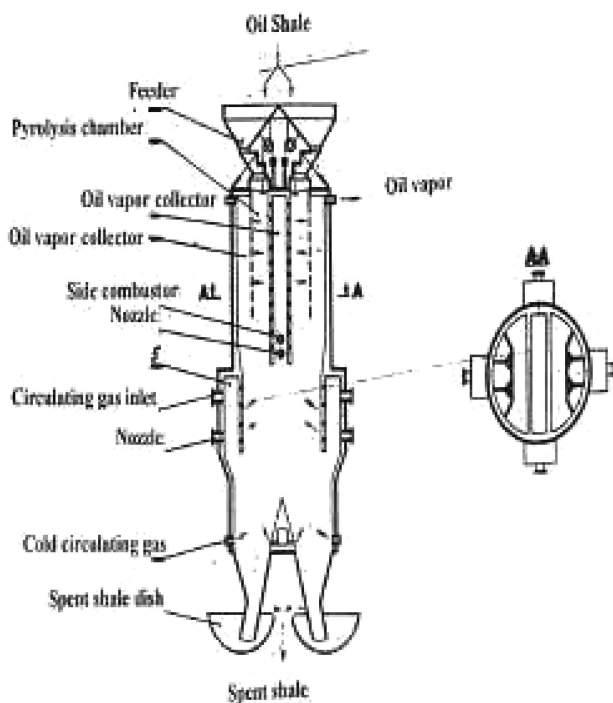


Figure 10. Kiviter Vertical Retort (16)

- Typically, in-situ processes require far greater heating time than surface approaches, resulting in longer lead-times and energy-investment periods before production of hydrocarbons begins.
- Product recovery is also constrained by inconsistent (heterogeneous) permeability and porosity in the shale formation, presenting challenges for recovering the produced hydrocarbon gases, vapors, and liquids.
- Subsurface heating – whether through direct combustion or in-situ heating - may leave residual carbon in the form of char on the remaining mineral body of the formation.
- In-situ combustion approaches use some of the shale itself as fuel for heating the rest of the formation. Many in-situ heating methods, however, require an external heat source, impacting energy efficiencies.
- As with conventional oil production, production efficiency can be relatively low. Effective means are required to “sweep” the produced hydrocarbons through the formation to the production well.
- Intrusion of groundwater into the heating area can result in inefficient heating and creation of unwanted steam, requiring effective methods for isolating the production area.
- Residual unswept hydrocarbons and char can both present contamination risks for groundwater, also requiring effective methods for isolating the heating area. Fracturing may also affect subsurface ground water patterns.

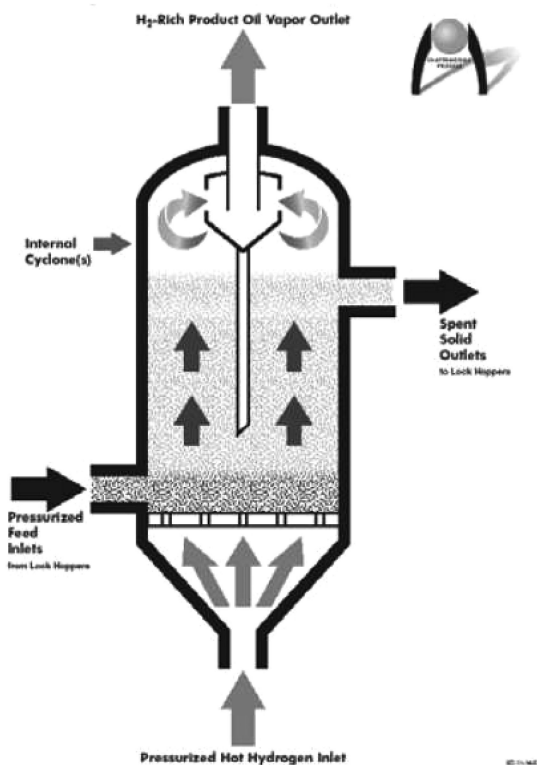


Figure 11. Chattanooga Process (17)

- Carbon dioxide may be produced by subsurface heating and degradation of the carbonate minerals that comprise most U.S. western oil shale. Carbon dioxide may also be generated in significant quantities by some energy sources used for subsurface heating.
- All of these potential disadvantages are targets for ongoing research, development, and demonstration efforts in government, industry, and the research community.

In-Situ Combustion Approaches

There are two general in-situ approaches:

- True in-situ (TIS) in which there is minimal or no disturbance of the ore bed, (Figure 16) and
- Modified in-situ (MIS), in which the ore bed is rubblized either through direct blasting or after partial mining to create void space (Figure 17).

Most early processes involved combusting some of the subsurface resource to generate heat needed to convert kerogen from the remaining resource to hydrocarbon liquids and gases, which could then be produced to the surface through conventional oil wells.

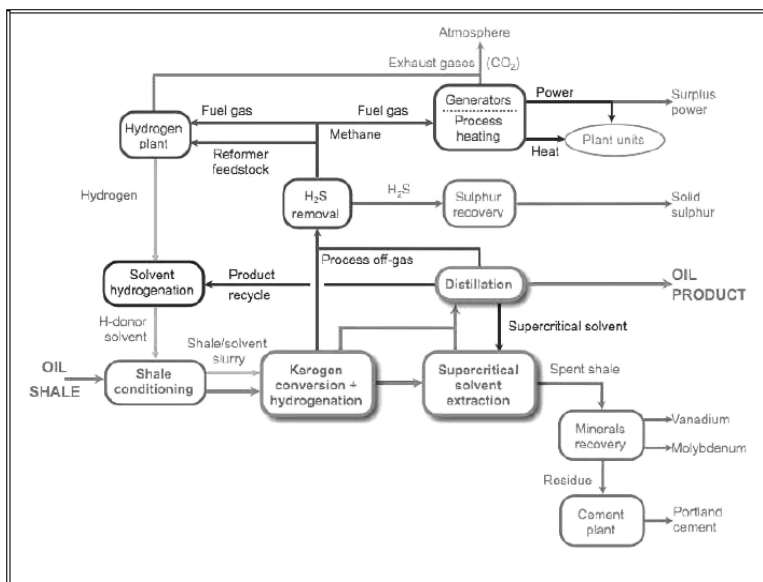


Figure 12. Rendall Hydrogen-Donor Solvent Process (19)

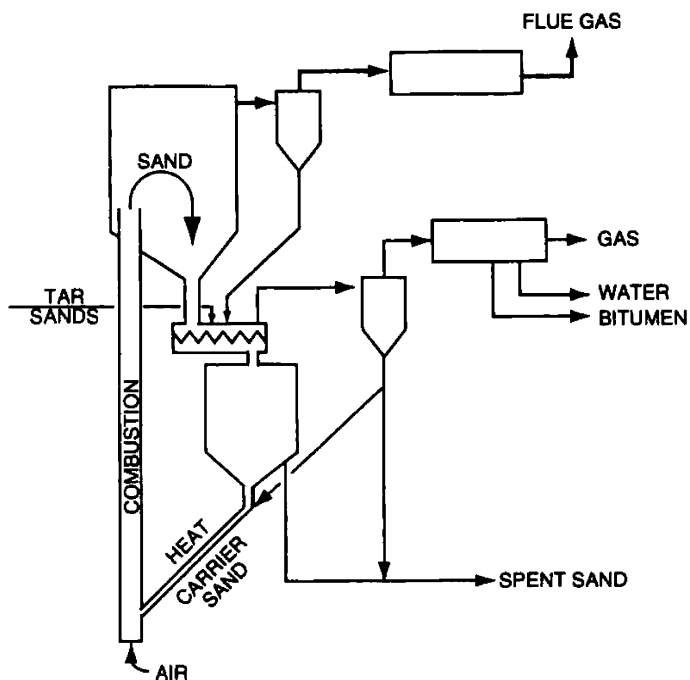


Figure 13. Lurgi Process (1)

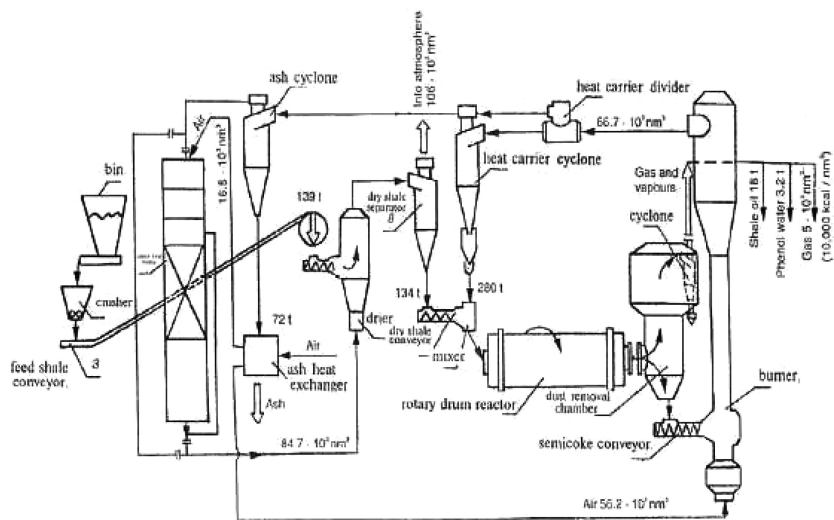


Figure 14. Galoter Process (21)

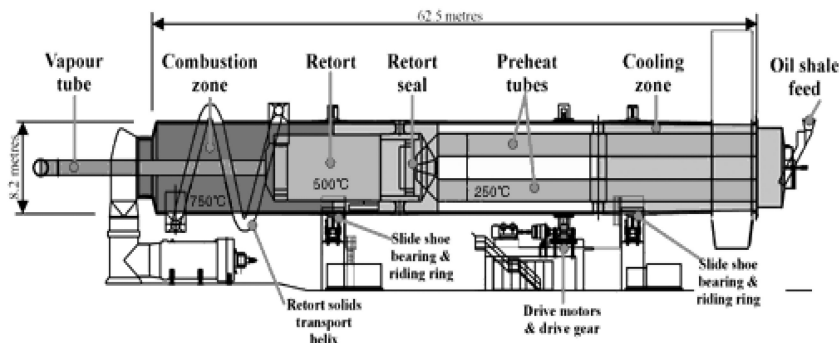


Figure 15. ATP Horizontal Rotator Kiln (2)

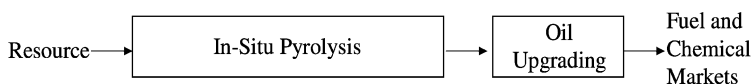


Figure 16. Conversion of Oil Shale to Products (True In-Situ Process) (2)

Both of these in-situ combustion approaches faced major challenges, however, primarily related to sustaining and controlling the subsurface combustion, directing and communicating heat through the target shale formation, generation of subsurface pollutants, and degradation of the subsurface environment, including groundwater quality. The MIS approaches achieved significant advances in terms of air, temperature, and combustion control, but emissions and subsurface environmental impacts continue to be challenges for MIS approaches.

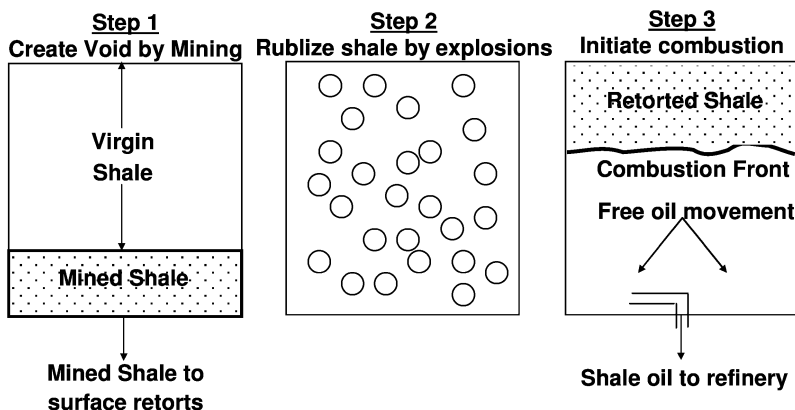


Figure 17. Conversion of Oil Shale to Products (Modified In-Situ Process) (22)

Table II provides an overview of the In-Situ Process that will be discussed in the following section.

Early In-Situ Approaches and Variations

Lessons learned from early attempts with true in-situ combustion led to a number of variations intended to address technical challenges associated with heat control, fracturing, and sweep efficiency. According to (Lee, 1991), Sinclair Oil and Gas attempted to use high pressure air to sweep produced hydrocarbons to the production wells. Equity Oil and Gas attempted to inject heated natural gas to serve as a heat carrier – in lieu of direct combustion – and to improve sweep efficiency. Dow Chemical, in experiments in eastern shale resources, applied blasting techniques to fracture shale formations. Dow also experimented with electric resistance heaters -- an approach later adapted by Shell. Geokinetics, Inc. laid the fundamental groundwork for modified in-situ processes with the use of mined, horizontal retort voids for use in thin deposits (23).

The Occidental Modified In-Situ Retort, completed in 1984, involved sinking a mine shaft and blasting and rubbleizing a portion of the shale body to allow void space for heating and retorting. The process integrated surface retorting operations for the mined shale. While technically a success in terms of process performance and product recovery and quality, the project also raised numerous potential environmental impacts associated with in-situ combustion approaches (24).

Table II. Classification and Status of Some In-Situ Oil Shale Retorting Technologies (3, 9)

<i>In-Situ Process</i>		
<i>Heating Method</i>	<i>Process</i>	<i>Last Status</i>
True In-Situ	Sinclair High Pressure Air	Pilot
Combustion	Laramie Energy Tech. Center	Pilot
Modified In-Situ	Geokenetics Horizontal	Pilot
Combustion	Occidental Surface Combination	Demonstration
In-Situ Heating		
Down Hole Heater	DOW Resistance Heating	Pilot
	Shell Electric Resistance Heating	Demonstration ^a
	IEP Geothermic Fuel Cell	Lab ^a
Radio Frequency	Radio-Frequency w/ Critical Fluids	Lab ^a
	P-W Borehole Microwave	Pilot Planned ^a
Direct Current	Electro-Frac TM	Pilot Plan ^a
Heat Gas Injection	Equity Hot CO ₂ Injection	Pilot
	Earth Search Sciences/Petro-Probe	Pilot ^a
	AMSO Deep Illite	Lab ^a
	MWE In-Situ Vapor Extraction	Pilot ^a
	Chevron CRUSH	Lab ^a
Groundwater	Shell Freezwall Technology	Pilot (in progress) ^a
Protection	EcoShale Incapsule	Field Pilot ^a

^a Currently in development.

New Approaches to In-Situ – Thermally Conductive Conversion

Much has changed, however, in the area of in-situ retorting. The most significant change is a major shift away from the concept of in-situ combustion, in favor of direct heating without combustion. Most current in-situ activity focuses on this new thermally-conductive conversion approach. Several new in-situ technologies are in varying stages of development and assessment. The recent advances in in-situ oil shale technology are both numerous and ground breaking. These new variations on the traditional approaches described above may offer:

- Improvements in thermal efficiencies
- Reductions in energy use
- Reductions in net water use
- More efficient capture of regulated emissions
- Effective carbon management
- Higher production yields, and/or

- Increased product quality as measured by API gravity and other standard measures.

New in-situ approaches can be classified into three groups:

- Downhole heaters
- Direct current heating
- Hot gas injection

One group employs downhole heaters – rather than mining or in-situ combustion – to heat the shale body to achieve pyrolysis and produce hydrocarbons. Another approach fractures and applies a direct current to heat the formation. The third approach, a variation on early concepts, injects heated gas to heat the shale and recover produced hydrocarbon gases and vapors. Each of these approaches is explored below.

Down Hole Heaters

Shell In-Situ Conversion Process (ICP)

For more than a quarter of a century, Shell's Mahogany Research Project has conducted research on Shell's innovative In-Situ Conversion Process (ICP) to recover oil and gas from oil shale in Colorado. ICP involves placing either electric or gas heaters in vertically drilled wells and gradually heating the oil shale interval over a period of several years until kerogen is converted to hydrocarbon gases and kerogen oil which is then produced through conventional recovery means. Electric heaters, inserted in heater wells, gradually heat shale beneath surface at a target depth zone 1,000 to 2,000 feet subsurface. The rock formation is heated slowly over a period of years to ~350°C (650 to 750°F), changing the kerogen in oil shale into oil and gas (Figure 18).

ICP, when applied to oil shale, produces a range of gases including propane, hydrogen, methane, and ethane, as well as high quality liquid products – jet fuel, kerosene, and naphtha – after the initial liquid product is hydro-treated.

ICP appears to improve heat distribution in the target deposit, overcoming heat-front control problems traditionally associated with prior in-situ combustion processes. Due to the slow heating and pyrolysis process, the product quality is much better and subsequent product treating is less complex as compared to oil produced by surface retorting or conventional in-situ approaches.

The gradual heating process is also expected to induce fracturing in the shale – assisting in uniform heating and providing pathways for produced gases and vapors to migrate to producing wells.

ICP produces approximately 1/3 gas and 2/3 light oil. Shell estimates that potential yields in the thickest and richest deposits could range from 100,000 to 1 million barrels of oil equivalent per acre. The process yields high quality feedstocks (>30 API gravity) that require only minimal upgrading to produce jet, diesel, and motor gasoline fuels. A recent field test on private Shell lands in Colorado demonstrated the efficacy of the ICP technology for producing significant volumes of high quality product.

Commercial scale application of the ICP technology using electric heaters will require extensive electric power generation facilities. Shell engineers have estimated that the process will generate three times the energy it uses. Hydrocarbon gases produced by the ICP may be used to generate electricity to reduce power requirements. Shell is also exploring the use of gas-fired heaters and other approaches to reduce electric power demand and improve thermal efficiency.

The slow, lower temperature heating process is expected to generate significantly lower carbon emissions than traditional surface retorting processes, because the lower heating temperatures preserve the integrity of the carbonate host rock. Ultimately, however, the carbon profile of an ICP project will depend largely on the energy source used for power or heat generation – coal, nuclear, gas, hydro, solar, or wind.

Shell has engineered and begun testing a freezeway technology to protect the heating zone from groundwater intrusion and to protect the groundwater from potential contamination (Figure 19). Once the hydrocarbons within a heating area have been produced and the subsurface area has been cleaned by repeated steam flushing, the freezeway is terminated allowing resumption of unimpeded groundwater flow.

The ICP requires no process water but would require water resources for post-production cleaning and site reclamation and restoration, as well as for product upgrading and site operations. Net water requirements are estimated to be less than 3 barrels per barrel of oil equivalent produced.

Field tests in Colorado on privately held lands expected to be expanded with several technology variations on three oil shale RD&D leases that were awarded to Shell by the U.S. Bureau of Land Management in 2006. Shell has also been awarded a concession from the Kingdom of Jordan to evaluate and apply the technology in deep oil shale deposits within the Kingdom.

IEP's Geothermic Fuel Cell

Another novel downhole heater approach is the application of geothermic fuel cells to produce heat and energy. Originated in Sweden during World War II, the use of geothermics has since expanded to applications to remove toxic wastes and to produce fuels from heavy oil, tar sands, and other resources.

Independent Energy Partners (IEP) has developed a heating technology applying a “geothermic fuel cell” to convert kerogen to shale oil, in-situ, while using minimal external energy sources (Figure 20). In the IEP concept, a high-temperature fuel cell stack is placed in the formation to heat the kerogen-bearing formation and release hydrocarbon liquids and gases into collection wells.

A portion of the gases are processed and returned to the fuel cell stack, with the rest available for sale. After an initial warm up period (during which the cells are fueled with externally sourced gas) the process becomes self-fueling from gases liberated by its own waste heat. The system, in steady-state operation, produces oil, electricity and natural gases. The GFC process developer estimates

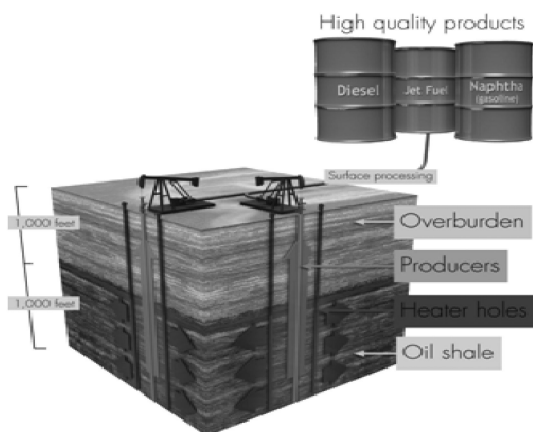


Figure 18. Shell's ICP Process (3)



Figure 19. Shell's Freezewall (3)

a potential net energy ratio of approximately 18 units of energy produced per unit used, when primary recovery is combined with residual char gasification and resulting syntheses gas.

According to IEP, Geothermic fuel cells heat formations by solid-to-solid conduction more efficiently than non-conductive applications. GFCs produce heat at a uniform rate along their length and therefore heat the formation uniformly

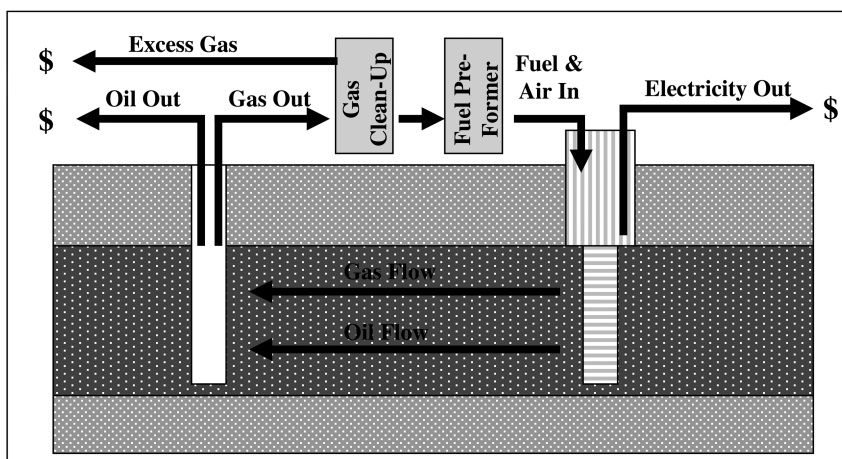


Figure 20. IEP's Geothermic Fuels Cells Process (3)

from top to bottom, leading to greater yields, improved recovery efficiency, and simplified production cycles.

Raising the formation temperature increases fluid pressure in the heated zone by 100 to 200 pounds per square inch (psi) over native pressure, which can be enough to fracture oil shale. Alternatively, the formation can be pre-fractured to enhance the hydrocarbon flow and communication between heating and producing wells.

Unlike other conductive approaches, geothermic fuel cells do not consume vast amounts of external energy — rather, they become self-fueling. IEP estimates the geothermic fuel cells would yield approximately 174 kilowatt hours (Kwh) of electric power per barrel recovered.

GFCs are also expected to produce only minimal air emissions. With no combustion involved – fuel cells produce electricity through an electrochemical reaction – there is negligible production of NO_x , SO_2 , particulate or toxic emissions.

GFCs are essentially self-sufficient in process water use. They produce steam as an exhaust which is re-circulated through fuel pre-reformers, thus obviating most if not all needs for outside process water.

GFCs produce minimal surface impact compared to mining and retorting operations that dispose of high quantities of waste “tailings” and dust. Since GFCs utilize a true “in-situ” approach, in which the ore body is left in place relatively undisturbed, waste disposal problems are eliminated.

IEP has entered into research and development relationships with the U.S. DOE Pacific Northwest National Lab and French oil company Total to advance the development of the GFC technology.

Radio-Frequency Heating

Working much like a microwave oven, radio frequency energy can also be used to generate heat for retorting. Extensive research has been conducted since the 1970s to design and test the application of radio frequency (RF) energy to improve oil shale retorting. There are several variations of RF energy applications for oil shale in development.

Schlumberger and Raytheon-CF Radio-Frequency with Critical Fluids

Raytheon and CF Technology have developed a patent-pending extraction methodology that uses radio frequencies to heat the shale to pyrolysis temperatures and supercritical carbon-dioxide to “sweep” the produced liquids and gases to production wells. With this technology, wells are drilled into the shale strata using standard oil industry equipment. Tuneable RF antennae, or transmitters, are lowered into the formation and then transmit RF energy to heat the buried shale.

Once heating and pyrolysis have occurred, super critical carbon dioxide is pumped into the shale formations to extract the produced oil from the rock and carry the oil to an extraction well. At the surface, the carbon dioxide fluid is separated and pumped back into injection wells, while the oil and gas are refined into fuels and other products.

This extraction technology can begin to produce oil and gas within only a few months, compared to years of heating required by other in-situ heating processes. The process is also “tunable” allowing heat to be directed consistently to the desired target and facilitating production of various products.

However, as with the Shell ICP, the RF/CF technology consumes significant electrical energy to generate the RF energy. According to Raytheon, for oil shale, this technology may recover four to five barrels of oil equivalent (BOE) for every barrel of energy consumed.

Ultimately, a self-sequestration approach, in which CO₂ is reinjected into the depleted kerogen-bearing formation, is expected to yield a neutral carbon foot print for process operations.

In 2007, Raytheon and CF Technologies sold the integrated technology to Schlumberger, one of the world’s largest oil field service companies, to commercialize the technology and facilitate its application in heavy oil and oil shale projects (3).

Another oil shale technology company, Phoenix-Wyoming, also seeks to apply borehole microwave heating technology. According to Phoenix-Wyoming, field tests have indicated that microwave technology can heat shale up to 50 times faster than in-situ heating using electric conduction methods. The effects of this faster heating approach on formation temperature, carbon profile, recovery efficiency, and product quality are not known.

Direct Current In-Situ Heating

Another novel approach to in-situ heating involves applying an electrical current through the oil shale formation to conduct heat to the shale.

ExxonMobil's Electrofrac™ Process for in-situ oil shale conversion is designed to heat oil shale in-situ by hydraulically fracturing the oil shale and filling the fractures with an electrically conductive material, thus forming a heating element (Figure 21). Electricity is conducted from one end of the fracture to the other, making the fracture a resistive heating element. Heat flows from the fracture into the oil shale formation, gradually converting the oil shale's solid organic matter into oil and gas. Using fractures created from horizontal wells is expected to allow Exxon to achieve a conductive zone that will heat the resources to pyrolysis temperature, forming liquids and gases that can be produced by conventional recovery technologies.

ExxonMobil screening of over thirty candidate technologies concluded that linear heat conduction from planar heat sources is likely to be the most effective method for "reaching into" organic-rich rock to convert it to oil and gas. According to ExxonMobil, planar heaters such as these should require fewer wells than wellbore heaters and offer a reduced surface footprint.

This process has the potential to provide cost-effective recovery in deep, thick formations with less surface disturbance than other proposed methods. Results from laboratory experiments and numerical modeling have been encouraging, and field tests have been initiated to test Electrofrac process elements on a larger scale. Many years of research and development may be required to demonstrate the technical, environmental, and economic feasibility of this breakthrough technology.

As with the Shell technology, the Exxon in-situ approach may also require strategies to prevent groundwater intrusion and protect groundwater from contamination by produced hydrocarbons and other compounds. Both the Shell ICP and Exxon Mobil Electrofrac™ technologies require the generation of significant quantities of electric power to provide process heat.

In-Situ Hot Gas Injection

Hot gas injection approaches, originally considered by Sinclair and others, have also attracted the attention of technology developers for potential application in oil shale development.

Chevron CRUSH

The Chevron CRUSH process builds on in-situ concepts developed by Sinclair, Equity, Geokinetics and others to use natural and induced fractures between wells to improve heat distribution and fluid-flow through oil shale formations and to circulate heated gases to convert embedded kerogen into hydrocarbon vapors and gases. Where early approaches used natural gas

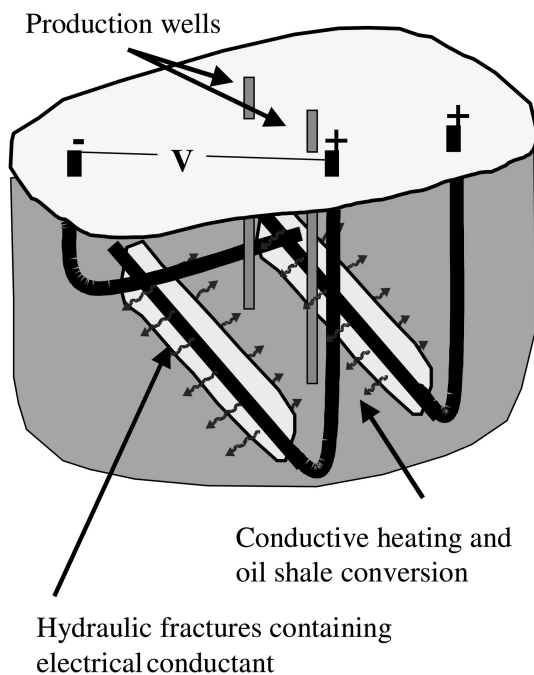


Figure 21. Electrofrac™ Process (3)

(methane), the Chevron process uses heated carbon dioxide as the gas heat carrier. The Chevron approach seeks to achieve uniform permeability through the targeted production zone by drilling wells and applying a series of complex fractures by injecting CO₂ to create a rubbleized production zone (Figure 22) (25).

The fracturing technology would allow large horizontal zones “approximately 1 to 5 acres wide and 50 feet high within the center of the 200 foot thick oil shale deposit.” to be rubbleized. Thus, a large vertical area of remaining shale, above and below the rubbleized “pocket” would remain as a natural, unfractured, and impermeable barrier protecting groundwater aquifers above and below the oil shale formation. This approach is intended to protect the heating zone from groundwater intrusion and protect groundwater from contamination by produce hydrocarbons and other heavy metals potentially released by in-situ heating.

The retorting process combines both in-situ heating and in-situ combustion. Initially, heated CO₂ is injected and cycled through the rubbleized zone to decompose the kerogen into producible hydrocarbons. The remaining organic matter in the previously heated and depleted zones would then be combusted to generate hot gases required to heat the circulated CO₂ for use in successive oil shale intervals or “pockets”, improving overall thermal efficiency of the process. The CO₂ will serve as a critical fluid to mobilize and sweep the produced hydrocarbon fluids to production wells.

Chevron Shale Oil Company, a part of Chevron U.S.A. Inc, has secured an RD&D lease tract in Rio Blanco County, Colorado where the company will

conduct oil shale research, development, and demonstration. Chevron plans to test the technology in several laboratory, bench, and small field tests. Chevron proposed a pilot test to BLM consisting of a minimum of 2-5 spot patterns (4 injectors and 1 producer per pattern) (25).

PetroProbe / Earth Search Sciences

Earth Search Sciences, Inc., has licensed a new processing system that it believes to have great potential for recovering oil from oil shale deposits. The in-situ process can gasify and recover products from oil shale deposits as deep as 3,000-plus feet.

In the PetroProbe process, air is superheated in a burner on the surface, its oxygen content carefully controlled. As superheated air travels down a borehole, it interacts with the oil shale and brings hydrocarbons to the surface in the form of hot gases. The gases are then condensed to yield light hydrocarbon liquids and gases (Figure 23). The process achieves a controlled and relatively quick production of product.

No mining is involved in the technology. The process begins by drilling into the body of oil shale and locating a processing inlet conduit within the hole. An effluent conduit is anchored around the opening of the hole at the ground surface. Pressurized air is introduced to an above-ground combustor, superheated and directed underground into the oil shale through the inlet conduit to heat the rock and convert the kerogen to a gaseous state.

Radiant heat in the inlet conduit produces a non-burning thermal energy front of predictable radius in the oil shale surrounding the hole. High temperatures and correct pressures cause the porous marlstone to gasify and allow its gaseous hydrocarbon products to be withdrawn as an effluent gas. Four products result: Hydrogen; 45°API gravity condensate; 1,000 btu methane gas, and water.

This is a self-sustaining system: effluent gas is transferred to a condenser where it is allowed to expand and cool; the gaseous fraction is separated from the liquid fraction and scrubbed to provide an upgraded synthesis gas; a portion of this gas is recycled and combined with other recycled feed stocks to create continuous fueling within the combustor – resulting in a significant product cost savings.

The process is environmentally sensitive. Produced CO₂ is compressed, and then pumped back into the oil shale body where it remains. Earth Search Sciences' patented remote sensing technology is used to establish a baseline before the project starts. Thereafter, continual monitoring during testing and production provides early-warning of problems, allowing them to be fixed quickly.

An important feature of the PetroProbe technology is its minimal surface footprint. Each complete plant will cover approximately one acre of land and produce for 10 to 20 years before depletion occurs. The surface plant's portable design allows it to be dismantled and moved to the next site. Subsurface, the formation retains 94 to 99% of its original structural integrity once the kerogen has been gasified.

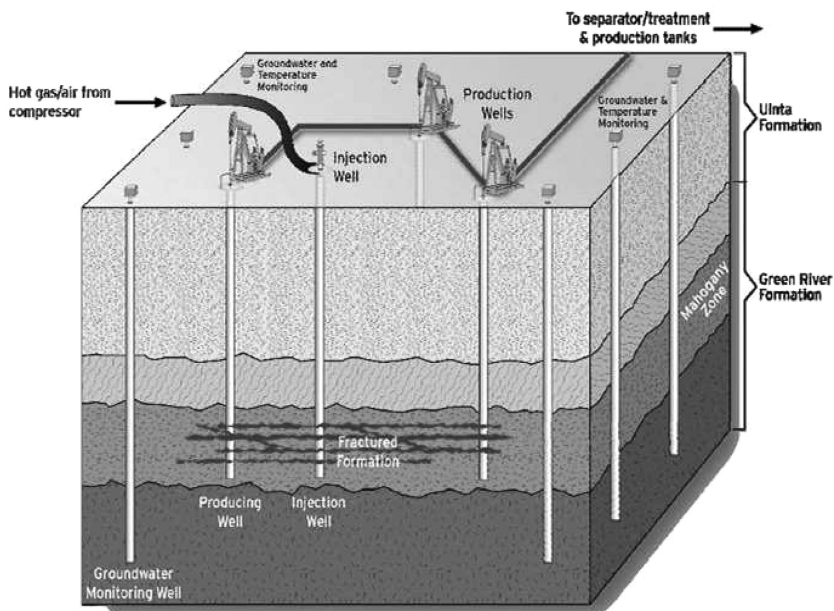


Figure 22. Chevron CRUSH (26)



Figure 23. PetroProbe Process (26)

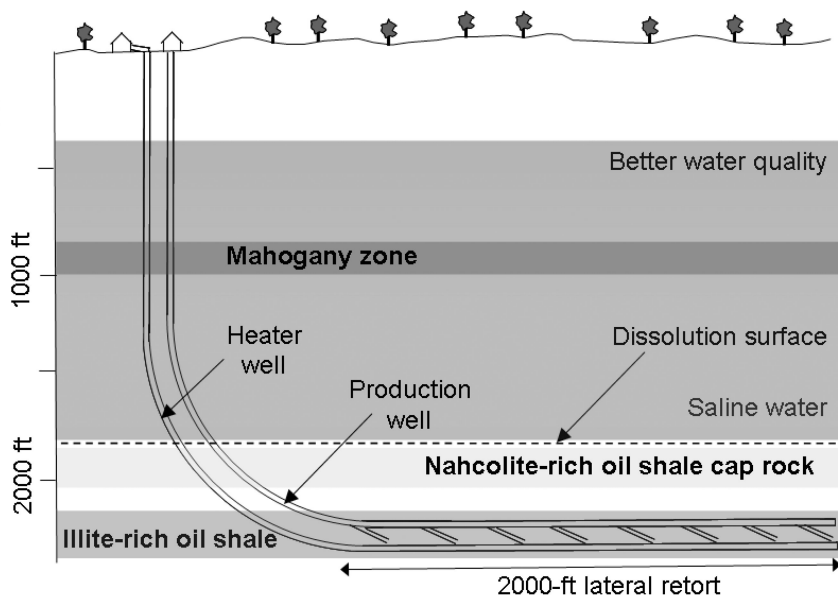


Figure 24. AMSO-EGL (26)

AMSO –EGL Technology

American Shale Oil, LLC (AMSO), formerly E.G.L. Oil Shale, LLC, is developing innovative, environmentally sustainable, in-situ shale oil extraction processes. AMSO is developing a new process for in-situ retorting of oil shale.

The AMSO-EGL Oil Shale process (patent pending) involves the use of proven oil field drilling and completion practices coupled with AMSO's unique in-situ retorting technology. The approach incorporates closed loop heating and lateral in-situ retorting to maximize energy efficiency while minimizing environmental impacts. Heat is introduced to the retort using a series of pipes placed near the base of the oil shale bed to be retorted (Figure 24). In many ways, this approach appears to emulate the successful Steam Assisted Gravity Draining (SAG-D) approach currently in use for heavy oil and oil sands development.

AMSO's proprietary process utilizes thermal spalling, convection and refluxing mechanisms to enhance heat distribution through the retort. The lateral retort approach efficiently distributes heat and minimizes surface disturbance by reducing the number of wells per area retorted.

After initial start-up, combustion of the gaseous hydrocarbons and hydrogen, co-produced with the shale oil, is expected to provide sufficient heat to liberate shale oil and gas from the deposit. In this way, shale oil is retorted without consumption of the produced shale oil or the use of external energy such as electricity and natural gas.

By targeting the illite-rich oil shale more than 2,000 feet below the surface, the technology and its application avoid the risk of contacting or degrading groundwater quality. This interval is hundreds of feet below the source of

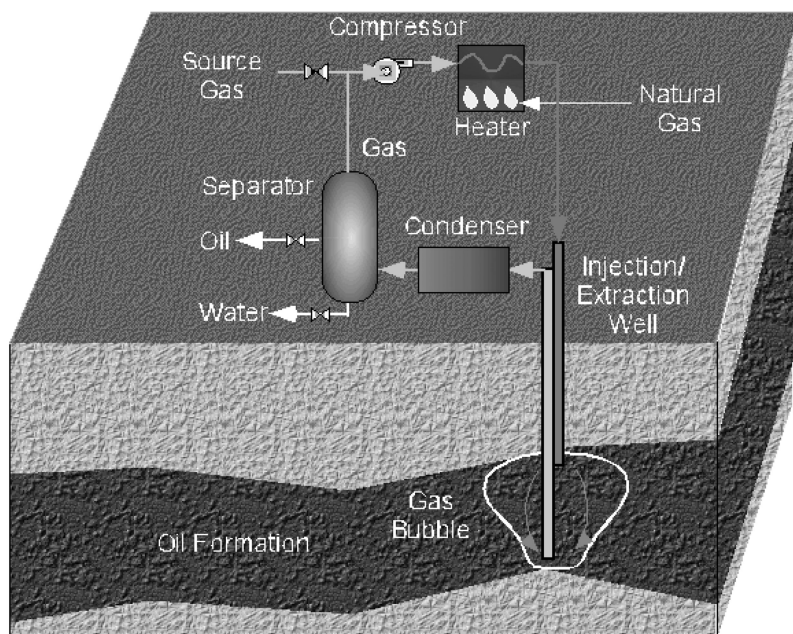


Figure 25. In-situ Vapor Extraction (IVE) Schematic (26)

useful ground water. Multiple geologic barriers, including 100 to 300 feet of nahcolite-rich oil shale, will protect usable ground water from retort impacts.

AMSO has just completed drilling operations and characterization of the site's geology and hydrology. A pilot retort experiment is scheduled to begin in 2010. The results of the pilot retort and additional field tests will demonstrate commercial viability.

In-Situ Vapor Extraction

Mountain West Energy (MWE) is developing in-situ vapor extraction (IVE) technology, a low-cost, scalable, fast, low-impact oil recovery process to produce oil from oil shale, oil sands, heavy oil reservoirs, and depleted conventional wells (Figure 25). In addition, IVE produces high-quality oil. MWE has demonstrated IVE in the laboratory, completed Phase 1 computer modeling, and started testing its technology in the field at the DOE's Rocky Mountain Oilfield Testing Center (RMOTC). MWE's technology is unique and innovative in that it vaporizes the oil and sweeps it to the surface as a gas, instead of a liquid.

MWE's IVE process uses a high temperature carrier gas injected into the target hydrocarbon formation to heat the oil by convection to the vaporization temperature. The carrier gas sweeps the oil vapors to the surface, where the oil is condensed and separated. The carrier gas is then re-circulated.

IVE recovers oil as a vapor, reducing the problems associated with flowing viscous, liquid oil through the formation. One implementation of IVE uses a

single, vertical or horizontal well, which reduces costs, improves profitability, and minimizes environmental impact.

IVE is capable of cost effectively recovering oil at any depth from 300 feet to 6,000 feet, which makes unconventional oil extraction technically and economically feasible for a large quantity of unconventional oil.

MWE's IVE technology has been successfully demonstrated on oil shale and conventional oil in a bench-scale system at the company's laboratory. IVE was able to recover 62% of the original-oil-in-place. Even higher recovery rates are expected by improving the sweep efficiency of the carrier gas with MWE's flow control technologies. In addition, MWE has completed Phase 1 computer modeling of IVE in conjunction with Dr. Milind Deo of the Petroleum Research Center at the University of Utah.

This technology has recently been selected by San Leon Energy for pilot testing and demonstration in Morocco's oil shale resources.

Conclusions

Oil shale technologies continue to improve and mature. Building on the lessons of past development efforts, oil shale technology developers are defining, testing, and demonstrating new approaches that overcome the technical issues of the past – such as energy use, thermal efficiency, oil yield, gas richness, water use, spent shale management, emissions controls, and ground water protection.

These new technologies are also responding to the new challenges presented by global climate change. More thermally efficient technologies require less energy inputs, produce higher yields, improve the quality of produced shale oil and gases, reduce and manage carbon emissions, and protect the environment. These and other innovations promise to improve operability and reliability, while maintaining capital and operating costs that will be competitive with conventional oil and gas.

Industry is making major investments in technology research development and demonstration to advance these technologies and innovations from bench and pilot scale to demonstration of economic and technical and economic feasibility at commercially representative scale

References

1. Johnson, H.; Crawford, P.; Bunger, J. *Strategic Significance of America's Oil Shale – Volume II: Oil Shale Resources, Technologies, and Economics*; U.S. Department of Energy, Office of Naval Petroleum and Oil Shale Reserves: Washington DC, 2003.
2. Biglarbigi, K. *Oil Shale Development Economics*; Presented at the EFI Heavy Resources Conference; Edmonton, Canada; May 16, 2007.

3. *Secure Fuels From Domestic Resources; The Continuing Evolution of America's Oil Shale and Tar Sands Industries*; U.S. Department of Energy, Office of Petroleum Reserves: Washington, DC, 2008.
4. *Proposed Oil Shale and Tar Sands Resource Management Plan Amendments to Address Land Use Allocations in Colorado, Utah, and Wyoming and Final Programmatic Environmental Impact Statement*; Department of the Interior, Bureau of Land Management: Washington, DC, 2008; p A-23; (Adapted from Nowacki, P.; 1981).
5. Crawford, P.; Biglarbigi, K.; Dammer, A.; Killen, J.; Knaus, E. *Advances in World Oil Shale Production Technologies*; Presented to Society of Petroleum Engineers, Annual Technical Conference and Exhibition; Denver, Colorado, 2008.
6. *Oil Shale Development in the United States: Prospects and Policy Issues*; The RAND Corporation: Santa Monica, CA2007; p 12.
7. *Proposed Oil Shale and Tar Sands Resource Management Plan Amendments to Address Land Use Allocations in Colorado, Utah, and Wyoming and Final Programmatic Environmental Impact Statement*; Department of the Interior, Bureau of Land Management: Washington, DC, 2008; p A-24; (Adapted from DOE; 1982).
8. *Oil Shale Development in the United States: Prospects and Policy Issues*; The RAND Corporation: Santa Monica, CA, 2007; p 12.
9. *Proposed Oil Shale and Tar Sands Resource Management Plan Amendments to Address Land Use Allocations in Colorado, Utah, and Wyoming and Final Programmatic Environmental Impact Statement*; Department of the Interior, Bureau of Land Management: Washington, DC , 2008.
10. *Secure Fuels From Domestic Resources; The Continuing Evolution of America's Oil Shale and Tar Sands Industries*; U.S. Department of Energy, Office of Petroleum Reserves: Washington, DC , 2008; pp 28-29.
11. *Proposed Oil Shale and Tar Sands Resource Management Plan Amendments to Address Land Use Allocations in Colorado, Utah, and Wyoming and Final Programmatic Environmental Impact Statement*; Department of the Interior, Bureau of Land Management: Washington, DC , 2008; p A-34.
12. *2007 Survey of Energy Resources*; World Energy Council; p 105.
13. *Proposed Oil Shale and Tar Sands Resource Management Plan Amendments to Address Land Use Allocations in Colorado, Utah, and Wyoming and Final Programmatic Environmental Impact Statement*; Department of the Interior, Bureau of Land Management: Washington, DC, 2008; p A-33.
14. Qian, J.; Wang, J. *World Oil Shale Retorting Technologies*; International Conference on Oil Shale: "Recent Trends In Oil Shale," Amman, Jordan, 2006.
15. Qian, J.; Wang, J. *World Oil Shale Retorting Technologies*; International Conference on Oil Shale: "Recent Trends In Oil Shale," Amman, Jordan, 2006; Adapted from Hou X. L *Shale Oil Industry in China*; The Hydrocarbon Processing Press: Beijing, 1986.
16. Qian, J.; Wang, J. *World Oil Shale Retorting Technologies*; International Conference on Oil Shale: "Recent Trends In Oil Shale," Amman, Jordan, 2006; Adapted from Sonne J.; Doilov, S. Sustainable Utilization of Oil Shale

Resources and Comparison of Contemporary Technologies used for Oil Shale Processing; *Oil Shale* **2003**, 20, (3S), 311–323.

17. *Secure Fuels From Domestic Resources; The Continuing Evolution of America's Oil Shale and Tar Sands Industries*; U.S. Department of Energy, Office of Petroleum Reserves: Washington, DC : 2008; pp 20–21.
18. *Secure Fuels From Domestic Resources; The Continuing Evolution of America's Oil Shale and Tar Sands Industries*; U.S. Department of Energy, Office of Petroleum Reserves: Washington, DC : 2008; pp 32–33, 70.
19. *Technical Review of the Rendall Process (A Proprietary Oil Shale Technology)*; RobSearch Australia Pty Limited: Abridged and Revised for Blue Ensign Technologies, Limited; 2005; pp 5–8.
20. *Proposed Oil Shale and Tar Sands Resource Management Plan Amendments to Address Land Use Allocations in Colorado, Utah, and Wyoming and Final Programmatic Environmental Impact Statement*; Department of the Interior, Bureau of Land Management: Washington, DC: 2008; p A-35.
21. Qian, J.; Wang, J. *World Oil Shale Retorting Technologies*; International Conference on Oil Shale, “Recent Trends In Oil Shale,” Amman, Jordan, 2006; (Adapted from Golubev N. Solid Heat Carrier Technology for Oil Shale Retorting, *Oil Shale* **2003**, 20, (3S), 324–332).
22. Crawford, P.; Biglarbigi, K.; Dammer, A.; Killen, J.; Knaus, E. *Advances in World Oil Shale Production Technologies*; Presented to Society of Petroleum Engineers, Annual Technical Conference and Exhibition, Denver, Colorado, 2008.
23. *Proposed Oil Shale and Tar Sands Resource Management Plan Amendments to Address Land Use Allocations in Colorado, Utah, and Wyoming and Final Programmatic Environmental Impact Statement*; Department of the Interior, Bureau of Land Management: Washington, DC, 2008; p A-42; Adapted from Lee, S.; 1991.
24. *Proposed Oil Shale and Tar Sands Resource Management Plan Amendments to Address Land Use Allocations in Colorado, Utah, and Wyoming and Final Programmatic Environmental Impact Statement*; Department of the Interior, Bureau of Land Management: Washington, DC, 2008; p A-43; Adapted from Lee, S.; 1991.
25. *Oil Shale Research, Development & Demonstration Project. Plan of Operation*; Chevron USA ,Inc.: 2006, (http://www.blm.gov/pgdata/etc/medialib/blm/co/field_offices/white_river_field/oil_shale.Par.37256.File.dat/OILSHALEPLANOFOPERATIONS.pdf)
26. *Secure Fuels From Domestic Resources; The Continuing Evolution of America's Oil Shale and Tar Sands Industries*; U.S. Department of Energy, Office of Petroleum Reserves: Washington, DC , 2008; p 22–23.

Chapter 3

Lake Level Controlled Sedimentological Heterogeneity of Oil Shale, Upper Green River Formation, Eastern Uinta Basin, Utah

William Gallin,¹ M. Royhan Gani,^{2,*} Milind Deo,³ Nahid DS Gani,² and Michael D. Vanden Berg⁴

¹Energy and Geoscience Institute, University of Utah, Salt Lake City, UT 84108

²Department of Earth and Environmental Sciences, University of New Orleans, 2000 Lakeshore Drive, New Orleans, LA 70148

³Department of Chemical Engineering, University of Utah, Salt Lake City, UT 84108

⁴Utah Geological Survey, Salt Lake City, UT 84114

*corresponding author email: mgani@uno.edu

The Green River Formation comprises the world's largest deposit of oil-shale and has enormous potential to meet global energy requirements, yet a detailed sedimentological characterization of these lacustrine oil-shale deposits in the subsurface is lacking. This study analyzed ~300 m of cores correlated to gamma and density logs in well P4 in the lower to middle Eocene (49.5–48.0 Ma), upper Green River Formation of the eastern Uinta Basin, Uintah County, Utah. In well P4, three distinct facies associations are identified that represent three phases of deposition linked to hydrologic evolution of the Lake Uinta.

The three phases of depositions are 1) an overfilled, periodically holomictic lake system, with deposition of primarily clastic mudstones, followed by 2) a balanced-filled, uniformly meromictic lake system, with deposition of primarily calcareous and dolomitic mudstones, followed by 3) an underfilled, evaporative lake system with nahcolite precipitation. The richest oil-shale zones were deposited during the second depositional phase. Although the studied interval is

popularly known as oil "shale", our bed-by-bed investigation shows that the interval is lithologically, thus chemically, quite heterogenous. This complexity has significant impact on modeling strategy for oil-shale exploitation.

Introduction

The Green River Formation, located in northeastern Utah, northwestern Colorado, and southwestern Wyoming (Figure 1) contains the world's largest deposit of oil-shale. Estimates of recoverable resources in Utah alone are often quoted in the hundreds of billions of barrels, ranging as high as 321 billion barrels (1). A recent meticulous report uses five key constraints to estimate Utah's potential recoverable oil-shale resource at 77 billion barrels (2).

As global fossil energy reserves are increasingly strained, the unconventional asset represented by the Green River Formation is obvious. Yet, sedimentology of the oil-shale bearing units of the Green River Formation is insufficiently documented, particularly in the subsurface. In outcrop, detailed investigation of oil-shale lithology is hindered due to weathering. Specifically, fine-grained mudstone laminations are much more clearly visible in slabbed core than in outcrop.

Previous work in the Green River Formation in the eastern Uinta Basin describes basin-margin depositional environments from outcrops, particularly for the lower and middle part of the formation (3–5). These studies are significant but lack information regarding subsurface lithological variation. Previous work interpreting well log data without core data (6) describes the strata in this region in a scope that is temporally too broad for the objectives of this study.

This study, focused on the upper Green River Formation farther towards the basin center than previous work, provides the first detailed account of subsurface sedimentology of the upper part of the Green River Formation in the eastern Uinta Basin of Utah. The study uses a ~300 m thick core correlated to gamma-ray and neutron density logs to meet the following two objectives: 1) detailed, bed-by-bed investigation of lithological variations of oil-shale, including distinguishing rich vs. lean zones of oil-shale, and 2) understanding the controls and environmental conditions that led to the deposition of oil-shale rich zones.

Regional Geology

As the Late Cretaceous Sevier fold-and-thrust orogeny waned during the late Campanian to early Maastrichtian, the onset of Laramide orogeny broke the broad foreland basin of the Western Interior Seaway into a series of perimeter basins, axial basins, and ponded basins (7, 8). The Uinta Basin formed as a ponded basin bounded to the west by the Sevier orogenic belt; to the south by the San Rafael, Uncompaghre, and Monument uplifts; to the east by the Douglas Creek arch; and to the north by Uinta uplift (Figure 1). The north-south trending Douglas Creek

arch separates the Uinta Basin from its time-equivalent neighbor, the Piceance Creek Basin in northwestern Colorado. The Douglas Creek arch acted episodically as a hydrological barrier and as a subsumed structural saddle between the Uinta Basin and the Piceance Creek Basin through the duration of deposition in these basins. The Piceance Creek Basin was, in turn, subject to inundation from the overfilled Greater Green River Basin in southwestern Wyoming (Figure 1).

The Green River Formation was deposited in the Uinta, Piceance Creek, and Greater Green River Basins in the early to middle Eocene, approximately 55 Ma to 44 Ma (9). Ash beds from volcanism in the Absaroka Mountains episodically blanketed the region, providing datable isochrons (9). As typical of ponded basins, the Uinta, Piceance Creek, and Greater Green River Basins were at times internally drained, depositing several thousand meters of profundal-lacustrine and evaporative strata in addition to fluvial-lacustrine, paludal, and alluvial strata (7).

Study Area and Local Geology

This study focuses on the oil-shale bearing profundal-lacustrine and evaporative strata of the Green River Formation in the eastern Uinta Basin of Uintah County, northeastern Utah (Figure 2). In study area and to the best of our knowledge, the highest quality core with available correlating well logs are from well P4 (also known as U059) which is housed at Utah Geological Survey (UGS) Core Research Center in Salt Lake City, Utah. Core P4, located in T10S-R25E, Uintah County, was recovered from 65 m (211 feet) to 357 m (1170 feet) depth zone, covering 292 m (959 feet) thick.

The present study follows marker-bed nomenclature of Remy (5) due to the prominence of those marker beds in core P4 and the precedent they set for subsequent literature (9). This nomenclature was defined in outcrops of fluvial-lacustrine and marginal lacustrine strata of Nine Mile Canyon in south-central Uinta Basin (Figure 2). Variations on Green River Formation nomenclature in literature and the stratigraphic position of core P4 in that system is summarized in Figure 3.

The present study also follows oil-shale nomenclature of Vanden Berg (2). This system consists of rich (R) and lean (L) oil-shale zones derived from well log data from the Uinta Basin. The Mahogany Zone is used for rich oil-shale zone 7 (R7); it is the richest kerogen zone (2). A-Groove and B-Groove are the names for L7 and L6 respectively that are from kerogen lean zones (Figure 3). These zones are identified in density logs with the Fischer Assay which correlates the presence of kerogen in the deposits with decreased bulk density (10). Richness of oil-shale zones varies, but estimated yield from rich zones is between 15 and 50 gallons per ton (2).

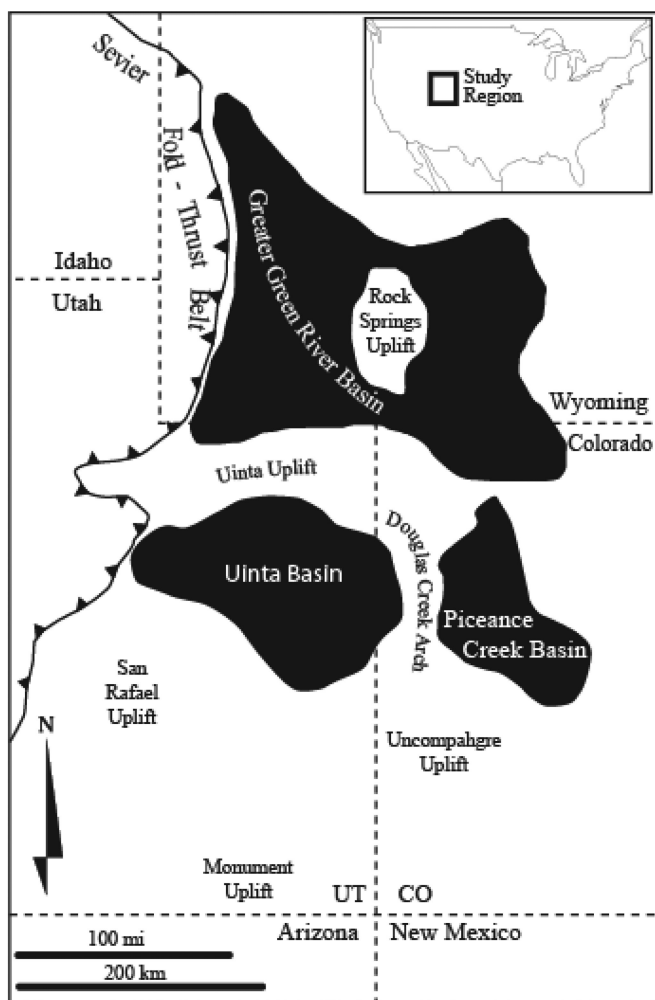


Figure 1. Location map of the study region in the western United States, showing the configuration of the Laramide lacustrine basins in which the Green River Formation was deposited in early to middle Eocene (49.5–48.0 Ma).

Methods

Lithology, sedimentary structures, and trace fossils (burrows) of core P4 were logged through visual investigation, using HCl and a light microscope when necessary. Using the methodology of Gani et al. (11), bioturbation intensity in the cores were quantified using a six-grade scale (6 being the highest) to generate a bioturbation index (BI) log. Photographs of key features were taken at various depths in the cores.

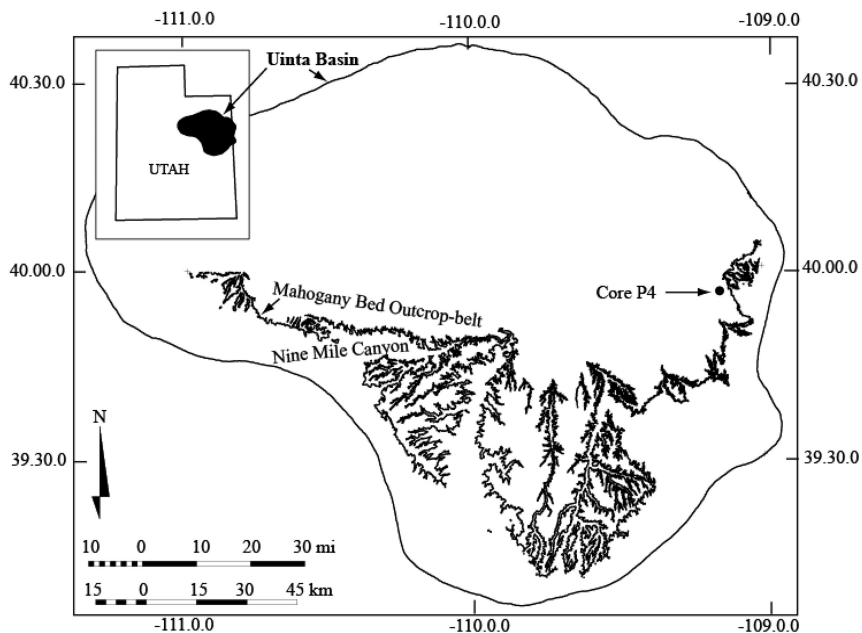


Figure 2. Location of well P4 (also known as well U059) in the eastern Uinta Basin of Uintah County, northeastern Utah. Note the location of Nine Mile Canyon, which is the site of many previous outcrop-based works on the Green River Formation.

Scanned images of Gamma and density well logs of P4 were acquired from UGS, and later digitized using NeuraLog software. These digital logs were uploaded in Landmark's Geographix software to pick stratigraphic surfaces correlated to core P4. These surfaces are defined as gamma kicks where gradual fluctuations in gamma values lead to, or are followed by, sudden changes in gamma values.

Results

Core Sedimentology

Figure 4 shows the graphic lithological log of core P4. Six lithofacies were identified that can be grouped into three broad intervals. The interval lying below the base of the Mahogany Zone (>235 m depth), is characterized by the preponderance of clastic mudstone facies. The middle portion of the core (125-235 m depth) is dominated by calcareous mudstone facies. The upper portion of the core (< 125 m depth) is characterized by evaporites. Oil-shale, not categorized here as facies, is unevenly distributed among the three intervals.

Sandstones are also unevenly distributed throughout the core as thin beds. However, two groups of thicker sandstones are found; one unnamed group lies near

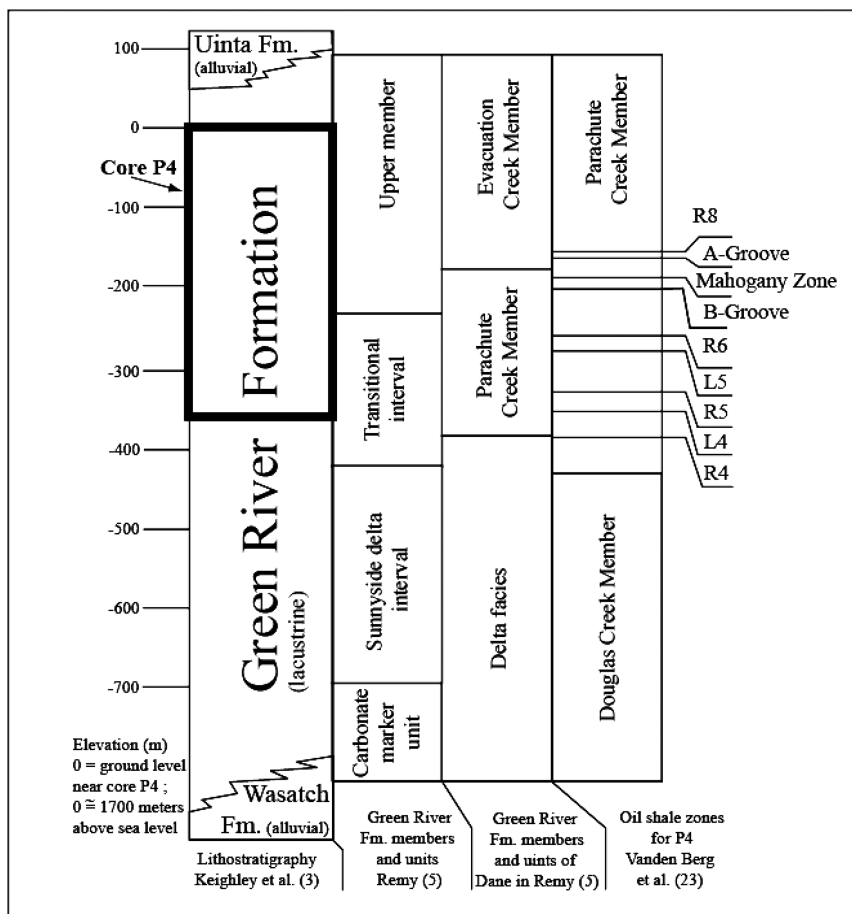


Figure 3. Stratigraphic nomenclature of Green River Formation in and around the study area. Core P4 belongs to the upper Green River Formation.

the base of the core, and another group, identified as the Horse Bench sandstone (5), lies near the top of the core (Figure 4).

Two main groups of tuffs are identified. The lower tuff, at the base of the Mahogany Zone is the Curly Tuff. The upper tuff, approximately 18 m above the top of the Mahogany Zone is the Wavy Tuff (5, 9).

Evaporites, identified only in the form of nahcolite, are found only above the Mahogany Zone. With the exception of current- and wave-ripples in the Horse Bench sandstone, nearly all sedimentary structures indicating agitation of the lake bottom appear below the Mahogany Zone.

Sedimentological description and interpretation of oil-shale and six lithofacies are as follows:

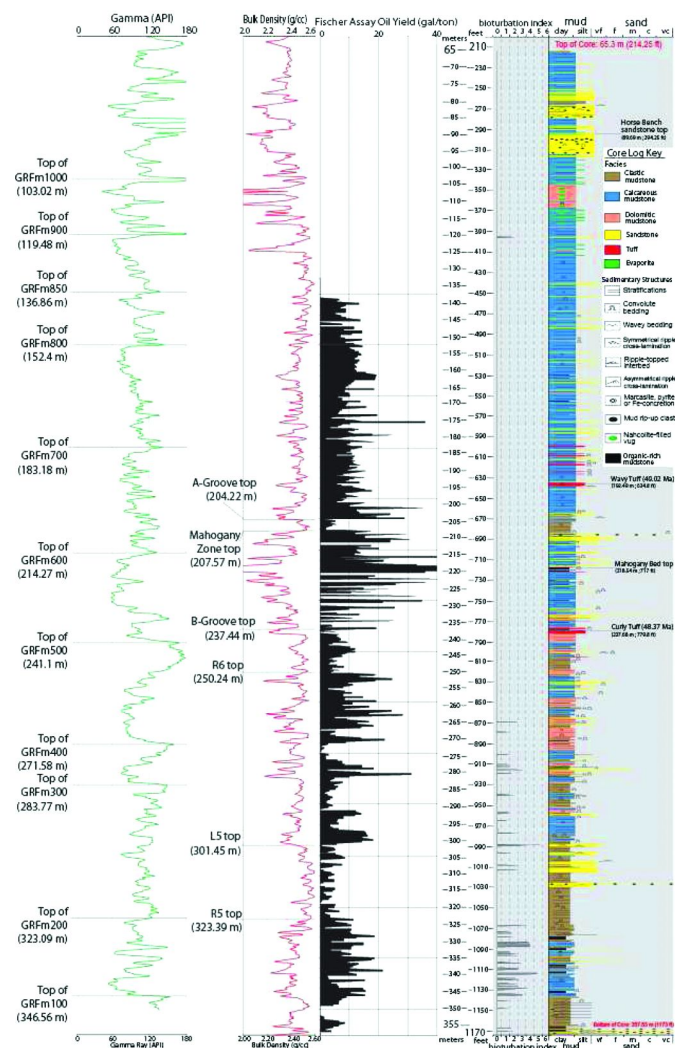


Figure 4. Geophysical, chemical, ichnological, and lithological logs for well P-4 (see Figure 2 for location). Prominent marker beds, rich (R) and lean (L) oil-shale zones, and genetic stratigraphic horizons (GRFm#) are labeled.

Oil-Shale

Description: The term oil-shale is lithologically ambiguous and perhaps scientifically misleading. Hence, oil-shale is not identified as a facies in this study. Lithologically, oil-shale in core P4 consists of kerogen-rich intervals of calcareous and dolomitic mudstones. The amount of kerogen-richness required for a mudstone to be considered as oil-shale is an economic question, not a sedimentological one.

The richness of oil-shale is represented in the Fischer Assay log of Figure 4 in terms of oil yield in gallons per ton (GPT). The Fischer Assay log shows the distribution of average rich versus lean oil-shale zones throughout core P4. The Mahogany Zone is the richest oil-shale zone. The Mahogany Bed of the Mahogany Zone is capable of yielding up to 75 GPT in the vicinity of core P4.

Kerogen-rich oil-shale does not react as strongly with HCl as the kerogen-poor calcareous and dolomitic mudstones due to the higher kerogen to carbonate ratio of oil-shale. Oil-shale appears distinctively dark brown to black and is finely laminated (<1 mm thick) in core P4 (Figures 5a, 5b, and 5c). Rich oil-shale beds of >20 GPT are rarely thicker than 30 cm. Oil-shale is often friable, and core samples tend to crack along oil-shale lamination planes.

Interpretation: Interpretation of oil-shale is discussed in the interpretation section of calcareous mudstones (Facies 2).

Facies 1: Clastic Mudstones

Description: The clastic mudstone facies consists of clay-rich to sometimes silty, grayish-beige to dark brown, finely-laminated (<1 mm thick) mudstones (Figure 6a). Light brown, beige, and gray laminations can be similar in color to calcareous mudstones or dolomitic mudstones facies (Facies 2 and 3, respectively), but the clastic mudstone facies never fizzes under HCl. The clastic mudstone facies is often interrupted by ripple-topped interbeds of siltstone or sandstone lenses (<2 cm thick). The facies shows varying degrees of soft-sediment deformation (Figure 6b); deformation due to post-depositional mineral and nodular growth of pyrite, siderite, and possibly marcasite; deformation due to overburden strata; and deformation due to bioturbation (Figure 6c). Despite local deformations and interruption by sand lenses, the clastic mudstone facies is most commonly horizontally laminated.

Interpretation: The predominantly horizontally laminated, non-calcareous, non-dolomitic, and very fine-grained nature of the clastic mudstone facies strongly suggests the deposition of siliciclastics in the deeper part of the lake basin, likely below storm wave base. Ripple-topped interbeds of coarser materials, especially those with scoured-bases and basal rip-up clasts, indicate event depositions when turbidity currents reached this distal depositional site.

Facies 2: Calcareous Mudstones

Description: The calcareous mudstone facies consists of microcrystalline, calcium carbonate-rich, yellow-beige to dark brown, finely laminated mudstones (<1 mm to 1 mm thick laminae). This facies reacts strongly to HCl. The richest oil-shale zones are dominated by calcareous mudstone facies (Figures 7a and 7b).

The calcareous mudstone facies shows signs of local soft-sediment deformation but rarely shows evidence of ripple cross-lamination or ripple-topped interbeds as does the clastic mudstone facies. When finely interlaminated with darker mudstones, calcareous mudstone facies is difficult to distinguish from the

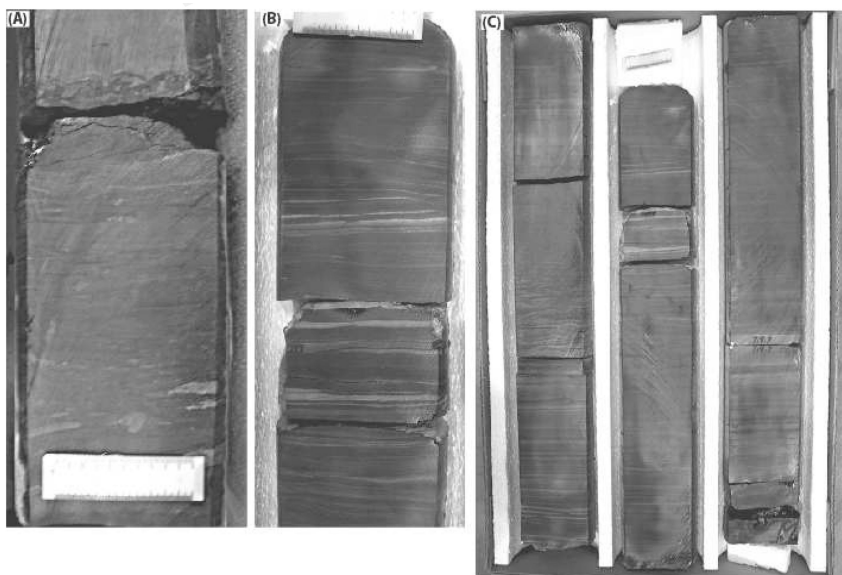


Figure 5. A) Black, organic-rich, and friable oil-shale (328.88 m depth in litholog of Figure 4). B) The Mahogany Bed, the richest oil-shale bed in the Mahogany Zone, which is the richest oil-shale zone in Green River Formation (219.46 m depth in Figure 4). Core base is bottom-right and top is upper-left. C) Details of the Mahogany Bed. Lighter interlaminae are kerogen-poor calcareous and dolomitic mudstones (218.54 m depth in Figure 4). Note that scale is 5 cm long in all photos.

clastic mudstone facies. However, as mentioned before, the calcareous mudstone facies will always react with HCl while the clastic mudstone facies will not. Evidence of bioturbation is more commonly found in the calcareous mudstone facies than in any other facies, although bioturbation is absent in the calcareous mudstone facies above the Mahogany Zone (Figure 7c).

Interpretation: Since there is no evidence of the production of calcareous shells, organic encrustations, or skeletal elements, and evidence for clastic allochthonous calcium input or post-depositional precipitation is lacking, the remaining possible source for calcium in the calcareous mudstone facies is from direct precipitation from the water column (12). The association of carbonate minerals with oil-shales is well documented (13), and, is often characteristic of deep lacustrine basins (14).

The conditions for the deposition of the calcareous mudstone facies in association with the oil-shale can be a meromictic, stratified lake with a slightly alkaline, nutrient-rich upper-layer and a high-pH, anoxic lower-layer. During seasonal algal blooms, dissolved CO₂ removal from the water column through photosynthesis raises upper-layer pH and allows for concentration of calcium and magnesium in algal sheaths. As algal blooms die, organic material deposits in the lake bottom where decomposition is inhibited by anoxic conditions. In this way, carbonate deposits in association with the organic constituents of oil-shale (15).

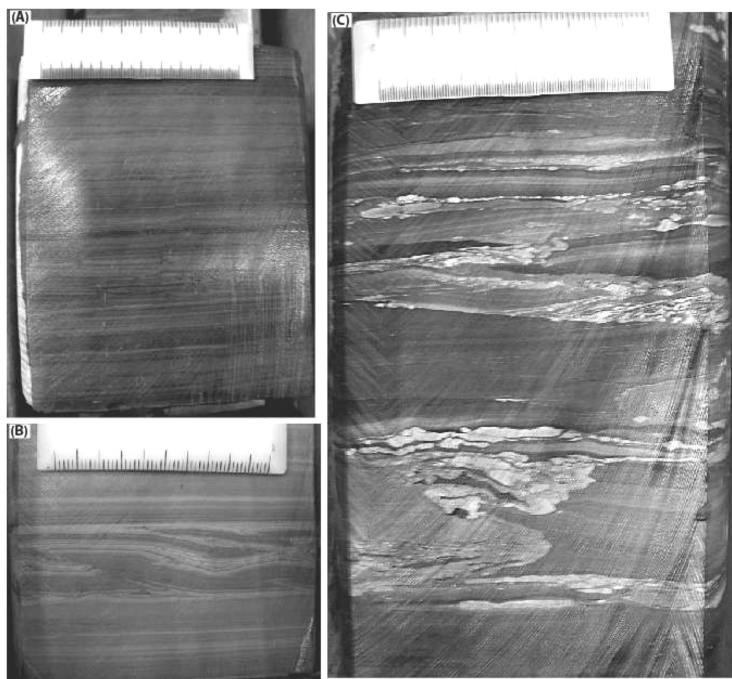


Figure 6. Clastic mudstone facies showing A) fine laminations (349.97 m depth in figure 4), B) soft sediment deformation (316.93 m depth in figure 4), and C) deformation due to bioturbation, where burrows are filled with dolomitic mudstones (327.05 m depth in figure 4). Note that scale is 5 cm long in all photos.

In order for the conditions to be met in which the calcareous mudstone facies are deposited rather than clastic mudstone facies, there must be meromictic lake conditions, and distance from overwhelming input of clastic mudstone. Both of these conditions are met in deep water lake basins. The fact that calcareous mudstone facies is usually finely laminated and undisturbed by wave or current-generated sedimentary structures further supports the interpretation of deposition of calcareous mudstone facies in deep water.

Facies 3: Dolomitic Mudstones

Description: The dolomitic mudstone facies consists of microcrystalline, light beige to light gray dolomite ($\text{CaMg}(\text{CO}_3)_2$) mudstone that reacts weakly with HCl. This facies is sometimes finely laminated (<1 mm to 1 mm thick laminae; Figure 8a) but is often deformed and often bears nodular growths of pyrite, siderite, and possible marcasite. The lower portion of the core exhibits a more even distribution of laminated dolomitic mudstone facies in association with oil-shale rich zones, calcareous mudstone facies, and clastic mudstone facies; whereas, near the top of the core, the dolomitic mudstone facies is closely associated with the evaporite facies (Facies 5). Dolomitic mudstone near the top of the core is massive rather

than laminated, deformed, and pocked by nahcolite dissolution vugs (Figure 8b). Although the dolomitic mudstone facies is generally lighter in color, it can often resemble calcareous mudstone facies or the clastic mudstone facies. However, the dolomitic mudstone facies will always react weakly with HCl while the clastic mudstone facies will not react with HCl, and the calcareous mudstone facies will react strongly with HCl.

Interpretation: Dolomitic mudstone facies are interpreted differently for the lower and upper portion of cores. In addition to Ca carbonate, Mg-Ca carbonate is also found in association with oil-shale (15). Certain algal blooms selectively remove Mg from the water column for concentration in algal sheaths. The laminated dolomitic mudstone in the lower portion of the core (>235 m depth) is interpreted to have formed under meromictic lake conditions similar to those that formed the calcareous mudstone facies. Slight variations in ecological conditions may have regulated the deposition of calcareous versus dolomitic mudstones.

Primary inorganic dolomite precipitate, as opposed to diagenetic dolomite, is often deposited in shallow, saline lakes (16). The association of massive dolomitic mudstone facies with evaporites in the upper portion of the core (<125 m depth) is interpreted to indicate shallow, saline conditions. The perceived problematic transition from deep water carbonates to shallow water evaporites without intervening basin-margin clastics is explained in the Discussion section.

Facies 4: Sandstones

Description: The sandstone facies consists mostly of yellow-beige to gray, very fine sandstones. Rarely, this facies contains coarser-grained sandstones, which can only be found in thin (1-3 cm) intervals. Most sandstone lenses are too thin to discern visible grading patterns. However, some thicker (>30 cm) sandstone beds show normal grading with erosive basal-contacts and rip-up mudstone clasts (Figure 9a). Asymmetrical and symmetrical ripple cross-laminations appear locally (Figure 9b). A prominent medium-grained, well-rounded tan sandstone layer lies at 279 m depth. Most individual sandstone beds are thin (1-3 cm) and show no ripples or graded relationship to overlying or underlying mudstones (Figure 9c). Thicker sandstone beds below the Mahogany Zone bear limited bioturbation (Figure 9d).

In core P4, sandstones are found mainly at two stratigraphic intervals (Figure 4). The lower sandstone interval lies between ~300-315 m. The upper sandstone interval, between ~80-95 m, is identified as the Horse Bench sandstone (5).

Interpretation: The deposition of sand facies in core P4 is interpreted to represent either 1) episodes of lower lake-level that brought the basin margin closer to the position of core P4, or 2) the periodic deposition of large turbidity flows capable of reaching the distal basin position of core P4. The sedimentary characteristics of most sandstone intervals indicate that most of these beds were not deposited from turbidity currents. The near absence of normal grading and the presence of oscillatory wave ripples suggest that these sandstone beds are related to periods of decreased distance between core P4 and the basin margin (i.e. decreased lake-level). In the upper portion of the core, the deposition of the Horse

Bench sandstone immediately following the deposition of bedded evaporites and shallow, saline-water dolomitic mudstones, suggests the onset of wetter climate and fresher water lake conditions following a period of aridity and salinity.

Facies 5: Evaporite (Nahcolite, NaHCO_3)

Description: The evaporite facies consists of brown to gray, bedded precipitation of nahcolite (Figures 10a and 10b) as well as vugs filled with nahcolite (Figure 10c). No halite was observed. The evaporite facies is only found above the Mahogany Zone. Nahcolite beds are generally < 3 cm thick and are mostly found interbedded with calcareous mudstone facies. Beds containing nahcolite vugs can be >5 cm thick and are found mostly in massive, deformed dolomitic mudstones.

Interpretation: The deposition of evaporites indicates conditions of shallow, saline water. Nahcolite can precipitate through shallow lake-bottom nucleation or as displacive intrasediment nodules (17). Bedded nahcolite in core P4 may represent bottom nucleates, and vug-filling nahcolite may represent original displacive nodules.

Nahcolite deposits in the Green River Formation constitute significant economic resources. While nahcolite deposits can serve to increase the value of otherwise costly surface or subsurface oil-shale mining operations (18), their potential assistance or detriment to in-situ electrical, air, or steam heating production of oil from oil-shale is yet to be modeled.

Whereas nahcolite-bearing strata in core P4 of the eastern Uinta Basin are found above the Mahogany Zone, the strata of the Piceance Creek Basin show a higher prevalence of saline water facies, including extensive nahcolite deposits, below the Mahogany Zone (9). This is interpreted to represent different hydrologic gradients at different times among the Eocene lake basins in which the Green River Formation was deposited. These hydrologic gradients are further explained in the Discussion section.

Facies 6: Tuff (Zeolite Sands)

Description: The tuff facies consist of biotite ash and zeolite (hydrous aluminosilicate) sands, possibly including analcime (hydrated sodium aluminosilicate) in a matrix of unidentified fused volcanoclastic mineral hash. Two large (~75 cm thick) ash beds (Figure 4) are identified as the Curly Tuff (Figure 11a) and Wavy Tuff (Figure 11b). At least 17 other distinct unnamed tuff beds are found in the core, ranging in thickness from 3–12 cm (Figure 11c). The tuff beds, together with underlying and overlying adjacent beds, are characteristically highly deformed.

Interpretation: Smith et al. (9) reported a $^{40}\text{Ar}/^{39}\text{Ar}$ laser-fusion date of biotite at 49.02 ± 0.30 Ma for the Curly Tuff and 48.37 ± 0.23 Ma for the Wavy Tuff (ages are weighted means with errors of 2σ). The Absoraka volcanic province in northwest Wyoming and southwest Montana and the Challis volcanic field in Idaho

were active at these ages and may be the source of the Curly and Wavy Tuffs (9). Zeolites represent volcanic glass altered after deposition in highly saline or alkaline waters (19). This supports the interpretation of high alkaline lake conditions during the deposition of calcareous and dolomitic mudstones.

Bioturbation

Bioturbation occurs almost entirely in the lower portion of the core, particularly at intervals where beds of calcareous mudstone facies alternate with beds of clastic mudstone facies (Figure 4). It is likely that the trace-making organisms periodically colonized the lake bottom during aerobic lake bottom-water conditions. Trace makers active during aerobic bottom-water, holomictic conditions were able to mine lower tiers of sediments that were deposited during anaerobic bottom-water, meromictic conditions. When stratification in water-column resumed, anaerobic bottom-water conditions precluded bioturbation. In the BI log of core P4 (Figure 4), such tiering of bioturbation is observed near the base of the core (325-350 m depth). Examples of this type of tiered bioturbation controlled by bottom-water oxygen-level is well documented in the literature of marine ichnology (20).

Meromictic conditions become more prevalent farther up the core (>235 m depth) as evidenced by the onset and eventual dominance of thick intervals of calcareous mudstones. Upward-decreasing trend of clastic mudstones suggests greater distance of well P4 from the shoreline, thus, possibly greater water depth and better conditions for lake stratification. The halt of bioturbation along with the increasing prevalence of calcareous mudstones above 235 m depth in core P4 further supports the interpretation of deep, anoxic bottom-water conditions in the middle portion of core P4 (125-235 m depth).

Gamma Log

Eleven picks of potential genetic-stratigraphic (i.e. isochronous) surfaces, were made in the upper Green River Formation from the gamma log of well P4. These eleven picks mark the top of stratigraphic units with names abbreviated as GRFm followed by a three to four digit numeral. The stratigraphic order of GRFm picks as well as rich/lean oil-shale zone picks in core P4 is shown in Figure 4. These eleven picks, along with six picks of rich and lean zones (2), are useful for ongoing subsurface stratigraphic correlation in the upper Green River Formation in the Uinta Basin.

The gamma log appears chaotic in the lower portion of the core, with at least two intervals of increasing-upward gamma values culminating at GRFm400 and GRFm500 immediately below the Mahogany Zone. The upper portion of the core, above the Mahogany Zone, shows a series of repetitive cycles of decreasing-upward gamma values. Each cycle of decreasing gamma values is topped by a sudden dramatic increase in gamma values. This pattern becomes less comprehensible above GRFm1000 (Figure 4).

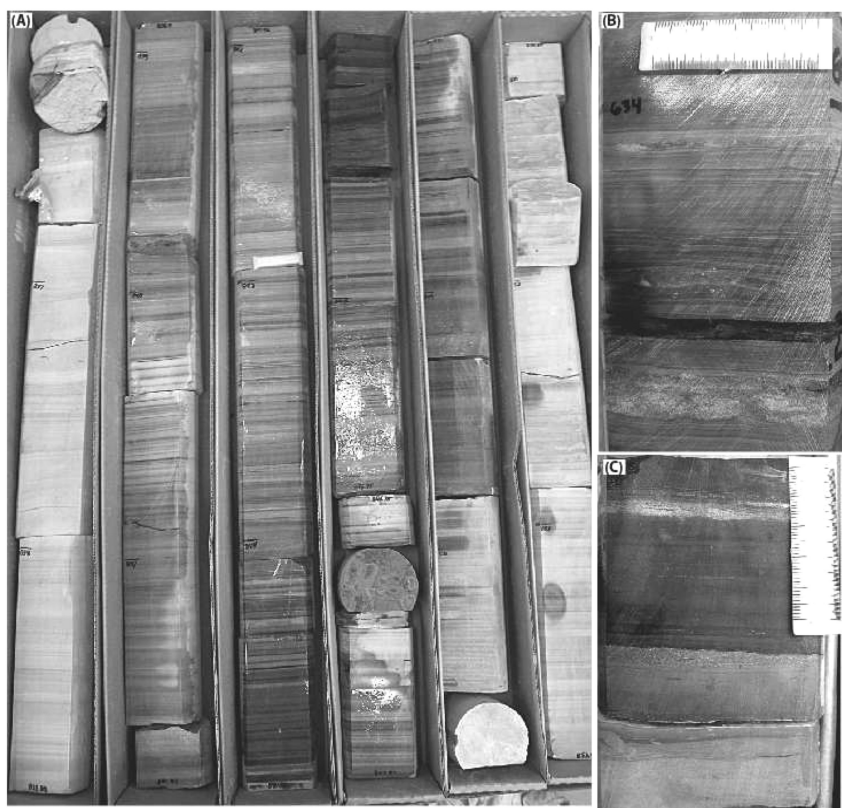


Figure 7. A) Typical, calcareous-mudstone-dominated rich oil-shale (259.69 –255.12 m depth in figure 4). Lighter rocks on either end of figure are dolomitic mudstones. Gray laminated rocks are kerogen-poor vs. kerogen-rich interlaminae of calcareous mudstones. Black rocks at the middle portion are calcareous mudstones highly rich in kerogen. Each core box is ~1 m long. Core base is bottom-right and top is upper-left. B) Details of calcareous mudstone facies. Light-colored granular beds are unnamed tuffs (193.24 m depth in figure 4). C) Bioturbated calcareous mudstones at the base of photograph, overlain by sandstone and, in turn, by kerogen-rich calcareous mudstones (332.54 m depth in figure 4). Note that scale is 5 cm long in all photos.

When correlated to core sedimentology, many of the highest gamma values correspond to clastic mudstone facies (e.g., depth interval 244-250 m). Many of the lowest gamma values correspond to calcareous mudstone facies (e.g., most of the Mahogany Zone in depth interval 215-235 m). Therefore, the gamma log of core P4 is, for the most part, a direct measure of the relative abundance of clastic vs. calcareous mudstones. This relationship, in turn, reflects interplay of lake-level, water-depth, and lake stratification.

Two scenarios can be invoked to compare the relative abundance of clastic vs. calcareous mudstones: 1) high gamma corresponds to clastic mudstones

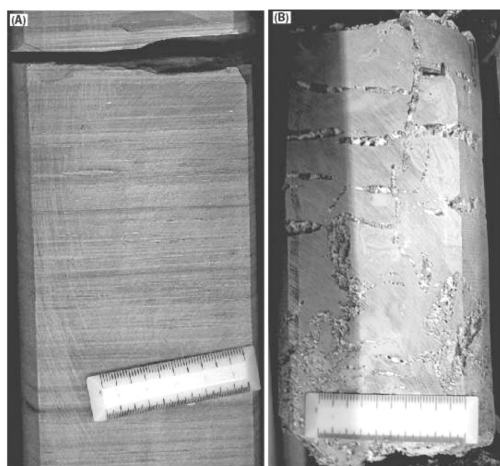


Figure 8. A) Finely laminated dolomitic mudstones (321.56 – 321.26 m depth in figure 4). B) Massive dolomitic mudstones with nahcolite vugs (110.64 m depth in figure 4). Note that scale is 5 cm long in all photos.

indicating wet climate favorable for delivering detrital-rich sediments (with K-feldspar, U, and Th) to the lake by surface runoff; whereas, low gamma corresponds to calcareous mudstones indicating less detrital input during dry climate; or, preferably, 2) high gamma corresponds to clastic mudstones indicating a fall in lake-level during which detrital input reaches the basin center (i.e. location of core P4); whereas, low gamma corresponds to calcareous mudstones suggesting a rise in lake-level generating deeper, stratified water conditions with little to no input of siliciclastic fines at the basin center. Notably, the second scenario is the inverse of gamma log interpretations of sand versus shale for marine and lacustrine environments (21).

Gamma signatures in the lower portion of the core (below the A-Groove) range from chaotic to bell-shaped (increasing-upward gamma). At least two bell-shaped trends at GRFm400 and GRFm500 indicate a sudden richness of carbonate lithology (deep water facies) followed by gradual increase in shale lithology (shallow water facies). Hence, these bell-shaped trends indicate shallowing-upward cycles, interpreted to be part of the lake system in which sediment and water supply exceeds (i.e., overfilled) or balances (i.e., balanced-filled) with accommodation.

The gamma curve in the upper portion of the core, above the Mahogany Zone, exhibits a sawtooth pattern with high gamma values decreasing gradually upward and then increasing suddenly. These patterns are clear in GRFm1000, 900, 850, and 700 (Figure 4). The characteristic pattern of the gamma log in the upper portion of the core exhibits aggradational to deepening-upward cycles. The persistence of deep water (i.e. calcareous mudstones) facies through the upper portion of the core along with gamma signature indicate that the basin was overall a deep balanced-filled lake system.

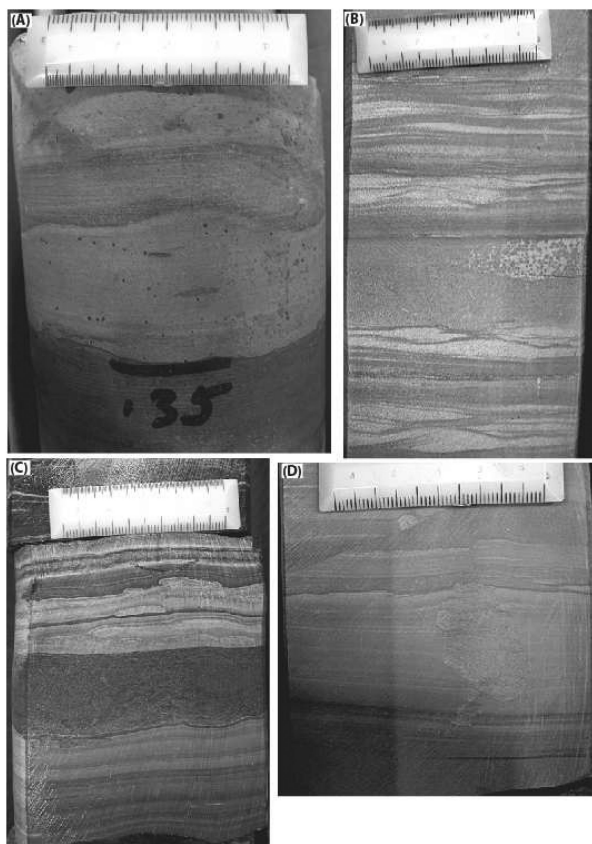


Figure 9. A) Sandstone facies (Horse Bench sandstone) with erosive basal contact and rip-up clasts (95.4 m depth in Figure 4). B) Wave ripple lamination (313.49 m depth in figure 4). C) Sandstone bed (darker layer in the middle) with sharp lower and upper contacts, underlain by calcareous mudstones and overlain by clastic mudstones (278.89 m depth in figure 4). D) Prominent solitary burrow in sandstone facies (278.59 m depth in figure 4). Note that scale is 5 cm long in all photos.

Discussion: Evolution of Lake Uinta

Sedimentology of core P4 is interpreted to represent a depositional environment distal from the basin margin and sediment-input sources. Sedimentary structures formed within storm or fair weather wave base, such as current and wave ripples, are only observed in limited places (the Horse Bench sandstone and other thin, scattered sandstones). However, the distance of core P4 from the shoreline varied over time, as reflected in the three facies associations found in the core.



Figure 10. A) Bedding plane view of bedded nahcolite (125.58 m depth in Figure 4). B) Small nahcolite vugs (113.45 m depth in figure 4). C) Large nahcolite vugs (122.83 m depth in figure 4). Note that scale is 5 cm long in all photos.

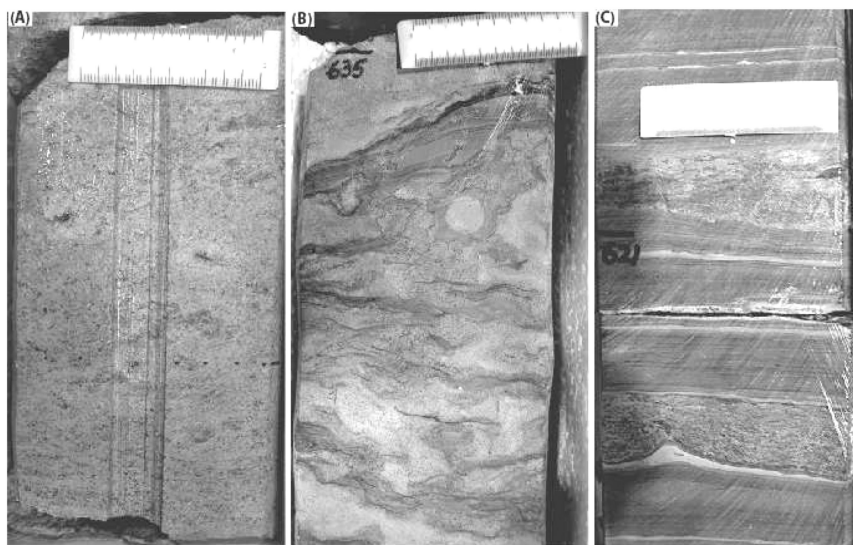


Figure 11. A) Curly Tuff (238.05 m depth in Figure 4). B) Wavy Tuff (193.55 m depth in figure 4). C) Thin, unnamed tuff beds (189.28 m depth in figure 4). Note that scale is 5 cm long in all photos.

Excluding the volcanic input of tuff, the six facies of core P4 are divided into three facies associations as follows: A) relatively shore-proximal facies association (235-358 m depth) including clastic mudstones, calcareous mudstones, laminated dolomitic mudstones, and sandstones; B) deep-basin facies association (125-235 m depth) including mostly calcareous mudstones with small amounts of clastic mudstones and sandstones; C) shallow water and evaporite facies association (60-125 m depth) including mostly sandstones, massive dolomitic mudstones, nahcolite, and some calcareous mudstones. The richest oil-shale deposits are found in facies association B.

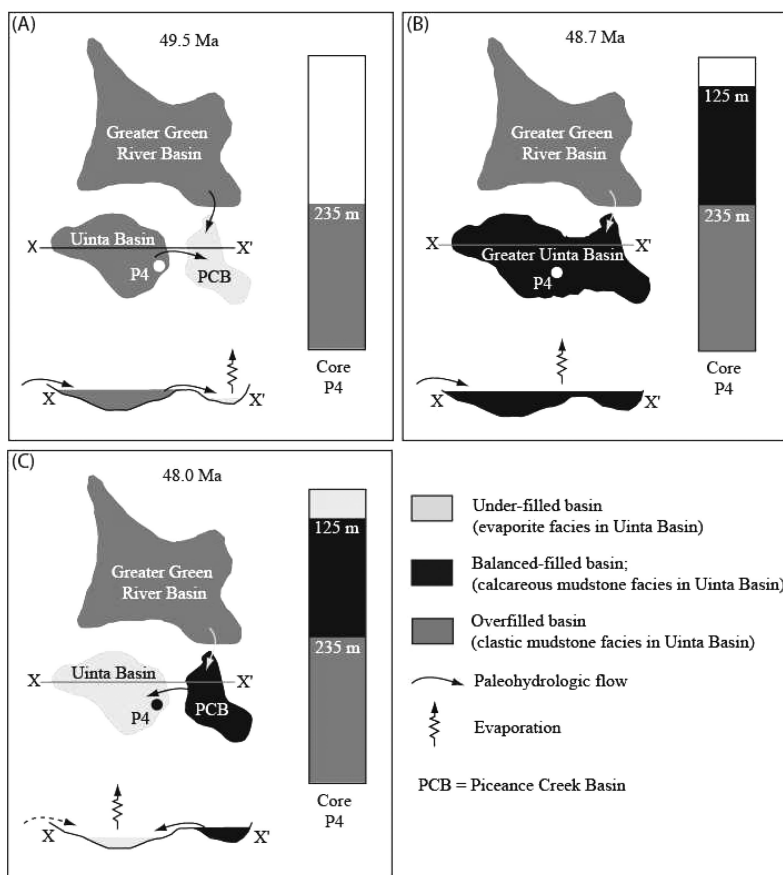


Figure 12. Schematic lake-level evolution of Laramide basins depositing the Green River Formation, 49.5–48.0 Ma ago. Schematic cross-sections show paleohydrologic flow according to published reconstructions (9). Schematic core litholog of P4 shows three facies associations deposited at each evolution stage of Lake Uinta. A) At ~49.5 Ma, the overfilled Greater Green River Lake and the Uinta Lake flow into the Piceance Creek Lake. As a terminal basin, the Piceance Creek Lake acts much as the present-day evaporative Great Salt Lake or the Dead Sea. B) At ~48.7 Ma, Uinta Lake and Piceance Creek Lake joined over a subsumed Douglas Creek arch, and balanced-filled conditions prevailed as freshwater input was proportional to evaporation rate. Under profundal, meromictic conditions, calcareous mudstones with the richest oil-shale zones were deposited at this time. C) At ~48.0 Ma, Lake Uinta became terminal, under-filled basin, probably by tectonic alteration of watersheds, that led to evaporative conditions in the basin.

The models of overfilled, balanced-filled, and under-filled lake basins (22) suggest that lake-basin type is a function of sediment, water supply, and accommodation due to basin subsidence. Under conditions of continuous basin

subsidence, sediment input and water supply should decrease relatively with time, changing basin systems from overfilled to balanced-filled to under-filled.

The distinctly different facies associations of core P4 (Figure 4) are related to a change in lake basin systems. In the lower portion of the core (> 235 m depth, facies association A), the decreasing-upward trend in the abundance of clastic mudstones, paired with the increasing-upward trend in calcareous mudstones, is interpreted to reflect the deepening conditions at core P4 in the Uinta Basin. This deepening was the result of overfilled lake conditions (excess of water and sediment input relative to accommodation; Figure 12a). The overfilled lake condition led to a balanced-filled condition (Figure 12b) as the Uinta and Piceance Creek Basins joined. This transition is characterized by the rapid waning of clastic mudstone facies and the predominance of the calcareous mudstone facies in the middle to upper portion of the core (235-125 m depth, facies association B). Balanced-filled conditions prevailed until evaporites deposited near the top (<125 m depth, facies association C) of the core, indicating an under-filled lake condition (Figure 12c).

The upward-decreasing trend in BI log and eventual cessation of bioturbation in core P4 (Figure 4) suggests implications for the relationship between bioturbation and overfilled, balanced-filled, and under-filled lake-basins. During initial overfilled conditions, bioturbation is active (BI: 2-3, and up to 5). During balanced-filled, deeper conditions, bioturbation decreases and ceases due to lack of oxygen indicated by the presence of oil-shale. Lack of bioturbation persists through the top portion of the core where massive dolomitic mudstones and nahcolite evaporite deposits indicate hypersaline, but shallower, conditions.

The lower portion of core P4 correlates with the transitional interval of Remy (5). The basin margin analysis made by Remy (5) describes the transitional interval as a period of lake level transgression. At this time, the Uinta Basin was separated from the Piceance Creek Basin by the Douglas Creek arch and the prevailing hydrologic gradient led overflow waters of both the Uinta Basin and the Greater Green River Basin to flow into the Piceance Creek Basin, which served as a closed terminal basin ((9); Figure 12a). Prior to the deposition of the Mahogany Zone, the Piceance Creek Basin and the Uinta Basin were joined over the Douglas Creek arch and formed a single Lake Uinta ((9); Figure 12b). After the deposition of the Mahogany Zone, conditions reversed and the Uinta Basin eventually became the terminal basin in the hydrologic system (Figure 12c).

Oil-shale was deposited in the upper Green River Formation during the deep stages of Lake Uinta. The richest oil-shale zones are the Mahogany Zone, R6, and the lower portions of R8 (2, 23). These zones were deposited during the transition from a small, over-filled basin of Lake Uinta, to a large, balanced-filled basin incorporating both Lake Uinta and Piceance Creek Basin. Anoxic conditions were obligatory for the preservation of organic materials comprising oil-shale deposits. Anoxic conditions at the bottom of Lake Uinta suggest that the lake was meromictic and profundal during the deposition of oil-shale.

The perceived problematic transition from deep-water calcareous mudstones to shallow-water evaporites without intervening basin-margin clastic input can be explained by the deposition of terminal fan deltas that are commonly developed at modern arid lake margins. Pusca (4) described the deposition of these terminal

fan deltas in the lower part of the Green River Formation. In the terminal fan delta model, clastic sediments are restricted to the circum-lacustrine alluvial plain during arid periods. Since surface runoff quickly infiltrates the arid soil or evaporates before reaching the lake, sediments are deposited as sub-aerial fans, and sediment input to the lake becomes negligible. Resuming wetter conditions would have delivered the clastic sediments of the Horse Bench sandstone to the site of core P4. Although Pusca (4) identifies terminal fan deltas in the lower part of the Green River Formation, the marginal lacustrine strata that deposited contemporaneously with the upper portion of core P4 are likely not preserved along the southern rim of the Uinta Basin due to Neogene and Quaternary erosion (8).

Conclusions

Oil-Shale

Oil-shale zones of the upper Green River Formation in the eastern Uinta Basin, Utah were deposited during profundal, meromictic lacustrine conditions. In core P4, oil-shale is a calcareous or dolomitic mudstone with high kerogen content.

Sedimentology of Core P4

- Core P4 has six facies: clastic mudstones, calcareous mudstones, dolomitic mudstones, sandstones, evaporite (nahcolite), and tuff.
- Six facies are divided into three facies associations: A) relatively shore-proximal facies association dominated by clastic mudstones (235-358 m depth), B) deep-basin facies association dominated by calcareous mudstones (125-235 m depth), and C) evaporating-basin facies associations, characterized by nahcolite and massive dolomitic mudstones (60-125 m depth).
- Facies associations A, B, and C were deposited in overfilled, balanced-filled, and under-filled lake basin, respectively.
- Bioturbation index log of core P4 can be used as a proxy for bottom-water oxygen level. The upward-decreasing trend in BI log supports the interpretation of overfilled, balanced-filled, and under-filled lake-basins.

Depositional History of the Upper Green River Formation in the Uinta Basin (49.5–48.0 Ma)

- First, an overfilled, fluctuating holomictic, and siliciclastic-influenced lake system transitioned to a balanced-filled lake system as water level rose in the Uinta Basin, subsuming the Douglas Creek arch and filling the adjacent Piceance Creek Basin.

- Second, a balanced-filled, profundal, and often meromictic lake system hosted the deposition of the richest oil-shale zones during the unification of the Uinta and Piceance Creek Basins.
- Third, an underfilled, evaporitic, and terminal fan-dominated lake system commenced as the Uinta Basin separated from the Piceance Creek Basin.

Future Work

Future work should target to correlate lithological characteristics, facies associations, bioturbation index patterns, and gamma signatures presented here to other cores and well logs in the Uinta Basin. These investigations would better assess the resource and extraction potential of oil-shale as well as the interplay of driving factors (e.g., tectonics and climate) in the evolution of the Uinta Basin.

Acknowledgements

Funding for this project was provided by DOE (grant #00056-55800308). Thanks to Utah Core Research Center (UCRC) for allowing us to study the cores. Thanks are also due to Raymond Levey of EGI, University of Utah. Beau Anderson painstakingly digitized well logs for this project. Landmark donated Geographix software that was used to interpret well log data. Comments of anonymous reviewers improved the manuscript.

References

1. Bartis, J. T.; LaTourrette, T.; Dixon, L.; Peterson, D. J.; Cecchine, G.; *Oil Shale Development in the United States: Prospects and Policy Issues*; The RAND Corporation: Santa Monica, CA; pp 1–68.
2. Vanden Berg, M. D.; *Basin-Wide Evaluation of the Uppermost Green River Formation's Oil-Shale Resource, Uinta Basin, Utah and Colorado*; Utah Geological Survey Special Study 128; Utah Geological Survey: Salt Lake City, UT, 2008; pp 1–19.
3. Keighley, D.; Flint, S.; Howell, J.; Moscariello, A. *J. Sediment. Res.* **2003**, *73*, 987–1006.
4. Pusca, V. A., Ph.D. Thesis, University of Wyoming, Laramie, WY, 2003.
5. Remy, R. R.; *Stratigraphy of the Eocene Part of the Green River Formation in the South-Central Part of the Uinta Basin, Utah*; U.S. Geological Survey Bulletin 1787; U.S. Geological Survey: Denver, CO, 1992; pp 1–79.
6. Johnson, R. C.; Roberts, L. N. R.; *Depths to Selected Stratigraphic Horizons in Oil and Gas Wells for Upper Cretaceous and Lower Tertiary Strata of the Uinta Basin, Utah*; U.S. Geological Survey Digital Data Series DDS-69-B; U.S. Geological Survey: Denver, CO, 2003; pp 1–33.

7. Dickenson, W. R.; Klute, M. A.; Hayes, M. J.; Janecke, S. U.; Lundin, E. R.; McKittrick, M. A.; Olivares, M. D. *Geol. Soc. Am. Bull.* **1988**, *100*, 1023–1039.
8. Johnson, R. C. Early Cenozoic History of the Uinta and Piceance Creek Basins, Utah and Colorado, with Special Reference to the Development of Eocene Lake Uinta. In *Cenozoic Paleogeography of West-Central United States*; Flores, R. M., Kaplan, S. S., Eds.; SEPM, Rocky Mountain Section: Denver, CO, 1985; pp 247–276.
9. Smith, M. E.; Carroll, A. R.; Singer, B. S. *Geol. Soc. Am. Bull.* **2008**, *120*, 54–84.
10. Tixier, M. P.; Alger, R. P. *Geophysics* **1970**, *35*, 124–142.
11. Gani, M. R.; Bhattacharya, J. P. MacEachern, J. A. Using Ichnology to Determine Relative Influence of Waves, Storms, Tides, and Rivers in Deltaic Deposits in the Cretaceous Western Interior Seaway, Wyoming-Utah, U.S.A. In *Applied Ichnology*; MacEachern, J. A., Bann, K. L., Gingras, M. K., Pemberton, S. G., Eds.; SEPM Short Course Notes 52; 2008; pp 209–225.
12. Reading, H. G.; *Sedimentary Environments: Processes, Facies, and Stratigraphy*; Blackwell Science: Oxford, England, 1996; pp 83–124.
13. Talbot, M. R.; Kelts, K. Paleolimnological Signatures from Carbon and Oxygen Isotopic Ratios in Carbonates from Organic Carbon-Rich Lacustrine Sediments. In *Lacustrine Basin Exploration: Case Studies and Modern Analogs*; Katz, B. J., Ed.; AAPG Memoir 50; AAPG: Tulsa, OK, 1990; p 340.
14. Eugster, H. P.; Kelts, K. Lacustrine Chemical Sediments. In *Chemical Sediments and Geomorphology: Precipitates and Residua in the Near-Surface Environment*; Goudie, A. S., Pye, K., Eds.; Academic Press: New York, 1983; p 439.
15. Ruble, T. E.; Philip, R. P. Stratigraphy, Depositional Environments, and Organic Geochemistry of Source-Rocks in the Green River Petroleum System, Uinta Basin, Utah. In *Modern and Ancient Lake Systems: New Problems and Perspectives*; Utah Geological Association Guidebook 26; Utah Geological Association: Salt Lake City, UT, 1998; p 328.
16. De Deckker, P.; Last, W. M. *Geology* **1988**, *16*, 29–32.
17. Warren, J. *Evaporites: Their Evolution and Economics*; Blackwell Science: Oxford, England, 1999; pp 262–267.
18. Dyni, J. R. Ph.D. Thesis, University of Colorado, Boulder, CO, 1981.
19. Klein, C. *Mineral Science*; Manual, ed. 22; John Wiley & Sons, Inc.: New York, 2002; pp 487–490.
20. Savrda, C. E.; Bottjer, D. J. *Palaios* **1989**, *4*, 330–342.
21. Van Wagoner, J. C.; Mitchum, R. M.; Campion, K. M.; Rahmanian, V. D.; *Siliciclastic Sequence Stratigraphy in Well Logs, Cores, and Outcrops: Concepts for High-Resolution Correlation of Time and Facies*; AAPG Methods in Exploration Series, n. 7; AAPG: Tulsa, OK, 1990; pp 1–55.
22. Bohacs, K. M.; Carroll, A. R.; Neal, J. E.; Mankiewicz, P. J. Lake Basin Type, Source Potential, and Hydrocarbon Character: An Integrated Sequence-Stratigraphic-Geochemical Framework. In *Lake Basins through*

- Space and Time*; Gierlowski-Kordesch, E. H., Kelts, K., Eds.; AAPG Studies in Geology, v.46; AAPG: Tulsa, OK, 2000; pp 3–33.
23. Vanden Berg, M. D.; Dyni, J. R.; Tabet, D. E.; Utah Oil Shale Database; Open-File Report 469; Utah Geological Survey: Salt Lake City, UT, 2006; pp 1–8.

Chapter 4

Thermodynamics of Shale Oil Production

James W. Bunger* and Christopher P. Russell

JWBA, Inc., Salt Lake City, Utah, USA

*jim@jwba.com

Oil shale represents the richest areal concentration of hydrocarbons on earth, measuring more than 1 million barrels per acre in Colorado, for example. Recovery technologies require the use of heat and can readily be designed to operate in an energy self-sufficient mode. 25 gpt oil shale contains enough energy to be totally self-sufficient while producing excess heat that can be converted to power for export. Overall thermal efficiencies depend primarily on grade, but variations in thermal efficiency will also depend on technology configurations. Of the three major process steps - mining, retorting, and upgrading - only the retorting step is unconventional. This paper provides the basis upon which the energy efficiencies of retort technology can be evaluated on a resource- and technology-specific basis.

Introduction

Oil shale must be heated to produce oil. Because of the large tonnages involved there is an impression that the energy required for this heating is prohibitive. Thermal analysis and experience show that energy cost is not prohibitive. The specific heat of oil shale is only about $\frac{1}{4}$ that of water, and much of the sensible heat can be recovered for use in heating fresh ore. The literature does not contain much information on the thermal efficiency for shale oil production, and this paper is an attempt to contribute thermal analysis to this technical area.

The importance of thermal efficiency can be seen in global energy trends. We are now at a stage in human economic development where the world's lowest-cost hydrocarbon resources have been produced. For conventional petroleum, the energy cost is increasing as reservoirs become deeper and more remote, the oil

being produced is heavier and contains more sulfur, and the specifications for end-use fuel become more stringent. Production of energy in the future will necessarily cost more, both financially and energetically.

In the near future shale oil production will be thermodynamically competitive with conventional petroleum. Similar thermodynamic efficiencies will translate into similar economics. In many regions of the world, including the United States, oil shale contains more energy per ton than Alberta oil sands that are being produced profitably today. Based on thermal analysis, oil shale should already be economically competitive with alternative fossil energy resources.

This paper quantifies the variables of thermal efficiency for producing oil from oil shale. An example is provided for Green River Formation, USA, oil shale and a generic gas combustion retort. Thermal efficiencies will vary with resource characteristics and technology approaches and the data and principles discussed in the paper can be applied to any oil shale resource and any technology approach. Details are provided for thermal properties of the retort portion of the process, which is the unconventional step. Energy costs for mining and upgrading (conventional technologies) are treated by analogy to industrial practice.

Resource Characteristics Important to Thermal Efficiency

When making an evaluation of energy requirements, it is necessary to select the recoverable intercept within the ore body. Figure 1 illustrates the tradeoff between grade, recoverable oil, and overburden-to-pay ratio, and shows that selecting a wider intercept yields more barrels per acre and reduces the overburden-to-pay ratio, but results in lower grade (gpt = gallons per ton).

Selecting the proper intercept, whether for mining-based or in-situ technologies, is an economic optimization problem. An illustration of simple optimization for a surface mine based on the core example shown above is shown in Figure 2. In this case, total tons-mined vs. bbl-produced yields the following family of curves, and shows a minimum exists between about 20 and 30 gpt. For in-situ or modified in-situ technologies, factors such as resource lease terms, reclamation requirements, energy losses at the edges, oil prices, or other variables may well favor larger intercepts and greater production per acre even though average grade is less. Conversely, throughput constraints on surface retort processes may favor richer zones, even at the expense of higher mining costs.

The typical Alberta oil sands condition is marked on the plot (Figure2). One point of this illustration is that there is wide range of resource richness characteristics that could be economically viable. Each resource location and technology approach will require its own optimization, and once the grade and intercept are selected, the methods of thermal analyses provided below can be applied.

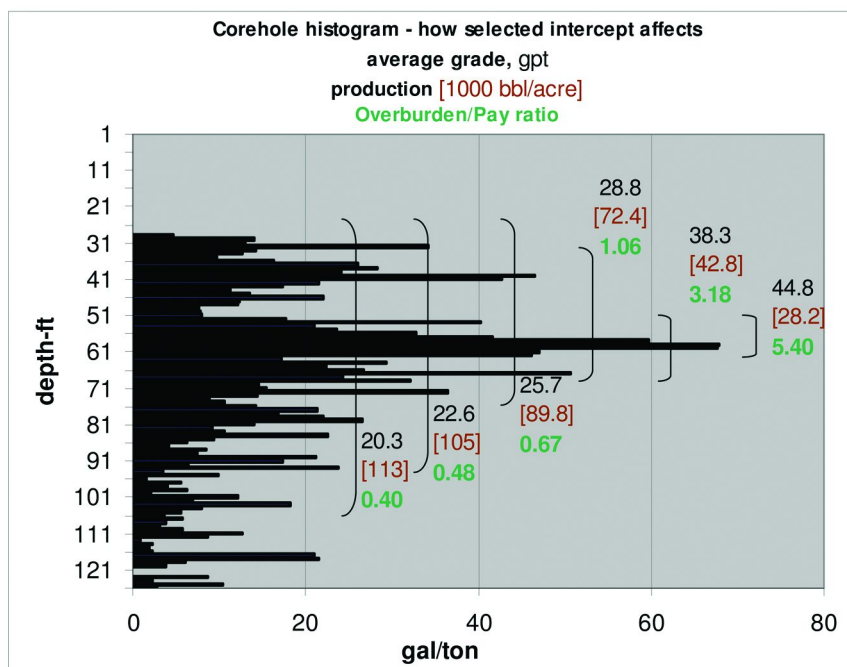


Figure 1

Mining Energy

Mining is a well-established industry, and estimates of mining energy costs can be made by analogy to these industries. There are many site-specific and technology-specific variables that will affect mining energy costs. However, as a benchmark, the experience from Alberta oil sands can be used as a guide. In Alberta the average yield of oil sands is about 21 gallon syncrude per metric tonne (19 gal per short ton), and the ore exhibits an average overburden to pay (O/P) ratio of 1 to 1, to give 4.4 ton/bbl total.

For Alberta oil sands mining energy costs are on the order of 4% of product Btu values, or roughly 240,000 Btu/bbl. About 20% of this energy cost is in the form of diesel fuel for haul trucks and bulldozers [For both Suncor and Syncrude daily consumption of diesel fuel is about 2000 bbl per million tonne mined (half million tonne overburden and half million tonne pay)]. The balance of energy requirements is in the form of fuel for power generation used in electric shovels and conveyers.

Oil shale may require a little higher per-ton cost for mining and ore preparation (crushing and screening) because the rock is consolidated. But offsetting the higher per-ton costs, is the richer ore, meaning fewer tons-mined/barrel-produced. For the base case illustrated in this paper (25 gpt, 1:1 O/P) total mined material is 3.36 ton/bbl or 24% less than Alberta oil sands.

For underground mining the efficiency will be better because no overburden needs to be mined. In the early decades of development grades will likely average

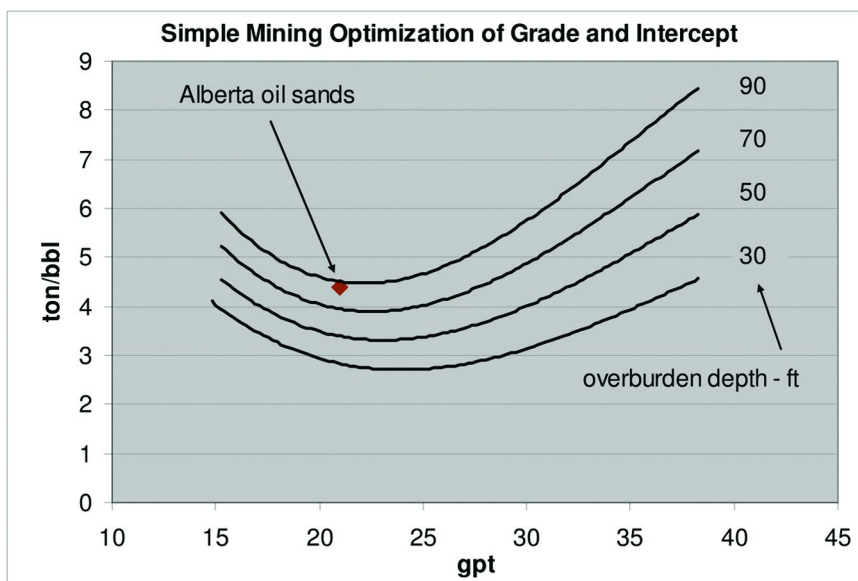


Figure 2

greater than 30 gpt (1.4 ton/bbl, not accounting for wastage). For varying grades and overburden/barren ratios a close approximation of overall mining efficiency can be made by prorating the ton/bbl in relationship to the aforementioned base-case efficiency.

In summary, applying factors from Alberta, the fuel cost for the base case is 35,714 Btu/ton-pay and the power costs for mining and ore preparation are 14.4 kW-hr/ton-pay (122,712 Btu/ton-pay). Overall first-law mining efficiency is about 96%.

The Thermal Cycle in Retorting Oil Shale

Mined, prepared ore is first preheated to dry the moisture content from the ore. The preheated, dry ore is then heated to full retort temperature. For in-situ or modified in-situ processes where heatup rate is slow, the maximum retort temperature may be in the range of 700 – 750 °F. For surface processes, where heatup rates are fast, the final retort temperature may be 900 – 950 °F.

Once the ore has reached its final retort temperature the technology will dictate whether or not the retort is ready for heat recovery or whether to continue with combustion of the coke remaining on the spent shale. If combustion is pursued, the temperature in the combustion zone is generally controlled below about 1200 – 1500 °F in order to minimize endothermic decarbonation reactions which, if uncontrolled, can rob the process of as much as 8% of the BTUs available in a 25 gpt ore (1).

Heat is reclaimed from the spent ore to improve thermal efficiency and to cool the spent shale for safe discharge. A customary approach to reclaiming heat is to

preheat combustion air or reheat recycle gas with hot, spent shale and use these hot gases to heat cold ore entering the reactor.

The most common sources of permanent heat loss are: sensible heat remaining in the final process streams, heat removed by coolers and condensers, heat lost to endothermic reactions of pyrolysis and gas production, and heat losses across the boundary to the environment. Heat is also needed to generate power, and none of the mechanical energy produced from electric power is recovered.

Retort Power Requirements

In any oil shale retort operation there will be a need for electrical power. Power may be generated by raising steam from excess energy resulting from coke combustion, or by combusting produced gases. In some cases, economics may favor purchasing power produced from coal, and sell the produced hydrocarbon gas because of its higher market value. But in most cases power will be produced on-site in an energy self-sufficient operation. This is particularly possible when the kerogen is very low in sulfur content, as it is in the western US.

Retorts that rely on movement of air or combustion gases require blowers. Power is needed to elevate the ore and convey tailings. (Power for ore preparation is included in the mining energy). Some energy is required for pumping of fluids, water and oil. Power is also needed for gas cleanup and water treatment. Power costs can be prorated to account for variations in grade, as some costs are ton-related and others are bbl-related. Quantitative estimates of power requirements for the retort and product cleanup units are given in the example below.

Mass Balance

Mass balance directly depends on grade and grade is somewhat dependent on the assay or retort method. The most commonly accepted assay method is the Modified Fischer Assay (ASTM D-3904), or MFA. The apparatus is a small, batch-type retort that is heated at a prescribed rate until a temperature of 932 °F (500 °C) is reached. The assay provides information on oil, water, and gas yield, the latter by weight loss, as well as the density of produced oil. Coke is not directly measured, and total organic content must be measured by other methods.

Information from the Synthetic Fuels Data Handbook (2) has been used to construct a mass relationship as a function of grade, for US Green River Formation (GRF) oil shale. This is shown in Figure 3, along with the quadratic equations (forced through zero) describing the least error fit to the data. *For all real retort processes the relative yield of organics between the gas, liquid and coke will vary from MFA.* Thus, to use the equations and property information provided in this paper, the user must first determine the yield distribution (between gas, liquid and coke) for the retort technology being analyzed. For deposits other than GRF oil shale, a thorough analysis of total kerogen content for specific deposits is needed.

Heat Balance Properties and Equations

The overall energy balance of a given process can be calculated using the following properties and equations.

Heat equations and data

1. Sensible heat for oil shale

$$C_p = 0.172 + 6.7E-5 \times T + 1.62E-6 \times G \times T$$

Where: C_p is in Btu/lb-°F

T is in degrees Rankine

G is the grade of oil shale in gallons/ton

2. Heat of vaporization of water

$$H_v = 970.33 \text{ Btu/lb}$$

3. Sensible heat for water

$$C_p = 1 \text{ Btu/lb-°F}$$

4. Heat of vaporization of oil

$$H_v = (79.223 \times T + 23218) / (T - 16.175)$$

Where H_v is in Btu/lb-oil-°F

T is in degrees Fahrenheit

5. Endotherm of retorting, including non-condensable gas formation

$$H_r = 0.228692 \times T \text{ °F} - 41.7556$$

Where H_r is in Btu/lb-liquid and T is the applicable retort temperature.

6. Dolomite decomposition endotherm^a

$$500 \text{ Btu/lb-CaMg(CO}_3)_2 \text{ (at 1200 °F)}$$

^aThe mineral most susceptible to decarbonation is dolomite ($\text{CaMg(CO}_3)_2$ MW = 184.4). Dolomite is present in a typical Green River oil shale in concentrations of about 33% of the inorganic matter. Experience shows decarbonation occurs at temperatures lower than the handbook value of 1350 °F, but at short contact times at 1200 °F, or below, very little dolomite will decompose. Calcite (CaCO_3), with a decomposition temperature of 1650 °F probably survives controlled combustion temperatures, although as with dolomite, the prospects of co-reactions with other minerals at lower temperatures cannot be discounted.

7. Sensible heat of barren rock – use oil shale Cp equation with $G = 0$ (this method neglects the effects of changes in mineralogy on Cp, which, while measurable are small overall).

8. Combustion heating value of kerogen and products

Kerogen –	17,927 Btu/lb
Gas –	20,000 Btu/lb
Oil –	18,500 Btu/lb
Coke –	15,100 Btu/lb

9. Power Equations

a. Blowers for air/gas movement

• Input terms

1. MW = avg molecular weight of gas (Dalton)
2. F_m = gas mass flow (lb/hr)
3. P = absolute inlet pressure (psi)
4. ΔP = pressure rise through blower (psi)
5. T = temperature ($^{\circ}$ F)
6. d = pipe diameter at blower exit – ft
7. e = blower efficiency (typically 0.6 unless otherwise known)

• Calculated terms

1. ρ = gas density (lb/ft³) = $0.5193 MW \times P / ((T-32/1.8)+273)$
 2. F_v = gas volumetric flow rate = ft³/hr = F_m / ρ
 3. V = gas velocity – ft/sec = $.000354 F_v / d^2$
 4. P_{kw} = blower power requirement – kW = $0.000054182 F_v (\Delta P + .0001085 \rho V^2) / e$
- b. Retort mechanical operation including production handling = 6 kW-hr/ton
- c. Gas cleaning, sour water treatment, etc. = 2.5 kW-hr/bbl
- d. Mining and upgrading power (see applicable sections elsewhere in this paper)

Example of Energy Balance (Retort Unit)

An energy balance example is calculated for 1 ton of 25 gpt ore fed to a gas combustion retort. Details of the calculations are not shown, but rely on the aforementioned properties and equations. Some values that are a consequence of changes of properties with temperature must be integrated over the applicable temperature range. Others are simple arithmetic applications of the equations. The use of decimal values in this example does not imply a commensurate degree of precision but is employed to minimized discrepancies resulting from rounding and approximations.

Basis: 1 ton (2000 lb) oil shale
 25 gpt MFA
 298.0 lb kerogen (calculated from equations in figure above)
 1% moisture content of ore = 20 lb
 33 % dolomite content of mineral portion of ore = 555.1 lb
 50% fraction of dolomite decarbonated at 1200 °F
 50 °F ambient ore temperature
 900 °F ore temperature when retorting is complete
 1200 °F shale temperature when combustion is complete
 200 °F spent shale and combustion gas temperature at process exit

Mass balance:

In:	2000.0 lb oil shale
	<u>905.7 lb</u> combustion air
Total In	2905.7 lb
Out:	190.4 lb oil
	36.4 lb gas
	20.0 lb water ^b
	1109.4 lb flue gas
	<u>1549.5 lb</u> spent shale
Total out	2905.7 lb

^bIn practice, some water is formed during pyrolysis of organics and minerals, but this production has not been estimated for this example, resulting in a slight overcounting of the mass of the spent shale.

Heat in	BTU
Heating of water (50-212°F)	3240.0
Evaporation of water	19406.6
Heating of oil shale to final retort T	463271.3
Heating of oil shale from retort T to final combustion T	143676.4
Heating of combustion air to final combustion T	265573.6
Endotherm of organic rx including gas formation	31236.7
Evaporization of oil	20360.7
Heat of decarbonation of dolomite (50% conversion)	138764.4
Losses to surroundings (3)	45400.0
Heat needed to generate power (30 kW/ton)	<u>196640.2</u>
Total Heat in	1327569.8
Heat out/generated	BTU
Generated from combustion of Coke	1075219.4
Recovery of heat from spent shale (200 °F final)	386954.4
Recovery of heat from flue gas (200 °F final)	<u>290172.8</u>
Total out	1752345.5
Excess heat (out – in)	424775.8

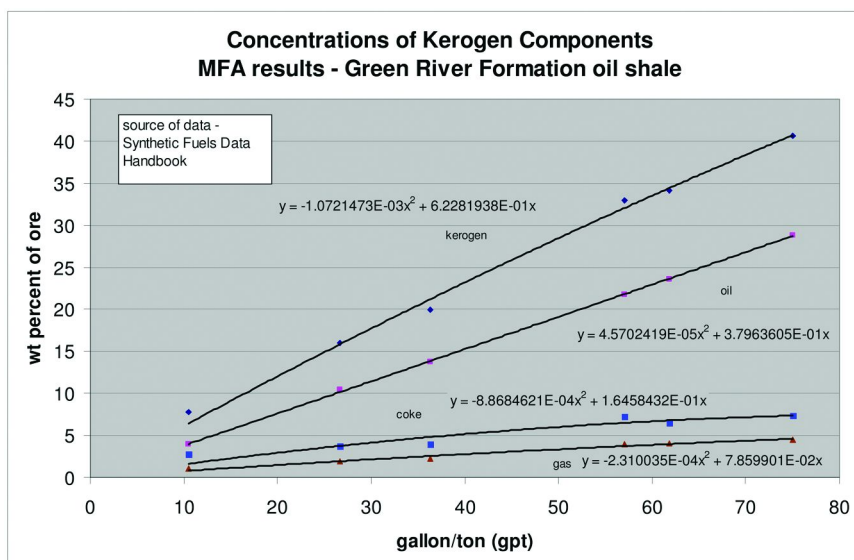


Figure 3

Thermal Balance Reconciliation

Kerogen in	5342386.7
Oil out	-3522202.1
Gas out	-728239.2
Excess heat out	<u>-424775.8</u>
Implied lost heat	667169.6

Loss accounting

Heating and evaporation of water	22646.6
Evaporation of oil	20360.7
Organic endotherm (incl gas formation)	31236.7
Carbonate endotherm	138764.4
Residual heat in spent shale	49088.5
Residual heat in flue gas	35698.1
Cooling of HC gases and oil	120956.4
Losses to surroundings	45400.0
Heat for power generation	<u>196640.2</u>

Total losses accounted 660791.5

Reconciliation (667169.6-660791.5) = 6378.0

Reconciliation agrees within 6378 Btu, or a little more than 0.1% of the total kerogen value of 5.34 million Btu. This high level of agreement lends validity

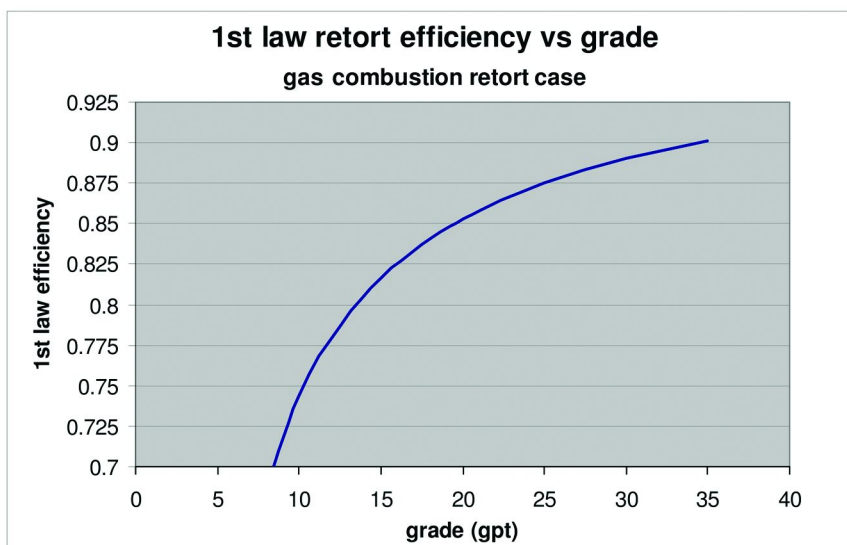


Figure 4

to the internal consistency of the thermal equations, heating values, and stream properties.

Retort Operation

Modern ‘gas combustion’ retorts such as Paraho use cool recycle gas and cool combustion air to control combustion temperatures. Gas or air may be introduced at the bottom or at intermediate zones within the combustion zone. Ore enters the top and gas enters the bottom, both at ambient conditions. The ore goes through preheating, followed by retorting, combustion and finally cooldown, all in a single bed. The net result is spent, clean ash exiting the bottom at about 200 °F and gas exiting the top at about 200 °F. The example shown above is representative of full utilization of energy, as might be the case for modern surface retorts.

Other technologies such as Red Leaf Resources EcoShale™ technology, in which a large encapsulated bed of oil shale is indirectly heated through combustion gas flowing through pipes laid in the bed, do not contemplate burning the coke for energy, and instead rely on burning the produced gas for heat and power. Calculating the energy balance for an EcoShale type retort can be performed by stopping the input energy at the retort stage. Heat may be recovered from the bed down to about 200 °F. Net heat and power may be supplied from the hydrocarbon gases produced.

Significantly, even without burning the coke for energy, but burning produced gas instead, the EcoShale technology promises energy self-sufficiency for oil shale grades down to about 13.3 gpt. Operating in an energy self-sufficient mode for leaner ores, the yield of saleable products is limited to the oil produced. Because

of the lower, slower retort heating, however, and the absence of oxygen in the retort zone, the quality of the oil is higher than for direct-fired gas combustion retorts.

Energy balances for electrically heated retorts, such as Shell's ICP and rf-type heating can be estimated from the above treatment by again stopping the input energy at the end of the retort stage, calculating the efficiency of producing electricity (field units are typically 40% on a Btu basis), and estimating the efficiency of utilization (close to 100% for resistance heating and something less for rf heating).

Effect of Average Grade on Efficiency

Overall efficiencies as a function of grade are displayed in Figure 4. Efficiencies fall off rapidly below about 13 gpt ton, and, in fact, gas combustion retorts such as the one illustrated need about 13 gpt ore to stay in heat balance by burning the coke alone. The first-law efficiency of the gas combustion process is about 78% and for the EcoShale process is about 79% for this breakeven point. For 25 gpt ore efficiencies for both cases are about 87%.

Liquids Upgrading

The quality of oil varies widely with retort technology and the choice of upgrading technology depends on the target markets. Severe upgrading to high quality syncrude has energetics and H₂ consumptions similar to resid hydrotreating, where minerals and heteroatom (S, N) contents are high. On a mole basis 1.8% nitrogen in typical shale oil raw liquids is roughly equivalent to 4.5% sulfur in typical bitumen coker distillate, meaning that upgrading hydrogen requirements are very similar, and on the order of 1800-2000 scf/bbl (The efficiency analysis in this paper ignores the energy content of the feedstock for producing H₂ and correspondingly, no energy credit is given for H₂ added to the oil. The analysis does account for the energy and utilities in H₂ manufacture. Rigorous accounting of hydrogen effects will change the efficiency numbers a little, but will not change the conclusions of energy self-sufficiency when producing shale oil.).

For liquid upgrading calculations based on published utility and hydrogen costs (4) reveal upgrading energy requirements on the order of 142,097 Btu/bbl, of which 73,756 is for heat and 68,340 is for power. This translates into a first-law efficiency of 97.5%.

Self-Sufficiency vs. Imported Energy

Concerns over energy efficiency of oil shale production are mitigated by the ability to be energy self-sufficient. Energy produced inside the battery limits does not compete with other economic uses of energy in the commercial markets. As is

shown in the examples above, there is no need to import energy, other than perhaps a small amount of diesel fuel, and in a facility with an upgrader, diesel fuel would be produced on-site. Except for the case where coal is the low-cost fuel for power generation, most oil shale technologies will be energy self-sufficient.

Overall Efficiencies

The overall efficiency for the base case, with upgraded syncrude is 81%. This is not far off from the 1st law efficiency of second-generation Alberta oil sands plants (5). Details are shown in the table below. If coke supplies all of the necessary heat, there is no net loss of saleable products for energy production. For a 25 gpt oil shale an additional 5 gallons-equivalent hydrocarbon gas is produced compared to Alberta oil sand, where syncrude recovery is about 19 gpt and all the produced gas is consumed internally. It becomes evident that oil shale is substantially richer, perhaps by 50% or more, than oil sands. Conversely, retorting is less efficient than water extraction and coking resulting in overall thermal efficiencies that are about equivalent.

The reason that comparisons between oil shale and oil sands are deceiving is because oil shale grade is measured by MFA as a liquid after the ‘coking’ reaction, whereas bitumen is measured before the coker. The comparison between oil shale and oil sands, which operate at a profit by any measure, is also made to reinforce the notion that if reliable technology can be proven, then oil shale should be economically competitive in today’s energy markets.

In summary, the net energy balance for 1 ton of 25 gpt oil shale is as follows:

	Product	BTU	% of total
In - Kerogen		5,342,387	100.0
Out			
	Gas produced for sale	728,239	13.63
	Oil produced for sale	3,522,202	65.93
	Excess heat produced for sale (difference)	93,071	1.74
	Sum of product outputs	4,343,512	81.30
Energy consumed in process (primary use)			
Fuel	Mining (diesel)	35,714	0.66
	Retort (coke)	464,151	8.69
	Upgrading (heat)	73,757	1.38
Power	Mining (shovels, conveying, ore prep – 14.4 kW-hr)	160,272	3.00
	Retort (ore movement, blowers, gas cleaning, water treat – 23.1 kW-hr)	196,640	3.68
	Upgrading (compression - 8.0 kW-hr)	68,340	1.29
	Sum of Energy Consumed	998,874	18.70
	Balance (Out + Consumed)	5,342,387	100.0

Conclusions

It is evident that net energy production is not an issue with oil shale. For a gas combustion retort there is ample internal energy in the coke to operate the process and the oil and gas produced is net to the consumer. Of the energy available in the kerogen, (for the gas combustion retort case) about 79.6% is produced as gas + liquid, about 18.7% is consumed in the process, and 1.74% is excess employed for power for sale. For a 50,000 bbl/day operation this excess power may amount to about 38 MW, not an insignificant amount.

References

1. *Synthetic Fuels Data Handbook*, Cameron Engineers: 1975; p. 33.
2. *Synthetic Fuels Data Handbook*, Cameron Engineers: 1975; tables 19, 20; p 32.
3. *Synthetic Fuels Data Handbook*, Cameron Engineers: 1975; table 61, p 77.
4. *Hydrocarbon Processing Refinery Process Handbook*, November, 2002; pp 128–129 for processing and p 123 for hydrogen.
5. Bunger, J. W.; Crawford, P.; Johnson, H. *Oil & Gas J.*, **2004**, *102.30*, 16–24; August 9.

Chapter 5

Molecular Composition of Shale Oil

James W. Bunger,* Christopher P. Russell, and Donald E. Cogswell

JWBA, Inc., Salt Lake City, Utah, USA 84152-0037

*jim@jwba.com

Molecular compositions of shale oils differ widely among deposits and retort technologies. Shale oils invariably contain high concentrations of heteroatom-containing compounds, and these characteristics will strongly influence approaches to processing of shale oil to marketable products. An advanced analytical method for identifying and quantifying molecular composition of shale oil, the Z-BaSIC™, method is illustrated and results are given. Results show that like conventional petroleum, compound types can be readily described by a limited number of homologous series. Detailed knowledge of composition will assist in the development of effective process steps needed to assimilate vast shale oil resources into the market-place.

Introduction

Shale oil is the pyrolysis product of kerogen, a primitive, high heteroatom-containing organic material found in oil shale. For example, Estonia kerogen is high in oxygen, Jordanian and Israeli kerogen is high in sulfur, and US kerogen is high in nitrogen. The molecular composition of the shale oils derived from these kerogen-containing ores reflects the high heteroatom content of their precursor material.

Shale oil may be used for three principal purposes. It may be simply burned as a fuel. This is possible when sulfur and nitrogen contents are low, as with Estonia shale oil. It may be upgraded and fed to a petroleum refinery to make conventional fuels and petroleum products. Upgrading is needed not only to stabilize the olefins but to remove heteroatoms of sulfur, nitrogen and metals. Or

it may be fed to a chemical refining process to extract and produce specialty and commodity chemicals, where the extraction raffinate is made into fuels (1, 2).

The value of shale oil for its respective markets depends strongly on its molecular composition, as well as the process technology available for upgrading or refining. Processing technologies are by no-means clearly established, and much of the development work in the future will be aimed at finding the optimum technologies and process conditions that yield products for the target markets.

For these reasons, it is useful to know the molecular composition of shale oil so as to understand what separations and conversions are economically desirable. This paper describes the results of an analytical method, called Z-BaSIC™ to quantify the molecular composition of shale oil.

Brief Description of Z-BaSIC

Z-BaSIC™ is an acronym for the **Z-Based Structural Index Correlation** method. Z-BaSIC describes the molecular composition of shale oil (or crude oils) in numerical form. More detailed descriptions of the method can be found in references (3–5).

First, compound types are classified by the generalized empirical formula:



Where ‘z’, ‘u’, ‘v’, ‘w’, ... are integer values that classify an individual molecule by a z-vector.

The ‘n’ value is the primary variable that defines a homologous series. As ‘n’ → ∞, all properties, P_i , approach the value for the corresponding property of an infinitely long paraffin. This adds confidence to the correlations of properties for heavy ends, where pure compound databases do not exist. The use of an empirical formula as a classification system and the definition of ‘n’ as the primary structural index correlating variable is the scientific foundation of the Z-BaSIC™ method.

Identification of the Z-BaSIC parameters for components in a mixture is made using capillary gas chromatography equipped with mass-, sulfur- and nitrogen-specific detectors (GC-MSD). A methodology has been developed using parent ions from 70eV electron impact ionization (mass selective detector) to classify the compound by z-vector (class). Within a class, variations in ‘n’ are rigorously associated with variations in MW by 14 atomic mass units (-CH₂). Where more than one z-vector gives rise to a common ion, GC retention time is used to distinguish between the z-vectors. Nitrogen and sulfur specific detectors are used to obtain the heteroatom distribution with respect to pseudoparaffin number (i.e. boiling point).

Quantification of the composition is accomplished by first measuring the elemental composition, density and boiling point distribution (determined by HTSD). A least-error fit is sought whereby the concentrations of the basket of compounds found by GC-MSD agrees with the measured data. The use of the

density property is possible because of the correlations of the ‘n’ parameter with physical properties for a given z-vector.

The combined information is used to prepare a composition-property, or ‘cp’ file. This file can then be used as input to a suite of software programs used to calculate properties, report molecular composition, and simulate refinery processes such as distillation, blending, and conversion processing. Z-BaSIC may also be used to prepare high-fidelity pseudocomponent files as input for LP models and process simulators.

Results

Bulk Properties

A sample of pilot plant oil produced by the EcoShale™ process on a Utah field site was analyzed by the Z-BaSIC method. EcoShale is a developing technology of Red Leaf Resources that involves indirectly heating a bed of oil shale using pipes buried in the bed. The pipes carry combustion gases in a closed loop. As oil is produced some oil drains to the bottom, where it is pumped, while vapors are collected overhead and condensed. The EcoShale 32 shale oil sample is a representative composite of the total oil produced.

Measured input data is shown in Table 1. Note the high nitrogen and low sulfur contents, typical of Green River formation shale oil. ‘cp’ files (earlier generation versions) have also been prepared on a Colorado surface retort shale oil (Unocal 23) and an Estonia surface retort (Kukersite 8) shale oil, and their input data is also given in Table 1.

It is clear from the bulk properties that large differences exist between various deposits and large variations result from different retort technologies applied to the same deposit. Whereas, the EcoShale process (a variation on a modified in-situ, MIS, approach) utilized 90 days to achieve temperatures between 700-750 °F, the Colorado and Estonia surface retorts achieve temperatures of greater than 900 °F in less than 1 hour. Under slow heating conditions the EcoShale 32 oil is higher in hydrogen and lower in boiling range than the Unocal 23. The variations in heteroatom content have yet to be explained, and could relate to deposit variations, or possibly differences in analytical accuracy (the Unocal 23 oil was analyzed nearly 20 years ago).

Measured high temperature simulated distillation data (HTSD) for EcoShale 32 are given in Table 2. Note that approximately 66 % of the oil boils between 304 and 676 °F, equivalent to the diesel fuel boiling range of C9 to C21. The high middle distillate yield results from the slow heating, as Unocal 23 shale oil sample only yields about 40% over this same range (detailed data not shown).

Table 1. Property data on three shale oils

<i>Property - units</i>	<i>EcoShale 32 Utah</i>	<i>Unocal 23 Colorado</i>	<i>Estonia Kukersite 8</i>
Measured input data for Z-BaSIC file construction			
Carbon – wt%	85.26	85.87	88.31
Hydrogen – wt%	12.45	11.74	8.06
Nitrogen – wt%	1.55	1.30	0.1
Basic Nitrogen – wt%	1.08	0.73	NA
Sulfur – wt%	0.249	0.918	0.557
Oxygen – wt%	1.24	0.17	2.98
Density @ 15.5 °C – g/cc	0.8643	0.9148	1.0189
API gravity - degrees	32.2	23.2	7.4
Additional property data on whole oils - Z-BaSIC output data			
UOP K factor	11.55	11.3	10.3
Average MW - Dalton	198	245	226
Conradson Carbon wt %	Non-detect	3.0	0.2
D-2887 distillation data			
10% point °F	330	384	528
50% point °F	560	716	702
90% point °F	801	935	915
Kinematic Viscosity @ 37.78 °C - cSt	4.00	23.3	259
Kinematic Viscosity @ 50.0 °C - cSt	3.04	NA	NA
Dynamic Viscosity @ 37.78 °C - cP	3.39	21.5	266
Dynamic Viscosity @ 50.0 °C - cP	2.55	14.4	136
ND = non-detect NA= not analyzed			

Summary Molecular Composition

A summary of the molecular composition for three shale oils is given in Table 3. For the EcoShale oil about 50% of the oil is saturated hydrocarbons, and that another 34% of the oil is nitrogen and oxygen types. These types, principally pyridines and pyrroles, are candidates for production of commodity and specialty chemicals by extraction and refining of the extract (1, 2). Only 15-16% of the oil is comprised of sulfur compounds and aromatic hydrocarbons. The Unocal 23 exhibits lower paraffins and higher aromatics. The Kukersite oil is extremely high in oxygen compounds, reflecting the potential value of that oil for producing phenols and resorcinols (2, 6).

Table 2. EcoShale 32 HTSD

Table 2 EcoShale 32 HTSD					
mass%	°F	mass%	°F	mass%	°F
0.5	148.2	34	483	68	644.4
1	175.2	35	488.8	69	651.4
2	206	36	491.4	70	654.4
3	247.4	37	493.4	71	660.8
4	258.8	38	499	72	667.4
5	275	39	504.6	73	673.8
6	295.4	40	509.2	74	677.6
7	304.4	41	512.8	75	685
8	316	42	518.4	76	692.4
9	328	43	521.6	77	697.4
10	340.2	44	523.6	78	704.6
11	346	45	529.4	79	712.2
12	350.2	46	535.8	80	718
13	360.4	47	541.8	81	725.2
14	373.4	48	548.4	82	733.8
15	383.8	49	551	83	739.6
16	386.4	50	554.8	84	748.2
17	388	51	560.6	85	755.8
18	396.4	52	564.8	86	763.2
19	407.4	53	570.6	87	772.4
20	415.4	54	576.4	88	779.6
21	421	55	578.6	89	789.2
22	423	56	581.4	90	795.8
23	425.8	57	587.2	91	806.2
24	430.4	58	592.8	92	814
25	436.8	59	598.8	93	824.2
26	443.6	60	603	94	833.6
27	448.6	61	605.6	95	845.8
28	454.8	62	611.6	96	860.4
29	457.4	63	617.4	97	881
30	459.8	64	624.4	98	908
31	466	65	628.6	99	950.4
32	472.2	66	631.4	99.5	997
33	477.8	67	638		

What is clear from these analyses is that oil compositions may be highly variable from one process to another and from one deposit to another. Measurable differences have been seen between oils produced by the same technology and deposit, but under different process conditions. Differences also exist during the progress of reaction, from beginning to end (data not shown).

Detailed Molecular Composition

The detailed molecular composition of EcoShale 32 is given in Tables 4 (a), 4 (b), 4 (c) and 4 (d). (This is one table, but broken up to fit the pages and make the entries readable.) The values given in the table are in weight percent of the compound type and carbon number indicated. The sum of all carbon numbers is given in the 'totals' column, and is repeated on each part. Dashes "-" found in the

Table 3. Summary of molecular composition

<i>Compound type</i>	<i>EcoShale 32 wt %</i>	<i>Unocal 23</i>	<i>Kukersite (Estonia) wt %</i>
paraffins	26.614	17.454	0.167
olefins	3.546	NA	NA
naphthenes	23.757	26.852	5.474
monoaromatics	4.553	12.122	15.905
diaaromatics	2.941	4.599	12.995
polyaromatics	0.567	1.368	4.909
sulfur compounds	1.821	6.916	3.728
pyrrolics	8.587	10.753	ND
pyridinics	17.706	10.2	ND
phenolics	8.399	1.267	30.717
Unidentified & >C36	1.506	8.471	26.104
Total	99.997	100.002	99.999

NA = not analyzed

ND = non-detect

table indicate that the compound type is infeasible for that carbon number. Zeros “0” indicate that the type and carbon number were sought, but if present, were below the detection limits of the GC-MSD.

Inspection of the table shows that shale oil can be described by homologous series of about 60 z-vectors, or compound types. For the most part, each type shows a single maximum in concentration, although that is not rigorously true for all molecular types. In our experience with a wide range of hydrocarbon mixtures, the total number of different z-vectors found for a variety of crude oils, bitumens and pyrolysis oils is less than about 100.

Discussion

The data shown in the Table 4 (a) imply a precision in analysis that does not, in fact, exist. The ‘cp’ file may contain more than 20,000 lines, and it becomes necessary to work in scientific notation. A higher number of decimal figures is required to avoid rounding discrepancies.

One could argue with the concentration of any one of the entries. However, for sake of instruction, if one entry in the matrix is changed to a different value, then all other entries in the entire table will change slightly. This is because the sum of all the entries must agree with the input data (elemental composition, density, and boiling point distribution). Thus, the quantitative solution is a least-error one, rather than a more deterministic one.

Table 4 (a). Compound type composition of EcoShale 32

Compound Type/number of carbons	Total	3	4	5	6	7	8	9	10
n-paraffins	12.62	0.00074	0.00529	0.0522	0.57	0.443	0.5	0.46	0.415
i-paraffins	13.99	-	0	0.0926	0.186	0.864	1.0999	1.3158	1.85677
monolefins	1.906	0	0.07775	0.0844	0.1132	0.05222	0.24776	0.41258	0.16459
mononaphthenes	5.12	-	-	0.0174	0	0	0.26062	0.36283	0.83718
diolefins	0.355	-	0	0	0	0.01738	0.0007	0.24711	0.08965
cyclomonolefins	0.356	-	-	0	0	0.02865	0.01889	0.03426	0.04901
dinaphthenes	7.671	-	-	-	-	-	0	0.22324	0.00611
triolefins	0.078	-	-	-	0	0	0.00604	0.00942	0.04258
cyclodiolefins	0.546	-	-	0	0	0.00147	0.09579	0.06701	0.2353
dicyclomonolefins	0.305	-	-	-	-	-	-	0.04001	0.20351
trinaphthenes	7.282	-	-	-	-	-	-	-	-
tetranaphthenes	1.927	-	-	-	-	-	-	-	-
pentanaphthenes	1.266	-	-	-	-	-	-	-	-
hexanaphthenes	0.081	-	-	-	-	-	-	-	-
heptanaphthenes	0.41	-	-	-	-	-	-	-	-
monoaromatics	2.068	-	-	-	-	0.00123	0.00257	0.09133	0.16839
vinyl benzenes	0.469	-	-	-	-	-	0.00001	0.02516	0.09907
naphthenomonoaromatics	0.286	-	-	-	-	-	-	0	0.00023
phenyldienes	0.81	-	-	-	-	-	-	-	0
dinaphthenomonoaromatics,indenenes	0.079	-	-	-	-	-	-	0	0
trinaphthenomonoaromatics	0.823	-	-	-	-	-	-	-	-
tetranaphthenomonoaromatics	0.018	-	-	-	-	-	-	-	-
diaromatics	1.828	-	-	-	-	-	-	-	0
acenaphthene/naphthenodiaromatics	0.883	-	-	-	-	-	-	-	-
dinaphthenodiaromatics	0.01	-	-	-	-	-	-	-	-
acenaphthalenes/fluorenes	0.22	-	-	-	-	-	-	-	-
triaromatics	0.33	-	-	-	-	-	-	-	-
naphthenotriaromatics/dihydroxyrenes	0.009	-	-	-	-	-	-	-	-
phenylnaphthalenes	0.159	-	-	-	-	-	-	-	-
tetraaromatics (peri-condensed)	0.006	-	-	-	-	-	-	-	-
tetraaromatics (cata-condensed)	0.029	-	-	-	-	-	-	-	-
naphthenofluorenes	0.001	-	-	-	-	-	-	-	-
pentaaromatics (peri-condensed)	0.033	-	-	-	-	-	-	-	-
naphthenosulfides/thiols	0.646	-	0	0	0	0.00782	0.08357	0.06192	0.01668
dinaphthenosulfides/thiols	0.649	-	-	-	-	-	0	0.01591	0.0263
thiophenes	0.159	-	0	0.00009	0.03345	0.0295	0.00053	0.00745	0.00346
trinaphthenosulfides/thiols	0.135	-	-	-	-	-	-	-	-
thiophenol	0.052	-	-	-	0	0	0	0	0
tetrahydrobenzothiophene	0.081	-	-	-	-	-	0.00002	0.00083	0.00034
tetranaphthenosulfides/thiols	0	-	-	-	-	-	-	-	-
benzothiophenes	0.091	-	-	-	-	-	0	0.00946	0.00482
benzodithiophenes	0.005	-	-	-	-	-	-	-	0
dibenzothiophenes	0	-	-	-	-	-	-	-	-
epithiophenanthrenes	0.002	-	-	-	-	-	-	-	-
benzodibenzothiophenes	0.001	-	-	-	-	-	-	-	-
pyrroles	2.397	-	0	0	0	0.23449	0.10358	0.23953	0.08642
indoles	6.112	-	-	-	-	-	0.00771	0.00755	0.01292
carbazoles	0.002	-	-	-	-	-	-	-	-
4-ring pyrrolics*	0.076	-	-	-	-	-	-	-	-
pyridines	13.63	-	-	0	0	0.49375	0.28503	0.42924	0.2128
quinolines	2.439	-	-	-	-	-	-	0	0.25984
phenanthridines	0.065	-	-	-	-	-	-	-	-
4-ring pyridinics*	1.573	-	-	-	-	-	-	-	-
phenols	4.758	-	-	-	0.00153	0.83679	1.8613	1.31773	0.09966
hydroxy tetralins	0.427	-	-	-	-	-	0	0.02065	0.04076
naphthols	0.933	-	-	-	-	-	-	-	0.4511
dibenzofuran	0	-	-	-	-	-	-	-	-
resorcinols	1.752	-	-	-	0.519	0.57	0.42405	0.1808	0.01932
dihydroxy tetralins	0.529	-	-	-	-	-	-	-	0.04558
unidentified	0.047	0	0	0	0	0	0	0	0
C36+	1.459	-	-	-	-	-	-	-	-

Likewise, if a compound type is not analyzed (such as the olefins for two of the shale oils), to the extent that such compounds exist in the oil, the concentrations of all other compounds are adjusted such that the distribution, properties and elemental composition still agree with the measured values. The consequence is that the composition portrayed is an accurate representation of the important chemical characteristics of the oil. Said another way, if the absolute concentrations of a given species are incorrect, there are offsetting concentrations of other types that keep the file consistent with measured values.

Table 4 (b). Compound type composition of EcoShale 32 (cont.)

Compound Type/number of carbons	11	12	13	14	15	16	17	18
n-paraffins	0.611	0.768	0.718	0.763	0.619	0.667	0.657	0.665
i-paraffins	1.248	1.10436	1.95195	1.5417	1.02604	0.61171	0.38169	0.1781
monolefins	0.182	0.2267	0.1979	0.05774	0.02204	0.03041	0.01491	0.01761
mononaphthenes	0.365	0.1785	0.19049	0.11073	0.37803	0.17858	0.30289	0.17165
diolefins	0	0	0	0	0	0	0	0
cyclomonolefins	0.154	0.07123	0	0	0	0	0	0
dinaphthenes	0.213	0.08683	0.21024	0.73238	0.84685	0.98276	0.74498	0.69734
triolefins	0.02	0	0	0	0	0	0	0
cyclodiolefins	0.146	0	0	0	0	0	0	0
dicyclomonolefins	0.061	0	0	0	0	0	0	0
trinaphthenes	0.019	0.29169	0.58301	1.05526	0.82152	0.81424	0.95462	0.57771
tetranaphthenes	-	-	-	-	-	0.07561	0.15053	0.27978
pentanaphthenes	-	-	-	-	-	-	0	0.46039
hexanaphthenes	-	-	-	-	-	-	-	-
heptanaphthenes	-	-	-	-	-	-	-	-
monoaromatics	0.296	0.35806	0.38682	0.11075	0.0593	0.09069	0.0708	0.01721
vinyl benzenes	0.048	0.21236	0.06844	0.00466	0.00422	0.00798	0	0
naphthenomonoaromatics	7E-04	0.00197	0.00171	0.00132	0.00079	0.00025	0.00055	0.00181
phenyldienes	0.121	0.61227	0.03097	0.03182	0.01095	0.00284	0	0
dinaphthenomonoaromatics,indenes	0.004	0.00045	0.00108	0.00169	0.00078	0.00094	0.00024	0.00391
trinaphthenomonoaromatics	-	-	-	-	0	0	0	0.00018
tetranaphthenomonoaromatics	-	-	-	-	-	-	-	0.00156
diaromatics	0.352	0.52723	0.19058	0.31254	0.23894	0.15778	0.01442	0.00637
acenaphthene/naphthenodiaromatics	-	0.0118	0.1029	0.0013	0.00218	0.00003	0.00597	0.03112
dinaphthenodiaromatics	-	-	-	-	-	0	0	0.00001
acenaphthalenes/fluorenes	-	-	0.00083	0.00101	0.00001	0.00367	0.00054	0.01092
triaromatics	-	-	-	0.00522	0	0	0.00715	0.01278
naphthenotriaromatics/dihydropyrenes	-	-	-	-	-	0.00001	0.00099	0.00205
phenylnaphthalenes	-	-	-	-	-	0.00001	0.00056	0.00259
tetraaromatics (peri-condensed)	-	-	-	-	-	0.00002	0.00003	0.0001
tetraaromatics (cata-condensed)	-	-	-	-	-	-	-	0.00017
naphthenofluorenes	-	-	-	-	0	0	0	0
pentaaromatics (peri-condensed)	-	-	-	-	-	-	-	-
naphthenosulfides/thiols	0.015	0.01132	0.11843	0.11035	0.05229	0.02266	0.01607	0.02608
dinaphthenosulfides/thiols	0.034	0.03927	0.01237	0.00668	0.00073	0.01236	0.10323	0.0663
thiophenes	7E-04	0.00174	0.00214	0.00357	0.00726	0.00078	0.00145	0.00889
trinaphthenosulfides/thiols	0.006	0.00864	0.00899	0.00011	0.00018	0.00293	0.00057	0.01265
thiophenol	0	0.05225	0	0	0	0	0	0
tetrahydrobenzothiophene	0.002	0.00257	0.0094	0.00635	0.00223	0.00282	0.00341	0.02318
trinanaphthenosulfides/thiols	-	-	-	-	0	0	0	0
benzothiophenes	0.004	0.01604	0.00409	0.03164	0.00466	0.00095	0.00125	0.00036
benzodithiophenes	1E-04	0	0	0	0	0	0	0
dibenzothiophenes	-	0	0.00001	0	0	0	0.00001	0.00001
epithiophenanthrenes	-	-	-	0	0	0	0	0
benzodibenzothiophenes	-	-	-	-	-	0	0	0
pyrroles	0.123	0.22043	0.6671	0.25167	0.03844	0.02791	0.03746	0.06033
indoles	0.011	0.00657	0.00381	0.00099	0.02541	0.134	0.297	0.428
carbazoles	-	0.0004	0.00002	0.00002	0.00005	0.00008	0.00008	0.00008
4-ring pyrrolics*	-	-	-	-	-	0.00009	0.00331	0.00601
pyridines	0.347	0.32269	0.25939	0.26161	0.10629	2.86113	0.92857	1.3336
quinolines	0.378	0.16693	0.06949	0.02862	0.0138	0.46495	0.25315	0.2595
phenanthridines	-	-	0	0	0.00088	0.00395	0.005	0.00634
4-ring pyridinics*	-	-	-	-	-	0	0.0273	0.08603
phenols	0.031	0.04166	0.02627	0.0094	0.40532	0.07684	0.05076	0
hydroxy tetralins	0.015	0.04157	0.02781	0.0148	0.14895	0.0809	0.03625	0
naphthols	0.091	0.19752	0.11298	0.06612	0.01414	0	0	0
dibenzofuran	-	-	0.00013	0.00001	0	0	0	0
resorcinols	0.037	0.00073	0.00171	0.00014	0	0	0	0
dihydroxy tetralins	0.004	0.17483	0.20546	0.096	0.00238	0	0	0
unidentified	0	0	0	0	0	0	0	0

A powerful capability of Z-BaSIC is that once a reference ‘cp’ has been created for the basket of compounds found in the oil, then changes in oil composition can be tracked by entering new input data. A file adjuster has been written which allows the concentration of all components to be either increased or decreased over the smallest distance possible to agree with the new measured

Table 4 (c). Compound type composition of EcoShale 32 (cont.)

Compound Type/number of carbons	19	20	21	22	23	24	25	26
n-paraffins	0.655	0.609	0.442	0.39	0.359	0.32	0.333	0.306
i-paraffins	0.271	0.22264	0.02898	0.00971	0	0	0	0
monolefins	0.002	0.00091	0.00107	0	0	0	0	0
mononaphthenes	0.238	0.20957	0.54735	0.153	0.12856	0.10266	0.07772	0.06796
diolefins	0	0	0	0	0	0	0	0
cyclomonolefins	0	0	0	0	0	0	0	0
dinaphthenes	0.527	0.43116	0.44128	0.311	0.2618	0.2047	0.1863	0.1517
triolefins	0	0	0	0	0	0	0	0
cyclodiolefins	0	0	0	0	0	0	0	0
dicyclomonolefins	0	0	0	0	0	0	0	0
trinaphthenes	0.332	0.205	0.2737	0.256	0.23854	0.19291	0.1487	0.11826
tetranaphthenes	0.187	0.35493	0.29247	0.1406	0.1098	0.08581	0.06438	0.04717
pentanaphthenes	0.346	0.2008	0.044	0.0489	0.03785	0.03031	0.02186	0.01566
hexanaphthenes	-	0.00952	0.01485	0.01503	0.01156	0.00889	0.00587	0.00505
heptanaphthenes	-	-	-	0	0.1271	0.09501	0.06368	0.04837
monoaromatics	0.006	0.00349	0.01187	0.0524	0.05034	0.04303	0.04181	0.03749
vinyl benzenes	0	0	0	0	0	0	0	0
naphthenomonoaromatics	0.033	0.02482	0.01818	0.02367	0.02228	0.02188	0.0193	0.01842
phenyldienes	0	0	0	0	0	0	0	0
dinaphthenomonoaromatics,indenes	0.001	0.00235	0.00426	0.00552	0.00569	0.00607	0.00566	0.00551
trinaphthenomonoaromatics	2E-04	0.09061	0.11337	0.11283	0.1002	0.08401	0.06658	0.05813
tetranaphthenomonoaromatics	0.002	0.00193	0.002	0.00197	0.00164	0.00152	0.00123	0.00106
diaromatics	0.003	0.00232	0.00215	0.00206	0.00213	0.00202	0.00188	0.00165
acenaphthene/naphthenodiaromatics	0.045	0.05782	0.06349	0.0603	0.05574	0.05646	0.06905	0.04919
dinaphthenodiaromatics	0.001	0.00113	0.00117	0.00097	0.00085	0.00074	0.00057	0.00042
acenaphthalenes/fluorenes	0.018	0.02246	0.02099	0.02098	0.01784	0.01536	0.01192	0
triaromatics	0.012	0.00962	0.01559	0.01607	0.01707	0.01577	0.01982	0.02298
naphthenotriaromatics/dihydropyrenes	0	0	0	0.00252	0	0	0	0.00223
phenylnaphthalenes	0.003	0.00723	0.00853	0.009	0.00695	0.00786	0.00957	0.01043
tetraaromatics (peri-condensed)	5E-04	0.00031	0.00039	0.00014	0.00015	0.00041	0.00035	0.00027
tetraaromatics (cata-condensed)	3E-04	0.00101	0.00106	0.00183	0.00196	0.00146	0.00098	0.00048
naphthenofluorenes	0	0.00002	0.00006	0.00013	0.00014	0.00014	0.00009	0.00005
pentaaromatics (peri-condensed)	-	0.00001	0.00046	0.00018	0.00012	0.00003	0.00004	0.00071
naphthenosulfides/thiols	0.015	0.0143	0.01052	0.0089	0.00863	0.00804	0.00766	0.00564
dinaphthenosulfides/thiols	0.052	0.04268	0.0368	0.02955	0.02849	0.02693	0.02314	0.0203
thiophenes	8E-04	0.00507	0.00636	0.00452	0.00607	0.00608	0.00559	0.00602
trinaphthenosulfides/thiols	0.01	0.01271	0.01056	0.0086	0.00849	0.00711	0.00597	0.00535
thiophenol	0	0	0	0	0	0	0	0
tetrahydrobenzothiophene	0.013	0.00218	0.00148	0.00131	0.00366	0.00111	0.0013	0.00131
trinanaphthenosulfides/thiols	0	0	0	0	0	0	0	0
benzothiophenes	7E-04	0.00125	0.00072	0.00078	0.0008	0.00098	0.00084	0.00105
benzodithiophenes	0	0	0.00001	0.00001	0.00001	0.00001	0.00002	0.00002
dibenzothiophenes	1E-05	0.00001	0.00002	0.00001	0.00002	0.00002	0.00002	0.00001
epithiophenanthrenes	0	0	0	0.00001	0.00001	0	0.00001	0.00001
benzodibenzothiophenes	1E-05	0	0.00001	0.00001	0.00001	0.00001	0	0
pyrroles	0.021	0.0625	0.0527	0.0385	0.0356	0.0236	0.0159	0.0156
indoles	0.543	0.6304	0.6027	0.5491	0.507	0.40837	0.4204	0.3234
carbazoles	7E-05	0.00006	0.00005	0.00005	0.00005	0.00007	0.00009	0.0001
4-ring pyrrolics*	0.004	0.00547	0.00736	0.00729	0.00867	0.00148	0.00108	0.0008
pyridines	1.741	0.49962	0.391	0.376	0.306	0.339	0.255	0.2368
quinolines	0.059	0.0696	0.06299	0.05807	0.05031	0.04508	0.04328	0.04741
phenanthridines	0.006	0.0055	0.00462	0.00374	0.0029	0.00216	0.00296	0.00396
4-ring pyridinics*	0.181	0.2598	0.341	0.2147	0.0499	0.0413	0.061	0.0606
phenols	0	0	0	0	0	0	0	0
hydroxy tetralins	0	0	0	0	0	0	0	0
naphthols	0	0	0	0	0	0	0	0
dibenzofuran	0	0	0	0	0	0	0	0
resorcinols	0	0	0	0	0	0	0	0
dihydroxy tetralins	0	0	0	0	0	0	0	0
unidentified	0	0	0	0	0	0	0	0

data. By this means insight into the conversion chemistry can be gained by correlating the change in compound types with changes in process conditions.

Molecular composition also gives insight into the conversion chemistry occurring. Rapid heatup results in production of higher molecular weight oils and discourages secondary reactions such as dehydrogenation and condensation

Table 4 (d). Compound type composition of EcoShale 32 (cont.)

Compound Type/number of carbons	27	28	29	30	31	32	33	34	35
n-paraffins	0.271	0.27	0.212	0.169	0.112	0.0779	0.0763	0.0478	0.0586
i-paraffins	0	0	0	0	0	0	0	0	0
monolefins	0	0	0	0	0	0	0	0	0
mononaphthenes	0.046	0.03778	0.03364	0.02162	0.01083	0.01823	0.02816	0.02307	0.02259
diolefins	0	0	0	0	0	0	0	0	0
cyclomonolefins	0	0	0	0	0	0	0	0	0
dinaphthenes	0.108	0.0899	0.06484	0.04531	0.01655	0.00536	0.0191	0.0253	0.0382
triolefins	0	0	0	0	0	0	0	0	0
cyclodiolefins	0	0	0	0	0	0	0	0	0
dicyclomonolefins	0	0	0	0	0	0	0	0	0
trinaphthenes	0.092	0.0817	0.07422	0.07069	0.04475	0.01751	0.01178	0.0056	0.00223
tetranaphthenes	0.036	0.0264	0.02091	0.01499	0.01079	0.00698	0.00701	0.01306	0.00409
pentanaphthenes	0.012	0.00815	0.00709	0.00629	0.00443	0.00455	0.00776	0.00406	0.00579
hexanaphthenes	0.003	0.00182	0.00141	0.00119	0.00087	0.00068	0.00049	0.00062	0.00002
heptanaphthenes	0.031	0.01569	0.01071	0.00674	0.00361	0.00354	0.00206	0.00091	0.0017
monoaromatics	0.034	0.03003	0.03335	0.02831	0.01778	0.01059	0.00534	0.00388	0.00554
vinyl benzenes	0	0	0	0	0	0	0	0	0
naphthenomonoaromatics	0.017	0.0155	0.01623	0.01438	0.00944	0.00689	0.00514	0.00841	0.00198
phenyldienes	0	0	0	0	0	0	0	0	0
dinaphthenomonoaromatics,indenes	0.005	0.00505	0.00523	0.00451	0.00319	0.00209	0.00153	0.00139	0.00058
trinaphthenomonoaromatics	0.042	0.03273	0.02718	0.03033	0.02432	0.01664	0.01946	0.00468	0
tetranaphthenomonoaromatics	8E-04	0.00058	0.00051	0.00055	0.0003	0.0003	0.00022	0.00012	0.00014
diaromatics	0.002	0.00195	0.00187	0.00138	0.00089	0.00044	0.00052	0.00086	0.00172
acenaphthene/naphthenodiaromatics	0.047	0.0455	0.04202	0.03957	0.02745	0.01644	0.01319	0.01336	0.02608
dinaphthenodiaromatics	4E-04	0.00034	0.0003	0.00032	0.00026	0.00031	0.00022	0.00018	0.00013
acenaphthalenes/fluorenes	0.013	0.01414	0.00933	0.00894	0.00644	0.00435	0.00762	0.00605	0.00554
triaromatics	0.021	0.02076	0.01927	0.02112	0.02273	0.02326	0.01586	0.03075	0.00095
naphthenotriaromatics/dihydroxyrenes	6E-04	0.00052	0.00001	0	0	0	0	0	0
phenylnaphthalenes	0.011	0.00709	0.00465	0.01566	0.0193	0.0258	0.00303	0.00395	0.00281
tetraaromatics (peri-condensed)	2E-04	0.00018	0.00058	0.00084	0.00122	0.00014	0.0002	0.00017	0.00014
tetraaromatics (cata-condensed)	7E-04	0.00358	0.00425	0.00657	0.00065	0.00129	0.00133	0.00138	0.00003
naphthenofluorenes	1E-05	0	0	0	0	0	0	0	0
pentaaromatics (peri-condensed)	0.003	0.00572	0.00051	0.00281	0.00664	0.0125	0.00002	0.00047	0.00027
naphthenosulfides/thiols	0.008	0.00271	0.00188	0.00134	0.00147	0.00217	0.00294	0.0034	0.0022
dinaphthenosulfides/thiols	0.017	0.01345	0.01401	0.00966	0.00563	0.00503	0.00417	0.00235	0.00078
thiophenes	0.006	0.00382	0.00283	0.00133	0.00068	0.00006	0.00045	0.00104	0.00146
trinaphthenosulfides/thiols	0.005	0.00464	0.00452	0.00462	0.00214	0.00143	0.0013	0.0018	0.00028
thiophenol	0	0	0	0	0	0	0	0	0
tetrahydrobenzothiophene	0.002	0.00016	0.00017	0.00026	0.00007	0	0	0	0
tetranaphthenosulfides/thiols	0	0	0	0	0	0	0	0	0
benzothiophenes	1E-03	0.00086	0.00059	0.00033	0.0005	0.00075	0.00098	0.00053	0.0008
benzodithiophenes	1E-05	0.00002	0.00001	0.00003	0	0.00053	0.00152	0.00003	0.00309
dibenzothiophenes	0	0	0.00001	0.00002	0.00003	0.00001	0.00002	0.00005	0.00002
epithiophenanthrenes	1E-05	0.00003	0.00005	0.0001	0.00005	0.00015	0.00077	0.00051	0.00001
benzodibenzothiophenes	1E-05	0.00003	0.00005	0.00002	0.00008	0.00035	0.00021	0	0.00003
pyrroles	0.013	0.0118	0.00986	0.00601	0.00063	0.0002	0.00022	0.00017	0.00014
indoles	0.312	0.33389	0.17416	0.17148	0.11525	0.04247	0.01665	0.0145	0.0126
carbazoles	1E-04	0.00014	0.00023	0.00002	0.00002	0.00003	0.00003	0.00003	0.00003
4-ring pyrrolics*	0.003	0.00231	0.00214	0.00187	0.00049	0.00712	0.00239	0.00272	0.00427
pyridines	0.284	0.2736	0.262	0.239	0.1451	0.1813	0.17052	0.0476	0.0409
quinolines	0.036	0.03114	0.02328	0.00159	0.00174	0.0015	0.00311	0.00477	0.00688
phenanthridines	0.004	0.00397	0.0035	0.00394	0.0007	0.00028	0.0002	0.00038	0.00039
4-ring pyridinics*	0.059	0.0518	0.0193	0.0136	0.0219	0.0249	0.0271	0.0329	0
phenols	0	0	0	0	0	0	0	0	0
hydroxy tetralins	0	0	0	0	0	0	0	0	0
naphthols	0	0	0	0	0	0	0	0	0
dibenzofuran	0	0	0	0	0	0	0	0	0
resorcinols	0	0	0	0	0	0	0	0	0
dihydroxy tetralins	0	0	0	0	0	0	0	0	0
unidentified	0	0	0	0	0	0	0	0.0208	0.0259

(coking). Slower heatup results in lower molecular weight compounds being produced, but produces more coke because of the enhanced secondary reactions.

Summary

As the world inevitably moves to produce abundant oil shale resources, details of reaction kinetics, composition, upgrading processes, product development and manufacture will unfold. It may be possible to develop new markets to take advantage of the heteroatom functionalities present. Once production is established, refineries can count on a consistent quality feedstock. Consistency in quality is a characteristic upon which markets place value, as evidenced by the ready marketing at sound prices enjoyed by Alberta syncrudes.

Acknowledgements

The supply of shale oil samples from Red Leaf Resources, Eesti Energia, Viru Keemia Grupp, and Unocal is gratefully acknowledged. Permission from Red Leaf Resources to publish the detailed composition of EcoShale 32 is acknowledged.

The financial support of the US Dept. of Energy contract number DE-AC21-93MC29240 is acknowledged. The authors gratefully acknowledge the on-going encouragement and helpful guidance of the late Hugh Guthrie, DOE COTR, a friend and mentor.

References

1. Bunger, J. W.; Cogswell, D. E.; Russell, C. P. Value-Enhancement Extraction of Heteroatom-Containing Compounds from Kerogen Oil. *Prepr. Am. Chem. Soc., Div. Fuel Chem.* **2001**, *46*, (2), 573–576; July.
2. Bunger, J. W., et al. *Shale Oil Value Enhancement Research*. Final Technical Report, DOE contract DE-AC21-93MC29240, April 2007.
3. Bunger, J. W.; Devineni, P. A. V.; Russell, C. P.; Oblad, A. G. Structure of Future Jet Fuels - A Model for Determining Physical and Chemical Properties from Molecular Structure. *Prepr. Am. Chem. Soc., Div. Pet. Chem.* **1987**, *30*, (1).
4. Devineni, P. A. V.; Bunger, J. W.; Russell, C. P. Prediction of Optimum Structure for JET Fuel Components using the Z-BaSIC Method. *Prepr. Am. Chem. Soc., Div. Pet. Chem.* **1989**, *34*, (4), 858–866.
5. Bunger, J. W.; Russell, C. P.; Cogswell, D. E. Quantitative Description of the Molecular Composition of Crude Oil. *Prepr. Am. Chem. Soc., Div. Pet. Chem.* **2001**, *46* (4), 355–360; August.
6. Koel, M.; Bunger, J. Overview of Program on US-Estonia Science and Technology Cooperation on Oil Shale Research. *Oil Shale* **2005**, *22*, (1), 65–79.

Chapter 6

Chemistry and Kinetics of Oil Shale Retorting

Alan K. Burnham*

American Shale Oil, LLC P. O. Box 1740, Rifle, CO 81650

*e-mail: alan.burnham@idt.net

Oil shale pyrolysis chemistry and kinetics are reviewed, with an emphasis on oil shale from the Green River Formation and work done by Lawrence Livermore National Laboratory during the 1970s and 1980s. Particular attention is given to measuring chemical kinetics of reactions generating oil in various kinds of reactors and of the reactions destroying oil by secondary coking and cracking. In addition, the relationship between the reaction kinetics and various industrial processes is explored, including a classification scheme based on heating method.

Oil shale can be converted to shale oil by many different processes, both *in situ* and *ex situ*. A classification scheme based on heat source and heat transfer method, modified from Burnham and McConaghy (1), is outlined in Table 1 along with examples of various implementations.

Processes differ considerably in the time-temperature-gas environment that the shale experiences, and many of these differences are reflected in the composition of the resulting shale oil, which affects subsequent upgrading and refining needs. Generally, *ex-situ* processes heat the shale faster, and the oil typically has a higher boiling range and higher nitrogen and olefin contents. *In-situ* processes typically heat the shale slower, and coking and cracking reactions decrease yields of heavy ends and polar compounds. Direct combustion processes, both *ex situ* and *in situ*, have lower naphtha content due to more difficult condensation associated with dilution of the offgas with combusted air. Pyrolysis conditions in most current processes and the resulting oil and gas yields fall within the understanding developed by the 1980s, which will be outlined in this paper.

To aid process design and evaluation, chemical kinetic models have been developed by many workers to quantify these changes over a wide range of

Table 1. Classification scheme for various oil shale processes (1)

<i>Heating Method</i>	<i>Above Ground (Ex Situ)</i>	<i>Below Ground (In Situ)</i>
Conduction through a wall (various fuels)	Pumpherson, Fischer assay, Oil-Tech, Hom Tov, EcoShale	Shell ICP (primary method), AMSO CCR, ExxonMobil Electrofrac
Externally generated hot gas	Union B, Paraho Indirect, Superior Indirect, PetroSix	Chevron CRUSH, Petro Probe, Mountain West IGE
Internal combustion	Union A, Paraho Direct, Superior Direct, Kiviter, Fushun	Oxy MIS, LLNL RISE, Rio Blanco, Geokinetics Horizontal
Hot recycled solids (inert or burned shale)	Galoter, Lurgi, Chevron STB, LLNL HRS, Shell Spher, ATP, Tosco II	
Reactive fluids	IGT Hytort, Xtract Technology, Chattanooga Process	Raytheon-CF Technologies
Volumetric heating		ITTRI, LLNL & Raytheon RF, Electro-Petroleum EEOP

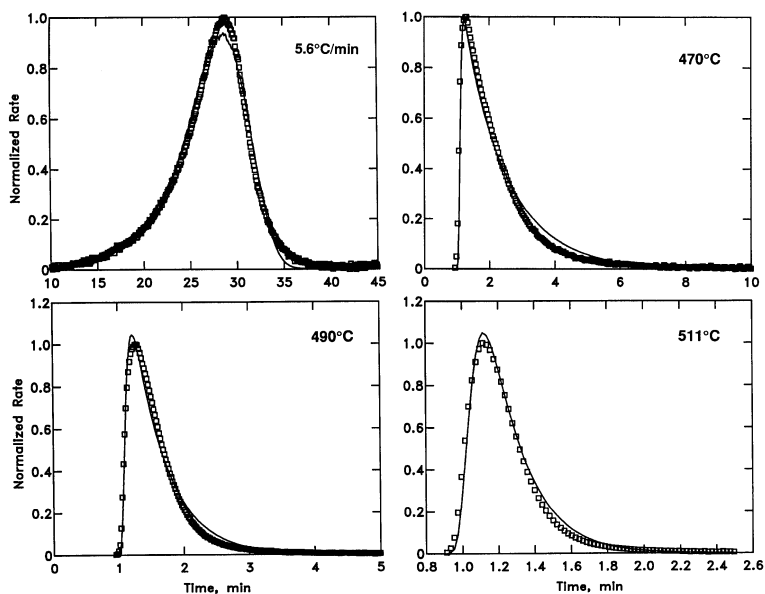
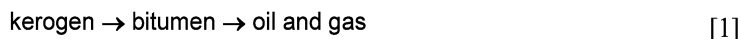


Figure 1. Comparison of a first-order kinetic model with oil and gas generation from Anvil Points oil shale dropped into a preheated bed of fluidized sand. A first-order reaction is mathematically incompatible with mechanism [1] except when bitumen formation is essentially instantaneous. Reproduced courtesy of LLNL from reference (10).

conditions, including corresponding changes in gas composition. In fact, a variety of kinetic models of different complexity were derived, as are described below. The emphasis is on work at Lawrence Livermore National Laboratory. The most detailed model developed for oil shale pyrolysis, which included oil fractions differing in molecular weight and chemical composition, was able to simulate effects of different heating rates and pressures up to 27 atm (2). This model was also applied successfully to oil formation in the Uinta basin (3). Further enhancements to pyrolysis models that are appropriate for application to true *in-situ* processes currently being explored were developed in the late 1980s and early 1990s for petroleum exploration purposes (4, 5), and these improvements should be folded back into the oil shale modeling community.

Kinetics of Oil Generation

One of the earliest kinetic models of oil and gas generation was the sequential reaction model proposed by Hubbard and Robinson (6):



The model was based on the definition that bitumen was the extractable organic matter within the reactor and oil was the condensable material that had escaped the reactor. The sequential model was assumed, because the extractable organic matter within the reactor built up faster than the oil that had escaped. However, it is important to note that the differentiation between bitumen and oil is based on a transport difference, not a chemical difference. There is a difference in average composition, of course, but there is a considerable overlap in the chemical compounds within bitumen and oil.

Braun and Rothman (7) reported a kinetic analysis of the Hubbard-Robinson data, including effects of heat transfer resistance, that yielded kinetic parameters for both bitumen and oil generation assuming the sequential model. Good agreement was shown for oil generation, but it was not noted that agreement was poor for bitumen generation. Subsequently, Ziegel and Gorman (8) showed that agreement with bitumen formation required an alternate pathway model:



More recently, Miknis and Turner (9) report an extensive set of bitumen and oil generation data and discuss the weaknesses of mechanism [1] for explaining their data. They acknowledge mechanism [2] but do not attempt to interpret their data with it.

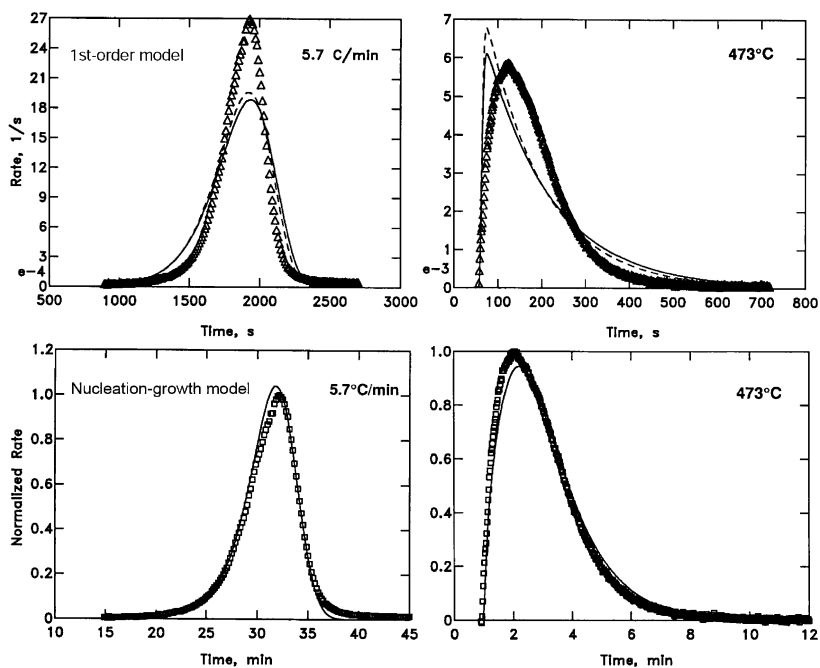


Figure 2. Comparison of first-order and nucleation-growth reaction models with oil and gas generation from Frejus boghead coal dropped into a preheated bed of fluidized sand. The first-order model does not work because of a substantial acceleratory. A nucleation growth model, which is difficult to distinguish from mechanism [1], works well. Reproduced courtesy of LLNL from reference (10).

The most definitive test of mechanisms [1] and [2] comes from a set of isothermal fluidized bed experiments in which the thermal heat-up time is kept small compared to the pyrolysis time (10). Mechanism [1] requires an acceleratory period prior to the maximum rate of oil and gas generation, while mechanism [2] does not. For most oil shales and petroleum source rocks, the maximum rate of oil and gas generation occurs as soon as the sample heats up, as shown in Figure 1 for an Anvil Points oil shale sample. A first-order kinetic model works very well, which is mathematically incompatible with mechanism [1], unless the conversion of kerogen to bitumen is essentially instantaneous.

For well-preserved kerogens in which algal bodies are still easily recognizable, an acceleratory period prior to peak oil and gas generation is usually observed (10). This is similar to pyrolysis characteristics of linear polymers (11). Such data can be fitted equally well with either a sequential model, i.e., mechanism [1], or a nucleation-growth model, as is shown in Figure 2. Nucleation-growth models originated for solid-state reactions with the observation that the reaction starts at a point in space and then grows geometrically in space. There are a variety of nucleation-growth models with different degrees of complexity. An analogous argument can be made for free radical reactions in which a single

initiation reaction can expand its effect through various propagation reactions (10).

Alternatively, Figure 3 shows two simple kerogen structures that can be examples of materials that would follow either mechanism [1] and [2] (11). The linear structure requires multiple bonds to break before a volatile fragment is formed, hence an acceleratory phase. The branched structure can form a volatile fragment by breaking only a single bond, hence a first-order reaction is possible. Walters *et al.* (12) have shown good agreement between a nonisothermal kinetic data and a mechanistic kinetic model based on measured molecular structures, but isothermal pyrolysis characteristics were not published. However, unpublished calculations for the Green River shale indicated that it was close to first-order in an isothermal simulation (Freund, personal communication, 2008).

Despite the overwhelming evidence that mechanism [1] is not correct in most cases, it persists as one of the most commonly cited models. One example is the hydrous pyrolysis work of Lewan and associates (13, 14). Although originally conceived for simulating natural petroleum formation, hydrous pyrolysis is now being considered by some for in-situ oil shale processing. The issue addressed here is not related to whether water participates in the oil generation reactions or the mechanism of expulsion; it is merely that a first-order kinetic analysis based on the appearance of oil is mathematically inconsistent with mechanism [1]. The mathematical issue is removed if one merely acknowledges that oil molecules can be formed either directly from kerogen or from a bitumen intermediate. There is still the issue of whether the typical hydrous pyrolysis data set can distinguish a first-order reaction from a more complicated reaction, but that issue is beyond the scope of this article.

One of the most widely used kinetic expressions in the literature for oil generation kinetics is that of Campbell *et al.* (15) They used a variety of isothermal and nonisothermal experiments. Although their method of using a single heating rate to derive nonisothermal experiment is not generally valid, oil generation from Green River shale is so close to a first-order reaction that it works well. Moreover, their cross-checking with isothermal oil generation experiments verified that assumption. Subsequently, two sets of fluidized-bed kinetic experiments for Green River shale suggested a long-time tail of heavy oil generation (16, 17). However, later experiments showed that the long-time tail was due to adsorption and desorption of heavy oil from dust collected in filters prior to the oil condenser. Oil generation was indeed first-order once that artifact was removed (18).

There have been problems historically in the literature in which kinetics from one apparatus do not agree well with those from another or that kinetics and where kinetics derived from isothermal experiments do not agree with those from nonisothermal experiments. The reasons for these problems are too numerous to describe in detail, but they generally result from poor temperature measurements (e.g., ignoring thermal gradients or finite heatup times) or poor kinetic analysis methods. Particularly egregious is the use of a single nonisothermal heating rate along with the assumption of a particular kinetic model. This common practice in the thermal analysis community motivated a kinetic analysis round robin and a publication stating unequivocally that multi-thermal heating methods are needed

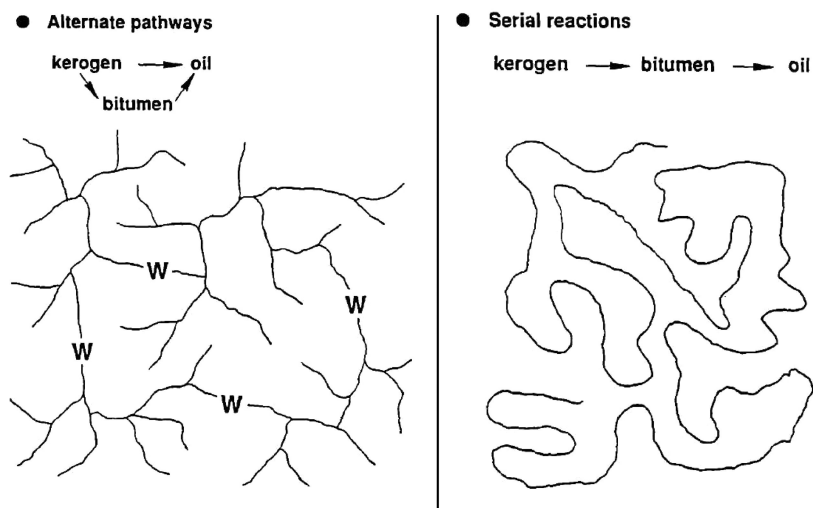


Figure 3. Two hypothetical kerogen structures that are compatible with mechanisms [1] and [2]. “W” represents an occasional weak link that would provide soluble but non-volatile fragments contributing to bitumen formation. Reproduced courtesy of LLNL from reference (11).

to derive valid kinetics (19). In addition, careful temperature measurements and proper kinetic analysis yield kinetic parameters that work for both isothermal and constant heating rates, as shown in Figures 1 and 2.

These problems were addressed thoroughly in the petroleum basin modeling community, which saw the need for methods that resulted in kinetic parameters able to extrapolate far outside their time-temperature range of measurement. Two similar instruments, Rock-Eval™ apparatus of various generations from the Institute Francais du Petrol (20), and the Pyromat™ from Lab Instruments (21, 22), were used extensively in this effort. A very wide range of petroleum source rocks were examined, which more than spans the range kerogen types in oil shales around the world. Marine kerogens typically required the use of distributed reactivity models, usually implemented via an activation energy distribution. Lacustrine kerogens are more typically close to a single first-order reaction. Particularly well-preserved algal kerogens required sequential reaction or nucleation-growth kinetics, as noted in Figure 2.

Workers at LLNL went one step further, seeking to relate the petroleum generation kinetic methods back to methods use more traditionally for oil shale processing (23, 24). Two methods examined in detail were the programmed microcopyrolysis (Pyromat II) and a Fischer-Assay-like apparatus, as shown in Figure 4. Also shown in Figure 4 is the fluidized-bed apparatus used for the data in Figures 1 and 2. The kinetics from all three methods agree well (22–24). The cumulative oil generation calculated from the Pyromat kinetics is compared to that measured from the self-purging reactor in Figure 5 for a variety of oil shales and petroleum source rocks. The agreement is excellent.

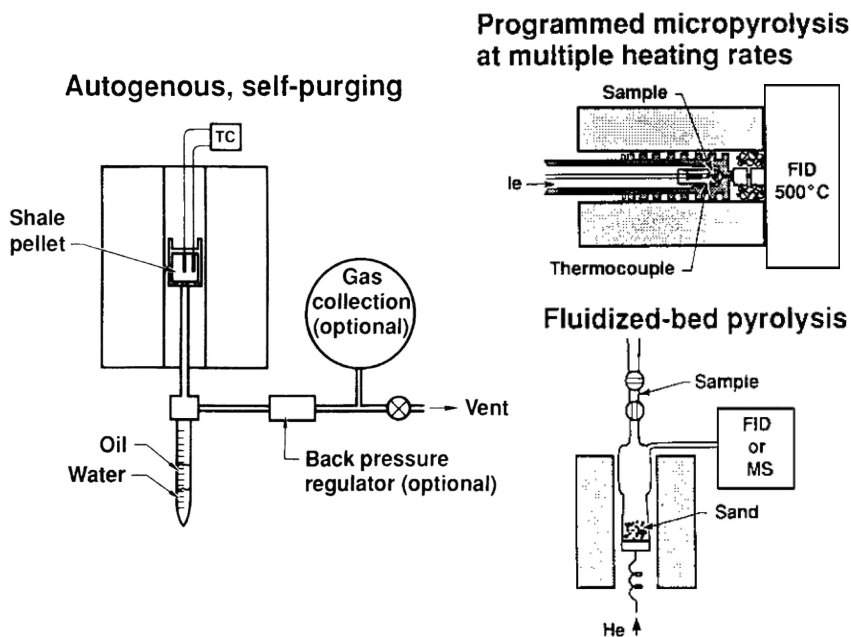


Figure 4. Three apparatus used to measure oil shale pyrolysis kinetics at LLNL. Adapted courtesy of LLNL from reference (23).

Kinetics of Gas Generation

Gas is cogenerated with oil from kerogen and from various minerals, and gas generation continues after oil generation is completed. The first extensive study of gas generation kinetics for oil shale was by Campbell *et al.* (25, 26), and later work at LLNL improved that method and characterized a wide variety of oil shales, petroleum source rocks, and coals (27–36). A few early selected results are shown in Figure 6. The three materials shown are representative of the range observed in subsequent work.

There are several general observations from these many measurements. Methane and hydrogen have more complex evolution profiles than do oil or tar. Evolution of hydrogen continues to a higher temperature than methane. The first peak (or shoulder) for methane and hydrogen occurs at a similar but slightly higher temperature than for oil or tar, and the prominence of the first peak in methane and hydrogen profiles is greater for kerogens with higher hydrogen content (typically lacustrine). There are small differences in the peaks of various light hydrocarbons, and propane and butane correspond closely to oil.

There is usually a single small peak for carbon monoxide with a maximum at a temperature similar to that for oil (27). Siderite, when present, generates a CO peak at a slightly higher temperature (33). Carbon dioxide evolution profiles are more complex and usually start at a lower temperature than for oil. Dawsonite and siderite (or ferroan), when present, have peak CO₂ generation rates roughly 100 °C lower (29) and 50 °C higher (27), respectively, than for kerogen

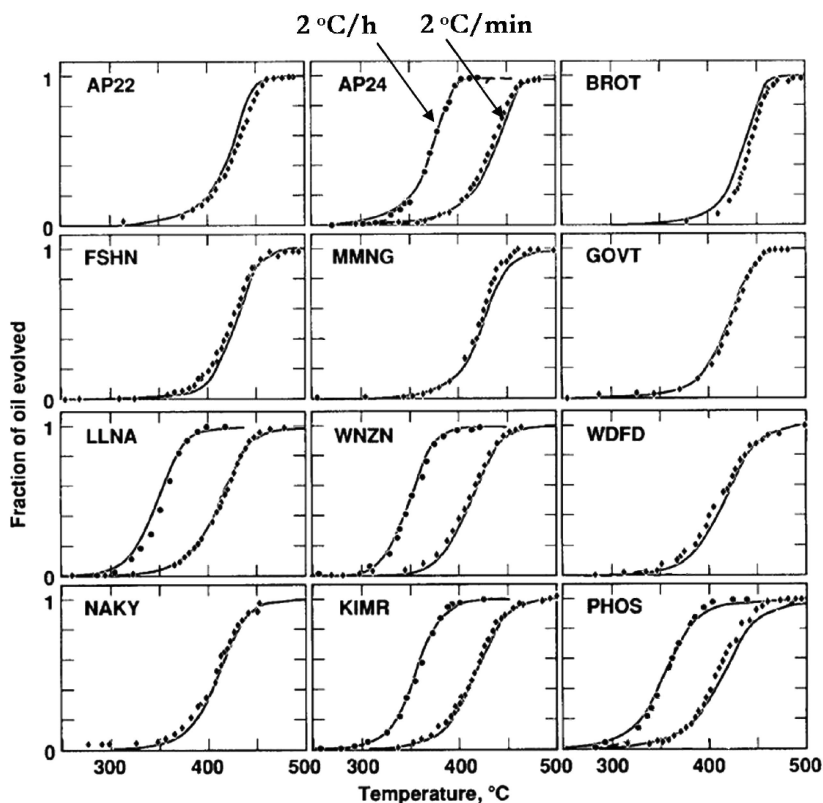


Figure 5. Comparison of oil evolution measured from a Fischer-Assay-like apparatus with that calculated from kinetics measured from programmed micropyrolysis. Measurements were made for all samples at 2 °C/min and for some samples at 2 °C/h, also. Samples: AP22 and AP24 are from Anvil Points Mine in Colorado; BROT and GOVT are from wells in the Uinta Basin; FSHN and MMNG are from China; LLNA is from Venezuela, WNZN is from Germany; WDFD, NAKY, and PHOS are from the eastern United States, and KIMR is from a well in the North Sea. Adapted courtesy of LLNL from reference (24).

pyrolysis. Hydrogen sulfide is also generated from kerogen decomposition, but most H₂S comes from reaction of organic matter with pyrite, so the story is much more complicated (34). Organic sulfur gases evolve at a temperature similar to hydrocarbons, while COS profiles are more similar to H₂S profiles and are obviously affected by gas-phase shift reactions (33, 35). Dolomite and calcite decomposition and the associated char gasification dominate higher temperature gas evolution (37–39).

Under isothermal conditions (Figure 7), the first gas to reach its maximum generation rate is CO₂, which is consistent with its earlier peak under a constant heating rate. Methane peaks shortly thereafter, and there is a shoulder for hydrogen generation. The substantial time lag prior to the maximum rate of hydrogen production compared to other gases indicates that it is not a primary

product of kerogen decomposition and is instead generated by secondary reactions of primary products, such as retrograde condensation (coking) reactions.

Kinetics of Oil Degradation

Both the yield and composition of oil depend on the heating conditions the oil shale and shale oil experience prior to quenching. Corresponding changes occur in gas composition, including the addition of gas from decomposition of carbonate minerals, if present, at temperatures higher than needed to pyrolyze kerogen.

Changes in oil yield and composition can be related to three classes of reactions: coking, cracking, and hydrogenation. Coking involves retrograde condensation reactions in the liquid phase when the generation temperature is low and oil tends to have a long liquid-phase residence time in the rock prior to evaporation and evolution from the reactor. Cracking involves the scission of carbon-carbon bonds in long chain alkyl groups, either in alkanes or alkyl-aromatics. Hydrogenation reactions occur under high pressure conditions, with autogenous or added hydrogen, and modify the coking and cracking reactions that occur at atmospheric pressure. Olefin content decreases, but depending upon the conditions, the heteroaromatic content can either increase or decrease. A qualitative representation of the coking and cracking mechanisms is shown in Figure 8.

The nature of oil coking was established most clearly by work at LLNL (40–42) and subsequent similar experiments at IMMR (43). The stoichiometry and an empirical kinetic model of oil coking were developed from a combination of pyrolysis and distillation experiments and different heating rates, e.g., Figure 9. The principal product of oil coking is a carbonaceous residue, and the amount of oil coking is independent of particle size in the absence of an external sweep gas. Hydrogen content in the oil increases and nitrogen content decreases. For Green River shale, the empirical formula of the oil that cokes, as determined by the change in oil composition versus yield loss, is $\text{CH}_{0.99}\text{N}_{0.38}$, compared to an empirical formula of $\text{CH}_{1.63}\text{N}_{0.19}$ for Fischer Assay oil. Methane and hydrogen are the principal gases formed from oil coking. The critical temperature for oil coking is between 250 and 400 °C, depending upon holding time. At lower temperatures, oil is not generated, and at higher temperatures, oil is generated in the gas phase and escapes from the reactor. Coking during shale oil distillation follows coking during oil generation from shale particles of all sizes. A gas sweep largely eliminates oil coking in fine particles by helping the oil evaporate. High pressure hydrogen acts to both inhibit coking and aromatization reactions (42, 44), as shown in Figure 10.

Later work determined the stoichiometry and kinetic models of oil cracking (45, 46). The principal product of oil cracking is lower molecular weight molecules, both liquid and gas. The boiling point distribution and hydrogen content of the oil decreases and the nitrogen content increases, just the opposite as for oil coking. Isoprenoid/normal and normal/aromatic ratios decreased with

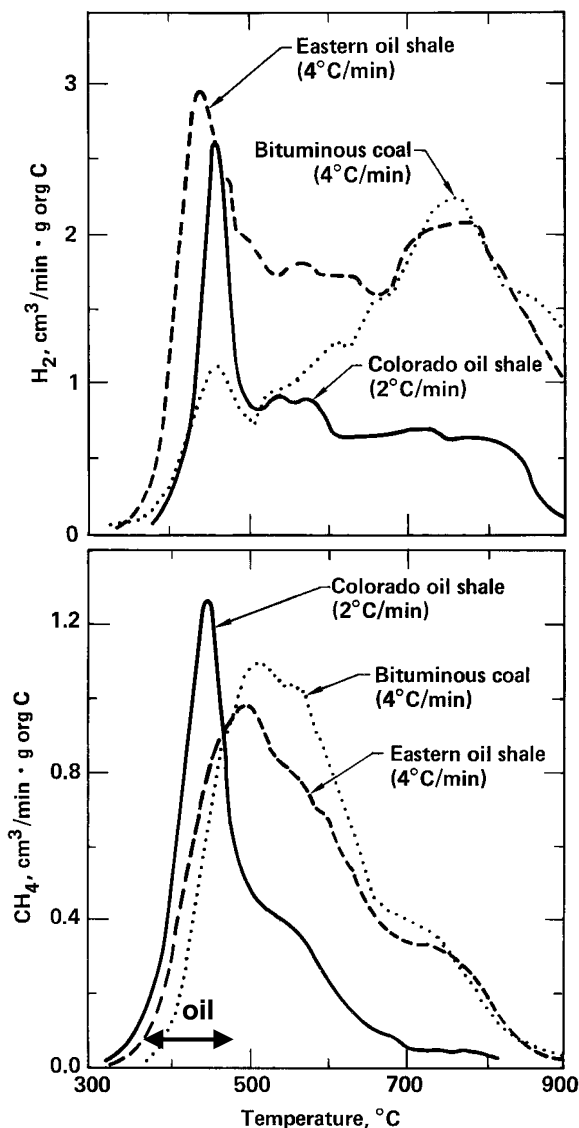


Figure 6. Comparison of methane and hydrogen evolution profiles for oil shale and coal heated at 2 or 4 °C/min. The eastern oil shale profile represents Ohio and Sunbury shales of Devonian-Mississippian age. Adapted courtesy of LLNL from reference (28).

severity. At high severity, Figure 11 shows that oil yield asymptotes to about 20% of the Fischer Assay yield, which roughly corresponds to the original aromaticity.

This mechanistic understanding was incorporated at the pseudo-component level into a detailed kinetic model (2). That model could match not only the atmospheric-pressure experiments (40, 41), as shown in Figure 12, but also the oil yield and composition from another set of experiments in which a back

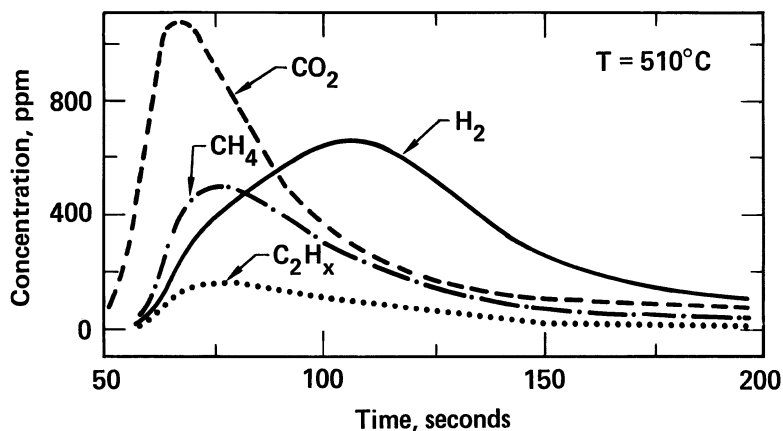


Figure 7. Generation rate of gases during fluidized-bed isothermal pyrolysis of Colorado oil shale at 510 °C. Adapted courtesy of LLNL from reference (28).

pressure regulator set at 375 psig was used to increase the residence time of generated oil in the heated zone, as shown in Figure 13 (47). No other published model has achieved agreement with experiment over such a broad range of conditions. In fact, the inability of the model to match the gas yields from the 375 psig experiments confirmed suspicions from material balance that a significant amount of gas, particularly hydrogen, leaked out of the collection system in those experiments. For conditions of interest to in-situ conversion process, the percentage of organic carbon being converted to C₅+ oil and char are approximately 46% and 35%, respectively. From material balance considerations, one can estimate that 19% of the raw-shale organic carbon is converted into gas. Consequently, gas constitutes about 30% of the volatile hydrocarbon products. Ammonia and hydrogen sulfide from organic and mineral sources increase the total gas yield by about a third, so the mass yield of gas is approximate half that of oil, which is substantially greater than for Fischer Assay.

While the LLNL work on Green River Shale is probably the most extensive collection of oil shale pyrolysis experiments, work on the Eastern U.S. Devonian shales, particularly at the University of Kentucky Center of Applied Research (formerly IMMR), is a close second. These shales are of marine origin and have lower initial hydrogen content more typical of a petroleum source rock. A smaller fraction of kerogen is converted to oil under Fischer Assay conditions, and the oil yield is more sensitive to heating rate than Green River Shale. Gas sweep inhibits oil yield loss as for Green River shale, and high pressure hydrogen provides a much greater increase in oil yield. Consequently, retort processes using high pressure hydrogen are much more advantageous for Eastern U.S. Devonian shale or most like for any other type II shale, typically marine deposition.

Correlations were also developed during the 1970s and 1980s between molecular markers in the oil and yield losses. Coking losses correlated with alkene/alkane ratios (48) and combustion losses correlated with naphthalene content (49). This method was used to separate yield losses due to chemical

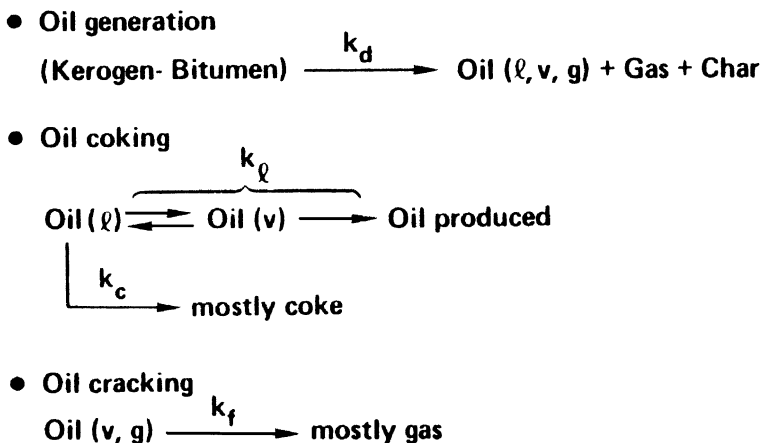


Figure 8. Qualitative mechanism for oil generation and degradation developed at LLNL in the 1970s and early 1980s. Adapted courtesy of LLNL from reference (45).

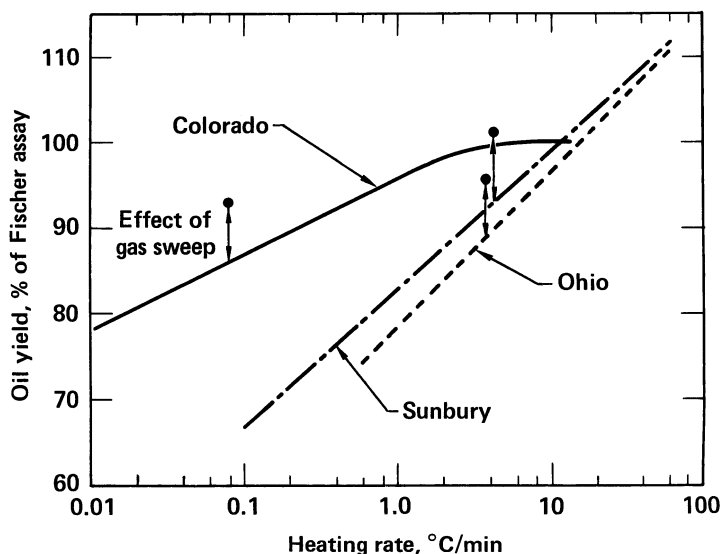


Figure 9. Summary plot of the effect of oil yield on heating rate for eastern and western US oil shales. Adapted courtesy of LLNL from reference (28).

means from those caused by sweep inefficiencies in modified in-situ retorts (50, 51). Similar correlations involving aromatic and isoprenoid compounds were developed for oil cracking losses in non-combustion retorts (46).

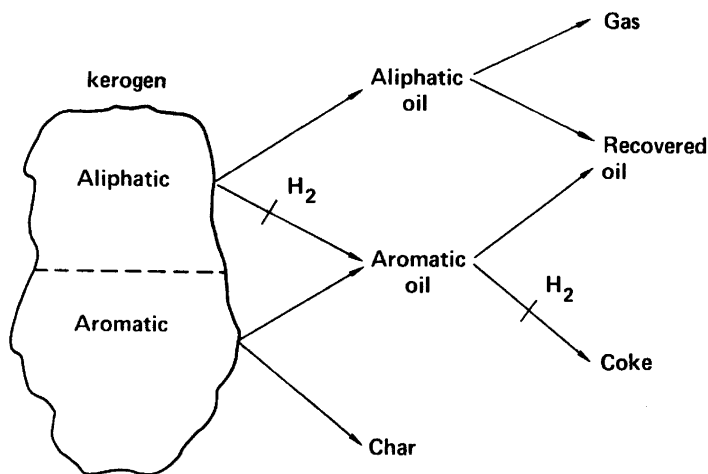


Figure 10. Schematic representation of the effects of high pressure hydrogen on the pyrolysis yields of oil and carbonaceous residue. Reproduced courtesy of LLNL from reference (42).

Recent In-Situ Processes

In-Situ Processing of oil shale has recently experienced a renaissance, primarily due to the work of Shell Oil. Shell has done extensive laboratory and field work (52, 53) directed towards demonstrating commercial viability of a true-in-situ retorting process using electric heaters similar to that developed during World War II in Sweden (54, 55). However, Shell's process incorporates much more modern technology, particularly with the use of an ice-wall to isolate the retort from groundwater in the permeable leached zone of the Green River formation. For this formation, the freeze wall is established, the water pumped out, the oil generated, and the residual shale cleaned of contaminants by flushing with cleaned water. The recovered oil has an API gravity is about 40 deg, which is the same as obtained by Burnham and Singleton at 1 °C/h and 27 bar. The boiling point distribution is also close that obtained by Burnham and Singleton, as shown in Figure 14.

Another advantage of slow, true-in-situ processing is that oil contains substantial less heteroatoms and metals. Burnham and Singleton found that the nitrogen and sulfur content was reduced by nearly two-fold compared to Fischer Assay by the coking and cracking reactions at 1 °C/h and 27 bar, and this benefit is demonstrated in Table 2 for both Equity BX oil, produced by superheated steam injection, and Shell ICP compared to typical superheated steam injection, and Shell ICP compared to typical aboveground processes. As and Fe levels are also reduced substantially by slow in-situ production. Ni and V may be reduced as well, but the limited available data is less clear on that issue.

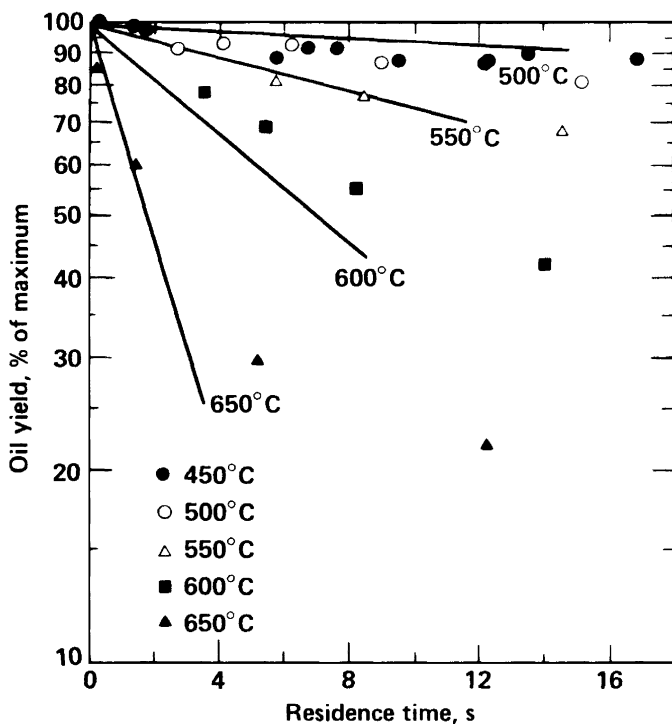


Figure 11. Oil yield as a function of cracking of the generated oil in a secondary reactor at various temperatures and residence times. The lines represent a first-order reaction, and the data clearly show a deceleratory reaction with an asymptotic yield of about 20 wt% of Fischer assay. Reproduced courtesy of LLNL from reference (46).

Other companies are also pursuing true-in-situ retorting in Colorado's Piceance Basin: ExxonMobil, Chevron, and AMSO. The AMSO process evolved from the original concept of EGL Resources (59) and is described in detail in an accompanying paper in this volume. Heat is distributed through the formation by refluxing oil, and permeability for the convective heat transfer is created by thermo-mechanical fracturing. Similar retorting times and pressures are expected to the Shell ICP process.

The most similar method to the Shell ICP is ExxonMobil's Electrofrac process (60). Calcined petroleum coke spheres are pumped into vertical hydrofractures to create a series of parallel plate electric heaters. As in the Shell ICP, the resistive heat reaches the oil shale mass by thermal diffusion. The advantage of the Electrofrac process is that the thermal diffusion time per well is smaller because of the greater surface area of a planar heater than a line source. However, the Electrofrac process is not applicable to the leached zone due to its high permeability, and ExxonMobil is targeting the saline zone with this technology. The overall process includes soda ash recovery.

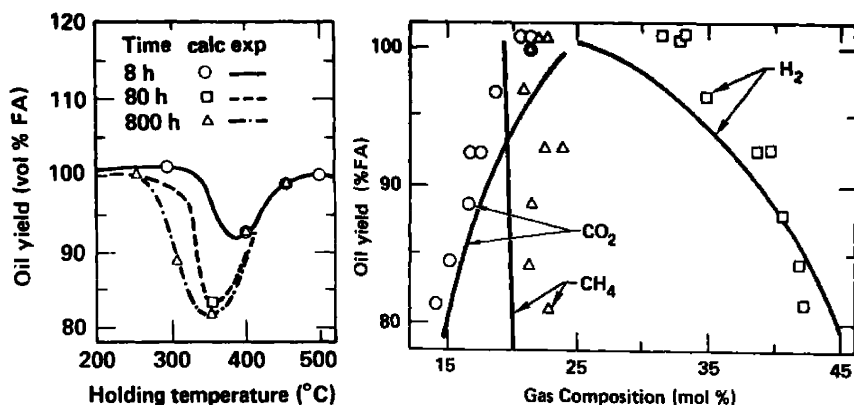


Figure 12. Comparison of calculated (2) and measured (40) oil yields and gas composition for experiments in which the heating at 12 °C/min to 500 °C was interrupted at various temperatures for various lengths of time. Reproduced courtesy of LLNL from reference (2).

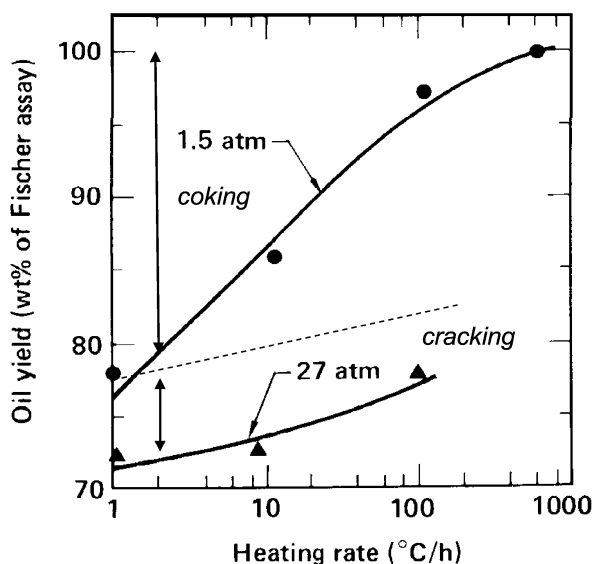


Figure 13. Comparison of calculated (2) and measured (47) oil yields as a function of heating rate at two pressures. The gas atmosphere in both cases was pyrolysis gas. Adapted courtesy of LLNL from reference (47).

The most different process being pursued is Chevron's CRUSH process (61). Permeability is created in the mahogany zone by a proprietary fracturing method. Organic matter is extracted from the fractured rock at a lower temperature than required by pyrolysis using supercritical extraction. Heat is created by burning

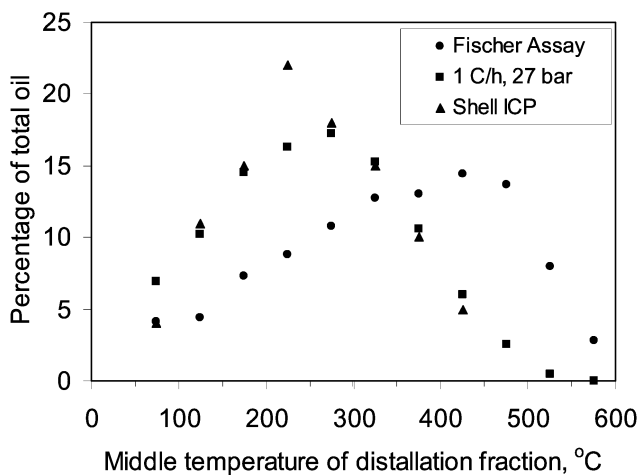


Figure 14. Distillation characteristics of Shell ICP oil compared to 1983 experiments of Burnham and Singleton (47).

Table 2. Concentrations of various elements in shale oil (56–58)

Oil Source	As ppm	Fe ppm	Ni ppm	V ppm	S Wt%	N Wt%	API gravity
Shell ICP		9	1	1	0.5	1.0	38
BX 100 (4/8/82)	0.1	4	8.1	1.1	0.3	0.8	37
BX 101 (8/24/82)	0.8	5	3.8	0.3	0.2	0.5	45
Gas Combustion	~30	108	6.4	6	0.7	2.1	20
TOSCO II	14	100	6	3	0.9	1.9	21
Unocal	~50	55	4	1.5	0.9	2.0	19
Paraho	22	38	3.3	0.3	0.6	2.1	20

the residual char in a spent retort and pumping it into an adjacent newly fractured retort.

Concluding Comments

Pyrolysis of oil shale was taken to a fairly advanced understanding during the 1970s and early 1980s. Mathematical modeling of pyrolysis kinetics and entire retorting processes reached a fairly sophisticated level. Subsequently, organic geochemists expanded the understanding of pyrolysis chemistry and kinetics and associated modeling for the related application of petroleum formation and basin modeling. Consequently, any new oil shale pyrolysis studies must pass over a relatively high bar to provide any new understanding of oil shale retorting. Even

so, advanced mechanistic understanding and modeling could advance the state of the art for those who understand what has been done in the past.

A major difference between today's oil shale activities and those of the 1970s and 1980s is the prominence of true in-situ methods, particularly the Shell ICP. Even though the products from such products are as expected from work prior to 1985, the technology has improved because of advances in engineering methodology, particularly drilling. Consequently, the current thrust in oil shale may finally crack the barrier of economic production, particularly given the imminent peak production of conventional crude oil.

References

1. Burnham, A. K.; McConaghy, J. M. Comparison of the Acceptability of Various Oil Shale Processes. 26th Oil Shale Symposium, Colorado School of Mines, Golden, CO, 2007; available on CD in Document CERI 2007-3.
2. Burnham, A. K.; Braun, R. L. *In Situ* **1985**, *9*, 1–23.
3. Sweeney, J. J.; Burnham, A. K.; Braun, R. L. *AAPG Bull.* **1987**, *71*, 967–985.
4. Braun, R. L.; Burnham, A. K. *Org. Geochem.* **1992**, *19*, 161–172.
5. Sweeney, J. J.; Braun, R. L.; Burnham, A. K. *AAPG Bull.* **1985**, *79*, 1515–1532.
6. Hubbard, A. B.; Robinson, W. E. *Thermal Decomposition Study of Colorado Oil Shale*, U.S. Bureau of Mines, Report Inv. 4744, 1950.
7. Braun, R. L.; Rothman, A. J. *Fuel* **1975**, *54*, 129–131.
8. Zeigel, E. R.; Gorman, J. W. *Technometrics* **1980**, *22*, 139–151.
9. Miknis, F. P.; Turner, T. F. In *Composition, Geochemistry and Conversion of Oil Shales*; Snape, C., Ed.; NATO ASI Series, Vol. 455; Kluwer: Dordrecht, 1995; pp 295–311.
10. Burnham, A. K.; Braun, R. L.; Coburn, T. T.; Sandvik, E. I.; Curry, D. J.; Schmidt, B. J.; Noble, R. A. *Energy Fuels* **1996**, *10*, 49–59.
11. Burnham, A. K.; Braun, R. L.; Taylor, R. W.; Coburn, T. T. *Prepr. - Am. Chem. Soc., Div. Pet. Chem.* **1989**, *34* (1), 36–42.
12. Walters, C. C.; Freund, H.; Keleman, S. R.; Peczak, P.; Curry, D. J. *Org. Geochem.* **2007**, *38*, 306–322.
13. Lewan, M. D. *Philos. Trans. R. Soc. London* **1985**, *315A*, 123–134.
14. Ruble, T. E.; Lewan, M. D.; Philp, R. P. *AAPG Bull.* **2001**, *85*, 1333–1371.
15. Campbell, J. H.; Koskinas, G. J.; Stout, N. D. *Fuel* **1978**, *57*, 372–376.
16. Wallman, P. H.; Tamm, P. W.; Spars, B. G. In *Oil shale, Tar Sands, and Related Materials*; ACS Symposium Series 163; Stauffer, H. C., Ed.; American Chemical Society: Washington, DC, 1981; pp 93–114.
17. Braun, R. L.; Burnham, A. K. *Fuel* **1986**, *65*, 218–222.
18. Coburn, T. T.; Taylor, R. W.; Morris, C. J.; Duval, V. In *Proceedings of the International Conference on Oil Shale and Shale Oil (21st Oil Shale Symp.)*; Yajie, Z., Ed.; Chemical Industry Press: Beijing, 1988; pp 245–252.
19. Brown, M. E.; Maciejewski, M.; Vyazovkin, S.; Nomen, R.; Sempere, J.; Burnham, A. *Thermochim. Acta* **2000**, *355*, 125–143.

20. Ungerer, P.; Pelet, R. *Nature* **1987**, 327, 52–54.
21. Burnham, A. K.; Braun, R. L.; Gregg, H. R.; Samoun, A. M. *Energy Fuels* **1987**, 1, 452–458.
22. Braun, R. L.; Burnham, A. K.; Reynolds, J. G.; Clarkson, J. E. *Energy Fuels* **1991**, 5, 192–204.
23. Burnham, A. K.; Braun, R. L. *Org. Geochem.* **1990**, 16, 27–39.
24. Burnham, A. K. *Energy Fuels* **1991**, 5, 205–214.
25. Campbell, J. H.; Koskinas, G. J.; Gallegos, G.; Gregg, M. *Fuel* **1980**, 59, 718–726.
26. Campbell, J. H.; Gallegos, G.; Gregg, M. *Fuel* **1980**, 59, 727–732.
27. Huss, E. B.; Burnham, A. K. *Fuel* **1982**, 61, 1188–1196.
28. Burnham, A. K.; Richardson, J. H.; Coburn, T. T. In *Proceedings of the 17th Intersociety Energy Conversion Engineering Conference*; IEEE Publishing: New York, 1982; Vol. 2, pp 912–917.
29. Burnham, A. K.; Huss, E. B.; Singleton, M. F. *Fuel* **1983**, 62, 1199–1204.
30. Coburn, T. T. *Energy Sources* **1983**, 7, 121–150.
31. Oh, M. S.; Coburn, T. T.; Crawford, R. W.; Burnham, A. K. In *Proceedings of the International Conference on Oil Shale and Shale Oil (21st Oil Shale Symp.)*; Yajie, Z., Ed.; Chemical Industry Press: Beijing, 1988; pp 245–252.
32. Burnham, A. K.; Oh, M. S.; Crawford, R. W.; Samoun, A. M. *Energy Fuels* **1989**, 3, 42–55.
33. Reynolds, J. G.; Crawford, R. W.; Burnham, A. K. *Energy Fuels* **1991**, 5, 507–523.
34. Burnham, A. K.; Kirkman Bey, N.; Koskinas, G. J. In *Oil Shale, Tar Sands, and Related Materials*; ACS Symposium Series 163; Stauffer, H. C., Ed.; American Chemical Society: Washington, DC, 1981, pp 61–77.
35. Wong, C. M.; Crawford, R. W.; Burnham, A. K. *Anal. Chem.* **1984**, 56, 390–395.
36. Wong, C. M.; Crawford, R. W.; Burnham, A. K. *Pepr. Symp. - Am. Chem. Soc., Div. Fuel Chem.* **1984**, 29 (3), 317–321.
37. Campbell, J. H. *The Kinetics of Decomposition of Colorado Oil Shale: II. Carbonate Minerals*; Lawrence Livermore National Laboratory Report UCRL-52089 Pt. 2, Livermore, CA, 1978.
38. Burnham, A. K.; Stubblefield, C. T.; Campbell, J. H. *Fuel* **1980**, 59, 871, 877.
39. Burnham, A. K.; Koskinas, G. J. *Effect of Oil-Shale Grade on Carbonate-Decomposition Rates in an Autogenous Atmosphere*; Lawrence Livermore National Laboratory Report UCID-18708; Livermore, CA, 1980.
40. Stout, N. D.; Koskinas, G. J.; Raley, J. H.; Santor, S. D.; Opila, R. L.; Rothman, A. J. *Quart. Colo. Sch. Mines* **1986**, 71, 153–172.
41. Campbell, J. H.; Koskinas, G. J.; Stout, N. D.; Coburn, T. T. *In Situ* **1978**, 2, 1–47.
42. Burnham, A. K.; Happe, J. A. *Fuel* **1984**, 63, 1353–1356.
43. Rubel, A. M.; Coburn, T. T. In *Proceedings of the 1981 Eastern Oil Shale Symposium*; Kentucky Institute of Mining and Mineral Research: Lexington, KY, 1981; pp 21–30.
44. Herschkowitz, F.; Olmstead, W. N.; Rhodes, R. P.; Rose, K. D. In *Geochemistry and Chemistry of Oil Shales*; ACS Symposium Series 230;

- Miknis, F. P., McKay, J. F., Eds.; American Chemical Society: Washington, DC, 1983; pp 301–316.
45. Burnham, A. K. In *Oil Shale, Tar Sands, and Related Materials*; ACS Symposium Series 163; Stauffer, H. C., Ed.; American Chemical Society: Washington, DC, 1981; pp 39–60.
 46. Bissell, E. R.; Burnham, A. K.; Braun, R. L. *Ind. Eng. Chem. Proc. Des. Dev.* **1985**, *24*, 381.
 47. Burnham, A. K.; Singleton, M. F. In *Geochemistry and Chemistry of Oil Shales*; ACS Symposium Series 230; Miknis, F. P., McKay, J. F., Eds.; American Chemical Society: Washington, DC, 1983; pp 335–351.
 48. Coburn, T. T.; Bozak, R. E.; Clarkson, J. E.; Campbell, J. H. *Anal. Chem.* **1978**, *50*, 958–962.
 49. Burnham, A. K.; Clarkson, J. E. In *13th Oil Shale Symposium Proceedings*; Gary, J. H., Ed.; Colorado School of Mines Press: Golden, CO, 1980; pp. 269–280.
 50. Tyner, C. E.; Parrish, R. L.; Major, B. H.; Lekas, J. M. In *15th Oil Shale Symposium Proceedings*; Gary, J. H., Ed.; Colorado School of Mines Press: Golden, CO, 1982; pp 370–384.
 51. Bickel, T. C. Analysis of Occidental Vertical Modified in Situ Retorts 7 and 8. *16th Oil Shale Symposium Proceedings*; Gary, J. H., Ed.; Colorado School of Mines Press: Golden, CO, 1983; pp 281–295.
 52. Vinegar, H. Shell's in-Situ Conversion Process. Presented at the 26th Oil Shale Symposium, Colorado School of Mines, Golden, CO, 2006; available on CD in Document CERI 2007-3.
 53. Beer, G.; Zhang, E.; Wellington, S.; Ryan, R.; Vinegar, H. Shell's in-Situ Conversion Process—Factors Affecting the Properties of Produced Shale Oil. Presented at the 28th Oil Shale Symposium, Colorado School of Mines, Golden, CO, 2008.
 54. Ljungstrom, F. Method of Electrothermal Production of Shale Oil. U.S. Patent 2634961, 1953.
 55. Weddige The gasification of oil-shale underground at Kvarntorp in central Sweden. *Gluckauf* **1955**, *91*, 778–781 (translated by S. Klosky, September 1955, U.S. Bureau of Mines).
 56. Johnson, H. R.; Crawford, P. M.; Bunger, J. W. *Strategic Significance of America's Oil Shale Resource. Vol. II. Oil Shale Resources, Technology and Economics*; U.S. Department of Energy: Washington, DC, 2004; pp 20–21.
 57. Paraho Commercial Feasibility Study, Description of Commercial Operations, Final Report Vol. 2-B, Contract DE-FG010RA50385.
 58. Huffman Laboratories analysis of Equity BX oil samples provided by American Shale Oil, LLC, 2008.
 59. Harris, H. G.; Lerwick, P.; Vawter, R. G. In Situ Method and System for Extraction of Oil from Shale. U.S. Patent Application US 2007/0193743 A1, August 23, 2007.
 60. Symington, W. A.; Olgaard, D. L.; Otten, G. A.; Phillips, T. C.; Thomas, M. M.; Yeakel, J. D. ExxonMobil's Electrofrac Process for in-Situ Oil Shale Conversion. Presented at the 26th Oil Shale Symposium, Colorado School of Mines, Golden, CO, 2006; available on CD in Document CERI 2007-3.

61. Nelson, D. C. Oil Shale: New Technologies Defining New Opportunities. Presented at the Platts Rockies Gas & Oil Conference, Denver, CO, April 26–27, 2007.

Chapter 7

Modeling of the In-Situ Production of Oil from Oil Shale

Jacob H. Bauman,¹ Chung Kan Huang,¹ M. Royhan Gani,²
and Milind D. Deo^{*,1}

¹Department of Chemical Engineering, University of Utah, Salt Lake City,
UT 84112

²Department of Earth and Environmental Sciences, University of New
Orleans, 2000 Lakeshore Drive, New Orleans, LA 70148

*milind.deo@utah.edu

Scarcity of conventional oil reserves amidst increasing liquid fuel demand in the world have renewed interest in oil shale processing because of the massive accessible resources. In-situ oil shale production has a lessened environmental impact, and likely lower cost than mining and surface processing. A few current processing strategies are briefly described. Heat transfer pathways, chemical kinetics, geomechanics, multiphase fluid flow, and process strategies all provide complexities to any in-situ oil shale production strategy. Understanding each of these phenomena, and appropriate model coupling is necessary to accurately model in-situ oil shale production processes. Results from in-situ oil shale modeling with the STARS simulator by the Computer Modeling Group (CMG) are discussed. Idealized energy efficiency and carbon footprint for this type of process were estimated as 3:1 net energy gain and 36 kg CO₂/bbl oil produced respectively.

Background

During the summer of 2008, oil prices rose to a maximum of about \$140 per barrel due to scarcity of oil reserves and high demand. These relatively high oil prices make oil shale resources an economically viable alternative for petroleum

production. There are an estimated 2.9 trillion barrels of oil from oil shale resource in the world. Most of this resource is in the United States, in the Green River Formation of Colorado, Utah, and Wyoming. The Green River Formation contains an estimated 1.8 trillion barrels of high quality oil shale (1).

Most large scale oil shale processing operations in the world are surface retorts. Oil shale is mined and processed at the surface. In-situ oil shale retorting is an attractive alternative to mining and surface retorting since there is less environmental impact. In-situ methods have a reduced environmental impact in terms of surface disturbance, water requirements, and waste management when compared to ex-situ technologies. However, in-situ technologies are still developing and include more uncertainty, especially at large scales. For in-situ oil shale processing, the shale must be heated underground by some method until the oil can flow. Kerogen is the organic component of oil shale. Kerogen is a solid and must be converted to a flowable fluid in order to be produced. As the kerogen is heated, oil can flow through the underground reservoir and be produced in a well. In order to model any type of in-situ process, understanding of the fundamental submodels is necessary. These fundamental submodels include heat transfer through the reservoir, chemical kinetics of kerogen pyrolysis or combustion, geomechanics, multiphase flow, and other factors due to process variations.

Current In-Situ Processing Strategies

Shell Oil company has been the most aggressive to this point with oil shale in-situ technology development. They have a pilot plant studying their InSitu Conversion Process (ICP) in the Green River Formation of Colorado. The ICP consists of resistive down hole heaters slowly supplying heat to the reservoir for a period of years before any oil is produced. After the initial heating period, they are reporting a high quality oil produced. They use a hexagonal heater pattern where each production well is surrounded by 6 heating wells. With their pilot scale ICP, they have surrounded their wells with a freeze wall. Coolants are circulated underground to create an ice barrier. The freeze wall is incorporated to prevent any possible groundwater flow contamination (2).

ExxonMobil developed a Hydrofrac process where they create hydraulic fractures in the oil shale reservoir. After fracture creation they inject conductive material into the fractures and use resistive heating to heat the reservoir. The purpose is to maximize heat transfer efficiency by increasing heat transfer area where the conductive material has been injected (3).

AMSO (American Shale Oil) is developing a process called CCR (Conduction Convection and Reflux). In this process they drill two horizontal wells at the bottom of the pay zone, a heater and a producer. They supply heat to the bottom of the reservoir, and expect as the kerogen decomposes to lighter products, the hot vapors will rise to the cooler top of the reservoir and reflux (4). This process can be engineered to create high quality oil.

Red Leaf Resources has recently developed their EcoShale In-Capsulation process that combines the benefits of ex-situ and in-situ processing strategies. In

their process a clay sealed hole, or capsule, is excavated at the surface. Natural gas burners are installed into the open capsule which is then filled with mined oil shale. The capsule is covered by native soil and overburden for environmental reclamation, and the shale in the capsule is slowly heated in-situ (5). This strategy is advantageous because the properties in the capsule are more easily controlled than in a traditional reservoir. Heat transfer is more efficient because the previously mined shale is fragmented. Mountain West Energy has developed their In-Situ Vapor Extraction (IVE) technology where hot methane gas is injected into the reservoir to pyrolyze the kerogen, and then the products are produced (6). Their test results are promising.

Modeling Considerations

For any in-situ oil shale retort, the kerogen in the reservoir must be heated to 350 °C – 500 °C pyrolysis temperature. Heat is supplied to the reservoir through a heating well, and transfers through the well by conduction in the rock, and convection. Kerogen pyrolysis requires a significant heat requirement. Acceptable heating efficiency is essential to any successful in-situ operation. Temperature control in a reservoir can also be a significant challenge. Temperature profiles will also become very complex when coupled with chemical kinetic models and multiphase flow and thermodynamic models.

Kerogen is the organic solid in oil shale. It is insoluble in most solvents, therefore pyrolysis is a common method for decomposing kerogen into liquid and gaseous components. The chemical mechanism and kinetics of kerogen pyrolysis is uncertain. Thermal Gravimetric Analysis (TGA) is often used to measure the kinetics of oil shale pyrolysis. In these TGA studies, the oil shale is crushed to minimize any heat transfer resistance. Results from these TGA studies give a distribution of activation energies, which add additional complexity to the kinetic model. The current consensus is that isoconversion models are theoretically and physically appropriate to describe kerogen pyrolysis. Kerogen structure is widely unknown, and may vary significantly within and between resources. Because of the complexity in kerogen structure, compositional behavior and decomposition mechanisms can be difficult to predict. Chemical lumping (grouping) can be used to model compositional behavior.

Combustion process options can be very attractive for oil shale production. In-situ combustion can significantly lower heat generation requirements for oil shale pyrolysis, making the process more efficient and economical. Understanding coke and kerogen combustion in the reservoir is important to appropriately engineer and predict the behavior of this type of process. For in-situ thermal processes, inorganic rock decomposition can also take place when temperatures are high. Carbonate rock decomposition could be a significant source of CO₂ emissions.

Geomechanics have a significant impact on the behavior of underground reservoirs. Geomechanics in oil shale reservoirs are somewhat unique because of the thermal treatment of the rock. Evidence suggests that permeability is created as the rock is heated. There is also concern about subsidence as rock is changed

Table I. Representative Component Molecular Weight and Hydrogen/Carbon Ratio

<i>Component</i>	<i>Molecular Weight</i>	<i>Hydrogen/Carbon Ratio</i>	<i>Hydrogen/Carbon Ratio (Alternate)</i>
Kerogen	670	1.05	1.50
Heavy Oil	441	1.64	1.52
Light Oil	152	2.27	1.52
Gas	54	2.5	1.62
Methane	16	4.0	4.0
Char	12.4	0.6	0.39
Coke	12.5	0.45	0.34

and weakened due to heating. Heterogeneity of the resources can also have a significant role in reservoir engineering. Detailed characterizations of many oil shale resources have been studied.

Flow characteristics in oil shale reservoirs can be quite complex due to the coupling of these submodels. Depending on the process design and reservoir characteristics, models are needed to accurately represent flow characteristics. Water, oil, gas, organic solid, and inorganic solid flow behavior in an oil shale reservoir is different to behavior in a conventional reservoir due to the high temperatures and other factors.

In-Situ Prototype Model

Oil can be produced from oil shale by pyrolysis. Kerogen is the hydrocarbon material in oil shale rock. Kerogen is pyrolysed to produce oil, gas, and residue. Kerogen is a complex material, and the resulting pyrolysis products are also quite complex. Kerogen pyrolysis was simulated using properties of lumped representative components. The following reaction mechanism, adapted from a previous study (7), was used in these simulations.

1. Kerogen \rightarrow Heavy Oil + Light Oil + Gas + CH₄ + char
2. Heavy Oil \rightarrow Light Oil + Gas + CH₄ + char
3. Light Oil \rightarrow Gas + CH₄ + char
4. Gas \rightarrow CH₄ + char
5. char \rightarrow CH₄ + Gas + coke

All reactions were assumed to be first order, and kinetic parameters from a previous study (7) were used. The heats of reaction were assumed to be 46.5 kJ/gmole for each reaction based on similar reactions from the template input files of the thermal simulator used in the study. Overall heats of reaction of kerogen pyrolysis to oil have been reported previously (8). Detailed thermochemical studies with individual products would be necessary to assign heats of reactions of individual conversions.

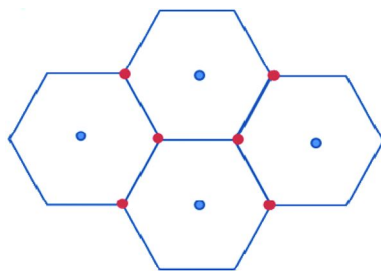


Figure 1. Aerial view of Shell ICP Well Geometry

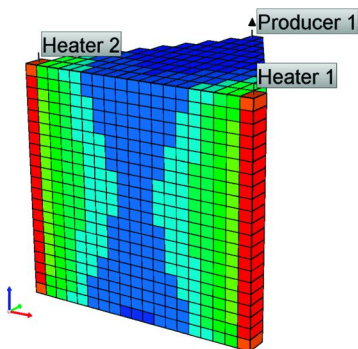


Figure 2. Simulated Triangular Wedge

Table II. U059 Well Survey Data

Depth (ft)	wt% of HC
665-670	12.5
671-680	12.5
681-690	14
691-694	15
695-700	16
700-710	25
710-715	16

Stoichiometry was approximated based on the molecular weights and hydrogen to carbon ratios chosen for each component to force a mass balance.

The hydrogen to carbon ratios of Green River oil shales are about 1.54 (9). Alternative simulations including a more realistic 1.50 hydrogen to carbon ratio for Green River oil shales, and more rigorous mass and elemental balances as shown in Table I, were run and showed comparable results and trends. It should be noted that stoichiometric coefficients used in this reaction scheme are not unique. They are simply estimated to force mass and elemental balances

based on approximated molecular weights and hydrogen to carbon ratios of each representative component.

STARS, a thermal-compositional simulator coupled with chemical kinetics developed by the Computer Modeling Group, was used to solve mass and energy conservation equations with necessary constraint equations and physical models (10).

Geometry

The well geometry used in simulation was loosely based on the pilot scale in-situ conversion process used by Shell Oil (2). Six heating wells surround one production well as shown in Figure 1. In this simulation the heaters were spaced 53 feet apart. The thickness of the simulated reservoir was 50 feet. Due to symmetry, only a triangular wedge was simulated as shown in Figure 2. The results from this simulated section can be repeated to represent the field.

The block was discretized using the CMG Builder into 21 vertical, 1-19 wide, and 1-10 length (10 blocks being the height of the triangle from an aerial view) blocks.

Initial Conditions

Gamma-ray log data from the Utah Geological Survey for the U059 well in the Uinta basin (11) was used to estimate the weight % of hydrocarbons (kerogen). The kerogen rich section of the well is from 665 ft to 715 ft deep, and the kerogen wt% varies from 12.5 wt% to 25 wt%. Table II shows the weight percent of kerogen at different depths in the well which was used to calculate the initial kerogen volume at each depth. The remaining volume was assumed to be inorganic rock.

The porosity of the initial rock was calculated for each layer with the assumption that kerogen nearly filled the pore space in the rock. The initial pressure and temperature assigned to the reservoir were a constant 1000 psi and 80 degrees F.

Production Strategy

The reservoir was directly heated with two vertical injection wells to simulate resistive or burner heaters. These heaters heated uniformly from the top to the bottom of the well. The heaters each supplied 50,000 BTU/day to the reservoir for a four year time period. The production was pressure controlled by the producer. The base case scenario used a BHP of 100 psi, but many simulations were run at different back pressures to estimate pressure sensitivity and numerical stability.

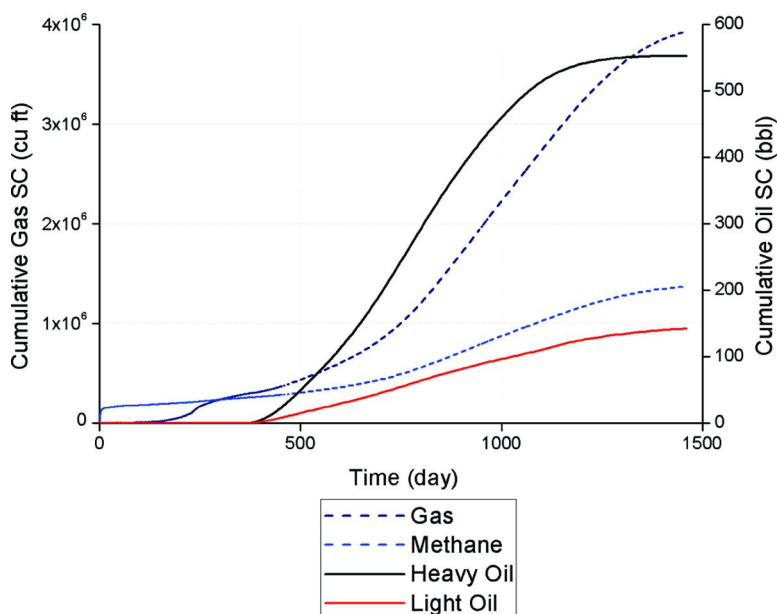


Figure 3. Cumulative Oil and Gas Production.

Results

The production results of the simulation are shown in Figures 3–9. The cumulative oil and gas production over a four year period are plotted in Figure 3. The production rates shown in Figure 4 show a maximum oil production rate of approximately 1.2 bbl oil/day. This maximum oil production rate occurs approximately two years after the heating is initiated. No significant oil is produced until after 400 days of heating. This time delay represents the time required to convert solid kerogen to producible oil with the given heating rate, well geometry, reservoir characteristics, and process parameters. These rates are multiplied by approximately 30 to convert the rate to bbl oil/day/acre. This oil production rate is fairly low, but oil production rate and quantity highly depends on temperature history in the reservoir. With the pyrolysis kinetic parameters and mechanism used in this simulation, much of the kerogen can convert to residue and gas. Figure 5 shows the energy efficiency of the heating strategy. After four years approximately 50% of the heat supplied to the reservoir is lost to overburden and underburden. Processes could be engineered to minimize the heat lost to overburden and underburden by changing heating patterns, histories, and strategies. Pyrolysis could be followed by in-situ coke combustion, for example, to improve heating efficiency.

Figures 6, 7, 8, and 9 show a comparison of 3 simulated grid blocks: one near the heater (block 18, 10, 11), one far from the heater (block 10, 1, 11), and one in the middle of the section (block 14, 5, 11). The reservoir is heated rapidly near the

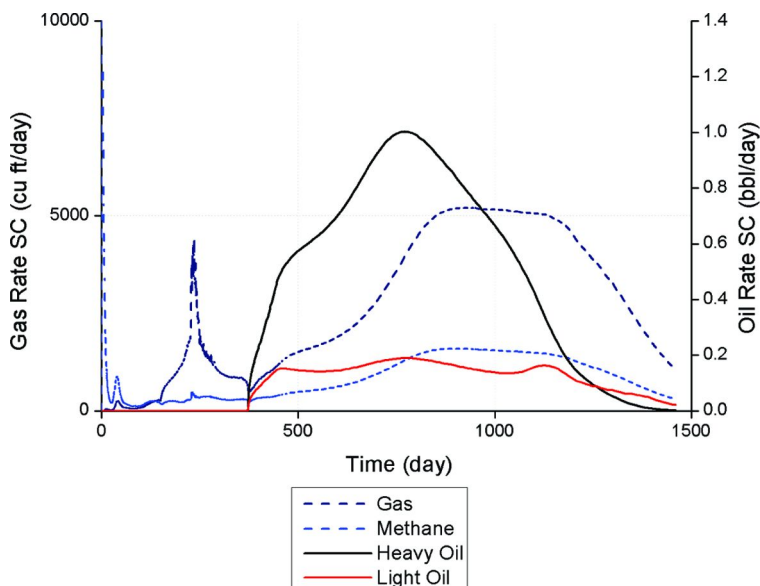


Figure 4. Oil and Gas Production Rates.

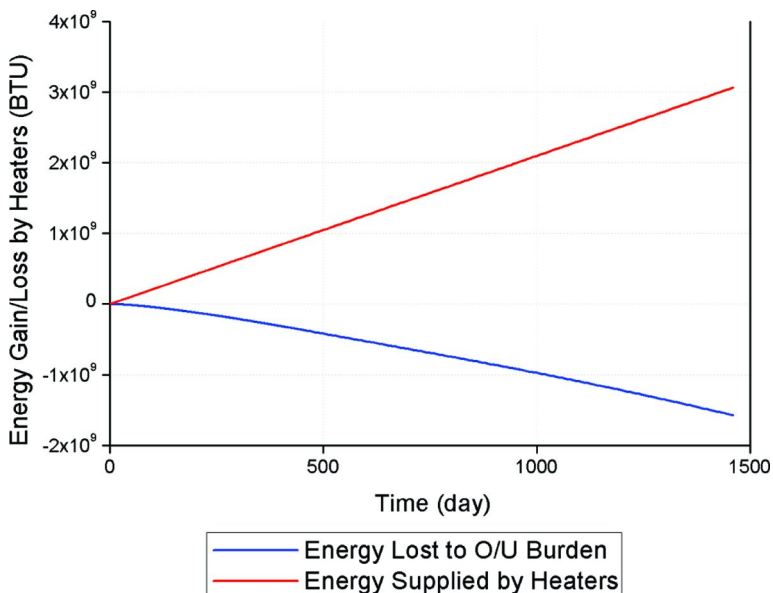


Figure 5. Energy Supplied to Reservoir and Energy Lost to Under/Over Burden.

heaters, and it can be seen that conduction through the reservoir is slow. Kerogen conversion is rapid at the high temperatures near the heater. The high temperatures near the heaters are excessive, yet somewhat high temperatures near the heaters may be required for enough heat to conduct through the reservoir in a reasonable time. The actual temperatures reported here are specific to the heat input strategy

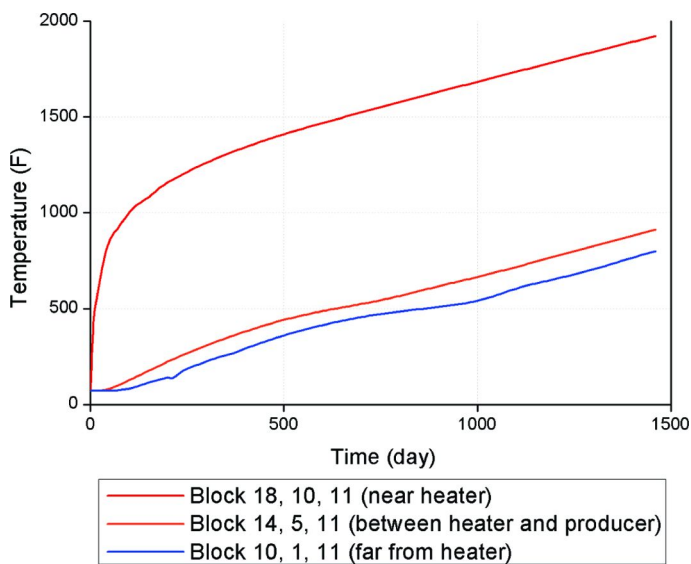


Figure 6. Temperature History Comparison for Three Distances From Heaters.

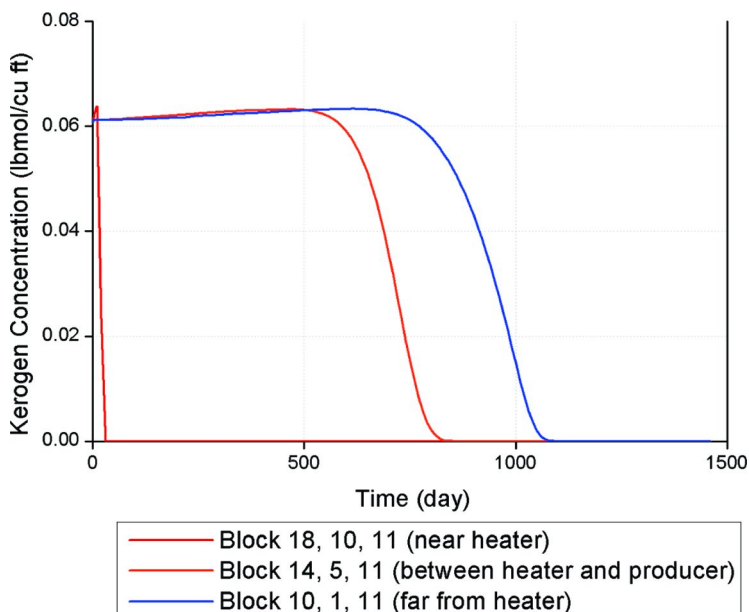


Figure 7. Kerogen Concentration Comparison for Three Distances From Heaters.

used in the simulations. It may take up to 700 days to supply sufficient heat for pyrolysis far from the heater under these conditions. Coking can be significant due to high temperatures near the heaters, as shown in Figure 9.

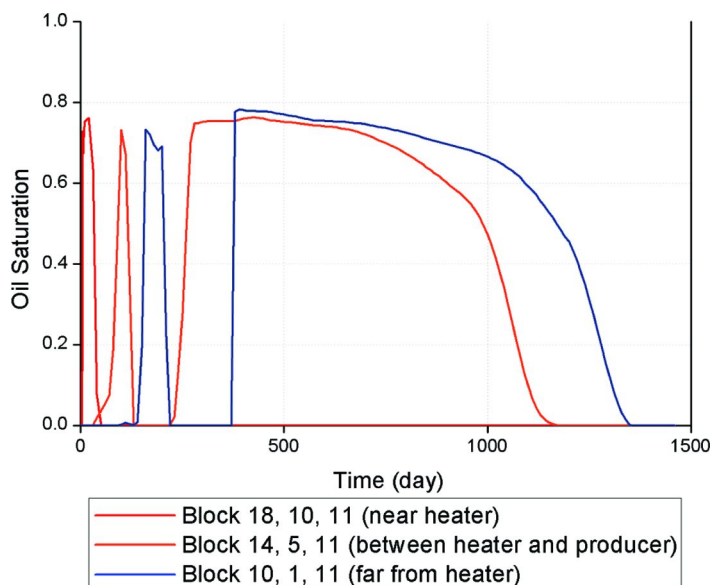


Figure 8. Oil Saturation Comparison for Three Distances From Heaters.

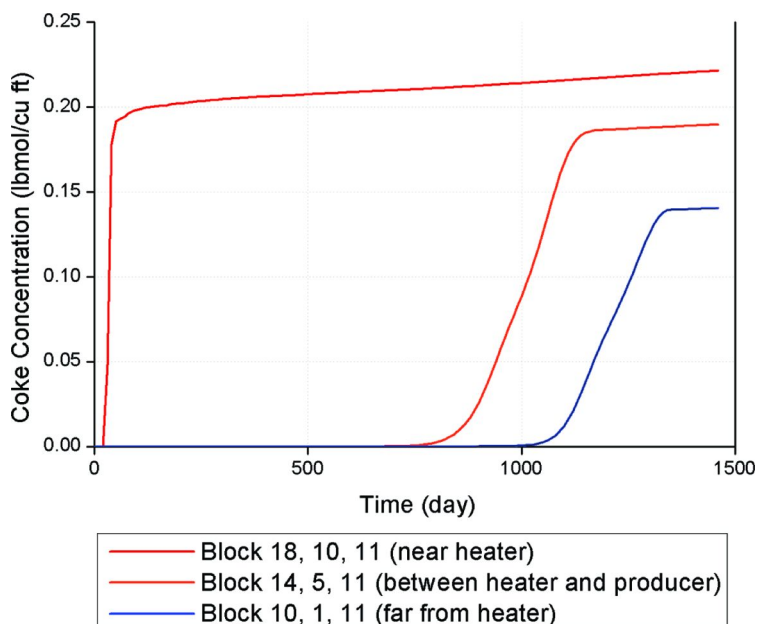


Figure 9. Coke Concentration Comparison for Three Distances From Heaters.

The net energy gain/loss was estimated for this type of process. This preliminary estimate assumed 15 wt% kerogen in the oil shale source rock, all kerogen converted to recoverable oil, the source rock was heated from 25 °C to 350 °C retort temperature, and the heat of reaction for kerogen conversion was

370 kJ/kg. In this idealized estimate, 17 units of energy produced per unit of energy required were calculated. The base case results of the simulation show about 50% reservoir heating efficiency at the end of 4 years. The pilot Shell Oil ICP estimates a net energy gain of 3 units out per unit required with resistive heating supplied. Assuming 36% electricity generation efficiency and 50% reservoir heating efficiency, about 3:1 net energy gain can be calculated with these assumptions. The net energy gain from the base case simulated results including gas and oil as products was 3.06 units energy out per unit energy required.

Preliminary estimates of the carbon footprint for this type of process were also calculated. Natural gas heating, 33 API crude oil produced, and the assumptions mentioned in the energy gain/loss estimate were assumed in these calculations. Assuming 100% heating efficiency, 18 kg CO₂/bbl oil are emitted. If 50% heating efficiency is assumed, 36 kg CO₂/bbl oil are emitted. These estimates only include emissions from the process, and do not include any CO₂ emissions due to combustion inefficiency or carbonate mineral decomposition. No estimates for water requirements were made because water is not necessarily required for in-situ oil shale conversion processes. When using resistive heating, water is required for electricity generation, but not directly required for the oil shale processing. Water is also required for mining operations associated with ex-situ processing strategies.

Acknowledgements

The authors would like to acknowledge the financial support from the United States Department of Energy for the Oil Shale and Oil Sands Program at the University of Utah. The authors would like to recognize the support of faculty and staff from the Institute for Clean and Secure Energy (ICSE) and the Petroleum Research Center at the University. Long-term support of Computer Modeling Group (CMG) by providing academic licenses to all of their simulators to the University of Utah is gratefully acknowledged.

References

1. Bartis, J. T.; LaTourrette, T.; Dixon, L.; Peterson, D. J.; Cecchine, G. *Oil Shale Development in the United States: Prospects and Policy Issues*; RAND Corporation: Santa Monica, CA, 2005; pp 5–9; http://www.rand.org/pubs/monographs/2005/RAND_MG414.pdf.
2. Wellington, S. L.; Berchenko, I. E.; Rouffingnac E. P.; Fowler, T. D.; Ryan, R. C.; Shalin, G. T.; Stegemeier, G. L.; Vinegar, H. J. U.S. Patent 6,880,633, 2005.
3. Symington, W. A.; Olgaard, D. L.; Otten, G. A.; Phillips, T. C.; Thomas, M. M.; Yeakel, J. D. ExxonMobil's Electrofrac™ Process for InSitu Oil Shale Conversion. Proceedings of the 26th Oil Shale Symposium,

Golden, CO, October 17, 2006, http://www.ceri-mines.org/documents/R05b-BillSymington-rev_presentation.pdf (accessed July 21, 2009).

4. Burnham, A. K.; Day, R.; Wallman, H. Overview of American Shale Oil LLC Progress and Plans. Proceedings of the 28th Oil Shale Symposium, Golden, CO, October 13–15, 2008 [CD-ROM]; 28th Oil Shale Symposium: Golden, CO, 2008; Session 16, Presentation 1.
5. Dana, T.; Patten, J.; Nelson, L.; Bungar, J. W. Ecoshale: Environmental Alternative Fuels. USTAR and the Salt Lake Petroleum Section of SPE. Nov. 13, 2008, http://ds.heavyoil.utah.edu/dspace/bitstream/123456789/7084/1/laura_nelson_spe%20presentation%2011-13-%2097%20version.pdf (accessed July 21, 2009).
6. Mountain West Energy. <http://www.mtnwestenergy.com/mwe.html> (accessed July 30, 2009).
7. Braun, R. L.; Burnham, A. K. PMOD: A flexible model of oil and gas generation, cracking, and expulsion. *Org. Geochem.* **1992**, *19*, 161–172.
8. Camp, D. W. Oil Shale Heat Capacity Relations and Heats of Pyrolysis and Dehydration. Proceedings of the 20th Oil Shale Symposium, Golden, CO, 1987.
9. Yen, T. F.; Chilingar, G. V. Introduction to Oil Shales. In *Oil Shale*; Yen, T. F., Chilingar, G. V., Eds; Elsevier Science Publishing Company: Amsterdam, 1976, pp 181–198.
10. *STARS User Manual*; Computer Modeling Group: 2007.
11. Vanden Berg, M. D.; Dyni, J. R.; Tabet, D. E. *Utah Oil Shale Database*; 2006; [CD-ROM]; Utah Geological Survey OFR 469.

Chapter 8

AMSO's Novel Approach to In-Situ Oil Shale Recovery

**Alan K. Burnham,^{*,1} Roger L. Day,¹ Michael P. Hardy,²
and P. Henrik Wallman¹**

¹American Shale Oil, LLC, P. O. Box 1740, Rifle, CO 81650

²Agapito Associates, 715 Horizon Drive, Suite 340, Grand Junction,
CO 81506

*E-mail: alan.burnham@idt.net

American Shale Oil LLC (AMSO) is one of three companies holding an Oil Shale RD&D Lease in Colorado from the U.S. Bureau of Land Management. AMSO is pursuing a unique strategy of recovering shale oil initially from the 2000-ft-deep illitic oil shale below the saline zone in order to isolate production from protected sources of ground water. Our method of heat distribution is also unique. We use refluxing oil to transport heat to the retort boundary, which will advance by thermo-mechanical fragmentation (spalling) due to the compressive stress caused by heating externally confined oil shale with an internal free surface. Heat is provided from a horizontal heater in an "L" shaped well using a downhole burner. Our commercial concept is to use panels of parallel horizontal heater and production wells about 2000-ft long and about 100-ft apart. Each well would produce about a million barrels over 2 to 4 years. Such an approach will disturb only about 10% of the land surface area.

Oil shale is a major possible source of liquid fuels, particularly from Colorado's Piceance Basin, which contains up to 1.5 trillion barrels of potentially recoverable shale oil (Johnson *et al.* (1)). In 2005, the U.S. Bureau of Land Management (BLM) issued a call for proposals to obtain RD&D Leases from the BLM. Upon demonstration of commercial viability and environmental

acceptability, the RD&D Lease could be expanded from 160 acres to 5120 acres. EGL Resources was one of three companies selected to test *in-situ* oil shale recovery processes in the Piceance Basin, and the lease was signed in January 2007. The lease was assigned to a wholly owned subsidiary, EGL Oil Shale LLC. EGL proposed a novel heat distribution method of using refluxing oil to transmit heat through a system of spider web wells (Harris *et al.* (2)). This generic in-situ approach was named a CCR™ retort (Conduction, Convection, and Reflux). In 2008, controlling interest in EGL Oil Shale was acquired by IDT Corporation, and EGL Oil Shale LLC was renamed American Shale Oil LLC (AMSO). In 2009, a US subsidiary of Total S. A. acquired 50% interest in AMSO LLC, and IDT retained 50%.

During 2007 and 2008, the CCR retorting approach was generalized to additional heat sources and well configurations, and an amended Plan of Operation was approved by the BLM. The modified approaches take advantage of the observation from nahcolite recovery from the Green River Formation by American Soda that a thermally fractured zone can propagate at least one hundred feet from the heating well (Ramey and Hardy (3)). The free volume for continued spallation is created by removal of roughly 25% of the rock volume by the nahcolite recovery. The analogy for oil shale recovery is the removal of a comparable fraction of the rock by conversion of kerogen to producible oil and gas.

In addition, the important issue of potential contamination and reclamation of protected sources of ground water inspired AMSO to conceive and pursue an approach to first process the illitic oil shale at the base of the Green River Formation. The name of the illite shale has not been formalized in the center of the basin, but it is the depositional equivalent of the Garden Gulch Member. Our goal is to demonstrate the isolation of any retort contamination from the protected waters by the intervening nahcolitic oil shale.

The Illite-Shale CCR Retort Concept

The CCR retort concept is shown schematically in Figure 1. The initial vertical permeability may be provided, for example, by a vertical well. The shale surrounding any high permeability conduit will want to expand as it is heated, but since it is confined by the surrounding cool shale, it undergoes compressive failure and fills the high permeability conduit with rubble. This basic process was demonstrated decades ago for oil shale by Prats *et al.* (4). A laboratory demonstration of spalling from a block confined on all sides except the heated face is shown in Figure 2. Finally, they showed the growth of a rubble cavity about 30-ft in diameter made during a field experiment recovering nahcolite.

More recently, American Soda (Ramey and Hardy (3)) pursued thermomechanical rubblization in commercial recovery of soda ash. Their data showing the decrease in strength and increase in stress of oil shale as a function of temperature is shown in Figure 3. The crossing point at about 175 °C is where one might expect spalling to occur, and this is substantially below retorting

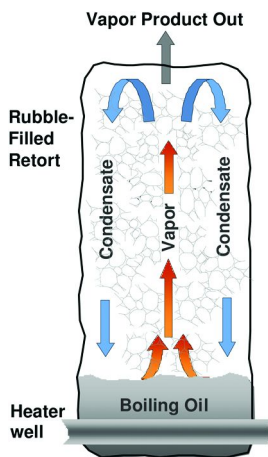


Figure 1. Schematic representation of refluxing oil distributing heat through a thermally fractured, retorted oil shale formation. Oil condensation and thermomechanical fracturing occur at the perimeter of the retorted region.

temperature. The boiling oil will be hot enough to bring the shale to retorting temperature, and the retorted shale is very weak in compression. Consequently, the thermomechanical fragmentation process is expected to propagate out to retort diameters of 100 or more feet in accordance with the experience by American Soda during nahcolite recovery shown in Table 1.

A conceptual picture of how we expect the thermomechanical wave to propagate through the retort is shown in Figure 4. Outside the retort, the shale will be in compression, because its thermal expansion will be confined by the surrounding cool formation. Fracture porosity will tend to be closed and any associated pore water would be expelled. On the inside of the compression wave, the shale will be prone to spall into the retort cavity, thereby relieving the circumferential stress, because the retorted shale has little compressive strength. The fracture porosity might be only a percent or so, but if the fractures have a width of only 100 μm , the estimated permeability would be about a Darcy. The thermal wave propagates outward, the kerogen in the fractured shale is converted to oil, gas, and char, which creates 20-30% porosity within the rubble particles. This porosity will have pore diameters of about one μm (Burnham (5)), and the resulting intraparticle permeability is in the range of 25 mDarcy (Baughman (6)). The strength of spent shale is very low (Duvall *et al.* (7)), so it should not be an impediment to continued spallation.



Figure 2. Thermomechanical fragmentation in a 1-ft cubic block heated with one face exposed to steam flowing at 520 °F. The block was confined on all faces except the one that underwent fragmentation. Reprinted by permission from reference (4). Copyright 1977 Society of Petroleum Engineers.

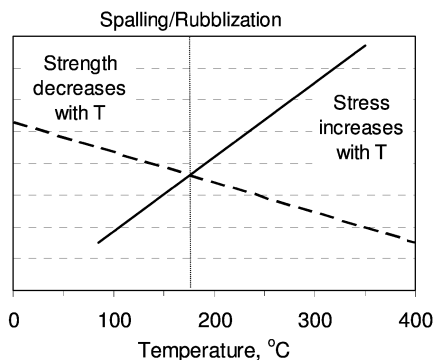


Figure 3. The decrease in strength and increase in stress with temperature causes confined oil shale to spall at about 175 °C.

Contamination of protected sources of ground water is a significant issue for oil shale recovery. Shell (8, 9), for example, proposes surrounding the retorted zone with an impermeable freeze wall, then remediating the residual contamination in the retorted zone by cyclic flushing with 20 pore volumes of treated water over two years. AMSO sought a simpler approach.

There is a largely unrecognized interval of reasonably rich illitic oil shale at the base of the Green River Formation. Combining the thermo-mechanical fragmentation concept with recovery of illite oil shale from the base of the Green River Formation gives the general retort concept shown in Figure 5. Here an “L” shaped heating well has replaced the “U” shaped heating well in the original EGL concept. In addition, for reasons explained more fully in the Heating Issues

Table 1. Cavity diameters formed during recovery of nahcolite by high-temperature solution mining (Ramey and Hardy, (3))

<i>Well</i>	<i>Tons of NaHCO₃ recovered</i>	<i>Cavity Diameter (ft)</i>
20-14	181,682	171
29-24	176,604	205
29-29	143,760	178
20-30	131,643	171
29-34	126,910	168
29-23	123,651	168
20-36	123,097	166
28-21	117,551	169
21-16	113,420	153
20-32	113,160	158

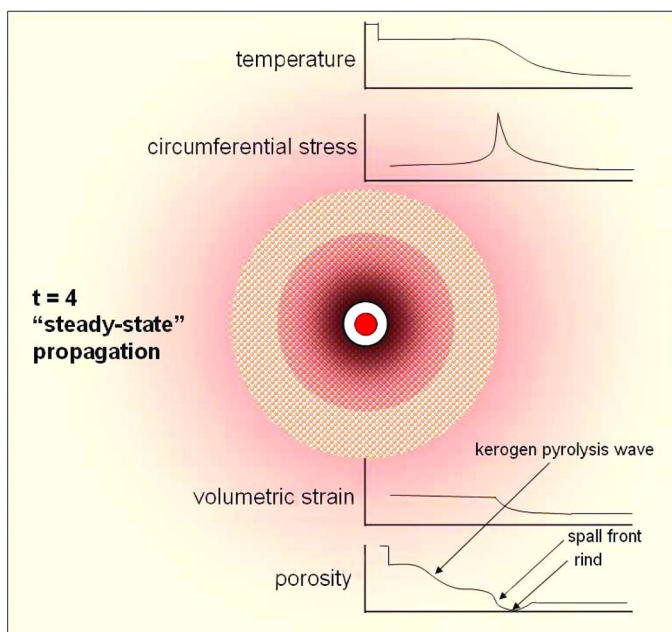


Figure 4. Conceptual picture of the propagation of the thermomechanical fracture wave at the retort boundary.

section, a downhole burner has replaced recirculating steam as the heat medium. In both cases, the heater well is isolated from the oil shale formation. In the example shown, several deviated boreholes from the horizontal production well provide the initial connectivity to the horizontal production well, which may or may not be cased.

A three-dimensional representation of how this concept might be applied in a commercial process is shown in Figure 6. Twenty or less well pairs, depending on the efficiency of the convective heat transfer through the rubblez shale, would form a panel of retorts that would eventually merge during the retorting process. The panels will be separated by pillars that are, for example, 200-ft thick. In this case, 80-90% of the chosen interval can be retorted, depending on how much of the barrier pillar is retorted. Furthermore, all the heater and production wells can be drilled along a 200-ft corridor, which means less than 10% of the area to be process needs to be disturbed and reclaimed. Depending on the exact well spacing, thickness, and richness of the oil shale, roughly a million barrels of shale oil will be recovered from a well over its lifetime of 2-4 years. For a 100,000 barrel/day production facility, about 6 panels will be operational at a time. For a 5120-acre commercial lease, about a billion barrels of shale oil could be recovered from the illite shale, depending on site-specific details.

Heating Issues

One of the most fundamental issues for oil shale retorting is how to get the heat into the oil shale. In general, the time scale for retorting is intimately related to the particle size of the shale to be retorted because of heat transfer resistance (Burnham (10)). Consequently, pyrolysis of particles with sizes up to a few mm can be accomplished in minutes at temperatures of about 500 °C, while pyrolysis of particles with sizes of tens of cm takes hours. In the absence of some fragmentation mechanism, it takes a few years to heat oil shale blocks of tens of feet, which is the closest conceivable well spacing for in-situ recovery. However, the advantage of such slow heating is that the retorting occurs at a lower temperature; hence, less heat is needed to heat the rock, and the quality of the oil increases substantially (Burnham and Singleton (11)). The improved oil quality comes at the price of a lower oil yield due to in-situ upgrading by coke deposition, but part of that oil-yield loss is made up by higher gas yields. Consequently, the energy content of the gas is more than sufficient to provide the heat required to sustain the retorting process.

The original EGL concept was to burn the gas aboveground to create steam, which would be circulated belowground in “U” shaped wells (Harris *et al.* (2)). Initial modelling showed that the process would work, in principle, given a plausible heat transfer coefficient between the steam tube and the boiling oil pool and a network of small-diameter wells to distribute the boiling oil. However, retorting in the upper part of the Green River formation using this approach as originally proposed would require extensive measures to protect usable groundwater. Consequently, we shifted our attention to the illite-rich shale below the saline zone.

This shift in target causes a fundamental change in the heat delivery issues, in that any heat being delivered from the surface has a much longer transit distance. This affects both the amount of energy lost due to thermal diffusion and pressure drops to be greater and the cost of protecting the shale surrounding the heat delivery pipe in regions not to be heated. Figure 7 shows heat delivery characteristics using

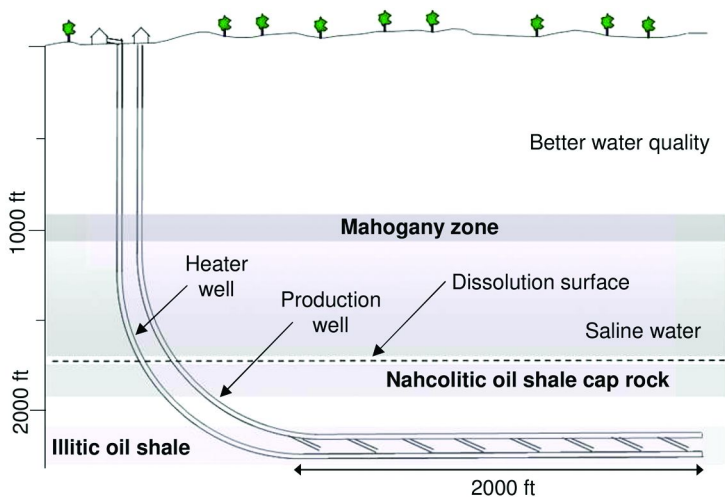


Figure 5. Cross section of a pair of horizontal heater and production wells in the illite-rich oil shale at the base of the Green River Formation.

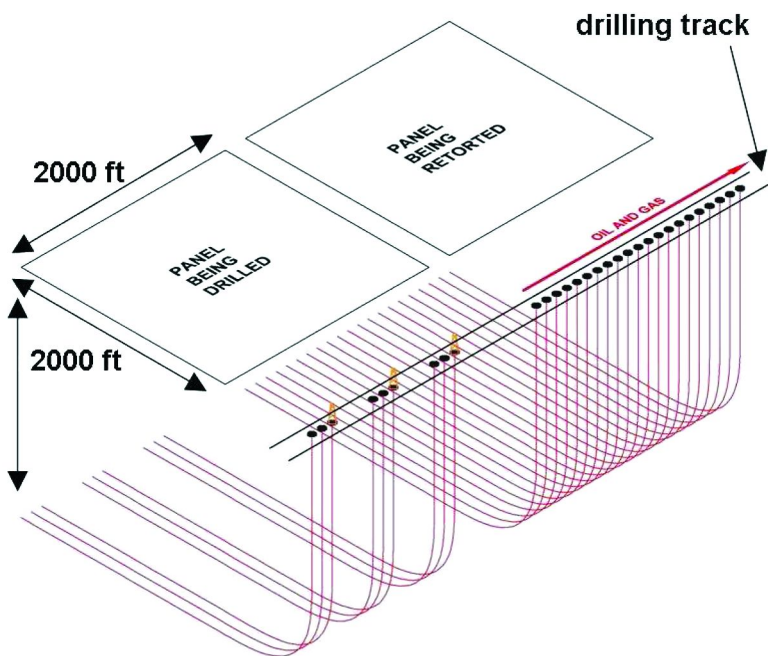


Figure 6. A possible commercial implementation of the CCR process applied to the illite-rich oil shale.

propane as the heat carrier down to a 2100-ft deep, 100-ft-long return-loop heat exchanger having an inlet temperature of 520 °C and maintaining a boiling oil pool at 360 °C. An injection pressure of 40 atm and a pressure drop of 10 atm were assumed over the 6050-ft roundtrip to and from the surface. While such a delivery system can deliver adequate power to a pilot-scale experiment, it does not work well at larger scales. As the length of the heat exchanger grows, an increasing fraction of the power is provided by electricity via the compressor. It would be better to just use an electric heater. Furthermore, as the VIT tube size grows to 8", excessive heating of the formation occurs surrounding the delivery pipe, as shown in Figure 8 and Table 2. Steam would be an alternative heat carrier to propane, but the pressure in the steam loop would have to be at least 170 atm to deliver the latent heat of steam at a temperature above 350 °C for effective use during pyrolysis.

These computational studies demonstrate that it is very desirable to deliver the energy to the retort using a downhole burner. Consequently, our commercial concept uses a downhole burner, and we are actively involved in developing such a device. This strategy retains the high energy gain (>5) of a non-electricity heated process and uses the coproduced gas to create a self-sustainable commercial operation.

Additional simulations have explored the potential advantages of convective heat transfer over conductive heat transfer. A pair of example calculations is shown in Figure 6 for a horizontal heating pipe held at 500 °C. Standard thermal conductivities (Baughman (6)) are used for the conduction case, and a sigmoidal increase in permeability from 1 mDarcy to 1 Darcy between 100 and 250 °C is used in the convective heat transfer case, with the boiling oil pool maintained at 360 °C by the heated pipe. The assumed permeability increase is related to the increase in porosity of 20-25% due to kerogen conversion and the associated thermomechanical fragmentation at the periphery of the retort, as discussed earlier for the analogous nahcolite solution mining experience by American Soda (Ramey and Hardy (3)). The conductive case is able to deliver only 0.1 kW/ft to the formation, while the convective case is able to deliver 4 kW/ft. In addition, the temperature for conductive decreases monotonically away from the heating well, while the convective case gives an approximately constant shale temperature of 350 °C away from the well until it decreases in sigmoidal fashion near the advancing thermally fractured zone. Of course, the assumptions associated with the convective case are probably optimistic. Counter-current diffusion from gaseous and vapor products generated at the retort wall will decrease convective heat flux. However, complex 3D flow in a real retort will decrease the impact of these generated products. The two cases in Figure 9 should be considered end members, with reality somewhere in between.

Water, CO₂, and Energy Gain Issues

Water usage is an important issue for an oil shale industry. Although our process design is in an early stage, it is possible to say that water usage will be

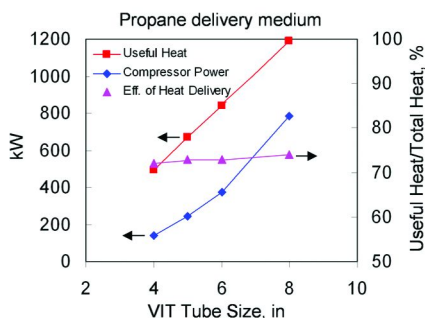


Figure 7. Heat delivery capacity at constant pressure drop for a 2100-ft-deep, 100-ft-long return-loop heat exchanger, using propane as a heat carrier, as a function of Vacuum Insulated Tubing diameter.

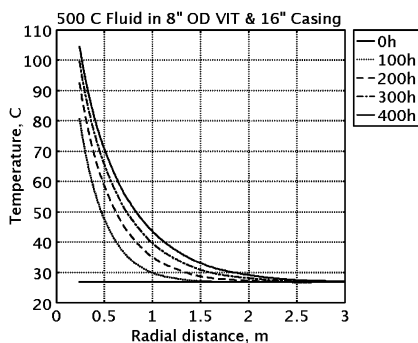


Figure 8. Calculated temperature around the Vacuum Insulated Tubing as a function of distance and time.

Table 2. Calculated temperatures around vacuum insulated tubing used to transmit a heating fluid downhole

VIT o.d., in	Fluid Temperature, °C	Initial heat loss rate, W/m of well	Temperature outside well
4	500	127	<100 °C after 2 years
4	360	89	<80 °C after 2 years
8	500	278	>100 °C after 400 hours
8	360	196	>100 °C after 3500 hours

less than one barrel of water per barrel of oil. The two major uses of water will be surface process cooling and dust control, both of which are estimated to be substantially smaller than one barrel water per barrel of oil, depending upon the amount of air cooling and asphaltic road surfaces. No water is required for cleaning the spent retorts, as they are isolated from usable groundwater. Furthermore,

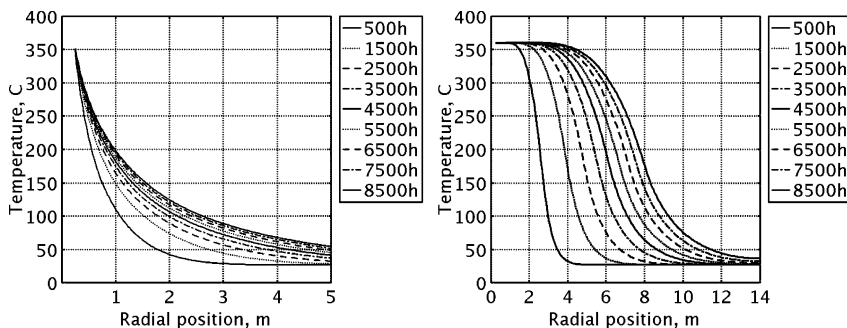


Figure 9. Comparison of heated regions around a 500 °C pipe based on conductive (left) and convective (right) heat transfer.

produced process water could be purified with reverse osmosis, for example, and used for other purposes, thereby reducing imported water needs.

Another issue facing oil shale recovery is the generation of CO₂ during production in excess of that generated during conventional oil recovery (Brandt *et al.* (12)). Using heat enthalpy equations of Camp (13), the heat of retorting 27 gal/ton illite shale up to 350 °C is 550 MJ/Mg shale, assuming 4.8 wt% water as measured in our core samples. Natural gas generates about 50 g of CO₂ per MJ of energy, giving 0.0275 Mg CO₂/Mg oil shale. Adding CO₂ from kerogen pyrolysis gives 0.0283 Mg CO₂/Mg shale. Assuming 80 vol% Fischer assay yield means 0.57 barrels of oil/Mg shale, which translates to 50 kg CO₂/barrel of oil. This compares to 450 kg CO₂/barrel of oil for its eventual combustion.

It is prudent for a variety of reasons to explore ways of capturing and using or sequestering the CO₂ produced during generation. Potential options are use in enhanced oil recovery, deep geological disposal, and mineralization in spent oil shale retorts. The first two are being explored by many organizations, primarily for the purpose of reducing CO₂ emissions from coal-fired power plants. The latter is unique and takes advantage of the special chemical properties of the illite-rich oil shale. There is sufficient porosity after retorting to convert all the CO₂ generated making process heat to carbonate minerals in the spent retort. We are exploring the optimal conditions by laboratory experiments and geochemical modelling.

Revisiting the energy gain issue, the heat of combustion of in-situ shale oil using the Boie equation reported by Muehlbauer and Burnham (14) is 44300 kJ/kg. A volumetric Fischer Assay yield of 80% for 27 gal/ton shale equals 7.5 wt% of the rock mass, so the energy content in the oil is 3323 MJ/Mg of rock. The energy content of the gas is less well known but may be as much as 1/3rd of the energy content of the oil for in-situ pyrolysis conditions, giving a total energy yield of about 4430 MJ/Mg rock. This corresponds to an total energy gain of about 8. There will be some thermal inefficiency and other energy use in practice, so the actual energy gain will be somewhat less but certainly greater than 5. Note that the produced gas contains more energy than required to heat the rock, so no imported natural gas would be needed.

Summary

American Shale Oil LLC is pursuing an oil shale strategy that seeks to minimize the environmental impacts of shale oil recovery. It seeks to first recover oil from the illite-rich shale at the bottom of the Green River Formation, which is isolated from protected sources of groundwater by nahcolite-rich saline zone oil shale. This initial recovery could yield a billion barrels of shale oil from only eight square miles. The process uses a unique convective heat transfer mechanism to minimize the number of wells needed to recover this oil, thus reducing the surface disturbance to only about 10% of the surface area. Use of the co-produced gas in a downhole burner maximizes energy efficiency for production and minimizes the risk to the overburden due to the heating wells. CO₂ sequestration by mineralization in the spent retorts offers the possibility of production of premium quality oil with negligible CO₂ released by the production process.

References

1. Johnson, R. C.; Mercier, T. J.; Brownfield, M. E.; Pantea, M. P.; Self, J. G. Assessment of in-Place Oil Shale Resources of the Green River Formation, Piceance Basin, Western Colorado; U.S. Geological Survey Fact Sheet 2009–3012, 2009, 6 p.
2. Harris, G. H.; Lerwick, P.; Vawter, R. G. In Situ Method and System for Extraction of Oil from Shale. Patent Application Publication US/2007/0193743 A1, 2007.
3. Ramey, M.; Hardy, M. The History and Performance of Vertical Well Solution Mining of Nahcolite (NaHCO₃) in the Piceance Basin, Northwestern Colorado, USA. In Solution Mining Research Institute, 2004 Fall Meeting, Berlin, Germany, 2004.
4. Prats, M.; Closmann, P. J.; Ireson, A. T.; Drinkard, G. Soluble-Salt Processes for In-Situ Recovery of Hydrocarbons from Oil Shale. *J. Petrol. Technol.* **1977**, *29*, 1078–1088.
5. Burnham, A. K. Reaction kinetics between CO₂ and oil-shale residual carbon. 1. Effect of heating rate on reactivity. *Fuel* **1979**, *58*, 285–292.
6. Baughman, G. L. *Synthetic Fuels Data Handbook*, 2nd ed.; Cameron Engineers, Inc.: 1978; pp 44–46.
7. Duvall, F. E. W.; Sohn, H. Y.; Pitt, C. H. Physical behaviour of oil shale at various temperatures and compressive loads. 3. Structural failure under loads. *Fuel* **1985**, *64*, 938–940.
8. *Designated Mining Operation Reclamation Permit Application for the Oil Shale Test*, Shell Frontier Oil and Gas, Inc.: 2007; p 8-4.
9. Vinegar, H. J. Shell's in-Situ Conversion Process for Oil Shale. Presented at the 26th Oil Shale Symposium, Colorado School of Mines, Golden, CO, October 16–20, 2006.

10. Burnham, A. K. Chemical Kinetics and Oil Shale Process Design. In *Composition, Geochemistry and Conversion of Oil Shales*; NATO Advanced Study Institute Series; Snape, C., Ed.; Kluwer: Dordrecht, 1993; Vol. 455, pp 263–276.
11. Burnham, A. K.; Singleton, M. F. High-Pressure Pyrolysis of Green River Oil Shale. In *Geochemistry and Chemistry of Oil Shales*; ACS Symposium Series 230; Miknis, F. P.; McKay, J. F., Eds.; The American Chemical Society: Washington, D.C., 1983; pp 335–351.
12. Brandt, A. R.; Boak, J.; Burnham, A. K. Carbon Dioxide Emissions from Oil Shale Derived Liquid Fuels. *Oil Shale: A Solution to the Liquid Fuel Dilemma*; ACS Symposium Series 1032; The American Chemical Society: Washington, D.C., 2010; Chapter 11, this volume.
13. Camp, D. W. Oil Shale Heat Capacity Relations and Heats of Pyrolysis and Dehydration. In *Twentieth Oil Shale Symposium*, Gary, J. H., Ed.; Colorado School of Mines Press: Colorado School of Mines, 1987; pp 130–144.
14. Muehlbauer, M. J.; Burnham, A. K. Heat of Combustion of Green River Oil Shale. *Ind. Eng. Chem. Proc. Des. Dev.* **1984**, *23*, 234–236.

Chapter 9

Shell's In Situ Conversion Process—From Laboratory to Field Pilots

Robert C. Ryan,* Thomas D. Fowler, Gary L. Beer, and Vijay Nair

Shell Exploration and Production Company, Houston, TX 77002

*robert.ryan@shell.com

Shell has been involved in developing oil shale technology for more than 50 years. A combination of laboratory and field testing covering a wide range of technologies from mining to steam processes to electric heaters has brought clearly into focus both the challenges and opportunities for a commercial oil shale project. To date, Shell has conducted eight Colorado field pilots in the oil shale resource with increasing scope, cost, and complexity. The majority of effort since 1981 has been devoted to actively studying important elements of the In-situ Conversion Process (ICP). The current focus is to complete the freeze wall test and to continue laboratory testing and modeling efforts to develop robust test programs to convert the three Research, Development, and Demonstration (RDD) leases under the terms of the Energy Policy Act of 2005.

Oil shale is the informal term used to describe the fine textured rock of sedimentary origin containing appreciable amounts of indigenous organic matter (kerogen) that yields liquid oil, gas, and water when heated to conversion temperatures. According to Thorne (*1*) et al “oil shale was formed by the deposition and lithification of finely divided organic matter and organic debris in the bottom of shallow lakes and seas. The organic debris resulted from the mechanical and chemical degradation of small aquatic organisms”. Kerogen is insoluble in benzene and has a complex chemical structure. Based on X-ray diffraction studies and elemental analysis an approximate molecular formula for kerogen is $C_{200}H_{300}O_{11}N_5S$ (*2*). However, it is recognized that this is an oversimplification of a complex system.

The current challenge of the energy industry is to find processes that are economically viable, environmentally responsible, and socially sustainable for converting oil shale to liquid transportation fuels. Such a process must crack this macromolecule to much smaller hydrocarbon pieces with essentially all the sulfur, nitrogen, and oxygen heteroatoms removed along with the associated metals such as iron, nickel, arsenic, and vanadium. Over the years a number of companies attempted to develop a viable process to commercialize this resource. The majority of the early work was carried out in the Green River Formation consisting of the Green River Basin in Wyoming, the Uinta Basin in Utah and the Piceance Basin in Colorado. Estimates of oil resource within the Green River Formation made over the years vary widely and depend on the minimum grade cutoff, but in every estimate, the oil resource is very large. In March 2009, the USGS released an in place estimate of 1.525 trillion bbls for just the Piceance Basin portion of the Green River Formation. The USGS did not make an attempt to provide an estimate of recoverable reserves because they point out that at present, there is no economic method to extract oil from the Green River Formation (3).

Major oil companies working alone or in partnerships have attempted to commercialize the oil shale resource for several decades. Usually the attempts involved mining the oil shale to supply large surface retorts in which the ore was raised to high temperature and converted to low API gravity shale oil and waste material called “spent shale” or ash. There were significant challenges with the surface retort approach including handling the massive volume of rock, disposing of the spent shale, upgrading the heavy oil, and operating problems with the retort itself. Because of the arid conditions in the region, high water usage was also a concern.

Shell took part in some of the early mining / retort attempts by industry to commercialize oil shale. However, Shell withdrew from the projects after a relatively brief time and strategically chose to stop work on the mining approach altogether in the mid 1990s to focus on in-situ methods of recovering shale oil. Shell’s decision was driven primarily by the desire to avoid the material handling and spent shale problems.

Shell’s Soluble Salt Process

A different approach to create permeability and generate initial porosity was proposed and field tested by Shell in 1971- 1972 (4). This method relies on the dissolution of the saline mineral nahcolite (sodium bicarbonate) present with the oil shale at concentrations of 30% (volume) in the center of the Piceance Creek Basin. The field test involved the injection of hot water to leach the nahcolite and other salts out of the formation. This technique was successful in leaching nahcolite and generating the required permeability and porosity. The field pilot employed saturated steam to raise the temperature of the resource. Based on work by Cummins and Robinson (5) conversion rate is highly temperature dependent. Raising the kerogen to 600°F by steam injection (requiring 1543 psia steam) would

enable conversion of 90% of the kerogen to oil and gas in approximately 85 days (Figure 1). Initial fieldwork indicated that at the 1,700 ft. depth of the resource, 1543 psia steam could be injected into the formation without loss of containment.

While more details can be obtained from the report by Prats et al (4) the results of the field test were generally disappointing. The nahcolite could be readily leached, as evidenced by the nahcolite solution mining industry within the Piceance Basin, but the rubbing of oil shale caused disaggregation of the shale and resulted in flow problems such that the steam could not be circulated at design rates. This reduced heat input resulted in the production of approximately 420 bbls of a bitumen/oil mixture plus associated gas. Because of the production and corrosion issues, this approach was not pursued.

Despite the technical problems during the test, Shell was sufficiently encouraged to move forward with in-situ technology. Lessons learned included: the nahcolite zone could be used for product containment, proper metallurgy is required to handle the significant amounts of acid gas that is produced and that production technology needs to be flexible to handle both light oil and heavy bitumen production.

Laboratory Testing

To better understand the results of the soluble salt test an extensive laboratory testing program was initiated. The basic setup is shown below in Figure 2. Approximately 2 kg of crushed oil shale is loaded in the reactor. This isothermal and isobaric lab reactor is used as a kinetic tool and a gross emulation of vapor phase field production. A wide range of heating rates and pressures were tested. Careful analysis of oil, gas, and water production along with that of the residual coke left in the reactor allowed for excellent mass balance. However, this system did not capture the void volume and permeability environment in the field.

From the reactor setup it is obvious that the pressure-volume-temperature behavior sets the phase and residence time for the reactions and also determines the product slate.

The strong impact of heating rate on the product quality is shown in Figure 3 (6). With no reactor backpressure and the very slow commercial heating rates of 0.5 – 2.0°C/day high, 34 – 38°API gravity product is obtained. This can be contrasted to the oil obtained in the Fischer Assay (actually modified Fischer Assay, ASTM D-3904, 1984), a common method to evaluate the liquid yield of a particular oil shale resource, measured in U.S. gallons per short ton of raw shale (gpt) (7). By convention, experimental results are usually reported as liquid barrels as a percentage of FA. The oil in this case is usually in the 23 – 25 °API range and was obtained at a heating rate in excess of 10,000°C/day. Additional data points were published by the Lawrence Livermore National Laboratory and show a nice progression of increasing API oil gravity as the heating rate is decreased (8).

Another difference between the rapid heating to temperatures in excess of 500°C and the very slow heating rate of ICP to temperatures below 400°C can

be seen by comparing the carbon number distribution of the ICP oil and that of material obtained in a surface retort which is closer to Fischer assay (Figure 4). For ICP over 85%wt is typically in the transportation fuel range with carbon numbers less than C20. An important feature of ICP is that the higher carbon number portion of the kerogen stays in the rock matrix as coke.

While progress was made with understanding the overall in-situ conversion process there was still a need to develop modeling capabilities to predict the evolution of products at various pressures and temperatures throughout the entire production history. A series of experiments were carried out at a heating rate of 10°C/day and a backpressure of 100 psig (Figure 5). The reactions were stopped at various temperatures and the produced vapor phase products were captured along with the “bitumen” (the material that was still in the reactor but was extractable with dichloromethane) plus any coke. Significant conversion of kerogen begins at approximately 300°C and is essentially complete at 365°C. About 58% of the original kerogen is extractable with dichloromethane at approximately 340°C and it decreases to zero at about 400°C. The produced distillable oil for the tests ending at 450°C is indicated by the crosses and the run at 365°C by circles. For clarity the produced oil from runs completed at lower temperatures are not included. As can be seen, the produced oil from the run ending at 450°C is approximately 74vol% of Fischer Assay. While the focus of the discussion has been on the liquid oil product it should be noted that approximately 1/3 of the ICP energy production is in the gaseous phase. When gas is converted to equivalent liquid barrels and included in the recovery efficiency calculation the result is closer to 90-100% of Fischer Assay. The results of these studies were used to develop models to predict product composition as a function of conversion level. As can be seen a good match between model and laboratory tests has been obtained.

While slow heating rates affect the relative reaction rates along with volatilization of various fragments, the pressure of the system also plays a role. A series of tests were carried out at 1°C/day heating rate and with different imposed backpressures. As can be seen in Figure 6, imposing backpressure changes the vaporization behavior leading to products enriched in hydrogen. This change could be due to alteration of chemical type/structure (aromaticity) or molecular weight.

To investigate this pressure effect a detailed product chemical composition was carried out using a gas chromatography / mass spectroscopy technique. The results are presented in Figure 7 and indicate that in this pressure range the impact on chemical composition is minor. Of particular note is the high paraffinic nature of Green River oil shale ranging from 40 – 45wt%. The simulated distillation data (Figure 8) confirms that for this pressure range the impact of increasing pressure is mainly reduction in molecular size and this is due to a combination of vaporization and secondary cracking.

Combining the laboratory test and modeling results, a picture of how this in-situ process would work commercially started to take shape. The subsurface would act as a large reactor where the pressure and heating rate could be designed to maximize product quality and quantity and minimize production cost. The key would be to maximize hydrogen content of the liquid products and minimize the hydrogen content of the coke in the subsurface.

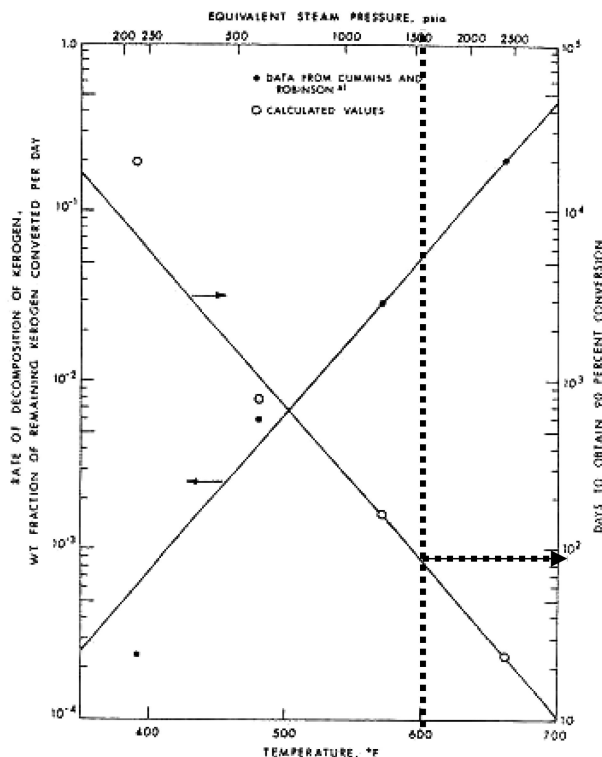


Figure 1. Days required to obtain 90% Conversion of Kerogen at Temperatures 350 – 700°F

While the laboratory testing was ongoing a review of possible subsurface heating techniques was initiated. As previously discussed, the methods that had been used in field testing had required the generation of permeability before substantial retorting could be achieved. However, because the thermal properties of bulk shale allow for propagation of energy through the solid shale itself, it was hypothesized that bulk heating with thermal conduction would generate permeability and that the gases generated during retorting will drive liquid oil from the pores of the shale. Of the various techniques that could be considered, the use of electric heaters appeared to be most promising.

Swedish History (1941-1960) of the In-Situ Conversion Process

The use of electric heaters to heat oil shale is not a new concept. At the beginning of World War II the Swedish government urgently ramped up oil shale development work in response to a blockade of imported oil in an attempt to supply liquid fuels to its indispensable fishing industry. Four shale oil recovery processes were developed simultaneously near Kvarntorp, Sweden (100 miles

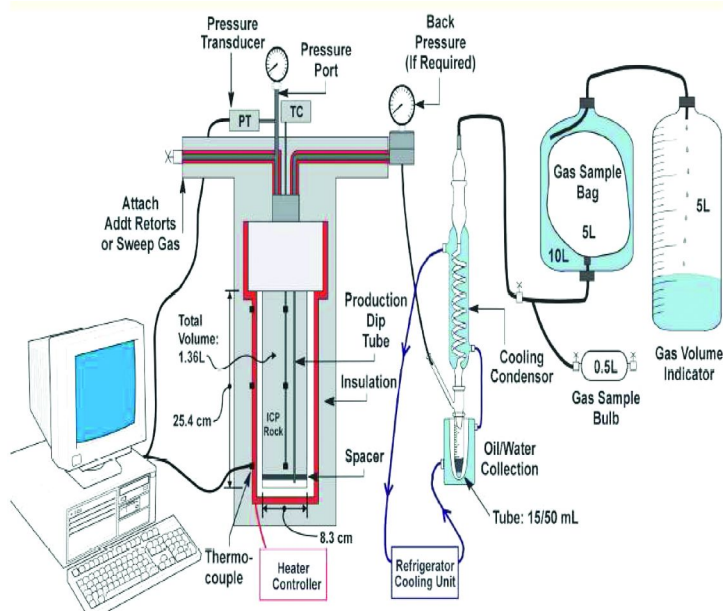


Figure 2. Laboratory Setup

SE of Stockholm) of which one was an in-situ process (invented by Dr. Fredrik Ljungström in 1940) known at the time as “the electrothermic method” or the “Ljungström in-situ” method (9). The Ljungström method was applied to a relatively thin (56 ft), moderately rich (16 gpt), shallow (overburden = 27 ft) oil shale deposit. The heating pattern consisted of a hexagonal array of heaters with a central producer on 7.2 ft spacing to allow for superposition of heat and uniform heating to conversion temperature. Each heater delivered 10 kW (~180 W/ft) to the resource and the heating rate was approximately 2°C/day with a final target temperature of 400°C. The pressure increase from heating and generation of gases drove the gaseous retorted products to the production well through pre-existing permeability. The average reservoir pressure during pyrolysis was 19 psig. A relatively light product with approximately 52%vol boiling less than 200°C was produced. This fraction was purified by treatment with caustic and sulfuric acid extractions.

Overall the technology was a success. The liquid recovery efficiency was above 60%FA and the ratio of energy out to energy in was 3.1:1. However, the project had several technical problems including corrosion (due to the presence of high, 25%vol, hydrogen sulfide), gas leakage (inadequate cap rock seal), bending and shearing of well casings, and water influx. After the war, cheaper supplies of imported oil became available again and the cost of labor and electricity increased. These factors eventually led to the closing of the in-situ project in 1960.

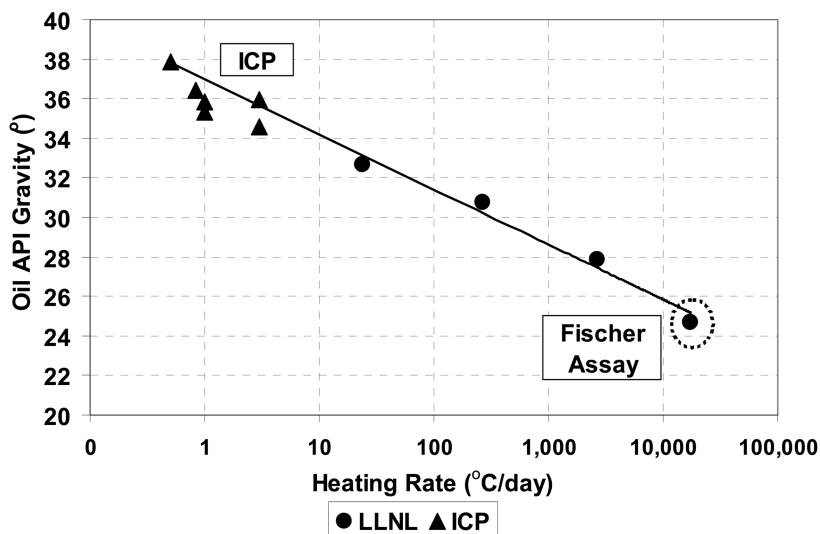


Figure 3. Relationship of API Oil Gravity and Heating Rate with no Reactor Backpressure

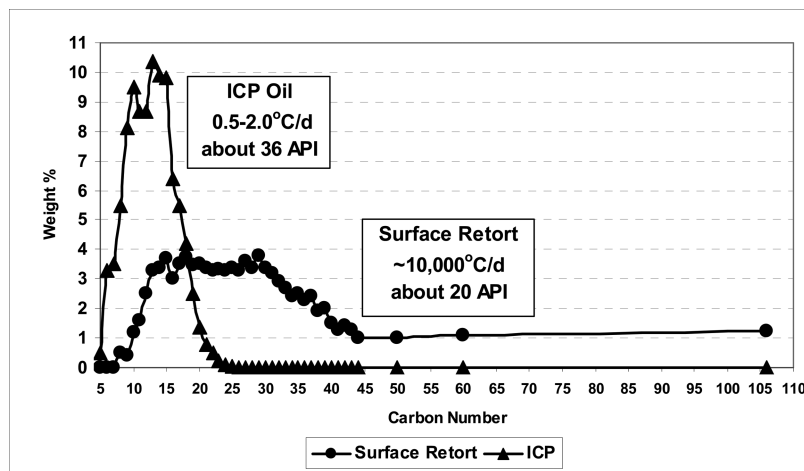


Figure 4. Comparison of Carbon Number Range of ICP and Surface Retorted Oil

Red Pinnacle Thermal Conduction Test (1981-1982)

With this background a field test was first proposed for the Green River oil shale by Shell's P. (Tip) Van Meurs and first piloted by Shell in Colorado at Red Pinnacle in 1981-82. The test was conducted in two phases. The first phase measured the oil shale thermal properties for comparison with the laboratory measurements while the second phase tested a new heater design, heated the oil shale to conversion temperature, and produced pyrolysis liquids and gases. The

second phase employed a seven-hole hexagonal pattern (2 ft spacing) comprised of alternating heater and producer holes around a central observer hole (Figure 9).

The heater was an early version of a mineral insulated heater. The 6 ft heated interval was selected because of its relatively high oil shale richness (>15 gpt) and sufficient thickness of competent oil shale above and below the target zone, to meet minimum overburden requirements, to reduce water influx, and to improve confinement of produced fluids.

Phase 2 heating began in early 1982. During the 55 day test heating period approximately 30 gallons oil, 2,000 scf gas and 20 gallons water were produced. Production was via a combination of vapor phase and artificial lift. During this time three different oil types were produced in sequence, each during about one-third of the heating period. Arrival times of these products at the three production wells varied but the major trends were unmistakable. The first oils (produced from day 6 through day 10) were light condensate of 42-44°API gravity. They were clear red amber colored fluids containing about 10 percent olefins, but no heavy (> C34) ends. The second type of product was bitumen with gravities from 8 - 15°API. They were produced as stable oil/water emulsions from day 18 through 28. These bitumens were typical depolymerized kerogen products, high in heterocompounds (70-80%), asphaltenes (6-17%), molecular weights (> C34, 40-70%) and acid numbers (3-5 mg KOH/g oil). The third type of oil, produced from day 38 to 55, was thermally altered oil with gravities from 21 to 22 °API. These contained high saturate (37%) and aromatic (21%) contents, but were lower in sulfur (~ 0.7%), asphaltenes (0.4-3%), heterocompounds (39-46%) and heavy ends (> C34, 39-46%) compared to the bitumen.

There were a number of significant accomplishments from this Red Pinnacle test and they include converting a high fraction of kerogen in place within the heated interval as determined by pre and post coring, capturing of oil and gas products, and operation of heaters at 800°C. One goal was to demonstrate that having porosity and permeability in the resource prior to heating was not necessary for having a successful project and this was accomplished. Although the test was initiated in a very competent and thus impermeable target zone, it was found that very good communication existed between injectors and producers at the end of the test. This fact was confirmed by pressure pulsing tests after power shutoff and by core examination during post test evaluations. One other learning from the test was that water influx from aquifers significantly impacted the energy balance of the system with an estimated 30% of the injected energy used to heat and boil water. It is interesting to note that the Swedish “Ljungström in-situ” method also found about the same percentage heat loss to water reflux despite employing dewatering wells.

Mahogany Field Experiment (1996-1998)

With the drop of the price of oil in the late 1980s together with the higher priority California thermal work, interest in oil shale gradually waned although a modest laboratory test program was continued. Shell’s interest in oil shale was

renewed in 1995 and the next year a larger, deeper project was designed and called the Mahogany Field Experiment (MFE). This pilot was conducted at Shell's Mahogany fee property in Rio Blanco County near the westernmost extent of the Piceance Basin.

The purpose of this test was to gain field confirmation of the oil quality produced in laboratory tests at a larger scale and greater depth than Red Pinnacle, to acquire data for numerical modeling, to understand aquifer effects and environmental impacts, and to evaluate heater performance.

A 57 ft interval was heated using a hexagonal array of heaters (Figure 10) consisting of nichrome wires threaded through electrically insulating ceramic beads and mounted on a metal support strip. The entire assembly was deployed in a 3.5 inch high alloy steel canister. To mitigate the effect of water influx a ring of six dewatering wells surrounded the heated pattern. To help with product capture a slight vacuum was used during the test. Heating began in mid 1997 and continued without incident until power was turned off in early 1998. Total oil production was 230 bbls with 1,300 mcf gas. Because one of the main goals of the project was to confirm laboratory produced oil quality in the field, a composite of the produced oil was analyzed. One measure that was used was to compare the carbon number distribution of the MFE oil to that produced in the laboratory (Figure 11). As can be seen, the simulated distillation of the MFE field pilot fits into the proper spot based on pressure.

The MFE was operated at pressures between 0 and 100 psig and the 38°API average composition of the produced oil agrees well with the laboratory data shown in Figure 7. The produced oil was primarily in the naphtha/jet/diesel fuel boiling range, as predicted.

This was the first time that a significant amount of product was produced to allow for extensive testing of upgrading technologies. One concern was the high nitrogen, approximately 1%wt, content. Detailed extraction and analyses revealed that the nitrogen compounds are primarily in aromatic ring compounds. However, it was found that in a lab-scale, one-step, hydrotreating process could produce a pipeline quality synthetic crude oil that could be readily refined to jet, diesel, and gasoline using conventional refining processes.

The MFE project provided much technical learning and helped to improve Shell's modeling of ICP (10). However, because of its small size, more testing would be required before a commercial project could be considered.

Mahogany Demonstration Project (Original) (1998-2005)

In 1997, during the early phases of the MFE heating, plans for the next oil shale pilot called the Mahogany Demonstration Project (MDP) were already being made. The project was conducted adjacent to the MFE. The primary purpose of the MDP was to determine the ICP recovery efficiency and energy balance. Secondary objectives included confirming product quality at greater depth, demonstrating technical capabilities including drilling, heater deployment and operation, and identifying pattern dewatering and scale-up issues. The original design (Figure 12)

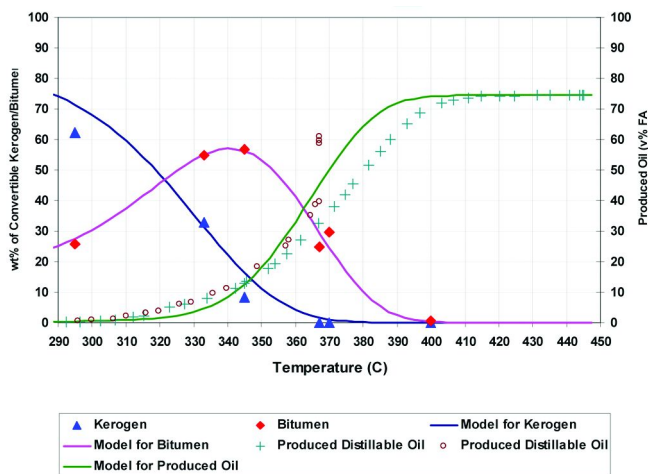


Figure 5. Kerogen Conversion and Bitumen and Oil Production

consisted of 38 heaters arranged in 20 ft. hexagonal patterns (with one additional test heater) and 15 producers at the center of each hexagon surrounded by a ring of dewatering wells.

In late 1998, prior to the installation of the heaters or the surface facilities, the project was suspended because of very low oil prices. In 2000, the project was restarted and heaters were deployed and facilities installed. A 150 ft interval was heated using bead heaters that were longer versions of the design used in the MFE. Heating began in late 2000. Within months, heaters began to fail. Over the next 2½ years in an attempt to inject sufficient heat to complete the project, many of the failed heaters were successfully pulled and replaced while others could not be removed (11). During this period heater failures continued.

By mid 2003, it was decided that the project could not be completed with the current heat delivery system. The average temperature achieved was well below the 650°F target and total oil production was less than 2% of design. Although the main objective of the test was not achieved there were several significant lessons learned that were incorporated in the next pilot test called the Mahogany Demonstration Project [South].

Mahogany Demonstration Project (South) (2003-2005)

The two primary objectives of the MDP[s] were: (1) reduce the uncertainty around the recovery efficiency compared to the MFE and (2) produce and capture a significant volume of oil (greater than 1,000 bbls). Because of the troublesome experiences at MDP[o], this project was designed with redundancy and other protective measures to maximize the probability of success. Several measures were employed to complete the project in a timely manner and to maximize the probability of success including: (1) utilizing as much of original MDP facilities as possible including separators and water treating, (2) designing a robust heater

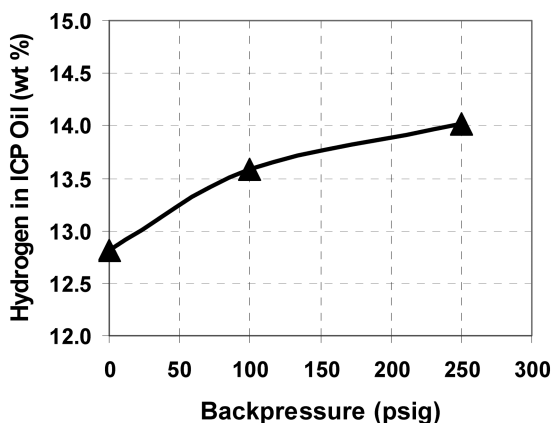


Figure 6. Hydrogen Content of ICP oil as a Function of Imposed Backpressure

system by combining a heavy wall canister with a mineral insulated (MI) heater, (3) including a permeable zone for production to minimize high pressure build-up in reservoir, (4) using a high density of heaters around the producers to create an early pyrolyzed zone, (5) using two different types of producers with one being vapor phase and the other being a sumped rod pump, and (6) enhancing product capture with use of surface vacuum. The heated pattern is shown in Figure 13.

Heating began in the spring of 2004 and continued for nearly 15 months with no heater failures. Although production dropped off dramatically after the heaters were turned off in mid 2005, production continued until November 2005 with the total oil production reaching 1,860 bbls. Post coring confirmed the liquid recovery efficiency to be above 60%FA, consistent with the Swedish project, Red Pinnacle, and MFE. The results of these field tests support the expectation that a commercial-scale ICP project would achieve total (oil+gas) recovery efficiency of approximately 90%FA with a total energy balance of close to 3.0 if it is based on electrical heaters.

A thermal reservoir simulator (9) was run and covered the majority of production (Figures 14 and 15). As can be seen there is an excellent match both in terms of predicting oil and gas rates as well as cumulative production. To obtain an accurate history match for the oil and gas production the model first matched the thermal history of the reservoir by using the heat injection rates for each heater and then tuning the water influx and the thermal properties of the formation.

Oil properties from MDP[s] were similar to the oil produced at MFE even though the field experiments pyrolyzed different oil shale zones. The nitrogen and oxygen concentrations were equivalent while the higher sulfur concentration for MDP[s] could be related to having a higher pyrite concentration in the pyrolysis zone. In addition, the concentrations of various hydrocarbon types, e.g., paraffins, cyclanes, and aromatics were similar along with the boiling point distributions (Table I).

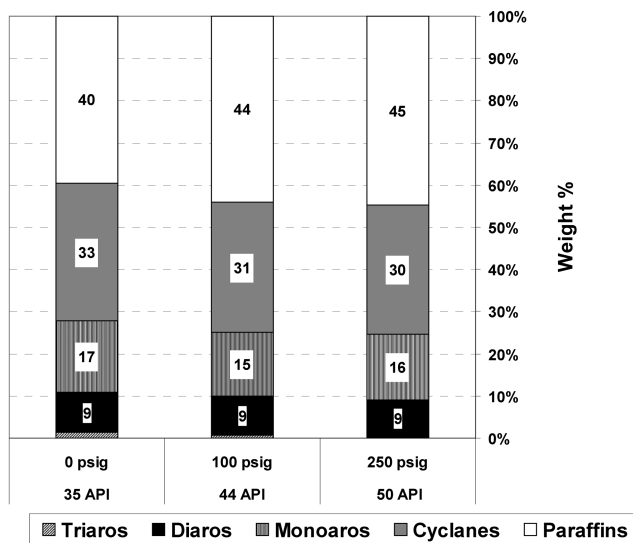


Figure 7. Chemical Composition Changes as a Function of Imposed Backpressure

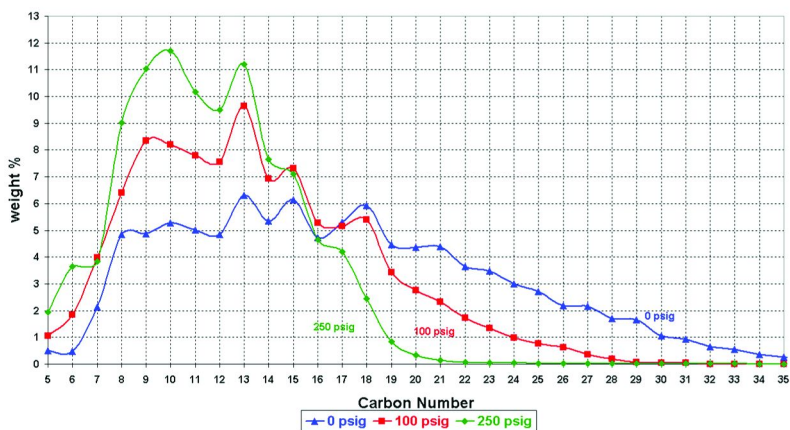


Figure 8. Carbon Number Distribution as a Function of Imposed Backpressure

Commercialization of oil shale using ICP technology requires not only an understanding of the subsurface heating, cracking, and coking but also a plan for handling the products once produced to the surface. Because of the scale of the MDP[s] test it was possible to obtain significant amounts of water, oil, and gas for analysis and also for laboratory upgrading. A scheme for handling the production from the wellhead to finished products is shown in Figure 16. Water, oil, and gas are first separated in a simple three phase separator. The desalting of the oil was relatively straightforward and no significant problems were encountered. The use of filtration was employed to separate clean permeate from the unfiltered oil

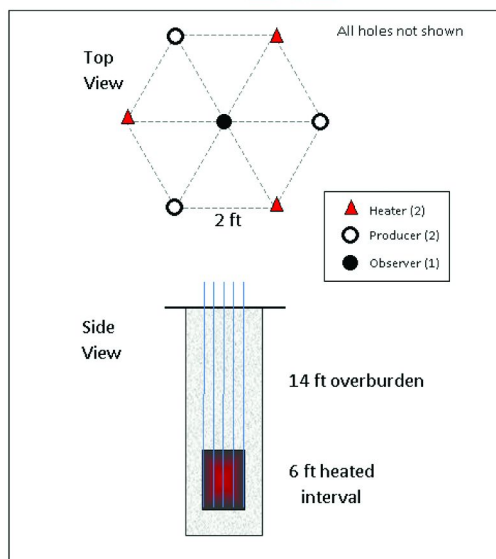


Figure 9. Red Pinnacle Thermal Conduction Test

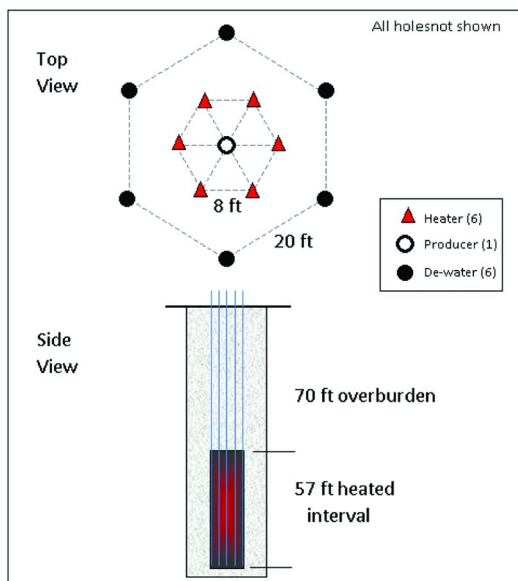


Figure 10. The Mahogany Field Experiment

where the particulates were concentrated and was processed separately. Based on extensive pilot plant testing of the water from MDP[s] the quality requirements in Colorado can readily be met with known technology.

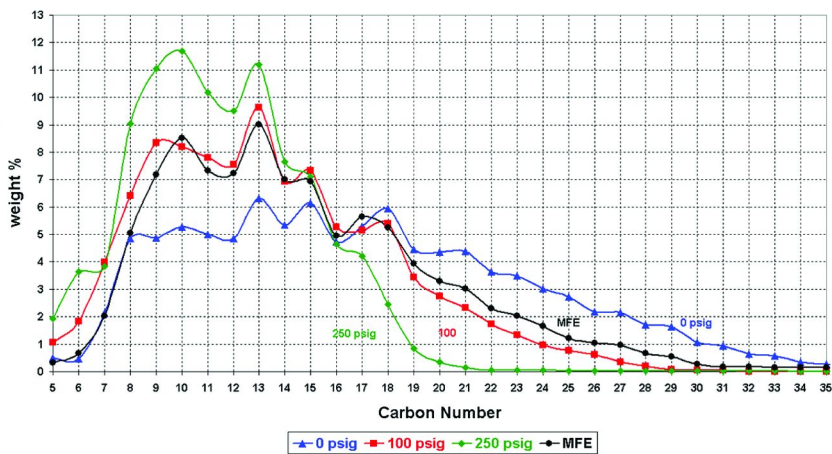


Figure 11. Carbon Number Distribution as a Function of Imposed Backpressure in Laboratory produced Oil Compared to Oil from the Mahogany Field Experiment

The upgrading of the oil to transportation quality products is outlined next. Raw filtered shale oil has a tendency to foul because of di-olefinic species but can easily be stabilized in a low pressure hydrotreating operation. The whole crude can then be hydrotreated and then fractionated, or fractionated and then hydrotreated. The hydrogen that is co-produced in the process can be used to meet some or all of the hydroprocessing demand. The paraffinic nature of the shale oil produces a low octane reformat feedstock but could also be used as a chemical feedstock for an olefin plant provided that hydrotreating removes essentially all the heteroatoms and in particular the nitrogen compounds. To help improve the octane of the gasoline product the C₃ and C₄ olefins can be alkylated to produce high octane gasoline components. While the paraffinic nature of the shale oil makes for a poor gasoline the paraffinic middle distillates make excellent jet and diesel products. The paraffinic shale oil vacuum gasoil can be subjected to various conversion processes, e.g. catalytic cracking, hydrocracking, or used for the production of lower olefins or base oil/bitumen.

To test this scheme the MDP[s] oil was upgraded using commercially available catalysts at moderate hydrotreating conditions. The results of JP-8 material prepared for the Department of Defense are presented in Tables II (12). JP-8 is the military equivalent of Jet A-1 with the addition of corrosion inhibitor and anti-icing additives; it meets the requirements of the U.S. Military Specification MIL-DTL-83133E. Jet A-1 is a kerosene grade of fuel suitable for most turbine engine aircraft and is produced to a stringent internationally agreed standard, has a flash point above 38°C (100°F) and a freeze point maximum of -47°C. For comparison the data from two previous surface retort shale oil tests along with product properties of jet fuel made from a Gas-to-Liquids (GTL) process and that from typical petroleum refining supplied by the Department of Defense are included.

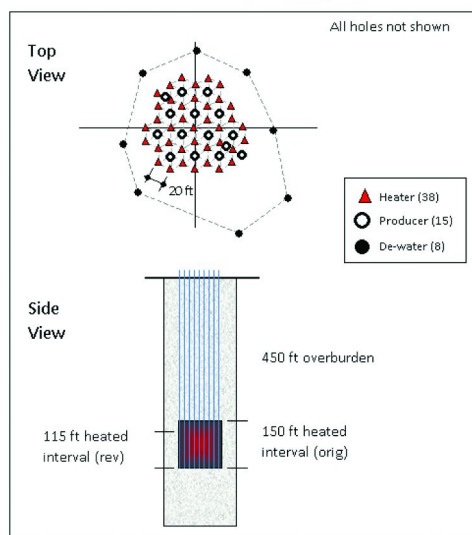


Figure 12. Mahogany Demonstration Project (original)

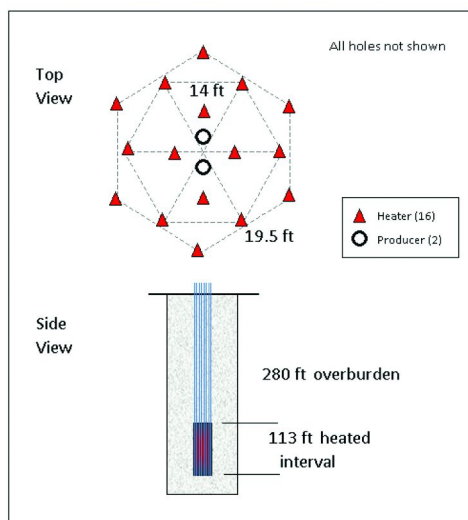


Figure 13. Heated Pattern of the Mahogany Demonstration Project (South)

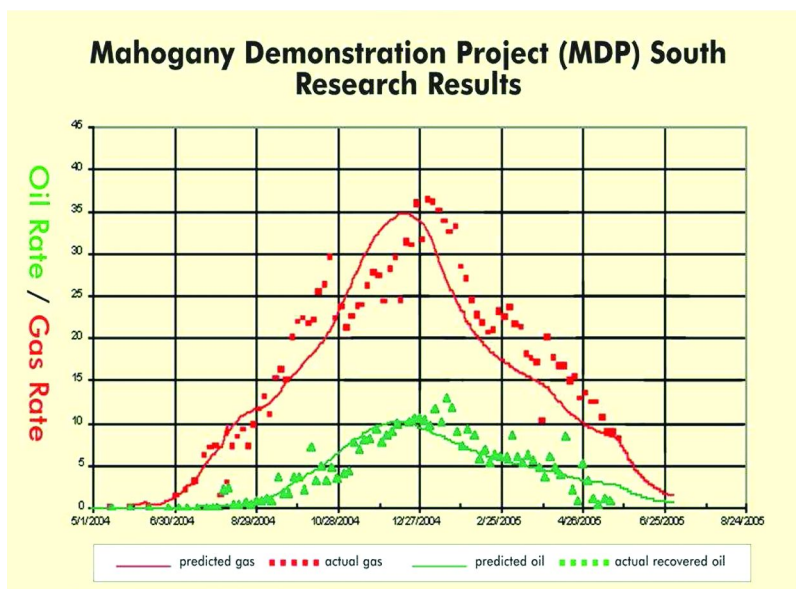


Figure 14. Oil and Gas Production Rates at MDP[s] and Model Results

To compare these products two key specifications, the freeze point and smoke point, will be examined. For high altitude operation a low freeze point fuel is required. As can be seen the Shell ICP shale oil, GTL, and typical petroleum JP-8 all meet the specification but the two previous shale oil materials from the 1970s do not. The smoke point is defined as the maximum flame height in millimeters at which jet fuel will burn without smoking, tested under standard conditions. It is used as a measure of the burning cleanliness of jet fuel and kerosene and higher smoke points are desired. The JP-8 fuel made from the Shell ICP shale oil has a smoke point that is superior to that of typical current JP-8 production and is similar to the fuel made from GTL oil. In summary this testing clearly established that the ICP shale oil can be converted into military grade jet fuel that meets current and anticipated future specifications.

While significant progress has been made in Shell's attempt to commercialize shale oil ICP, two major issues remain and they are the development of a cost effective and robust heater system and a cost effective method for product containment and exclusion of water from the pattern. Although the MDP[s] heaters worked extremely well, the use of thick wall canisters in a commercial project is not feasible. As far as water and product capture is concerned the use of vacuum, as was used at MDP[s], is also not practical and the use of dewatering wells is not suitable for minimizing water influx into the heated pattern.

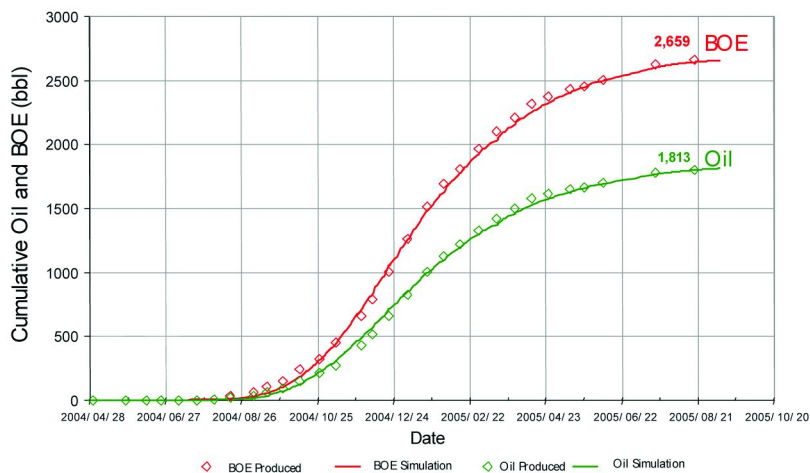


Figure 15. Cumulative MDP[s] Production and Model Results

Table I. Comparison of MFE and MDP[s] Oil Properties

<i>Pilots</i>	<i>MFE</i>	<i>MDP[s]</i>
API Gravity	37.9	35.5
Specific Gravity (calc)	0.8352	0.8473
C, % wt	84.97	85.11
H, % wt	12.95	12.57
O, ppm	4700	4600
S, ppm	4790	8330
N, ppm	10030	11100
Boiling Ranges, % wt		
Naphtha (IBP-375°F)	28.6	26.7
Jet (375-500°F)	28.1	28.6
Diesel (500-650°F)	27.2	28.2
Bottoms (650°F+)	16.1	16.4
Hydrocarbon Type, % wt		
Paraffins (Total)	40.5	44.4
Normal	23.8	28.2
Iso	16.7	16.2
Cyclanes	31.2	29.4
Phenols		0.2
Monoaromatics	17.9	16.4
Carbazoles		0.3
Diaromatics	9.9	7.7
Triaromatics		1.5
Tetraaromatics		0.1

To address these problems work was initiated in 2001 to field test heaters in oil shale and in 2002 to test a freeze wall concept to prevent water influx.

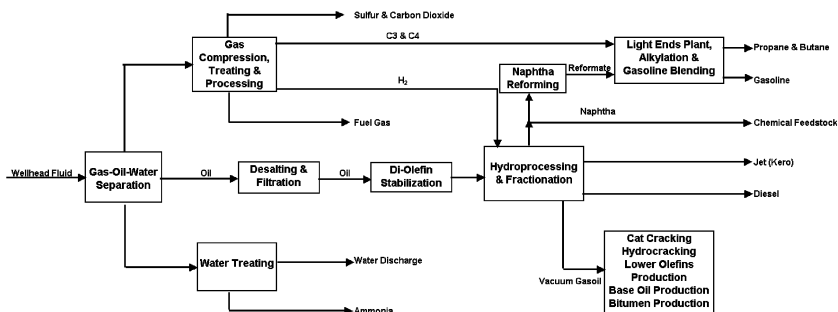


Figure 16. Shale Oil Refining General Process Flow Scheme

Deep Heater Test (or Mahogany Test Experiment) (2001-Present)

For a successful oil shale project it is necessary to develop and field test a commercial heater. To facilitate the development of a commercial heater, a pilot called the Deep Heater Test (DHT) was designed at Shell's Mahogany site and is located adjacent to the MDP and MFE. The purpose of this pilot was to enable field-testing of a variety of potential commercial heaters in near commercial conditions (up to 410 ft in length). The testing allowed the evaluation of threats posed by geomechanical stresses, thermal stresses and property variations, water influx, wellbore stability, and high temperature corrosion. Heater testing began in 2002 and continued through 2007. A total of 17 heaters have been tested representing multiple heater types such as pipe-in-pipe and mineral insulated heaters. The tests have helped identify many technical challenges including: (1) heater hot spots caused by variations in oil shale thermal conductivity, (2) geomechanical strength of the formation as a function of temperature, (3) impact of high geomechanical stresses on heater performance, (4) non-uniform formation gripping of the heater, (5) shear stresses near the top and the bottom of the heated intervals, (6) refluxing, (7) control of low impedance heaters, and (8) hole stability as a function of temperature. Other tests were conducted at the DHT location in holes used to measure the impact of rock deformation on heaters.

Mahogany Isolation Test (2002-2004)

Commercialization of oil shale using the ICP technology requires a method of preventing water influx to the heated pattern and also a method of ensuring capture of the products of pyrolysis both to maximize recovery and protect local aquifers. A freeze wall is a relatively common practice in some underground mining operations and may be a solution to both of these problems. A field pilot was executed with the objective of proving that a freeze wall could be formed using conduction cooling, and ICP fluids could be contained within the freeze wall during retorting and the heated oil shale interval could be remediated. A diagram

Table II. MDP[s] Shale Oil JP-8 Jet Fuel

<i>Specification Test</i>	<i>Shell ICP Shale Oil JP8 2007</i>	<i>Shale Oil JP5 1974</i>	<i>Paraho Shale Oil JP5 1978</i>	<i>GTL JP8</i>	<i>Petroleum JP8</i>
Total Acid Number, mg KOH/g	0.002		0.001	0.004	0.005
Aromatics, % vol	3.2	25.95	24	0.0	20.3
Olefins,	0.7	2.29	1.6	0.0	0.6
Mercaptan Sulfur, % mass	0.000		0.01	0.000	0.000
Total Sulfur, % mass	0.00	0.05	0.04	0.00	0.07
Distillation:					
IBP, °C	146	171	186	144	160
10% recovered, °C	166	191	193	167	177
20% recovered, °C	171	199	196	177	183
50% recovered, °C	186	219	207	206	200
90% recovered, °C	219	254	232	256	237
EP, °C	245	282	253	275	255
Residue, % vol	1.3	1.0	1.2	1.5	1.2
Loss, % vol	0.5	1.2	0.2	0.9	0.7
Flash Point, °C	44	65.5	66	45	52
Cetane Index (calculated)	52.4	49.5	44.6	66.0	45.1
Freeze Point, °C	-53	-22.5	-46	-51	-49
Viscosity @ -20°C, cSt	3.7	5.1		4.9	4.2
		(@ -18°C)			
Viscosity @ -40°C, cSt	6.7		7.99	9.5	8.3
			(@ -34°C)		
Heat of Combustion (measured), BTU/lb	18740	18532	18561	18870	18470
Hydrogen Content, % mass	14.7	13.7	13.7	15.4	13.8
Smoke Point, mm	40	22	21	42	23
Copper Strip Corrosion	1a	1a	3b	1a	1a
Thermal Stability @ 260°C					
Tube Deposit Rating	0	Fail	0	1	1
Change in Pressure, mm Hg	0		0	0	1
Existent Gum, mg/100ml	0.2	81.7	0	0.6	0.2
Particulate Matter, mg/ml	0.1	164.2	0.6	1.0	NR
Filtration Time, minutes	3			10	NR
Water Reaction	1			1	1
Specific Gravity @ 15°C	0.778	0.8058	0.807	0.756	0.798
Nitrogen, ppm	0	895	1.0	0	

of the test layout is shown in Figure 17. The two heaters and one producer well were drilled on the vertices of an equilateral triangle with a 7 ft side.

After approximately 5 months of cooling the formation of the freeze wall was completed with total isolation of impacted water zones. The heating phase began in mid 2003 and lasted six months. There was no artificial lift or vacuum used and so production was via vapor phase. Approximately 2.6 barrels of oil and 73 MSCF of gas were produced. An important concern for a commercial project is the reclamation of ICP products of pyrolysis, particularly the water-soluble organic compounds (primarily BTEX - benzene, toluene, ethyl benzene, and xylene). A reclamation test was carried out at the MIT and demonstrated that a “pump and treat” approach could be successfully used to meet regulatory requirements.

While the MIT successfully achieved its three main objectives of creating and sealing a freeze wall, converting oil shale to products without water influx, and reclaiming the interior of the freeze wall the size of the test was too small to be considered sufficient to derisk a commercial project.

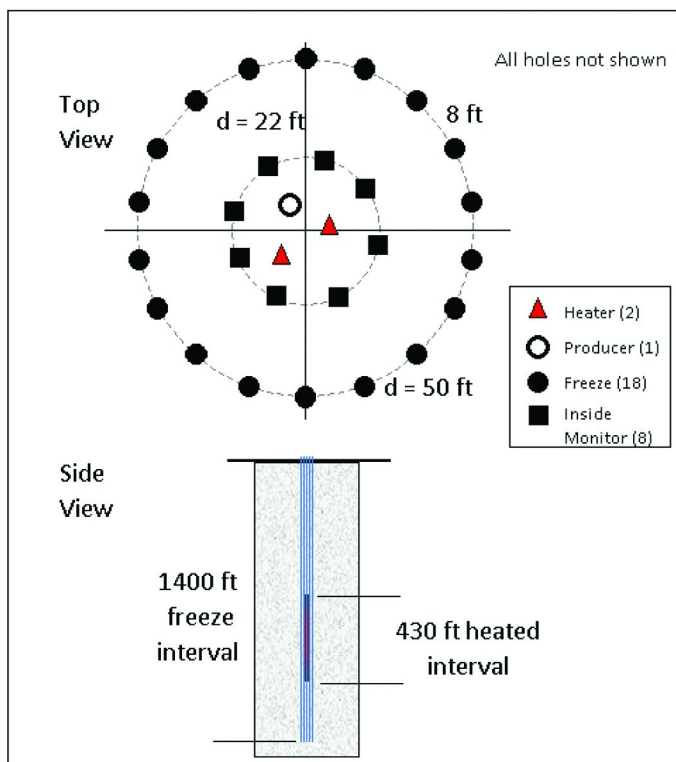


Figure 17. Mahogany Isolation Test

Freeze Wall Test (2005-Present)

As a follow-up to the successful MIT freeze wall test a large field pilot, Shell's largest and most ambitious to date, was designed to investigate the viability of using freeze wall containment for a commercial oil shale project, to test a grout wall as an alternate containment option, and to test possible wall repair methods. The test layout is shown in Figure 18.

The test was started in 2005 and freezing began in early 2007. The shallowest zones were completely frozen in late 2008 and the middle zone froze in April 2009. As of July 2009, the freeze wall is continuing to form in the deeper zones. Testing to determine its robustness and reparability will be conducted later in 2009 and 2010.

Research, Development, and Demonstration Pilot(s)

While progress has been made by Shell in moving forward on the development of oil shale ICP, the field testing has been basically limited to work on land that Shell owns in fee. To truly unlock this resource Shell needs access to large

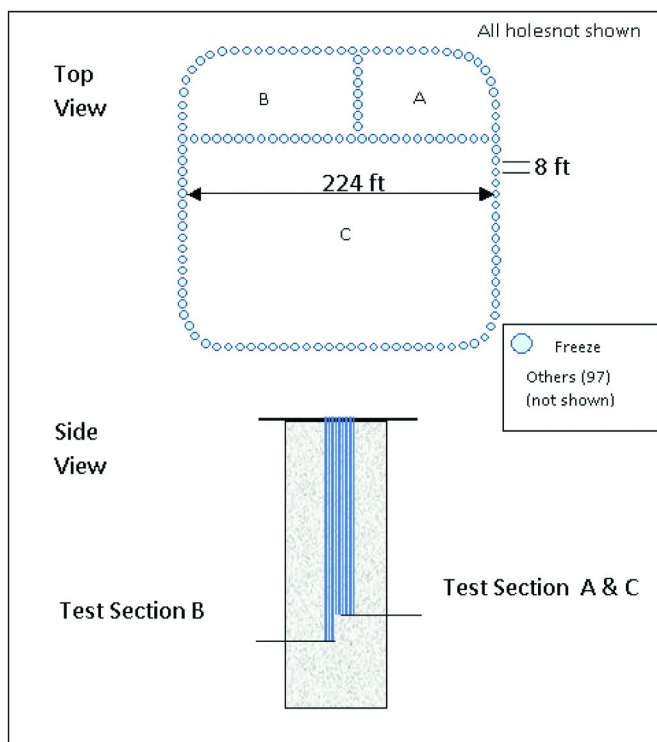


Figure 18. Freeze Wall Test

areas of resource and this means working with the Federal government that owns approximately 80% of the oil shale in the Piceance Basin. President Herbert Hoover signed an executive order that prohibited the leasing of federal oil shale lands. This ban has only been lifted twice, most recently with the Energy Policy Act of 2005 that allowed leasing of oil shale properties in 160-acre parcels for Research, Development, and Demonstration (RDD) purposes. Most recently with the Energy Policy Act of 2005 that allowed leasing of oil shale properties in 160-acre parcels for Research, Development, and Demonstration (RDD) purposes. If the RDD work meets the agreed upon terms, the RDD leaseholders can earn a preferential right to convert the 160-acre RDD lease to a 5,120-acre commercial lease. Under terms of the leasing program, a different technology is required for each lease. Shell was successful in obtaining three leases to test: (1) base ICP, (2) advanced heater ICP, and (3) nahcolitic oil shale ICP. Planning of the RDD field tests and the follow-up commercial activities is in progress.

Summary

Shell has been active in the development of oil shale technology for more than 50 years. A steady progression of lessons learned from both laboratory and field testing covering a wide range of technologies from mining to steam processes to electric heaters has brought clearly into focus both the challenges and opportunities for a commercial oil shale project. To date, Shell has conducted eight Colorado field pilots in the oil shale resource with increasing scope, cost, and complexity. The majority of effort since 1981 has been devoted to actively studying important elements of the In-situ Conversion Process. The current focus is to complete the freeze wall test and to develop robust test programs to convert the three RDD leases under the terms of the Energy Policy Act of 2005.

References

1. Thorne, H. M.; Stanfield, K. E.; Dinnean, G. U.; and Murphy, W. L. *Oil Shale Technology, A Review*; Inf. Conf. Circ. 8216; U.S. Department of the Interior, U.S. Bureau of Mines, Washington, DC, 1964; p 1–24
2. Yen, T. F. Structural Investigations on Green River Oil Shale. In *Science and Technology of Oil Shale*; Yen, T.F., Ed.; Ann Arbor Science Publishers: Ann Arbor, MI, 1976.
3. Johnson, R. C., et al. *An Assessment of In-place Oil Shale Resource in the Green River Formation, Piceance Basin, Colorado*; Fact Sheet 2009-3012; United States Geological Survey: March, 2009.
4. Prats, M.; Closmann, P. J.; Ireson, A.T.; Drinkard, G. *Soluble Salt Processes for In-Situ Recovery of Hydrocarbons from Oil Shale*; SPE Paper No. 6068; 1976.
5. Cummins, J. J.; Robinson, W. E. *Thermal Degradation of Green River Kerogen at 150°C to 350°C*; RI 7620; U.S. Bureau of Mines, Laramie Energy Research Center: Laramie, WY, 1972.
6. Beer, G.; Zhang, E.; Wellington, S.; Ryan, R.; Vinegar H. *Shell's In-Situ Conversion Process – Factors Affecting the Properties of Produced Shale Oil*; In Colorado Energy Research Institute Document: CERI-2009-2; Presented at 28th Oil Shale Symposium, Golden, CO, 2008
7. Dyni, J. R. *Geology and Resources of Some World Oil Shale Deposits*; U. S. Geological Survey Scientific Investigations Report 2005-5294.
8. Burnham, A. K.; Singleton, M. F. High Pressure Pyrolysis of Green River Oil Shale. In *Geochemistry and Chemistry of Oil Shale*; Miknis, F. P., McKay, J. F., Eds.; ACS Symposium Series 230, American Chemical Society: Washington, DC; 1983; pp 335–351.
9. Salomonsson, G. *The Ljungström In-Situ Method for Shale-Oil Recovery Oil Shale and Cannel Coal*; Proceedings of the Second Oil Shale and Cannel Coal Conference; Institute of Petroleum: London, 1951; Vol. 2, pp 260–280.

10. Chen, C. *Reservoir Simulation Study of an In-situ Conversion Pilot of Green-River Oil Shale*; SPE 123142-PP, SPE Rocky Mountain Petroleum Technology Conference, Denver, CO, 2009.
11. Fowler, T. D.; Vinegar, H. J. *ICP Oil Shale - Colorado Field Pilots*; SPE 121164, Presented at the SPE Western Regional Meeting, San Jose, CA, March 24–26, 2009.
12. Nair, V.; Ryan, R.; Roes, G. *Shell ICP – Shale Oil Refining*; In Colorado Energy Research Institute Document: CER1-2009-2; Presented at 28th Oil Shale Symposium, Golden, CO, 2008.

Chapter 10

ExxonMobil's Electrofrac™ Process for *In Situ* Oil Shale Conversion

W. A. Symington,* R. D. Kaminsky, W. P. Meurer, G. A. Otten, M. M. Thomas, and J. D. Yeakel

ExxonMobil Upstream Research Company, P. O. Box 2189, Houston, Texas, 77252-2189

*bill.symington@exxonmobil.com

ExxonMobil is pursuing research and development of the Electrofrac process for *in situ* oil shale conversion. The process heats oil shale *in situ* by hydraulically fracturing the oil shale and filling the fracture with an electrically conductive material, forming a resistive heating element. Heat generated in the fracture is thermally conducted into the oil shale, converting the organic matter into oil and gas which are produced by conventional methods.

Electrofrac has the potential to recover oil and gas from deep, thick oil shale formations with less surface disturbance than mining and surface retorting or competitive *in situ* heating techniques. Laboratory and numerical modeling results have been encouraging, and field experiments are underway to test Electrofrac process elements at a larger scale. Several years of research and development will be required to demonstrate the technical, environmental, and economic feasibility of this breakthrough technology.

Electrofrac is an energy-efficient method for converting oil shale to producible oil and gas (*I*). As shown in Figure 1, the method heats oil shale *in situ* by hydraulically fracturing (a conventional oil field technology) the oil shale and filling the fracture with an electrically conductive material to form a heating element. The produced shale oil and gas are recovered by conventional methods.

The use of fractures in Electrofrac is consistent with early screening research at ExxonMobil, aimed broadly at producing oil and gas from organic-rich rocks. This research explored over 30 technologies that potentially could be applied to this general problem. Basically, the research concluded:

- that *in situ* methods are preferred,
- that heat conduction is the most practical way to “reach into” organic-rich rock and convert it to oil and gas, and
- that linear conduction from a planar heat source is more effective than radial conduction from a wellbore.

The effectiveness of planar heat sources results in their requiring far fewer heating wells for development of an oil shale resource.

Electrofrac is depicted in Figure 1 in what is expected to be a preferred geometry, using longitudinal vertical fractures created from horizontal wells and conducting electricity from the heel to the toe of each heating well. This is not the only workable geometry, and one can envision many variations within the scope of Electrofrac. The process is applicable with either vertical or horizontal fractures.

The Electrofrac conductant must have an electrical resistivity high enough for resistive heating, yet low enough to conduct sufficient electric current. This means it must be significantly less conductive than most metals and significantly more conductive than most insulators.

The remainder of this chapter reviews ExxonMobil’s research on Electrofrac, which has been focused on critical technical issues for process success. These issues include:

- Identification of a suitable Electrofrac conductant,
- Ascertaining whether electrical continuity through a fracture can be maintained when the rock is heated,
- Assessing whether oil and gas will be expelled from oil shale heated under *in situ* stress,
- Estimating the chemical composition of generated shale oil and understanding the factors that control this composition,
- Designing a completion strategy for creating fractures that can deliver heat effectively, and
- Developing *in situ* conversion methods that allow coproduction of other mineral resources.

Research addressing these issues has consisted of core-plug-scale laboratory experiments and numerical models. Results have been encouraging and specifically have included the following.

- Calcined petroleum coke has been identified as a candidate Electrofrac conductant.
- Experiments with simulated Electrofrac fractures have verified that, at least at core-plug scale, electrical continuity can be maintained even as kerogen is being converted to oil and gas.
- Hydrocarbon expulsion from oil shale under *in situ* stress has been verified by experiments conducted in a miniature load frame designed to fit in a pressure-sealed heating vessel.

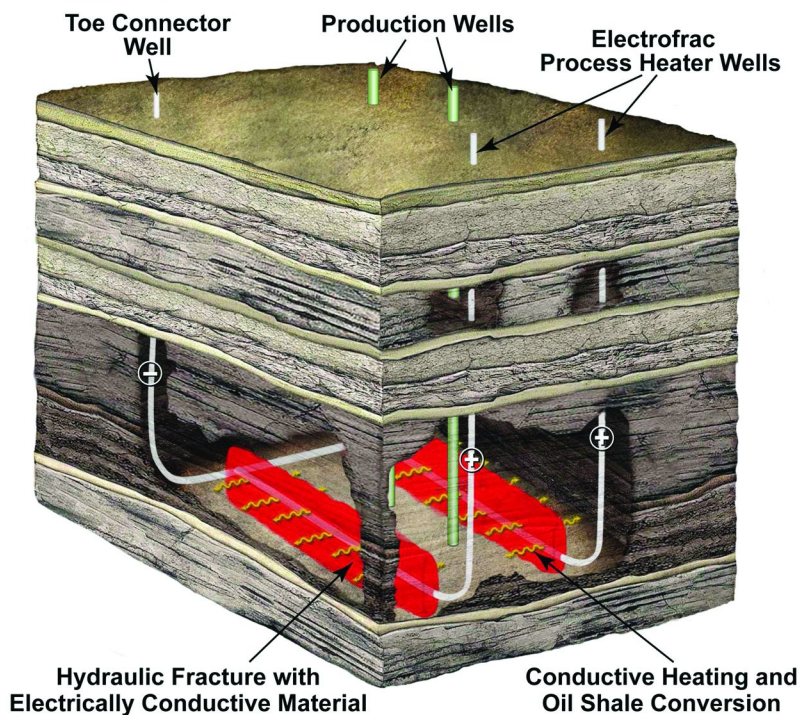


Figure 1. Electrofrac process schematic diagram.

- An equation-of-state phase behavior model for the fluids generated from kerogen suggests that volume expansion upon conversion is a large potential drive mechanism for expulsion.
- Geomechanical modeling indicates most of the Piceance Basin Green River oil shale is in a stress state favoring vertical, rather than horizontal, fractures. Completion strategy work has therefore focused on vertical fracture scenarios.
- Effective heating has been verified with screening tools based on heat conduction models coupled to kinetic models of kerogen conversion.
- In Piceance Basin, it should be possible to coproduce oil shale by *in situ* conversion, and sodium minerals by subsequent solution mining.

The remainder of this chapter provides additional detail regarding these research results and is organized around the important technical issues addressed. In several instances, examples are drawn from potential Electrofrac application to the Green River oil shale in the Piceance Basin of Colorado. This is appropriate because the Piceance Basin contains what is probably the world's largest oil shale resource. Although Piceance Basin examples are described herein, ExxonMobil's expectation is that Electrofrac is broadly applicable to global oil shale resources of sufficient richness and thickness.

Electrofrac Conductant Identification

As stated above, calcined petroleum coke has been identified as a candidate Electrofrac conductant. This is coke that has been heated to high temperature (1200-1400°C), usually in a rotary kiln (2). Calcined petroleum coke is relatively pure carbon, with higher calcining temperatures increasing its purity. It is a granular material with physical characteristics that make it amenable to being pumped into a fracture. Figure 2 shows photographs of calcined petroleum coke and a 20/40 mesh fracture proppant.

The electrical resistivity of calcined petroleum coke is in the desired range for an Electrofrac conductant and is relatively temperature-insensitive. This temperature insensitivity is illustrated by the data presented in Figure 3. These measurements were made on commercially available calcined coke. Two experiments are represented in Figure 3, each showing the measured resistivity as the sample is first heated and subsequently cooled. The data have been normalized by dividing by the measured resistivity at 25°C.

In addition, the resistivity of calcined coke should be controllable to some extent by specifying the calcining temperature. This is illustrated by the data of Hardin et al. (3), reproduced in Figure 4.

Because the coke is calcined at temperatures higher than it will experience in the Electrofrac process, it should also have good chemical stability. Finally, this material is generally available and relatively inexpensive. It is used in aluminum smelting, cathodic corrosion protection, and as packing material for industrial electrical grounding.

Electrical Continuity

A number of experiments were conducted to verify that electrical continuity can be maintained as kerogen adjacent to the fracture converts to oil and gas. Simulated fractures were created in core-plug samples by cutting the sample in half, milling a tray in one half to accept the conductant, and assembling an oil-shale conductant oil-shale sandwich. Conductants used were calcined petroleum coke and cast steel shot. The steel shot was used as a proxy prior to the identification of calcined coke. During assembly, stress was applied to the sandwiches using hose clamps to achieve electrical continuity. The samples were then heated to oil shale conversion temperatures. Construction of samples with simulated fractures for these electrical continuity experiments is illustrated in Figure 5.

Concern about maintaining electrical continuity stems from the idea that heated oil shale will soften, allowing a granular conductant to lose contact between individual particles. If the conductant particles embed too deeply in the walls of the fracture, continuity could be lost in this manner.

The results of one electrical continuity experiment are illustrated in Figure 6. In this experiment, cast steel shot was the conductant. The assembled sandwich axially confined in a steel frame but no axial stress was applied. The entire assembly was heated externally in a pressure-sealed heating vessel to 360°C for

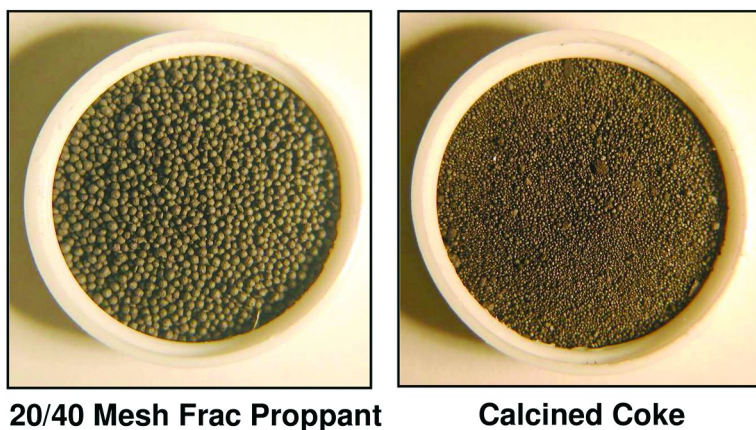


Figure 2. Photos of 20/40 mesh fracture proppant and calcined petroleum coke.

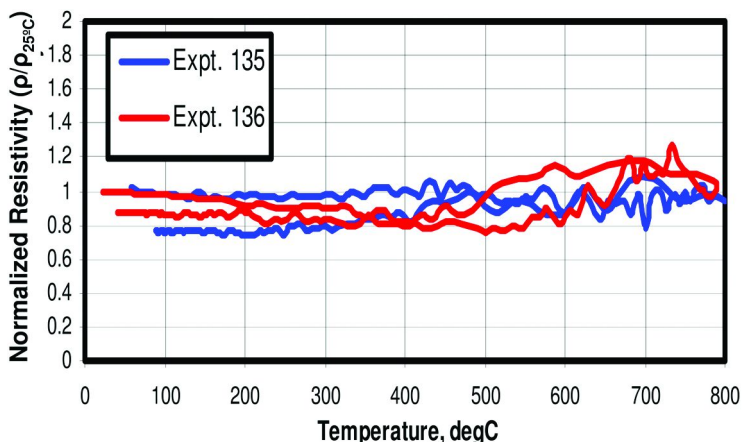


Figure 3. Resistivity measured on commercially available calcined coke.

24 hours, achieving 90% conversion of the oil shale to oil and gas. After the sample was cooled and removed from the heating vessel, its electrical continuity was found to be intact. A saw cut was made across the diameter of the sandwich, and photographs of the simulated fracture were taken. The rock indentations in the fracture face, visible in Figure 6, indicate that a minor degree of embedment did occur, but this did not disrupt the circuit.

Figure 7 illustrates the results of a second electrical continuity experiment. This experiment was heated internally by supplying electric current to the simulated fracture. Because the thermal conductivity of oil shale is relatively low, in a short-term, internally heated experiment, it is possible to maintain a substantial temperature difference between the simulated fracture and the periphery of the sample. The sandwich in this experiment was again constructed with cast steel shot as the conductant. To permit connection of the power leads, no axially confining frame was used in this experiment. The circuit was heated

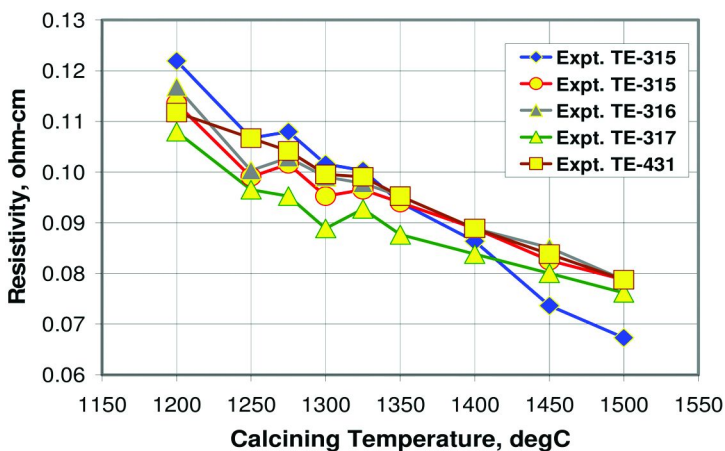


Figure 4. Calcining temperature controls coke resistivity. After Hardin et al. (3)

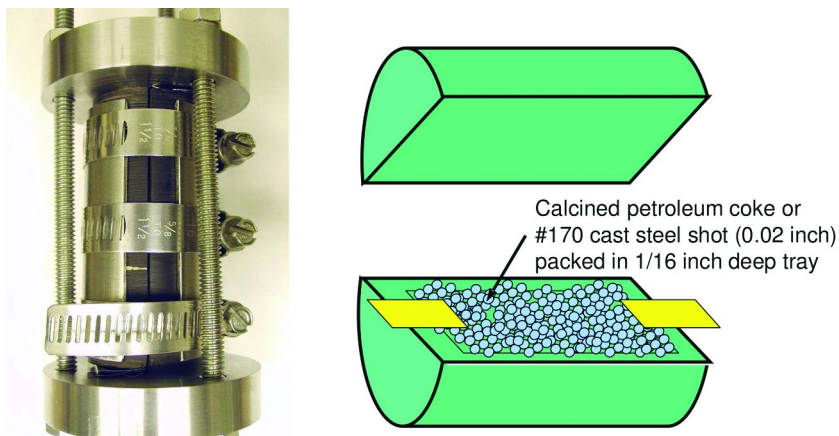


Figure 5. Construction of oil shale-conductant sandwiches for electrical continuity experiments.

with 20 amps of current for 5 hours. The power dissipated was around 60 watts, and at no time in the experiment was any disruption of the circuit encountered.

A thermocouple embedded in the sample reached a temperature of 268°C, from which it was estimated that the simulated fracture was at 350–400°C. Thermal expansion caused several fractures in the sample that allowed hydrocarbons to escape from the crescent of converted rock adjacent to the simulated fracture. The photo in the upper right portion of Figure 7 shows the simulated Electrofrac fracture and a rock surface that became exposed due to one of these thermally induced fractures.

The photomicrograph shows a section of the rock perpendicular to the exposed rock face shown in the photo. The steel shot in the simulated fracture, the spent oil shale, and a thermal crack cutting through the partially converted and unaltered

oil shale are all clearly visible. The ultra-violet fluorescent lighting highlights, in a bluish color, fractures through which hydrocarbons have migrated.

Hydrocarbon Expulsion under *In Situ* Stress

Another critical technical issue for the success of Electrofrac is the expulsion of hydrocarbons from oil shale heated under *in situ* stress. While it is well established that oil shale heated under no external stress will expel oil and gas (4), we were concerned that under significant *in situ* stress, hydrocarbons might not escape from the rock. To address this issue, some experiments were performed in which oil shale samples were heated under simulated *in situ* stress.

To accomplish this, a spring-loaded frame was constructed which could apply stress to a 1-inch diameter sample. A photograph of the frame is shown in Figure 8. The entire device was placed in a pressure-sealed heating vessel and heated to conversion temperature. In this suite of experiments, samples were heated to 400°C for 24 hours, achieving 95% conversion. Using different sets of springs, the samples were loaded with up to 1000 psi pressure. Samples were encased in Berea sandstone cylinders, jacketed, and clamped to limit lateral strain. This uniaxial loading is similar to what the oil shale would experience *in situ*. Special alloy springs ensured that the spring load did not diminish as the springs were heated along with the sample. As might be expected, oil shale samples initially expanded volumetrically, but by the end of the experiment they were smaller than their original size. The maximum expansion was recorded by a piece of gold foil wrapped on one of the load frame support posts.

We concluded from these experiments that hydrocarbons will escape from heated oil shale even under *in situ* stress. Experiments under stress recovered 21 to 34 gal/ton from samples with a Fischer assay of 42 gal/ton.

To better understand these expulsion experiments, an equation-of-state (EOS) phase behavior model was constructed for the hydrocarbon fluids generated from kerogen. Results of the model are illustrated in Figure 9 and Figure 10. The hydrocarbon composition used to construct the model was derived from Micro-Sealed Spherical Vessel pyrolysis experiments (5). While these experiments and the resulting composition will not be discussed here, this technique is generally used to study pyrolysis of conventional oil and gas source rocks.

A phase diagram derived from the model is shown in Figure 9. From the diagram we can see that fluids created from kerogen at Electrofrac conditions will be about 75% vaporized on a molar basis. Effectively, we will be boiling the oil out of the rock as it is created. This certainly helps explain our expulsion experiment results.

This can be viewed in another way as shown in Figure 10. Before conversion, a ton of Green River oil shale would occupy 16.5 cubic feet. After conversion, the kerogen has become hydrocarbon liquid, hydrocarbon vapor, and coke. At Electrofrac conditions the system would occupy 27.3 cubic feet. This 65% volume expansion provides a large drive mechanism for expelling hydrocarbons from the rock.

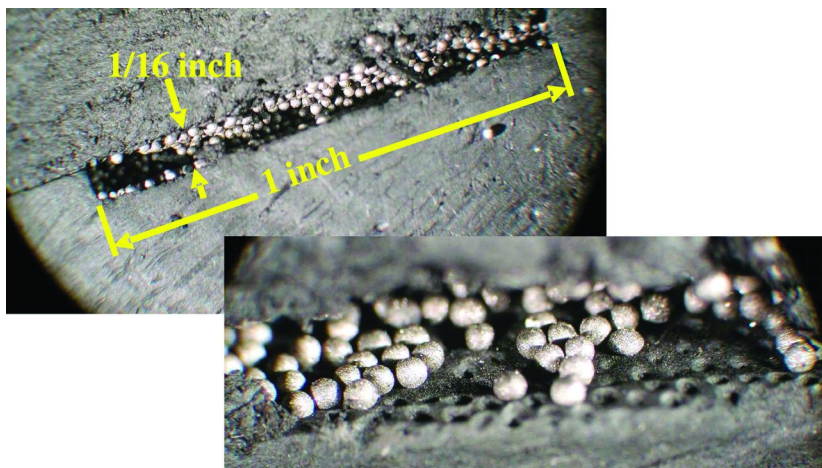


Figure 6. Results of an externally heated electrical continuity experiment.

Chemical Composition of Generated Oil

The chemical composition of shale oil generated by an *in situ* conversion process is a key factor influencing process viability. Shale oil composition is, at least in part, governed by intensive parameters such as pressure, temperature, and stress state. Understanding how variations in these parameters relate to shale oil composition provides an opportunity to optimize a conversion strategy to generate an improved hydrocarbon product. In this section we discuss how effective stress and hydrostatic pressure influence the molecular composition of shale oils generated in laboratory experiments that simulate *in situ* pyrolysis such as that occurring during the Electrofrac process (6).

A variety of intensive parameters (independent of system mass) govern *in situ* pyrolysis (7, 8). These include hydrostatic pressure, stress state, maximum temperature, heating duration, and source composition. Using a variety of techniques, all of these parameters can be controlled or at least influenced during pyrolysis.

We conducted a series of experiments that focused on two of these parameters, the stress state and hydrostatic pressure.

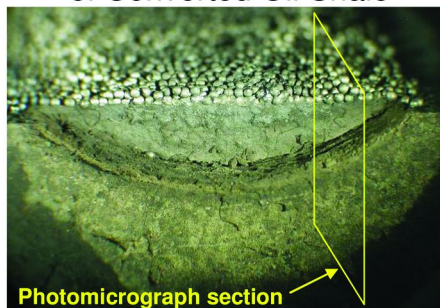
Experimental Protocol

A primary objective of these experiments was to identify the effects of hydrostatic pressure and effective stress on the compositions of oils produced during heating of oil shale. All experiments were conducted in a 465 ml Hastelloy Parr vessel heated externally by a custom furnace regulated by thermocouple feedback. The experiments were closed-system and run for 24 hours. The vessel assembly was placed in a furnace and brought to 393°C over 1.5–2 hours. After

Post-Experiment Oil Shale Sample



Simulated Fracture and Crescent of Converted Oil Shale



Photomicrograph under Fluorescent Light

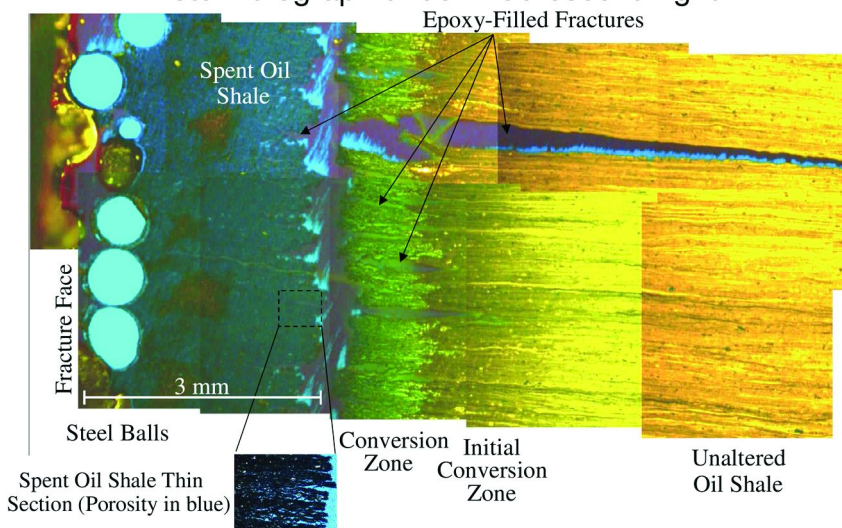


Figure 7. Results of an internally heated electrical continuity experiment.

24 hours at temperature, the furnace was turned off and the vessel was removed and allowed to cool passively. The gas pressure was then bled off gradually, the vessel opened, and the liquid and solid products collected. Monitoring instruments included: two thermocouples on the exterior vessel wall, another near the sample in the vessel's interior, and an internal pressure transducer (data points every 10 seconds). All monitoring instruments measured heat-up, run, and cool-down periods.

All experiments used the same block of oil shale as starting material. The block, shown in Figure 11, was collected in Hell's Hole Canyon, Utah, and is typical of relatively rich oil shale from the Mahogany Zone of the Green River Formation (4). It was cut parallel to layering to yield a block suitable for drilling cores from the same stratigraphic interval. This was done to assure homogeneity of the starting material.

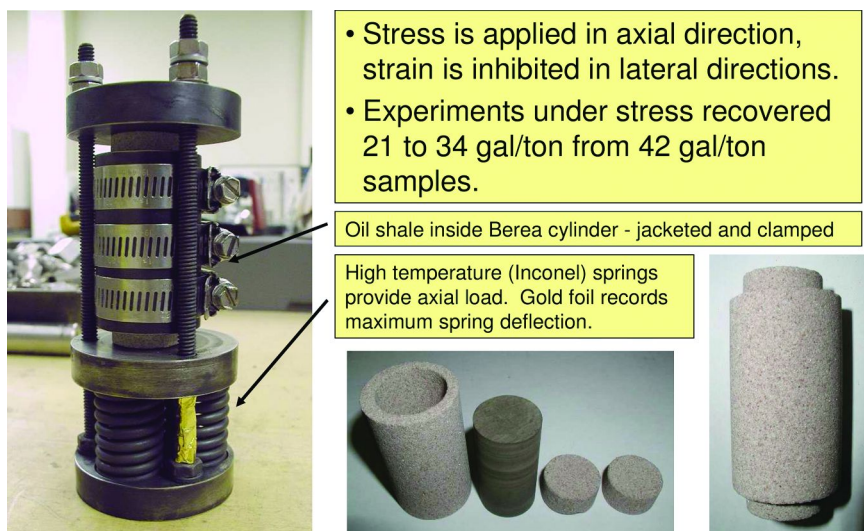


Figure 8. Spring-loaded frame and sample preparation used in expulsion experiments under simulated in situ stress.

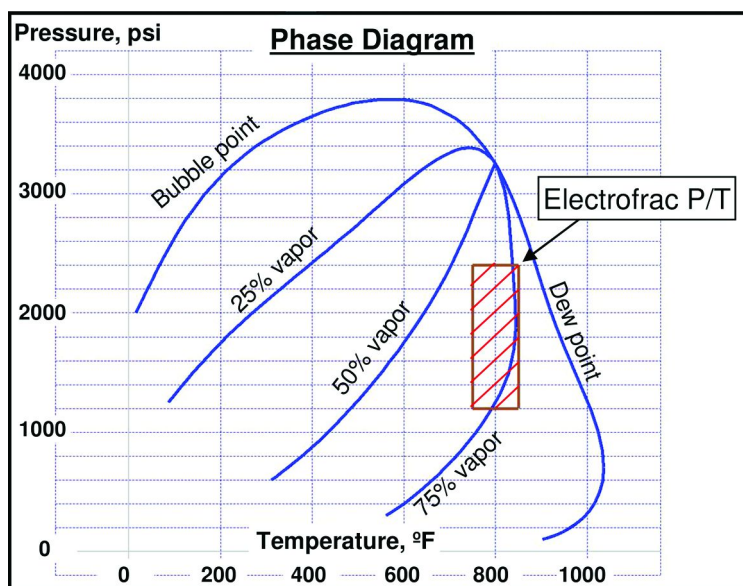


Figure 9. Phase diagram derived from EOS model for kerogen products.

Argon (Ar) was used to supply a hydrostatic pressure. The vessel was sealed, flushed and pressurized with Ar. Initial Ar-pressures used were 50, 200, and 500 psi. The hydrostatic pressures at temperature were more than double the initial pressures because of heating of the Ar and generation of gas from the oil shale kerogen.

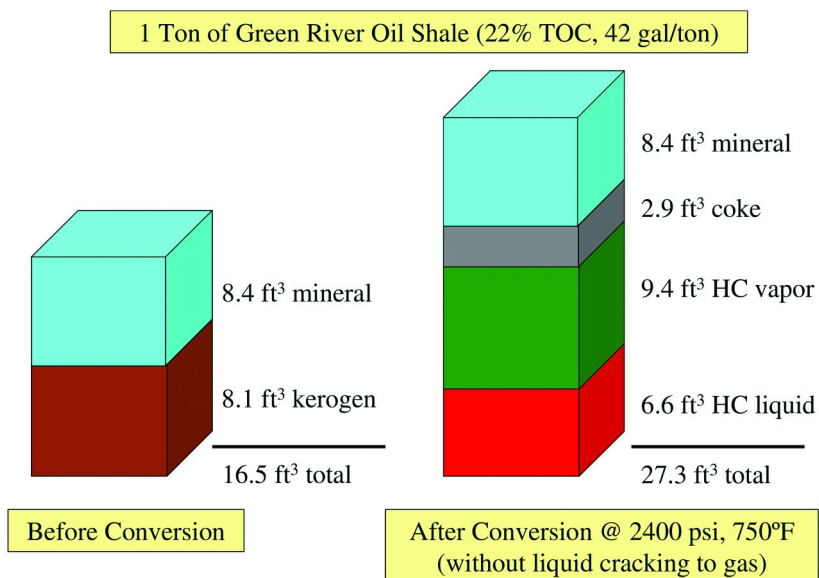


Figure 10. Results of phase behavior modeling of kerogen products.

To examine the role of effective stress on the pyrolysis products, we used the spring-loaded frame described earlier and shown in Figure 8. The entire frame was inserted in the vessel, along with the sample. Effective stress, in this context, refers to the portion of the lithostatic load that is directly supported by the solid framework of the rock. An effective stress of either 400 or 1000 psi was exerted on the sample using one of two sets of three springs compressed a fixed amount by appropriately torquing nuts on threaded rods connecting the top and base plates of the load frame.

Experimental Results

Oils were analyzed by a variety of techniques. Here we focus on the results of whole oil gas chromatography ($nC_5 - nC_{40}$) and detailed gas chromatography ($nC_4 - nC_{19}$). These techniques provide some overlap and demonstrate internal consistency of the results.

The following general relationships were documented for the influence of effective stress and hydrostatic pressure on shale oil composition.

Increasing effective stress causes:

1. a decrease in n -alkanes heavier than $\sim nC_7$ to nC_8
2. an increase in aromatic ring concentrations
3. an increase in saturated ring concentrations
4. a decrease in isoprenoid concentrations

Increasing hydrostatic pressure causes:

1. essentially no compositional effect in the absence of effective stress
2. reduces the effective stress effect

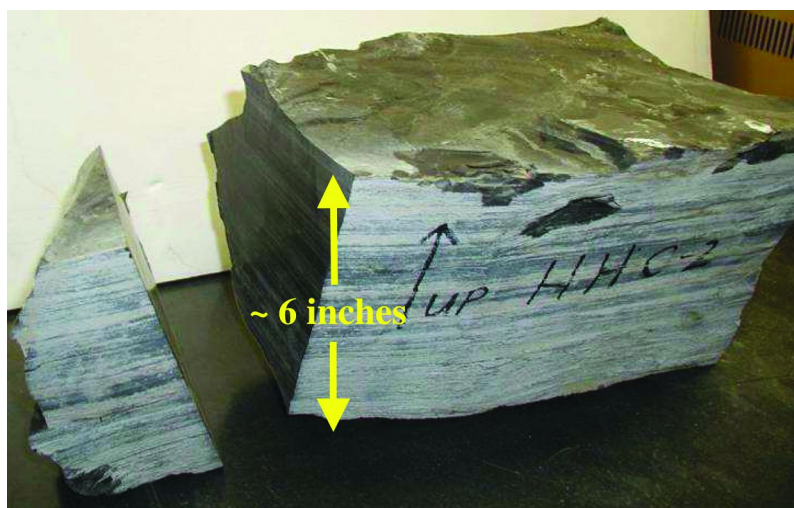


Figure 11. Block of oil shale used as starting material for all experiments.

The decrease in longer *n*-alkanes with increasing effective stress is readily seen in the simplified whole oil chromatograms presented in Figure 12. By comparing experiments conducted at the same temperature (393°C), duration (24 hours), hydrostatic pressure (initial Ar pressure = 500 psi), and with the same starting material, the effect of changing the effective stress is isolated. Among these three experiments, the 0 psi effective-stress result has the highest proportion of long chain alkanes and the proportion decreases as the effective stress increases to 400 psi and 1000 psi.

The simplified whole-oil chromatograms provide an adequate way to visualize some results. However, as the number of compounds considered increases, contrasting raw or modified chromatograms becomes less illustrative. To simplify the data presentation we have adopted the use of normalized chromatograms, as shown in Figure 13.

Normalized chromatograms are generated by first normalizing the integrated areas of all identified peaks for each sample to 100%. The compounds in each normalized analysis are then renormalized by dividing by the same compound in a reference analysis. This yields a smoothed plot showing the ratios of the two analyses. Two experiments that yield identical results have a ratio of unity for all compounds. Therefore, systematic deviations from unity can be viewed as relative enrichments or depletions in the numerator experiment(s) relative to the denominator experiment.

The choice of the normalizing analysis allows deviations to be interpreted in terms of a desired analytical or experimental parameter. For example, Figure 13 shows the ratios for the 0 psi and 1000 psi effective stress experiments depicted in Figure 12. The plot provides quick visual confirmation that the 1000 psi effective stress experiment is relatively depleted in larger molecules (plot falls below one). The normalized chromatograms allow compounds present in low concentrations to be compared alongside those present in much greater proportions. Unfortunately

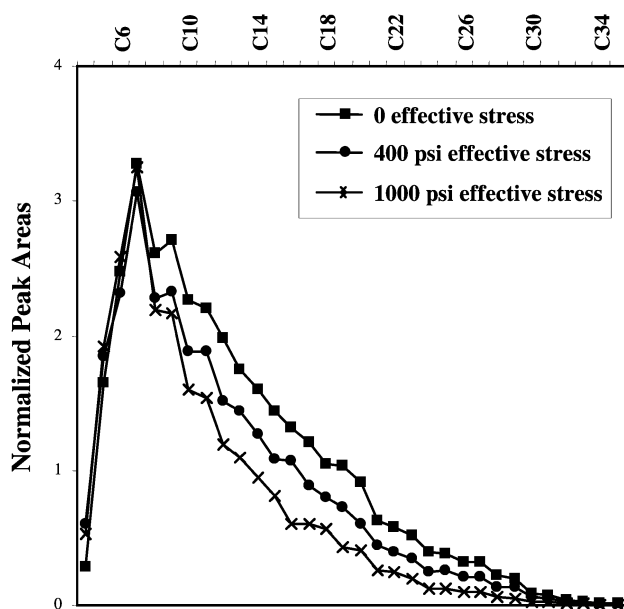


Figure 12. Simplified whole oil chromatograms showing the impact of effective stress on the proportions of straight-chain alkanes.

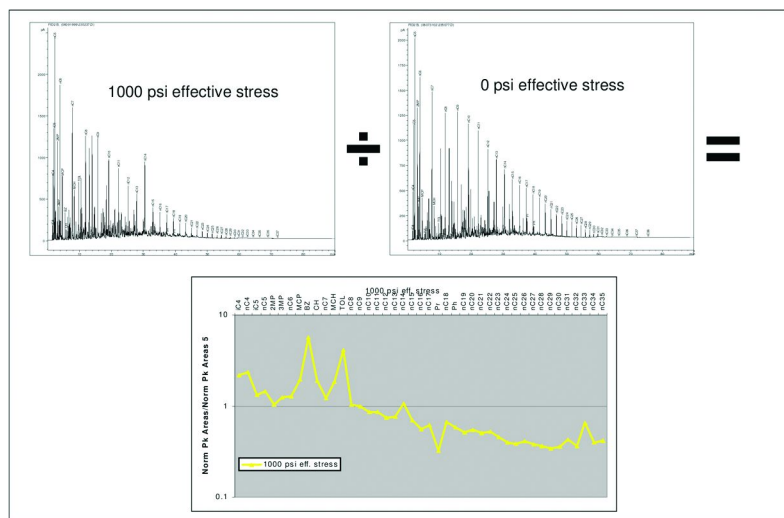


Figure 13. Methodology for normalizing whole-oil chromatograms, illustrated using experiments for 0 psi and 1000 psi effective stress as an example.

compounds close to the detection limits, and therefore not well-quantified, can generate anomalous spikes. These should be ignored in interpreting the results.

The results presented in Figure 12 can be usefully revisited using normalized chromatograms, and are presented again in Figure 14. In this presentation it is clear that not only does the 1000 psi effective stress have the lowest proportion of heavy molecules it also has a higher proportion of smaller molecules (although similar to that of the 400 psi effective stress experiment).

That higher effective stress leads to more aromatic ring compounds can be seen by examining the detailed C₃-C₁₉ chromatograms from these same experiments. Normalized versions of the detailed chromatograms are presented in Figure 15. The 1000 psi effective stress experiment has the highest concentrations of both single ring (benzene, toluene, xylene) and double ring aromatics (naphthalenes). Similar trends are seen for the 400 psi experiment, although certain variably-methylated naphthalenes are not substantially different from the 0 psi effective-stress experiment.

As with the aromatic rings, the proportion of saturated rings increases with increasing effective stress. This is shown in Figure 16, which depicts the same analyses as Figure 15, but with the saturated rather than aromatic rings highlighted. Both the cyclopentane-based and cyclohexane-based molecules are present in the highest proportions in the 1000 psi effective stress experiments. As with the aromatic rings, most saturated rings show an increase in proportion going from 0 to 400 to 1000 psi effective stress.

Increasing effective stress also leads to selective decimation of isoprenoids relative to adjacent *n*-alkanes. This is illustrated in Figure 17, which again presents the same data but highlights isoprenoid compounds. Isoprenoids are branched-chain alkanes with a direct biological origin. Because they are of biological origin, their proportion relative to an adjacent *n*-alkane provides a measure of cracking in a hydrocarbon system. This is a consequence of no new isoprenoids being generated by cracking while new *n*-alkane molecules can be generated by cracking of longer chains. The 1000 psi effective stress experiments show the most pronounced decimation of the isoprenoids. The 400 psi effective stress experiments show essentially the same relationships but more subdued.

The compositional response to changes in hydrostatic pressure is more complicated than the response to effective stress. In the absence of effective stress, changes in the hydrostatic pressure have a negligible compositional effect. Figure 18 compares two experiments with a pressure difference of more than two times (200 versus 500 psi Ar initial). The shale oil compositions are nearly identical, resulting in a normalized plot that falls at or near unity for most compounds. The large deviation from unity in the light hydrocarbon range is caused by volatile loss. The spikes at higher carbon numbers are related to higher uncertainties for concentrations near detection limits.

In the presence of effective stress, an increase in hydrostatic pressure modifies the consequence of that effective stress. This result is demonstrated by the plots presented in Figure 19. Both plots show experiments conducted at either 400 psi (upper plot in Figure 19) or 1000 psi (lower plot in Figure 19) effective stress. The results are normalized to experiments conducted at 0 psi effective stress but otherwise the same conditions. In each plot the general variation from unity reflects the consequence of effective stress as described above. The amount of deviation from unity is greater in the lower graph because the experiments were

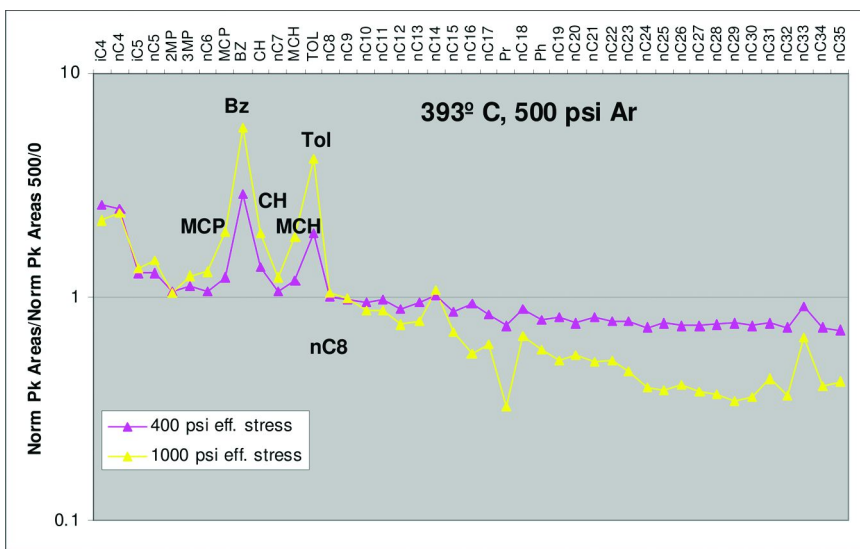


Figure 14. Normalized whole oil chromatograms showing the impact of effective stress on the proportions of heavier straight-chain alkanes.

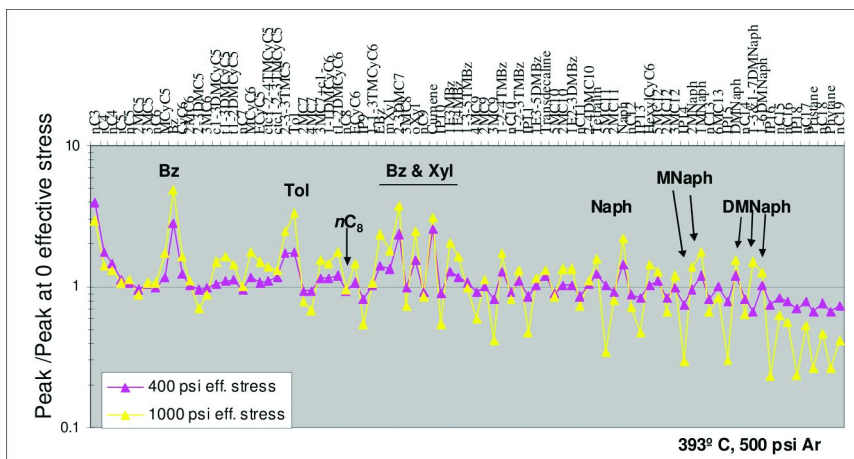


Figure 15. Detailed normalized chromatograms highlighting relative enrichment in aromatic ring compounds with increasing effective stress.

conducted at higher effective stress. The key feature of these graphs is that the experiments conducted at higher hydrostatic pressure (500 psi versus 200 psi Ar initial pressure) plot closer to unity for both effective stress conditions. Thus, increasing the hydrostatic pressure, in the presence of an effective stress, reduces the compositional consequence of that effective stress.

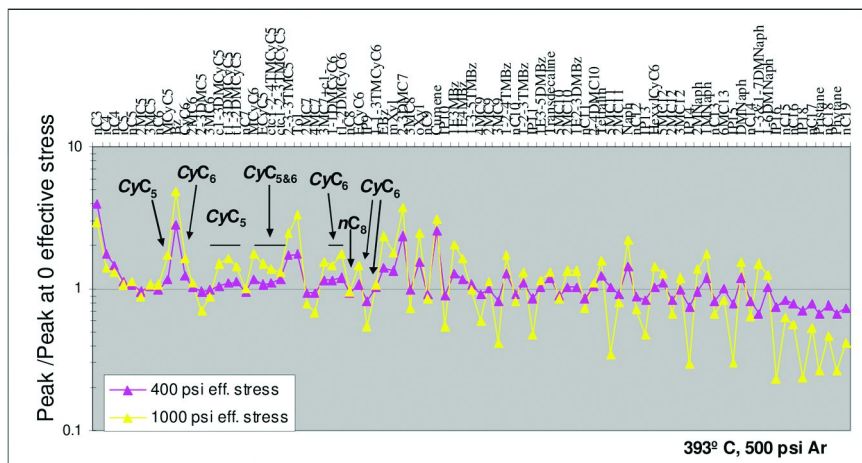


Figure 16. Detailed normalized chromatograms highlighting relative enrichment in saturated ring compounds with increasing effective stress.

Summary of Compositional Experiments

This investigation of the compositional influence of effective stress and hydrostatic pressure demonstrates clearly that by modifying these intensive parameters during *in situ* conversion of oil shale, it is possible to generate an improved hydrocarbon product. Our conclusion is that variations in effective stress exert a substantial control on the composition of *in situ* generated shale oil. Therefore knowledge of the stress field in an oil shale is critical for planning an optimized *in situ* conversion technology. In our experiments, systematic changes in effective stress generated systematic changes in the composition of shale oil generated. This demonstrates the robustness of the result. Another important observation is that changes in hydrostatic pressure have a minimal effect in the absence of effective stress, and otherwise act to merely modify the effective-stress effect.

Electrofrac Completion Strategy

The schematic design of a completion strategy for effective heating includes an estimate of how many Electrofrac fractures will be required, how they will be arranged geometrically, and what their dimensions will be. An important question for such a design is the orientation of the fractures. Hydraulic fractures open normal to the least principle *in situ* stress. So, to predict the orientation of Electrofrac fractures in the Piceance Basin of Colorado, a basin-wide geomechanical model of *in situ* stress was constructed. While the model is site-specific it is nevertheless important because the Piceance Basin is by far the world's largest oil shale accumulation. This model is illustrated in Figure 20, and is described by Symington and Yale (9). The model includes the effects of

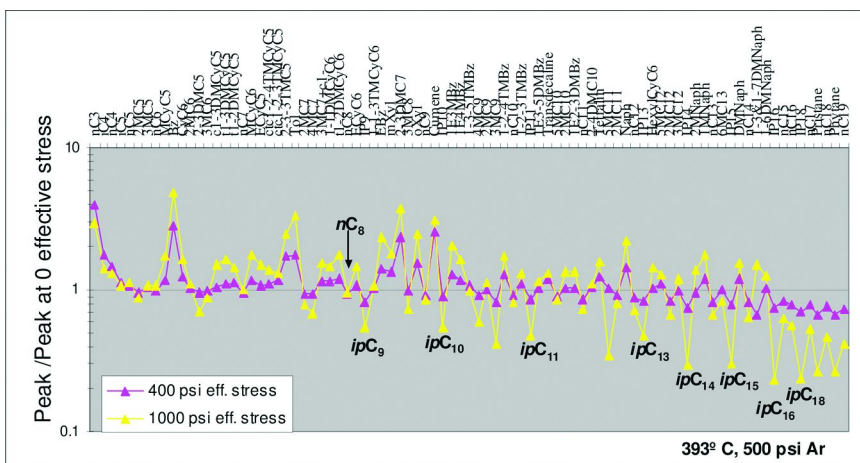


Figure 17. Detailed normalized chromatograms highlighting decimation of isoprenoids relative to adjacent *n*-alkanes with increasing effective stress.

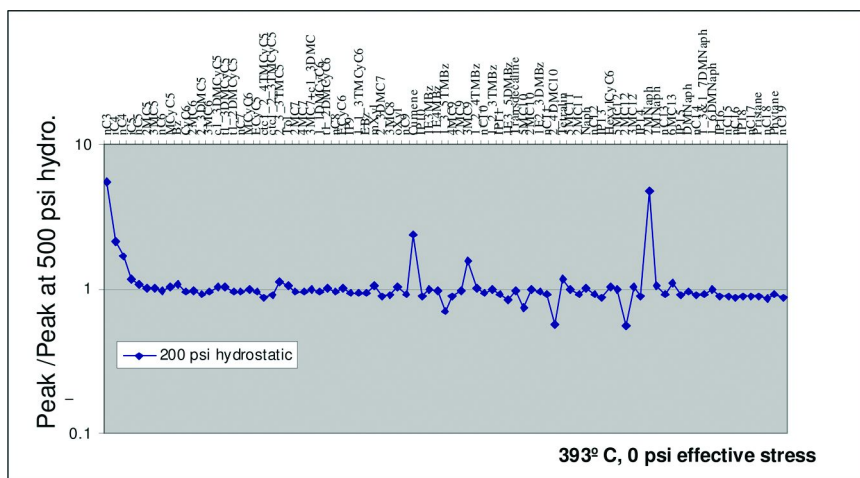


Figure 18. Comparison of two experiments conducted with no effective stress shows no dependence of composition on initial Argon pressure.

topography, tectonics, and recent erosion. It is calibrated to a variety of data including:

- Fracture stimulations that constrain the minimum principle stress,
- Borehole breakout and ellipticity observations that constrain the horizontal stress difference, and
- 1960's-vintage fracture tests that establish the depth of the horizontal-to-vertical orientation transition at one location.

From the model, the elevation of the transition between shallow horizontal fracturing and deeper vertical fracturing was extracted. From this elevation it was concluded that most of the Piceance Green River oil shale is in a stress state

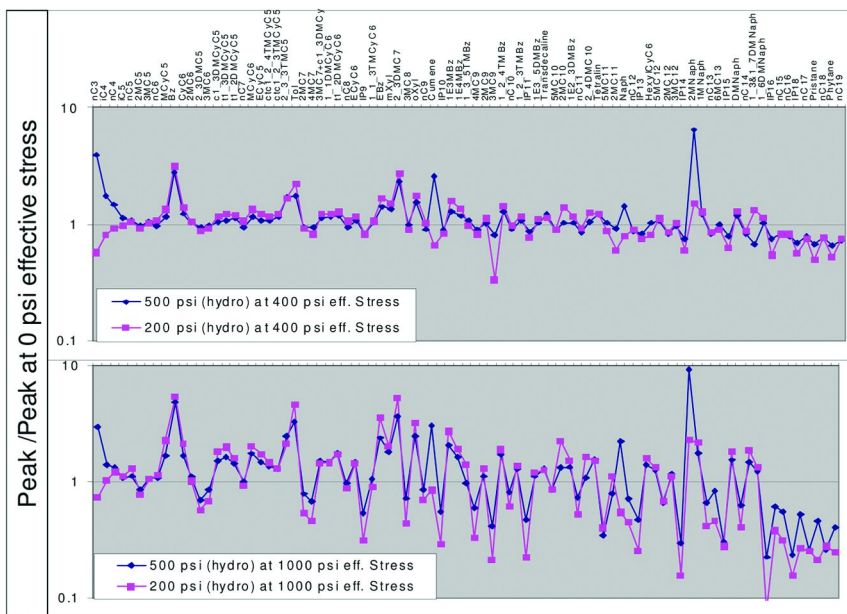


Figure 19. Under effective stress, composition is influenced by initial Argon pressure. Experiments under stress are normalized to experiments conducted with equal Argon pressure, but no effective stress.

favoring vertical fractures. Completion strategy work has therefore focused on vertical rather than horizontal fractures.

The resulting design is depicted in Figure 1, which will now be discussed in more detail. Heating wells in this scenario are drilled horizontally, perpendicular to the least principle *in situ* stress. Vertical longitudinal fractures are created from the horizontal wells and filled with Electrofrac conductant. Electrical conduction is from “heel” to “toe” in each of the heating wells. Connector wells are drilled through the fracture near the toe of each well, and the horizontal sections of the wells are constructed of electrically nonconductive material. For reasonably spaced heating fractures, the induced stresses should not alter the least principle stress direction. This is important because it enables development using a series of fractures with known consistent orientation. Finally, multiple layers of heating wells may be stacked to increase heating efficiency.

The effectiveness of stacking multiple layers of heating wells is illustrated by thermal conduction models used to optimize the Electrofrac heating efficiency. The models were constructed with a set of screening tools developed at ExxonMobil for application to *in situ* oil shale conversion processes (10). Figure 21 shows a schematic diagram for a heating scenario with two layers of stacked Electrofrac fractures. The next several paragraphs describe ExxonMobil’s screening tools, and their application to this completion design.

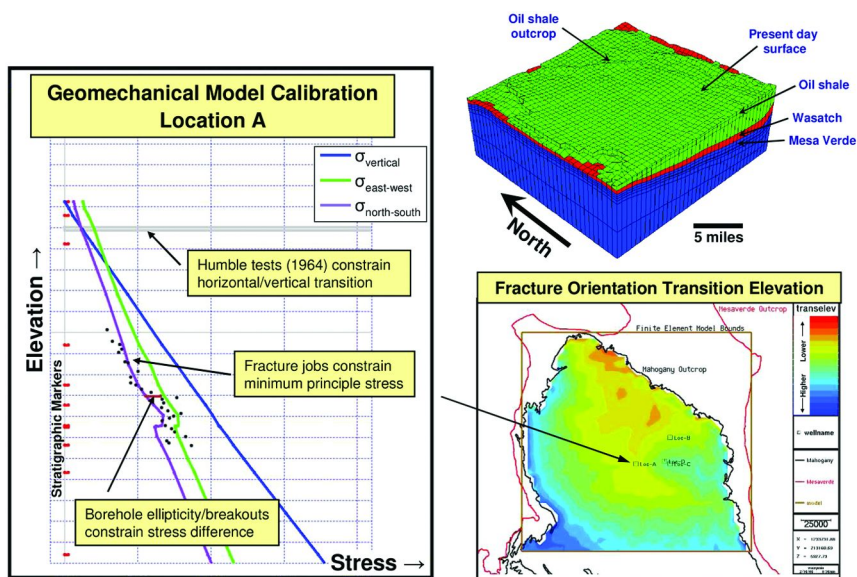
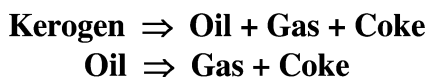


Figure 20. Piceance Basin geomechanical model for the prediction of *in situ* stress and the orientation of Electrofrac fractures.

Thermal Conduction Screening Tools

ExxonMobil's screening tools effectively combine linear heat conduction theory and basin modeling source rock calculations. Using linear conduction theory, arbitrary arrangements of heat sources are modeled by superposing time sequences of an initial value problem for an "instantly heated" rectangular solid embedded in an infinite medium. The basic initial value problem used in this superposition approach is illustrated in Figure 22, along with its mathematical solution as described by Eckert and Drake (11). The mathematical solution is represented in terms of error functions, and computers can easily handle the superposition of many heaters. Complex heating programs are treated as a series of heaters turned on and off, and basic anisotropy can be included using direction-dependent thermal diffusivities, represented by "*a*" in the equations in Figure 22. Another advantage of the approach is that calculations are performed only at sites of interest, rather than over an entire numerical grid.

The temperature histories calculated in this manner are input to a kinetic model of kerogen decomposition. Basin modeling tools, used in conventional oil and gas exploration, offer a ready-made library of these kinetic models. The models can either use end-member source rock types (usually based on Van Krevelen types (12)) or measured kinetics. They usually implement a simple chemistry model such as the one below.



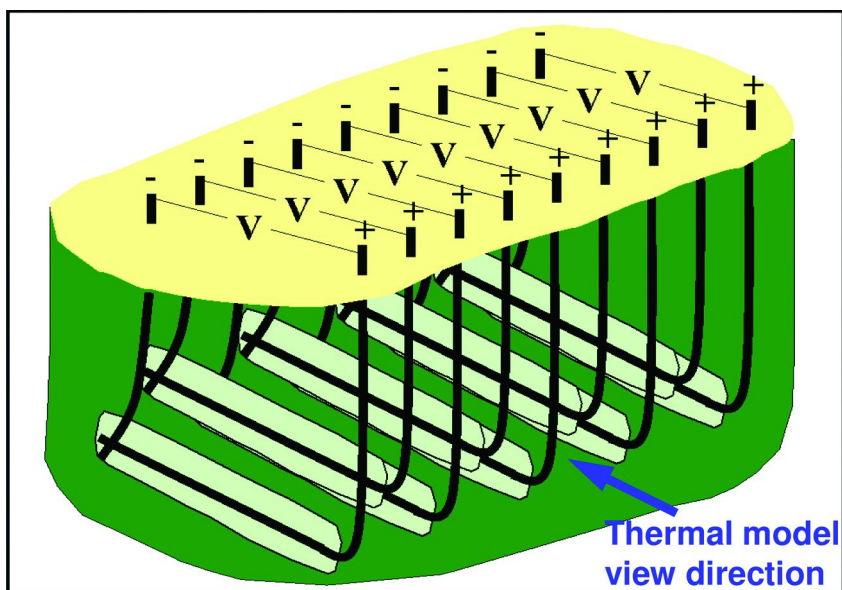


Figure 21. Schematic Electrofrac configuration with two layers of stacked heating wells.

In this model, kerogen decomposes to oil, gas, and coke. The oil then further decomposes to gas and coke. The kerogen decomposition obeys first order reaction kinetics, modeled using a spectrum of activation energies as illustrated in Figure 23.

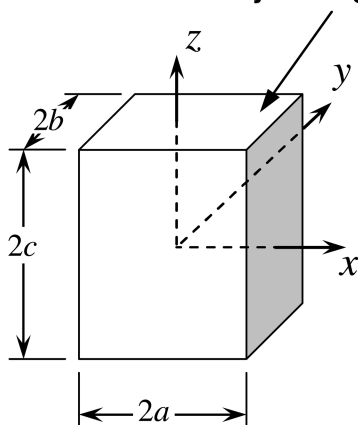
Example calculations from a model of this type are shown in Figure 24 for constant heating rates spanning a geologic rate of $3\text{ }^{\circ}\text{C}/\text{Ma}$ to *in situ* conversion rates of $50\text{--}100\text{ }^{\circ}\text{C}/\text{year}$. At *in situ* process heating rates, the conversion temperatures are relatively insensitive to the heating rate. Therefore the fraction of kerogen converted can be estimated from the maximum temperature achieved by the rock, using a nominal heating rate characteristic of the process as a whole. This technique is frequently used to increase the number of screening cases that can be considered.

Combining linear heat conduction theory and kinetic modeling of kerogen decomposition leads to a general procedure for screening calculations, which is illustrated in Figure 25. The procedure starts in the upper left corner of the figure and continues around clockwise.

First, the heating scenario being evaluated is described as a set of rectangular volumetric heaters, which are turned on and off to mimic the field operation. The description must include all the heaters that impact the zone of interest. Often this results in several thousands of “mathematical heaters”.

This list of heaters is processed by a computer program that calculates temperature and outputs it to a display program. The display program used by the authors has source rock models from ExxonMobil’s proprietary Stellar™ basin modeling software built into it, but other, more generally available, basin modeling software might just as easily fill this role. The display program

**Rectangular solid heated
by ΔT degrees at time, $t = 0$**



$$T = T_0 + \Delta T f(x,t) g(y,t) h(z,t)$$

where :

$$f(x,t) = \frac{1}{2} \left(\operatorname{erf} \left(\frac{a-x}{2\sqrt{\alpha_x t}} \right) + \operatorname{erf} \left(\frac{a+x}{2\sqrt{\alpha_x t}} \right) \right)$$

$$g(y,t) = \frac{1}{2} \left(\operatorname{erf} \left(\frac{b-y}{2\sqrt{\alpha_y t}} \right) + \operatorname{erf} \left(\frac{b+y}{2\sqrt{\alpha_y t}} \right) \right)$$

$$h(z,t) = \frac{1}{2} \left(\operatorname{erf} \left(\frac{c-z}{2\sqrt{\alpha_z t}} \right) + \operatorname{erf} \left(\frac{c+z}{2\sqrt{\alpha_z t}} \right) \right)$$

Figure 22. Basic initial value problem used to calculate temperature by linear superposition for screening tool applications.

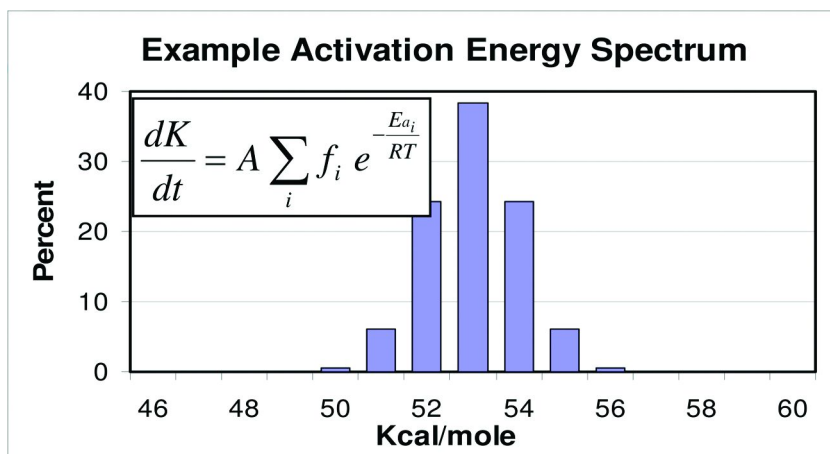


Figure 23. Example activation energy spectrum for kerogen decomposition.

assembles thermal histories and convolves them with the source rock model to calculate the oil and gas generation history. As already mentioned, a “full-math” source rock model may be used, but frequently the fraction of kerogen converted is simply estimated from the maximum temperature achieved at a given point. Finally, the display program can sum up the oil and gas generated for comparison to the total heat energy input.

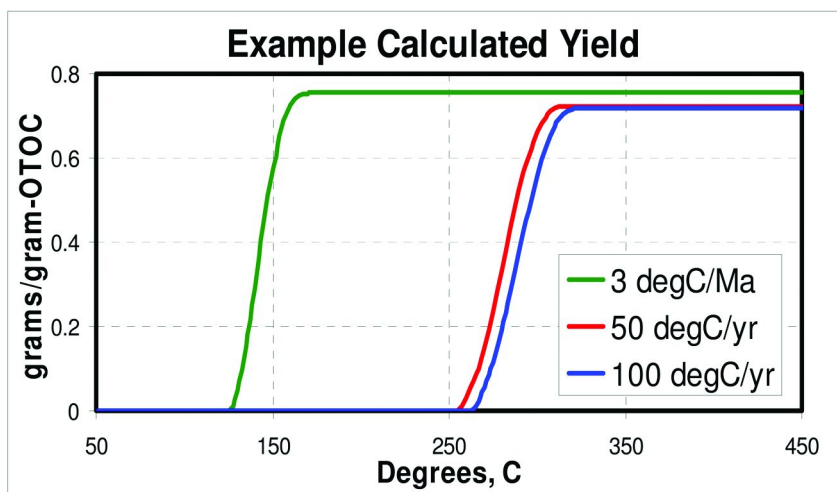


Figure 24. Example calculated yields (in grams/gram of Original Total Organic Carbon) from a kerogen chemical decomposition model.

Application of Screening Tools to a “Typical” Electrofrac Case

The previously described screening procedure has been applied as part of ExxonMobil’s Electrofrac process development work. The rock physical properties used for these calculations are summarized in Table I and are based on Green River oil shale. Important parameters for heat conduction are the heat capacity, density, and thermal conductivity, which result in a thermal diffusivity of 0.607 ft²/day. Our calculations assumed a relationship between fractional kerogen conversion and maximum temperature achieved, with a conversion temperature window of 500-615°F. Finally, we assumed a nominal oil shale richness of 30 gal/ton by Fischer assay.

Screening calculation results for the schematic completion design shown in Figure 21 are presented in Figure 26. This case is considered “typical”. It includes five years of heating with a total heat input sufficient to convert a 325-foot section of oil shale. The fracture spacing is 120 feet, and two staggered layers of Electrofrac fractures are used. The fractures are 150 feet high (75 feet up and 75 feet down from the heating wellbore). The resultant heating efficiency is 74%, meaning the applied heat, sufficient to convert a 325-foot section, actually only converts 240 feet. The remaining heat is lost to over- and underlying rocks heated to below-conversion temperatures.

It is interesting that the details of the heating pattern are quickly forgotten after the 5-year heating period ends. The heating efficiency is therefore mostly governed by more global parameters such as the heat input, heating duration and thickness heated. Details of the heat input distribution have more impact on the number of heaters required than on the efficiency. In this “typical” case we anticipate that the heated area will require only one heating well every 1.5 acres, minimizing the surface disturbance required for an Electrofrac project. This is a vivid illustration

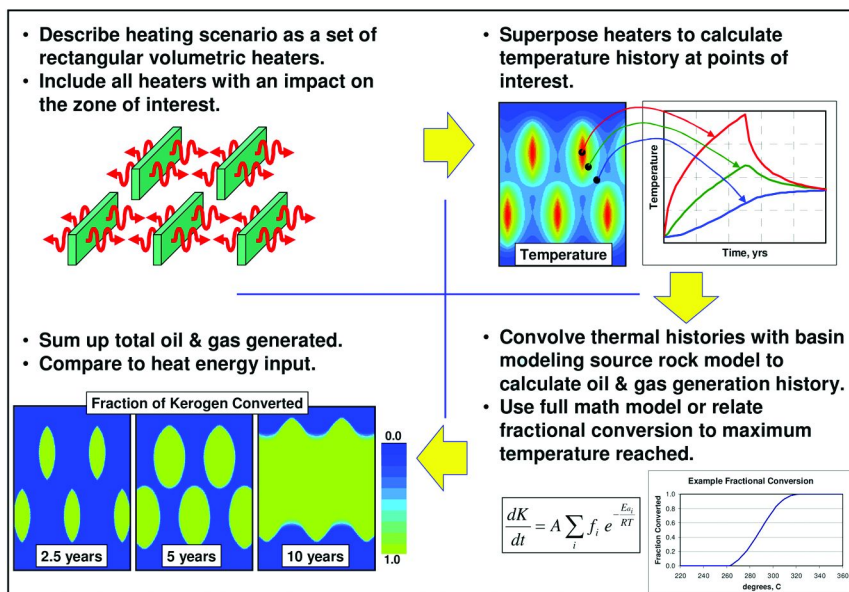


Figure 25. Generalized procedure for in situ oil shale screening calculations.

of the desirability of planar rather than radial heat sources, which might require nearly 20 times as many wells.

In summing up the fractional kerogen conversion to calculate the heating efficiency, a profile of hydrocarbon generation through time can be produced. Figure 27 shows the profile for this typical case, presented in a normalized fashion. Interestingly, the peak generation rate does not occur until about 15 months after the heating period ends, and significant generation continues until almost three years after heating. It is probably also worth noting that these screening tools calculate hydrocarbons generated; calculating hydrocarbons actually recovered would require a full-physics simulation of the problem.

Production of Sodium Minerals Associated with Oil Shale

In the Piceance Basin of Colorado, the Green River oil shale is associated with potentially valuable sodium minerals. Principally, these minerals are nahcolite [NaHCO₃] and dawsonite [NaAl(OH)₂CO₃], as described by Beard et al., 1974 (13). These evaporite minerals were formed in several Eocene lakes that once covered areas of Wyoming, Utah, and Colorado, as described by Dyni, 1987 (14).

Table I. Rock physical properties for Electrofrac screening calculations

Electrofrac Screening Analysis Parameters (Based on Green River Oil Shale)	
Heat Capacity (BTU/lb-°F)	0.3
Thermal Conductivity (BTU/day-ft-°F)	25
Density (lb/ft³)	137
Thermal Diffusivity (ft²/day)	0.607
Temperature window for conversion at 180 °F/year (°F)	500 to 615
Oil Shale Richness (gallons/ton)	30

Sodium resources in the Piceance Basin are significant. The nahcolite resource is estimated by Dyni, 1974 (15) to be 32 billion short tons. Beard et al., 1974 (13) estimate total dawsonite in-place resources to be 19 billion short tons.

Nahcolite is the more important sodium mineral in the basin and has been commercially exploited by solution mining. Nahcolite has a wide variety of industrial and manufacturing uses, including the manufacture of glass and industrial chemicals, and the removal of sulfur dioxide from flue gases. Dawsonite may be a potential source of aluminum for manufacturing.

Coproduction of oil shale and nahcolite may provide the most feasible means of recovering both these resources. ExxonMobil has developed a method to coproduce nahcolite and oil shale resources. As described by Kaminsky, et. al. (16), the method could maximize the resource potential for both oil shale and nahcolite in the Piceance Basin. In the remainder of this section, we describe ExxonMobil's approach to coproduction of oil shale and nahcolite and indicate some of its implications for remediation after shale oil production by *in situ* techniques. While the technology is described within the context of Electrofrac, it would likely be applicable with other *in situ* techniques that rely on heating for conversion.

Coproduction of oil shale and nahcolite with Electrofrac will preserve and possibly enhance sodium-mineral value. Chemical-equilibrium modeling and experimental work indicate that pyrolysis of oil shale will result in the transformation of nahcolite (sodium bicarbonate or baking soda) to sodium carbonate (natrite or soda ash). Like nahcolite, sodium carbonate is a water-soluble mineral. After oil shale recovery is complete, water injection into the pyrolysis zone can be an effective method for recovering the sodium carbonate. The enhanced permeability of the pyrolyzed oil shale will make access to the sodium minerals more efficient and should result in increased recovery.

Nahcolite occurs as beds, nodules, and finely disseminated crystals within and between beds of oil shale within the Parachute Creek member of the Green River formation. Dyni, 1974 (15) estimated that 85% of the nahcolite is intimately mixed with oil shale as either nonbedded crystalline aggregates or finely disseminated

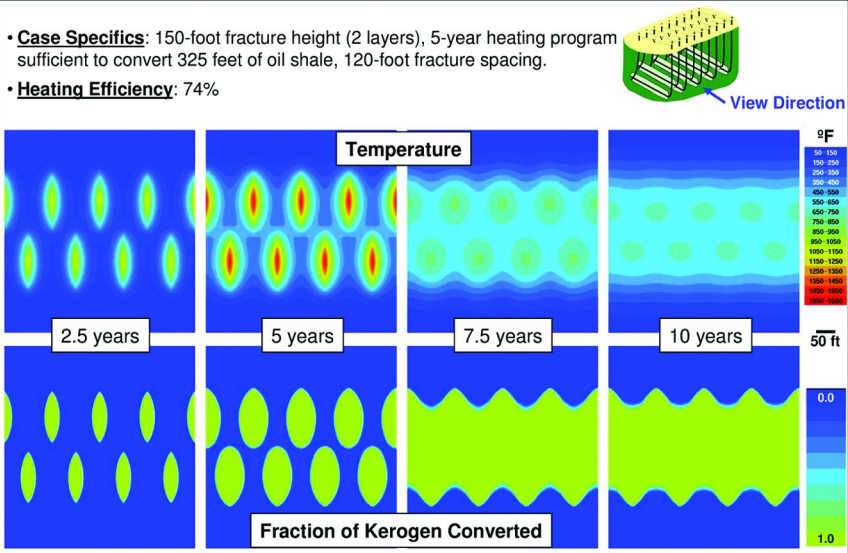


Figure 26. Temperature and kerogen conversion history for a "typical" case with two layers of staggered Electrofrac.

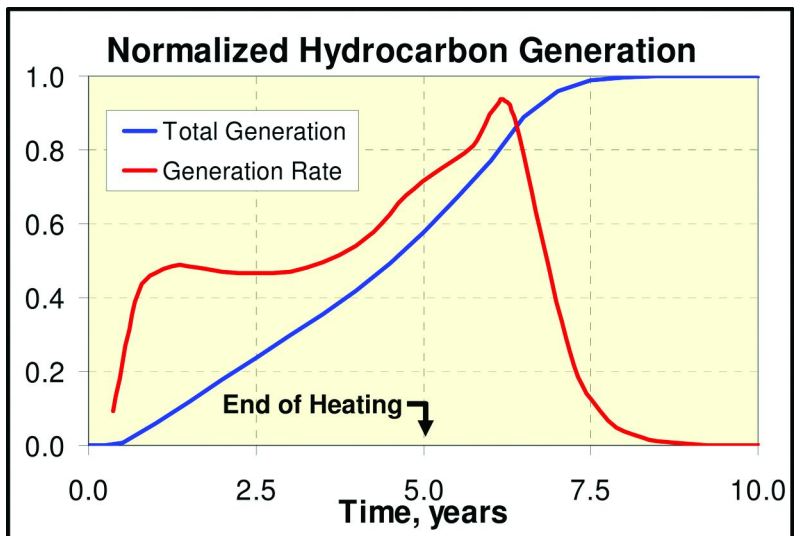


Figure 27. Normalized profile of hydrocarbon generation through time for a "typical" Electrofrac case.

crystals. This analysis implies that access to the bulk of the nahcolite resource is dependent on finding methods that increase the permeability of the oil shale and thus allow water to pass through the formation for dissolution.

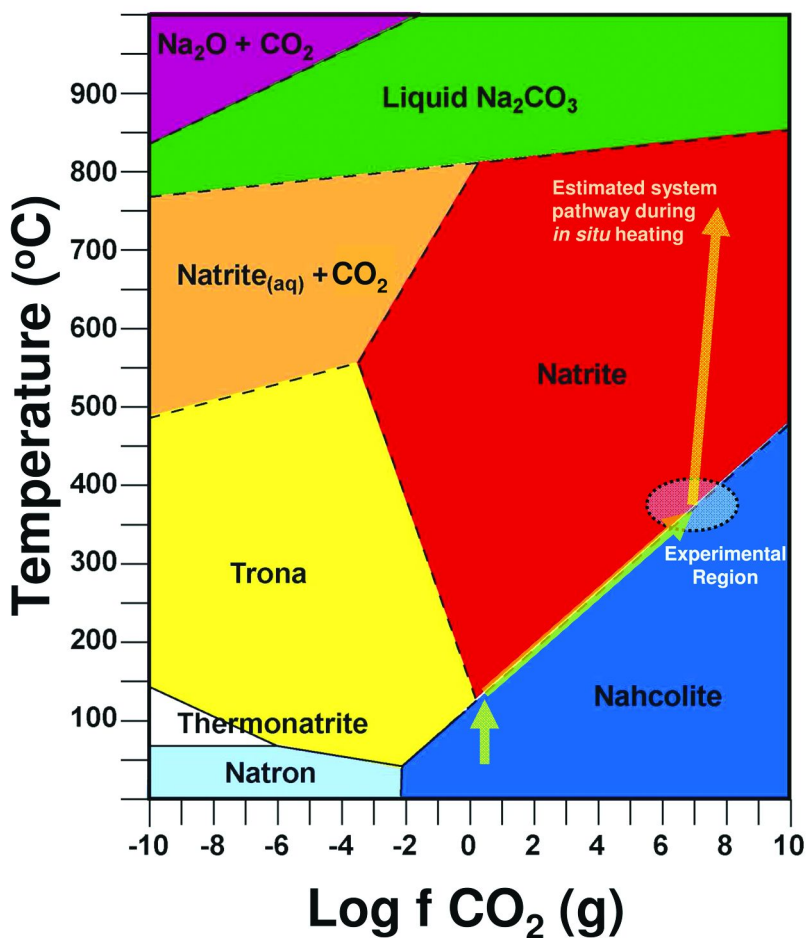
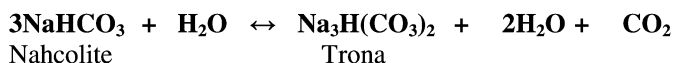
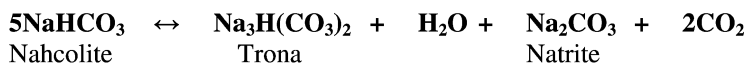


Figure 28. Phase diagram for the sodium carbonate mineral system.

It is well established that, as temperature increases, nahcolite loses carbon dioxide. Depending on the partial pressure of water and carbon dioxide, the resultant minerals are trona or natrite.



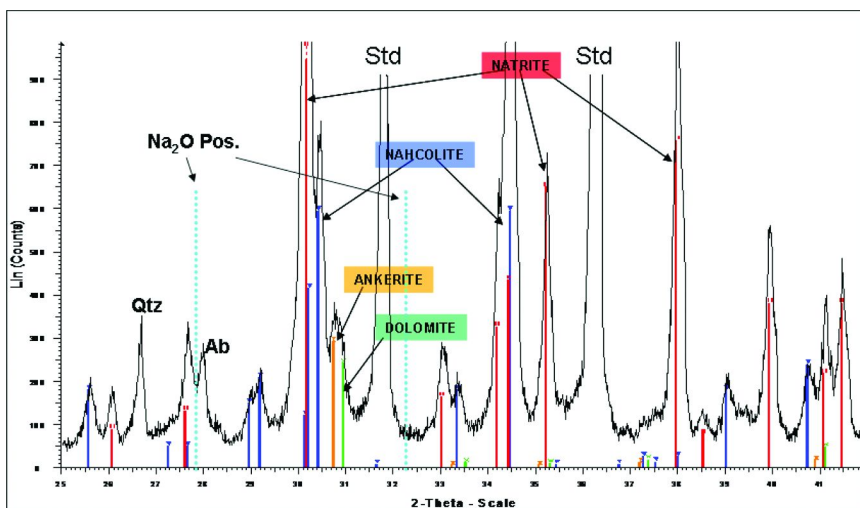


Figure 29. X-ray diffraction pattern of a nahcolite-oil shale mixture after oil shale pyrolysis

Both trona and natrite are readily water soluble. It is only at very high temperatures that natrite or trona will break down to form sodium oxides. However, the temperature at which this transformation occurs ($>800^{\circ}\text{C}$) is highly dependent on the partial pressure of carbon dioxide in the system.

The phase diagram of the sodium carbonate mineral system displayed in Figure 28 is based on publicly available thermodynamic data as well as ExxonMobil experimental results. This diagram, from Yeakel, et. al. (17), shows the relationship of sodium-mineral phases as a function of temperature and carbon dioxide fugacity, assuming abundant water with a pH of 8.5. Although not shown on the diagram, several of our experimental data points lie along the boundary between natrite and nahcolite. Heating simulations of rich oil shale (>25 gpt) support the estimated system pathway shown by the arrows. It follows the boundary between natrite and nahcolite, increasing the partial pressure of CO_2 , until nahcolite is consumed. If the rock is heated to 500 to 600°C , calcite and dolomite will begin to decompose, forming additional carbon dioxide. This will keep natrite stable, even to temperatures exceeding 900°C , which is well above Electrofrac process temperatures for the bulk of the rock. Thus, one can expect the majority of nahcolite will be converted to natrite, and the natrite will be stable at the temperatures anticipated during *in situ* conversion.

Experimental results further support this hypothesis. Layered sandwiches and random mixtures of oil shale and nahcolite were prepared, using ground up oil shale and baking soda pressed to make artificial rocks, to simulate bedded and disseminated nahcolite. These mixtures were placed in a Parr heating vessel and heated to 375 or 393°C ; the mixtures were maintained at those temperatures for 24 hours to completely pyrolyze the oil shale. X-ray diffraction analysis of the products, an example of which is shown in Figure 29, demonstrates that some nahcolite was preserved and some was converted to natrite.

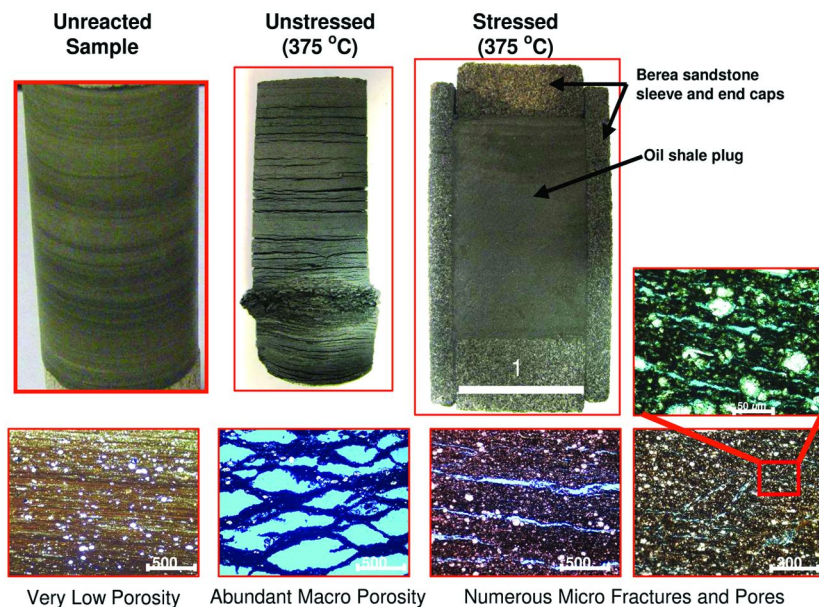


Figure 30. Thin sections and core plugs – Green River oil shale.

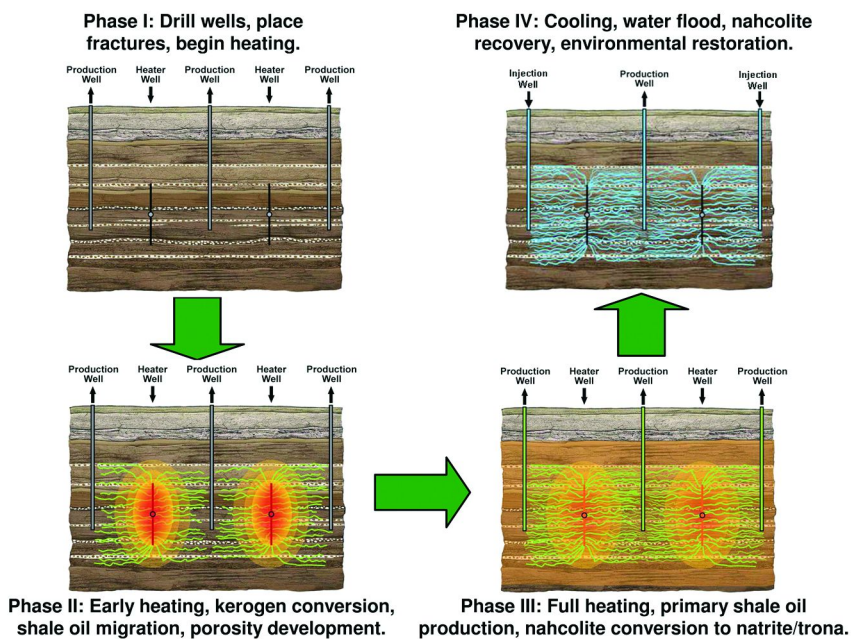


Figure 31. ExxonMobil's concept for recovery of both shale oil and nahcolite.

Experimental results not only demonstrate the preservation of sodium-mineral value, they indicate that oil shale pyrolysis makes the sodium minerals more accessible to solution mining by enhancing the porosity and permeability of the formation. Experiments on oil shale heated to 375°C under stressed and unstressed conditions confirm that porosity is enhanced by the kerogen conversion process. Figure 30 shows the plugs and thin section photo-micrographs of unreacted and pyrolyzed oil shale under different stress conditions. Unreacted shale has a porosity of <0.5%. The thin section is dominated by organic matter mixed with a matrix of clay and calcite/dolomite. The larger white specs are quartz grains (rounded) or calcite rhombs.

The heated but unstressed oil shale sample shows ample evidence of splitting along laminae, presumably where organic material was most abundant. The thin section shows a network of large pores and cracks. Both the plug and the thin section exhibit the swelling associated with kerogen conversion and the resultant porous network that developed.

If the oil shale is heated under conditions of 1,000 psi overburden stress using the miniature load frame described earlier and shown in Figure 8, the overall rock maintains its integrity while small pores and fractures are formed. The plug photograph is a slice through a reacted oil shale plug inside its sandstone sleeve. Note the lack of expansion cracks and the preservation of lamination. In the thin sections, we observe small fractures that occur in clusters within the oil shale. These fractures are 50 to 100 microns wide. Some fractures are oriented parallel to lamination while others are oriented at various angles to lamination. In addition to the fractures, the ground mass of the oil shale contains numerous small pores that form a microporous network. These pores and microfractures are <50 microns in size. This set of experiments clearly indicates that, even under conditions of overburden stress, the kerogen conversion and expulsion process creates porosity and permeability that was not present in the original oil shale.

These results clearly establish that the sodium-mineral value will be preserved and that porosity and permeability are expected to increase as the rock is heated.

Figure 31 illustrates ExxonMobil's concept for oil shale conversion and recovery with subsequent nahcolite recovery (Kaminsky et al. (16) and Yeakel et al. (17)).

In Phase I, Electrofrac fractures are constructed in the oil shale interval of interest.

In Phase II, the Electrofrac fractures are heated, and oil shale begins to convert to hydrocarbons that migrate to the production wells. At this stage some nahcolite may convert to natrite.

Phase III represents the main stage of heating and hydrocarbon recovery, during which kerogen is converted to oil and gas that are then produced. Hydrocarbon production will be facilitated by the fracture and porosity network that develops in the oil shale and by the expansion of the hydrocarbon volume when kerogen converts to oil and gas. At this stage, nahcolite will be converted largely to natrite.

After the heating phase ends, the rocks begin to cool, and primary hydrocarbon production begins to diminish. Some fractures and pores are likely to close under lithostatic pressure; however, some will remain open. As cooling continues into

Phase IV, some production wells may be converted to water injection wells. Water will be injected into the fracture network. This water will be heated upon entry into the hot oil shale and will dissolve the natrite; the water will be produced and the natrite recovered. Natrite could then be converted to sodium bicarbonate, as needed, with the addition of carbon dioxide.

Summary

In summary, ExxonMobil's Electrofrac process is an energy-efficient method for converting oil shale to producible oil and gas. Early Electrofrac research has focused on critical technical issues for the process and has included laboratory experiments and numerical models. The experiments demonstrate:

- That calcined coke is a suitable Electrofrac conductant,
- That electrical continuity is unaffected by kerogen conversion, and
- That hydrocarbons will be expelled from heated oil shale even under *in situ* stress.
- That shale oil composition is influenced by *in situ* stress and hydrostatic pressure. Understanding these controls on composition should facilitate generation of an improved product.
- That sodium-mineral value is preserved during *in situ* pyrolysis. Oil shale pyrolysis makes the sodium minerals more accessible to solution mining by enhancing the porosity and permeability of the formation.

The modeling results include:

- A phase behavior model that shows volume expansion is a large potential drive mechanism for expulsion,
- A geomechanical model that shows the dominant stress state of the Piceance Basin Green River oil shale favors vertical fractures,
- A thermodynamic model that explains the preservation of sodium minerals during *in situ* pyrolysis and shows that nahcolite will be at least partially converted to soda ash, and
- Heat conduction screening models that show several fracture designs can deliver heat effectively. A "typical" case requires one Electrofrac heating well every 1.5 acres, improving process economics and reducing the land disturbance required for an Electrofrac project. This vividly illustrates the desirability of planar rather than radial heat sources, which might require nearly 20 times as many wells.

These early research results from laboratory experiments and numerical models are quite encouraging. As a result, ExxonMobil has initiated field experiments to test Electrofrac process elements at a larger scale. Many years of research and development may be required to demonstrate the technical, environmental and economic feasibility of this breakthrough technology.

Acknowledgements

The authors wish to thank ExxonMobil for supporting this research and for permission to contribute to this publication.

References

1. Symington, W. A.; Olgaard, D. L.; Otten, G. A.; Phillips, T. C.; Thomas, M. M.; Yeakel, J. D. *ExxonMobil's Electrofrac Process for In Situ Oil Shale Conversion*; 26th Oil Shale Symposium, Colorado School of Mines, 2006.
2. Ellis, P. J.; Paul, C. A. *Tutorial: Petroleum Coke Calcining and Uses of Calcined Petroleum Coke*; Great Lakes Carbon Corporation, Presented at AIChE 2000 Spring National Meeting, March 5-9, 2000; http://www.glcarbon.com/tech_articles.htm.
3. Hardin, E. E.; Beilharz, C. L.; Melvin, L. L. A Comprehensive Review of the Effect of Coke Structure and Properties when Calcined at Various Temperatures. In *Light Metals*; Das, S. K., Ed.; The Minerals Metals and Materials Society: 1993; pp 501–508.
4. Baughman, G. L. *Synthetic Fuels Data Handbook*, 2nd ed.; Cameron Engineers, Inc.: 1978.
5. Curry, D. J.. Personal communication, 2003.
6. Meurer, W. P.; Symington, W. A.; Braun, A. L.; Kaminsky, R. D.; Olgaard, D. L.; Otten, G. A.; Phillips, T. C.; Thomas, M. M.; Wenger, L. M.; Yeakel, J. D. *Parameteric Controls on the Composition of Oil Generated by In Situ Pyrolysis of Oil Shale*; 28th Oil Shale Symposium, Colorado School of Mines, 2008.
7. Lewan, M. D. Experiments on the Role of Water in Petroleum Formation. *Geochim. Cosmochim. Acta* **1997**, *61*, 3691–3723.
8. Price L. C.; Wenger L. M. The Influence of Pressure on Petroleum Generation and Maturation as Suggested by Aqueous Pyrolysis. In *Advances in Organic Geochemistry 1991; Part 1, Advances and Applications in Energy and the Natural Environment*; Eckardt, C. B., Maxwell, J. R., Larter, S. R., Manning, D. A. C., Eds.; *Org. Geochem.*, **1992**, *19*, 141–159.
9. Symington, W. A.; Yale, D. P. *Interpolation/Extrapolation of Measured In Situ Earth Stresses: An Example from the Piceance Basin in Western Colorado*; ARMA/USRMS 06-1124, Golden Rocks Conference, June 19-21, 2006.
10. Symington, W. A.; Spiecker P. M. *Heat Conduction Modeling Tools for Screening In Situ Oil Shale Conversion Processes*; 28th Oil Shale Symposium, Colorado School of Mines, 2008.
11. Eckert, E. R. G.; Drake, R. M. *Analysis of Heat and Mass Transfer*; McGraw-Hill, Inc.: 1972
12. Tissot, B. P.; Welte, D. H. *Petroleum Formation and Occurrence*; Springer-Verlag: 1984.

13. Beard, T. N.; Tait, D. B.; Smith, J. W. Nahcolite and Dawsonite Resources in the Green River Formation, Piceance Creek Basin, Colorado. In *Rocky Mountain Association of Geologists Guidebook*; 1974; pp 101–109.
14. Dyni, J. R. The Origin of Oil Shale and Associated Minerals. In *Oil Shale, Water Resources, and Valuable Minerals of the Piceance Basin, Colorado: The Challenge and Choices of Development*; Taylor, O. J., Ed.; U. S. Geological Survey Professional Paper 1310, 1987; pp 17–20.
15. Dyni, J. R. Stratigraphy and Nahcolite Resources of the Saline Facies of the Green River Formation of Northwest Colorado. In *Rocky Mountain Association of Geologists Guidebook*; 1974; pp 111–122.
16. Kaminsky, R. D.; Symington, W. A.; Yeakel, J. D.; Thomas, M. M. In Situ Co-Development of Oil Shale with Mineral Recovery. United States Patent Application, Publication No. US2007/0246994, 2007.
17. Yeakel, J. D.; Meurer, W. P.; Kaminsky, R. D.; Symington, W. A.; Thomas, M. M. *ExxonMobil's Approach to In Situ Co-Development of Oil Shale and Nahcolite*; 27th Oil Shale Symposium, Colorado School of Mines, 2007.

Chapter 11

Carbon Dioxide Emissions from Oil Shale Derived Liquid Fuels

Adam R. Brandt,^{*,1,4} Jeremy Boak,² and Alan K. Burnham³

¹Energy and Resources Group, University of California, Berkeley CA 94024

²Center for Oil Shale Technology & Research, Colorado School of Mines,
Golden CO 80401

³American Shale Oil LLC, Rifle, CO 81650

⁴Current address: Department of Energy Resources Engineering, Stanford
University, Stanford, CA 94305-2220

*abrandt@stanford.edu

Without mitigation or technology improvements, full-fuel-cycle carbon dioxide (CO₂) emissions from oil shale derived liquid fuels are likely to be 25 to 75% higher than those from conventional liquid fuels, depending on the details of the process used. The emissions of CO₂ from oil shale derived fuels come from three stages: retorting of shale, upgrading and refining of raw shale oil, and combustion of the finished transportation fuels. Emissions from these stages represent approximately 25-40%, 5-15%, and 50-65% of total fuel-cycle emissions, respectively. The most uncertain source of emissions is the retorting stage, due to variation in emissions with shale quality and retorting technology used. Mitigation options include higher thermal efficiency, minimizing carbonate decomposition, CO₂ sequestration by geologic injection, enhanced oil recovery, mineralization in spent retorts, or the use of non-fossil sources for process heat.

Introduction – Carbon Dioxide and Oil Shale

The world resource of oil shale likely consists of trillions of barrels of hydrocarbon (HC) product, with significant resources distributed worldwide (1).

Both scientific investigation and production of oil shale resources have been episodic, coinciding with peaks in the price of oil. This is due to the high cost of oil production from shale. Recent oil price increases have driven a resurgence of interest in oil shale development around the world.

Current methods of producing HCs from oil shale involve mining and retorting shale at the surface to convert immature kerogen to liquids and gas (*ex situ* retorting). Common fuel sources for *ex situ* retorting are pyrolysis gas and “char,” a shale oil coke generated during the production of liquid HCs from kerogen. *In situ* conversion of kerogen to HCs holds promise, but a major increase in production is more than a decade away. Methods considered for *in situ* heating include borehole electrical heaters, electrical heating through fractures propped with conductive material, fluid heat transport through boreholes, and borehole-installed fuel cell heaters (2).

Given current concern about anthropogenic climate change, a major hurdle for production of fuels from oil shale is the quantity of carbon dioxide (CO₂) emitted from oil shale processing. Early analysis of this problem presented a very wide range of possible emissions consequences (3). Recent research attention has focused on this problem (4–10), but significant uncertainties remain. This chapter summarizes the state of knowledge regarding CO₂ emissions from oil shale retorting, and discusses the remaining uncertainties.

This chapter explores emissions from the full liquid fuel production cycle, and generally uses parameters derived from the Green River Formation (GRF) oil shale of the Western United States, the largest resource of oil shale in the world (1). This fuel cycle includes three stages: retorting raw shale to produce crude shale oil, upgrading and refining of crude shale oil, and combustion of the final refined fuel. Emissions from the first stage, oil shale retorting, are the most uncertain, and will be the primary focus of this chapter. Key sources of CO₂ from oil shale retorting include CO₂ generated by the breakdown of carbonate minerals, by the oxidation of kerogen during pyrolysis, by combustion of fuels to provide thermal energy for retorting, and by fossil fuel power plants used to generate electricity used in the retorting process. Emissions from the last two stages are less uncertain and will be described in less detail. Note that this chapter focuses solely on conversion of kerogen to liquid and gaseous HCs, and does not address the use of oil shale for power generation.

For the calculations presented in this chapter, energy requirements and CO₂ emissions are reported either per tonne (t) of raw shale processed, or per megajoule (MJ) of refined fuel delivered (RFD) to the end consumer. The refined fuel of comparison will be reformulated gasoline (U.S. Federal standard). We use the higher heating value (HHV) basis of fuels.

Sources of Carbon Dioxide from Fuel Production Stages

Carbon dioxide is directly emitted in all three primary stages of producing and consuming fuels from oil shale. First are emissions resulting from the retorting of oil shales to generate unrefined hydrocarbons (HCs), including crude shale oil and

HC gases. Second are emissions from the upgrading and refining of crude shale oil to refined fuels (e.g., gasoline or diesel). Third, direct emissions result from combustion of the refined fuel by the consumer. Additionally, there are minor indirect emissions from the consumption of materials such as steel or cement used in oil shale extraction.

Emissions from Generating Crude Hydrocarbons through Oil Shale Retorting

Emissions from oil shale retorting process can be divided into three components: CO₂ emitted due to the thermal energy requirements of retorting, CO₂ emitted from other energy uses associated with retorting, and CO₂ emitted from the shale itself. These emissions sources will be discussed in order.

Carbon Dioxide Emissions from Thermal Requirements for Retorting

A major source of emissions is the thermal energy requirement for retorting. These thermal requirements can be met by direct combustion of fuels, or indirectly by combustion of fuels for electric power generation.

The thermal energy demands of retorting can be defined as the heat of retorting, which is an overall heat requirement that includes ((11), p. 32):

- a) The heat content of shale mineral matter at final temperature of the retorted shale (which could be lower than the retorting temperature, as in the Paraho process where heat is recovered from spent shale);
- b) The heat of reaction of kerogen decomposition;
- c) The heat of reaction of mineral reactions in shale (e.g., decomposition of carbonates);
- d) The heat to vaporize generated hydrocarbons and water contained in shale (both bound and free water);
- e) The heat contents of gas, water, and oil vapors at the temperature of exit from the retort.

The heat of retorting varies with shale character and with the retorting technology used. Measured values vary significantly between samples and studies, and it is difficult to generalize about the heat of retorting ((12), p. 149). Reported heats of retorting range from as low as 240 MJ/t to as high as 880 MJ/t across a variety of studies ((12), Table 8.10). We will explore the reasons for this variability below.

Because of factors (a) and (e) above, the heat of retorting depends strongly on the rate at which heating takes place. This is because slower retorting results in lower temperatures of complete kerogen decomposition. At a heating rate of 0.5°C/day, kerogen will be effectively decomposed upon reaching 340-360°C, as compared to 500°C for the Fischer Assay at 12°C/min (FA – the standard process for measuring liquid content of oil shale). This 150°C temperature difference will result in an increase in the heat of retorting by 140 MJ/t from the slow to the fast process due solely to the change in enthalpy of the shale mineral matter (13). (These values do not account for decomposition of any saline

or carbonate minerals, as these factors are discussed below.) Also with faster retorting, produced HCs leave as vapor at a higher temperature, which increases heat requirements by <10 MJ/t. [Camp (13) notes that the change in sensible heat of kerogen between 350 and 500 °C will be 50 kJ/kg of kerogen larger than that of the retort products if oil is in the vapor phase. Since the organic content of GRF shale is 16-20% for 110-150 l/t shale, this amounts to <10 MJ/t of shale processed.]

The heat of retorting varies little with changes in the mineral composition of shale (13). Because the enthalpies of typical mineral components of GRF shale do not vary greatly, Camp (13) found that large shifts in the percentage composition of shale mineral matter were required to cause even a 1% change in the weighted heat capacity of the minerals (note that this excludes the effects of bound water and mineral decomposition, which can have large effects and are discussed below).

The above values for mineral matter are only strictly true in simple retorting systems with no heat recovery from spent shale. In retorts with beneficial heat recovery from the spent shale (e.g., the Alberta Taciuk Processor [ATP], a modern ex situ retort with countercurrent heat exchange), the net heat requirement depends on the temperature of the spent shale as it exits the retort. This does not include spent shale that is water cooled, unless the heat of the steam is used for a beneficial purpose.

Because of factor (b) above, the heat of retorting increases as the organic content of the shale increases. An increase in organic content corresponding to a yield increase from 20 to 200 l/t will increase the heat of retorting from ~600 to ~800 MJ/t (14). Mraw and Keweshan (15) found empirically that a 110 l/t Green River shale will have a heat of retorting of about 700 MJ/t, while a 150 l/t shale will require about 750 MJ/t. [This is calculated using their enthalpy relationship $H(773\text{ K}) - H(298\text{ K}) = 569 + 1.181G$, where G is the FA yield in l/t. Similar relationships were found in two earlier studies (15).] The richest shales studied (>300 l/t) have heats of retorting approaching 1000 MJ/t (15).

Because of factor (c) above, the heat of retorting varies with reactions involving shale mineral matter, including mineral dissociation and dehydration. Many of these reactions are endothermic, adding to the required energy inputs of retorting. Common reactions that occur in shale are shown in Table 1, numbered and grouped by species. Many of these reactions also result in release of inorganic CO₂, but here we are only concerned with their effects on the heat of retorting (see below for discussion of mineral CO₂ emissions).

The relevant mineral reactions can be grouped into reactions involving calcite (CaCO₃), dolomite (MgCa(CO₃)₂), sodium minerals, and pyrite (FeS₂). Reactions involving calcite, dolomite and sodium minerals are endothermic, and therefore add to the heat of retorting. Reactions involving pyrite are either endothermic or exothermic, depending on whether oxidation is involved. Oxidation reactions can contribute 107-320 MJ/t per wt% S in raw shale (14).

Not all of the reactions in Table 1 will occur in a specific shale retorting system. One reason is that shale can lack the required mineral constituents. For example, the saline minerals nahcolite (NaHCO₃) and dawsonite (NaAl(OH)₂CO₃) are present in large quantities in the saline zone of the GRF, but will not be present in large quantities in most shales undergoing retorting (<1 wt% in the Mahogany

zone). Another reason is that some retorting processes will discourage reactions. For example, during in situ retorting (like the Shell in situ conversion process - ICP), the dolomite and calcite reactions will not occur to any significant extent because of the low retorting temperature.

A complication that prevents generalizations about heat demand from mineral reactions is that endothermic decomposition of a species can result in differing thermal demand depending on the end products generated. For example, the reaction of CaCO_3 with SiO_2 (reaction 2 in Table 1) has about half the thermal demand of decomposition of CaCO_3 to CaO and CO_2 (reaction 1). The relative strength of these reactions is governed by the partial pressure of CO_2 during retorting, which varies with the process used (16).

As a simple example, a GRF oil shale that is (by weight) 25% ankeritic dolomite, 12% calcite, and 1% nahcolite, retorted in a surface retort fueled by shale char combustion, could experience approximately 50% decomposition of the dolomite, 10% decomposition of the calcite, and complete decomposition of nahcolite. If 80% of the calcite CO_2 is emitted through the silicate reaction, (Reaction 2), then the total thermal demand from mineral decomposition will be ≈ 130 MJ/t of shale processed. Note that this is a significant fraction of the heat of retorting. In a low-temperature process (e.g., conductive in situ retorting), this thermal demand will be greatly reduced because carbonate decomposition will be limited.

Lastly, because of factor (d), the amount of water that must be driven off of the shale can contribute significantly to the heat of retorting. This water can be free water or water bound to clays or other mineral matter. Bound water has a lower heat capacity than free water because it has less vibrational freedom than liquid water (13). But the energy burden of dehydration is larger than the heat of vaporization. Replacing 1 wt% of mineral matter with free water will result in ≈ 20 MJ/t addition to the heat of retorting, while adding the same amount of bound water would add ≈ 30 MJ/t (13). [The exact difference will depend on the heat capacity of the mineral species contained in the shale. It will also change with the heats of dehydration for bound water, which are uncertain (13). Nevertheless, the heat capacity of water is ≈ 4 times that of shale mineral matter, and the heat of vaporization or dehydration is significant, resulting in an energy burden from additional water content (on a volumetric basis water has ≈ 2 times the heat capacity because it is less dense).]

All of the above factors make it difficult to generalize about the heat of retorting. There is a large diversity of oil shale processes and oil shale types. And even for what is nominally the same type of process, the details of the engineering implementation can affect the thermal history of the shale, which affects the heat of retorting. Consequently, each process must be analyzed in detail before reliable estimates can be made of the amount of CO_2 generated from retorting energy inputs.

Illustrative estimates of the general heat of retorting demands can, nevertheless, be made for three cases of GRF shale retorting [In the cases outlined, shale has the mineral composition from Camp (13), specifically: 16.7% organic matter (≈ 110 l/t), 25% ankeritic dolomite with the formula $\text{Mg}_0.72\text{Fe}_0.28(\text{CaCO}_3)_2$, 15% calcite, and 1.3% bound water.]:

Table 1. Enthalpy change with mineral reactions^a

<i>Reaction</i>	<i>T (°C)</i>	<i>ΔH (J/g or MJ/t) @ 298K</i>
Calcite:		
1. $\text{CaCO}_3 = \text{CaO} + \text{CO}_2$	600-900	1764
2. $\text{CaCO}_3 + \text{SiO}_2 = \text{CaSiO}_3 + \text{CO}_2$	700-900	878
3. $2\text{CaCO}_3 + \text{SiO}_2 = \text{Ca}_2\text{SiO}_4 + 2\text{CO}_2$	700-900	1133
Dolomite:		
4. $\text{CaMg}(\text{CO}_3)_2 = \text{CaO} + \text{MgO} + 2\text{CO}_2$	600-750	1680
5. $\text{CaMg}(\text{CO}_3)_2 = \text{CaCO}_3 + \text{MgO} + \text{CO}_2$	600-750	715
6. $\text{CaMg}(\text{CO}_3)_2 + 2\text{SiO}_2 = \text{CaMgSi}_2\text{O}_6 + 2\text{CO}_2$	700-900	849
7. $\text{CaMg}(\text{CO}_3)_2 + \text{SiO}_2 = \text{CaMgSiO}_4 + 2\text{CO}_2$	700-900	1049
Saline minerals:		
8. $2\text{NaHCO}_3 = \text{Na}_2\text{CO}_3 + \text{CO}_2 + \text{H}_2\text{O}$	100-150	1324
9. $2\text{NaAl}(\text{OH})_2\text{CO}_3 = \text{Na}_2\text{CO}_3 + \text{Al}_2\text{O}_3 + 2\text{H}_2\text{O} + \text{CO}_2$	350-400	842
10. $\text{NaCO}_3 + 2\text{SiO}_2 = \text{Na}_2\text{Si}_2\text{O}_5 + \text{CO}_2$	700-900	849
11. $\text{NaCO}_3 = \text{Na}_2\text{O} + \text{CO}_2$	>850	3031
Dehydration of clays ^{bc}	Various	2555
Pyrite:		
12. $\text{FeS}_2 + 2\text{H} = \text{FeS} + \text{H}_2\text{S}$ (during pyrolysis)	440-475	523 ^d
13. $\text{FeS}_2 + \text{H}_2\text{O} + \text{C} = \text{H}_2\text{S} + \text{FeS} + \text{CO}$ (w/ steam)	350-500	1619
14. $\text{FeS} + \text{H}_2\text{O} = \text{FeO} + \text{H}_2\text{S}$ (w/ steam present)	450-700	572
15. $2\text{FeS}_2 + 5\frac{1}{2}\text{O}_2 = \text{Fe}_2\text{O}_3 + 4\text{SO}_2$	<600	-6900

^a Values are from Campbell (16) except that for clay (13) and sulfur reactions (17, 18). The experimentally derived ΔH for some of these reactions was observed to be somewhat smaller than values from the reference literature ((16), Table 7). ^b The dehydration of clays must also include a correction term to the heat capacities of hydrated minerals to account for the heat capacity addition due to the bound water before it is liberated. Camp (13) cites a heat capacity value of $1.68+0.0022T$ (temperature in K) for bound water, which is lower than that for free water. ^c The clay dehydration data of Camp (13) includes all clays as a single species. ^d Depending on the source of the hydrogen donor, this reaction could be more or less endothermic.

- Slow in situ retorting (0.5°C/day) to 350°C,
- Fast retorting to 515°C at 30°C/min heating rate, and
- Fast retorting to 515°C as above with the spent shale used as at heat carrier and heated to 750°C. In this case there is heat recovery from the spent shale (as in the ATP retort). [This calculation uses a simple model to account for carbonate decomposition. It uses the Thorsness (19) OSP model (described below) and assumes a mass-weighted residence time at 750 °C of 9.5 min. This results in

significant decomposition of dolomite, but not significant decomposition of calcite.]

The resulting heats of retorting for these three cases are outlined in Table 2.

Lastly, the efficiency of thermal energy transfer to shale also must be accounted for. Thermal losses to the surroundings through the retort shell (in ex situ retorting) or to the surrounding formation (during in situ retorting) will increase the thermal energy requirements of retorting. Data suggest that between 5% and 20% of the heat may be lost during retorting (6, 20).

The heat of retorting values calculated in MJ/t for a given retorting process, can be converted to CO₂ emissions using the CO₂ intensity of thermal energy sources (Table 3). Care is required when electricity is used as the thermal energy source because the carbon intensity of electricity can vary significantly depending on its primary energy source, the efficiency of generation, and transmission losses. We see that for natural gas used directly in case *a* (as with natural-gas-fired downhole heaters), emissions might be 22.5 kgCO₂/t shale processed, while the use of char in case *b* might result in emissions of nearly 70 kgCO₂/t shale processed, if char combustion could be accomplished without carbonate decomposition. The use of electricity will, in general, increase these values. These carbon intensities of the thermal demand of retorting can be converted to fuel basis, and they range generally between 10 and 20 gCO₂/MJ RFD. [We assume here: a 110 l/t shale is retorted, with 95% of FA liquid yield recovered; the shale oil has characteristics of Paraho raw shale oil (21) (HHV = 44.4 MJ/kg, API gravity = 21.4); there is 90.1% energetic conversion to refined products output (see discussion below); and 10% of thermal energy inputs to retorting are wasted by loss to the surroundings. These values result in crude shale oil yield of 4300 MJ/t, and refined fuel yield of 3875 MJ RFD/t.]

Carbon Dioxide Emitted Due to Auxiliary Energy Use in the Retorting Process

Carbon dioxide is also emitted due to energy consumed in non-thermal energy requirements of retorting. For ex situ retorts, these non-thermal energy uses include: mining the raw shale, transport of raw shale to the retort, crushing and pre-processing raw shale, operation of the retort, transport of spent shale to disposal site, and handling of crude shale oil. For in situ retorts, the mining energy requirements above are replaced with drilling and casing wells, along with other subsurface operations. These miscellaneous emissions are difficult to calculate without actual project data, as they depend on specifics of a given facility.

In one report of emissions from the ATP ex situ retort, emissions from electricity consumption and mining diesel use were estimated at 11.3 and 10.3 gCO₂/MJ RFD, respectively ((25), *p.* 104). In a report of emissions from ATP technology applied to the Stuart shales of Queensland, emissions from electricity and diesel use were reported to be 8.0 and 0.3 gCO₂/MJ RFD, respectively (26).

For an in situ case, an analysis of the Shell ICP suggests that emissions from non-thermal retorting energy use were between \approx 4 and 8 gCO₂/MJ RFD, for uses such as drilling, freeze wall maintenance, pumping, and site reclamation (6).

Table 2. Estimated heats of retorting for three illustrative cases^a

	<i>Unit</i>	<i>Case a</i>	<i>Case b</i>	<i>Case c</i>
Heating rate	K/sec	5.8x10 ⁻⁶	0.4	0.4
Final temperature	°C	350	515	515/750
Dolomite decomposition	%	0	< 2	45
Calcite decomposition	%	0	~ 0	2
Enthalpy of retorting	MJ/t raw shale	450	730	520-670^b

^a These heats of retorting calculated using the shale characteristics of 16.7% organic matter (≈ 110 l/t), 25% ankeritic dolomite with the formula $\text{Mg}_0.72\text{Fe}_0.28(\text{CaCO}_3)_2$, 15% calcite, and 1.3% bound water. ^b This includes a total heat demand of 820 MJ/t, with heat recovery from spent shale of 150 – 300 MJ/t of raw shale. This value is only approximate because the amount of heat recovery depends on the specifics of operation of the retort.

These are estimates not based on data from commercial scale operations, and were conservatively calculated, so actual emissions could be higher.

Carbon Dioxide Emitted from Oil Shale

Lastly, CO_2 is emitted from shale during retorting. This is due to two processes that occur with the heating of shale: formation of CO_2 from kerogen and bitumen, and formation of inorganic CO_2 from mineral reactions.

Organic CO_2 is emitted in retorting due to the elimination of existing oxygen in the organic matter as CO_2 in the presence of retorting heat. Because the chief reaction is thought to be decarboxylation of organic acids and esters within the kerogen, the amount of CO_2 generated in this manner scales with the organic content of the shale and has little to do with the mineral content of the shale (23).

Kerogen from Green River oil shale contains 5 to 6 wt% oxygen (see Table 4), while raw shale oil contains only trace amounts of oxygen. In theory this means that up to 8% of the mass of kerogen contained in the shale could leave as CO_2 if all organic oxygen were converted to CO_2 . In practice, however, water vapor is also formed. Empirical results from Stanfield (27) reported that 2.4% to 4.7% kerogen mass is emitted as CO_2 , (These values are for 4 samples of GRF oil shale ranging from 44 to 257 l/t richness.), whereas more recent analyses suggest values ranging from 4.1% to 5.3% of kerogen mass (23, 28). [The Huss and Burnham data also include CO, which oxidizes quickly in the atmosphere and is therefore included in CO_2 emissions estimates ((29), *p.* 2-8)]. A study of 66 shale samples (30) provides a well-grounded correlation for CO_2 yield, including both mineral and organic CO_2 , as a function of shale grade (see Figure 1). From this and other data, 4.1% of the kerogen mass is emitted as CO_2 . [This value also includes carbon in CO, as it is quickly oxidized to CO_2 in the atmosphere. This value is lower than some other studies, possibly because the fraction of oxygen in kerogen was overestimated in prior studies due to oxidation during analysis.] Thus, for shale that is 16% organic matter, emissions will be 6.5-8.5 kgCO_2/t shale processed, or 1.7-2.2 gCO_2/MJ RFD.

Table 3. Carbon intensity of thermal energy sources

<i>Thermal energy source</i>	<i>Carbon intensity of thermal energy sources</i>		
	<i>Carbon density (gC/g fuel)</i>	<i>CO₂ intensity (gCO₂eq./MJ)</i>	<i>Source</i>
Natural gas	> 0.75	49-51	(22)
Coal	< 0.75 to > 0.92	88-97	(22)
Shale char ^a	0.87 to 0.92	88-100	(23)
Electricity - Nat. gas ^b	NA	111	
Electricity - Coal ^c	NA	280	
Electricity - Colorado ^d	NA	206	(24)

^a These values from formulas for char produced from secondary pyrolysis at $\approx 550^\circ\text{C}$ and tertiary pyrolysis at $\approx 750^\circ\text{C}$ ((23), Table 3). HHV of the char is calculated using the Dulong formula. This does not include the associated carbonate decomposition. ^b Assumes combined-cycle turbine with 45% efficiency of generation and transmission. Assumes 50 gCO₂/MJ natural gas. ^c Assumes pulverized coal boiler with 30% efficiency of generation and transmission. Assumes 92.5 gCO₂/MJ of coal. ^d Data from EIA (24) for total electricity generation (MWh) and total emissions (Mt CO₂) in Colorado.

Organic CO₂ is emitted before the peak rate of oil generation, with peak generation occurring at around 400°C in the FA ((23), Figure 3). Later reactions such as secondary and tertiary pyrolysis ($>550^\circ\text{C}$ and $>750^\circ\text{C}$, respectively) do not result in organic CO₂ emissions because the oxygen has been consumed well before these temperatures are achieved (23).

If a retorting process occurs with oxygen input, as in a directly heated ex situ retort, the emissions of CO₂ from organic sources will be a combination of CO₂ derived as above, and CO₂ derived from the combustion of organic material to provide retorting process heat. These emissions were covered above in the thermal requirements of retorting.

Additional CO₂ is emitted from shale due to reactions of inorganic mineral matter during retorting. The most important of these reactions were listed and numbered in Table 1.

Common saline mineral reactions (such as decomposition of nahcolite and dawsonite, reactions 8 and 9 in Table 1, respectively) occur at low temperatures. Because these temperatures are below those at which retorting occurs, these minerals will completely decompose during retorting. Thankfully, these minerals are not prevalent except in the saline zone of the GRF. For every 1 wt% of nahcolite that decomposes, 2.6 kgCO₂/t is emitted. The decomposition of carbonate minerals dolomite and calcite occurs at higher temperatures and will therefore be most problematic in retorting systems where the spent shale is combusted to utilize the heating value of the shale char. For every 1 wt% of dolomite that undergoes primary decomposition (reaction 5), 2.3 kgCO₂/t is emitted, whereas the same figure for calcite (reaction 1) is 4.4 kgCO₂/t.

There is uncertainty about the kinetics of carbonate decomposition in shales. This is partly due to the difficulty of modeling the complex reactions in

a heterogeneous substance such as oil shale (16). Some generalities about the mineral reactions do, however, exist. First, decomposition increases with both the maximum temperature achieved and the amount of time spent at that temperature (Figure 2). Also, the primary decomposition of dolomite (reaction 5) occurs much more quickly at low temperatures than calcite decomposition.

Also of great importance is that simple decomposition of calcite (reaction 1) is significantly inhibited by the presence of gaseous CO₂. This can be seen in the divergence in Figure 2 between the decomposition of calcite at 0.25 atm CO₂ (dashed lines) and 1 atm CO₂ (solid). The temperature at which decomposition begins increases with higher partial pressures of CO₂, and the dominant reaction changes from reaction 1 to reactions 2 and 3 (Table 1). Given the likely high partial pressures of CO₂ in the immediate gaseous environment of retorting particles, most CO₂ release from calcite will occur from the reaction of calcite with silica, rather than decomposition to CaO. [In Campbell's (16) empirical results, simple decomposition of CaCO₃ was only dominant at P_{CO₂} = 0, a condition not likely to hold for any period of time in the atmosphere directly surrounding decomposing shale mineral matter. At higher partial pressures of CO₂, the overwhelming reaction was with silica ((16), Table 44). Overall, the silica reaction resulted in about 4/5 of the evolved CO₂ ((16), Table 7).]

Despite these regularities, there are significant differences in the reaction rates found by different models of carbonate decomposition. Campbell (16) reported reaction kinetics for carbonate decomposition processes in shale. More recently, Thorsness (19) reported two models: the OSP model, which was based on the work of Jukkola (31), and a "Fast Kinetics" model based on results from the Lawrence Livermore National Laboratory (LLNL) 4TU-Pilot retort.

The OSP model is in general agreement with Campbell's decomposition model (results from this model are presented in Figure 2). Unfortunately, this model performed poorly in predicting decomposition in the LLNL retort, with predictions 12-17% low on an absolute basis (a significant deviation when absolute decomposition rates tend to be below 50%). Thorsness created the Fast Kinetics model to match empirical data from the LLNL retort. This model predicts very high levels of carbonate decomposition, significantly in excess of those predicted by Campbell and the OSP model. Also, this model was not generated for modeling in situ retorting, so the usefulness of this model under those conditions is unknown (e.g., it is thought to overestimate rates of decomposition at slow heating and low temperatures).

As an example of the divergence between model results, the OSP model predicts decomposition of dolomite of 24% and 50% when shale is heated to 700°C for 2 minutes and 5 minutes, respectively. On the other hand, the Fast Kinetics model predicts decomposition fractions of 79% and 98% for the same conditions. This gross divergence suggests that more research on carbonate decomposition is needed. Part of the solution may be the use of fractional order kinetics, as would be expected for shrinking core reactions.

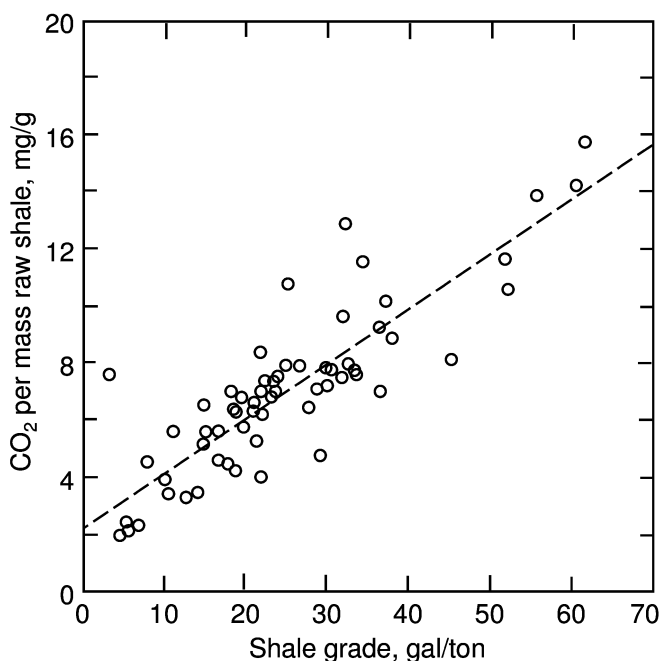


Figure 1. CO_2 yield as a function of shale grade for 66 Green River oil shale samples [adapted from (30)]. The non-zero intercept probably represents CO_2 from nahcolite at an apparent concentration of 0.8 wt%.

Table 4. Composition of kerogen in Green River shale

	Elemental kerogen composition (wt %)			
	Smith ^a	Singleton et al. ^b	Campbell et al. ^c	Huss and Burnham ^d
Carbon	80.52	80.97	80.32	81.72
Hydrogen	10.30	10.19	10.31	10.22
Nitrogen	2.39	2.36	2.62	3.05
Sulfur	1.04	1.08	1.07	–
Oxygen	5.75	5.36	5.68	5.01

^a These values are the average of 10 sample of cores of Mahogany zone oil shale from Colorado and Utah. The composition across samples was reported to be very consistent. Source: ((11), Table 33). ^b Source: (30), based on the empirical formula derived from 66 Green River shale samples: $\text{CH}_{1.50}\text{N}_{0.025}\text{O}_{0.05}\text{S}_{0.005}$. ^c Source: (28) This is based on the empirical formula $\text{CH}_{1.54}\text{N}_{0.028}\text{S}_{0.005}\text{O}_{0.053}$, derived from shale from the Anvil Points Mine. ^d Source: (23) This is based on the empirical formula $\text{CH}_{1.50}\text{N}_{0.032}\text{O}_{0.046}$, derived from 7 samples of varying organic content from the Anvil Points Mine and Colorado lease tract C-a.

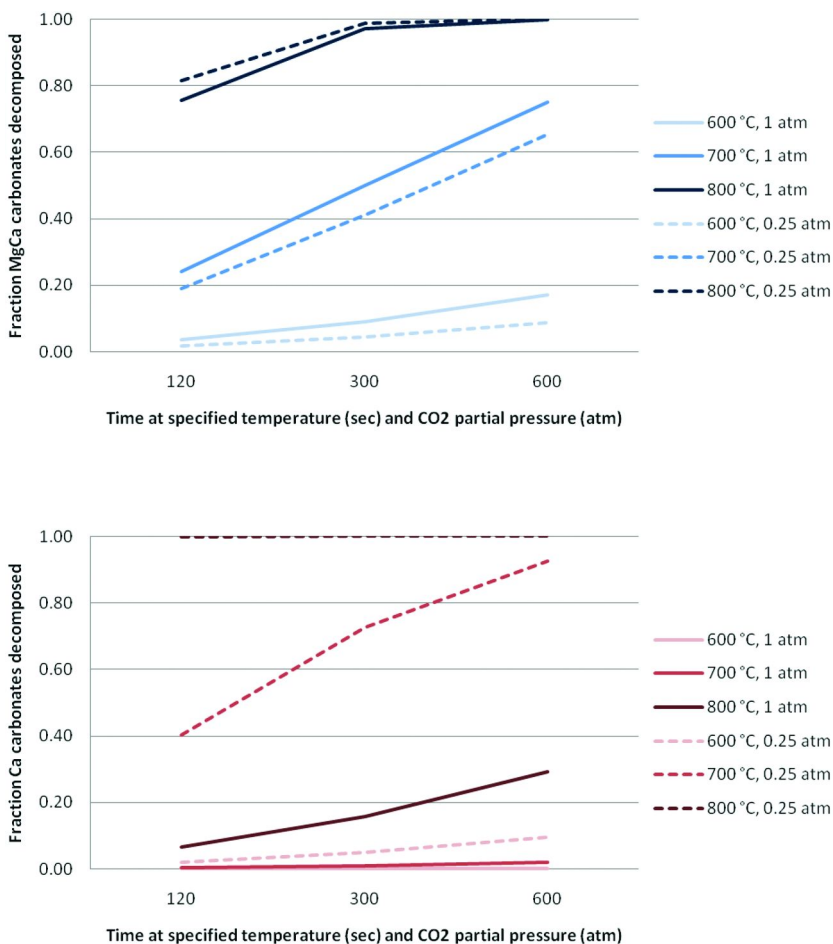


Figure 2. Fraction of carbonate minerals (calcite bottom, dolomite top) decomposed as a function of time (x-axis) and temperature (y-axis). Kinetics based on OSP model (19). In dashed lines the partial pressure of CO₂ is assumed to be 0.25 atm, whereas for solid lines it equals 1 atm. Note the very strong response of calcite to CO₂ pressure.

Upgrading and Refining of Oil-Shale-Derived Hydrocarbons

After crude shale oil is produced, it must be upgraded and refined. This upgrading can include anything from simple stabilization of the raw shale oil for transport to complex fractionation and upgrading systems (32). At least some upgrading is required before refining, because raw shale oil, at least from the GRF, is generally:

- Unstable and therefore not able to be pipelined due to formation of gums (33);
- Affected by suspended solids which must be removed [For example, shale oil produced by the Paraho retort contained 0.5 wt% suspended solids, most of

which settled out after the oil/water emulsion was broken. About 250 ppm of fine solids remained after settling ((21), p. 1011).];

- c) High in nitrogen content (approximately 2%, compared to about 0.2% for conventional crude oils); and
- d) High in arsenic, iron and nickel ((21), p. 1005).

It is difficult to generalize about oil shale upgrading (21). This is because the properties of raw shale oil differ greatly depending on the retorting process used and the raw shale retorted. For example, the Paraho retort produces 21°API crude, while tests of the Shell ICP process have produced crudes of 36°API (34) with substantially lower nitrogen and metals content. The energy inputs to and emissions from upgrading will also vary because numerous upgrading pathways and technologies are possible (21).

Due to this variability, wide ranges of hydrogen requirements for upgrading are cited. Speight cites H₂ requirements of between 1400 – 2060 scf H₂/bbl of raw shale feed (21). Probstein and Hicks reported that upgrading of Paraho crude would have a stoichiometric hydrogen demand of 2.1 kg H₂ per 100 kg of raw shale oil (32) (This calculation assumed upgrading from CH_{1.59}O_{0.014}N_{0.02}S_{0.003} to finished crude of CH_{1.8} plus water, ammonia, and H₂S.) They reported that actual demand could be nearly twice this high, or 40 m³ H₂/100 kg shale oil, due to the formation of H-rich HC gases. More recently, Johnson *et al.* reported energy requirements of 126.6 MJ/bbl of raw shale feed (35).

These values are converted to consistent units of gCO₂/MJ of crude shale oil feedstock below in Table 5. [In this table, we assume as in Probstein and Hicks (32) that the total energy use in upgrading is approximated by the hydrogen demand.] This table shows that there is considerable variation in the figures, especially considering the much lower value implied by the energy use cited by Johnson *et al.*

After upgrading of the crude shale oil, it must be refined into finished liquid fuels. [In all calculations present here, we assume for simplicity that upgraded synthetic crude has the same energy content as the raw crude oil input to the upgrading process ((32), see p. 357).] In 2006, U.S. refineries had the following gross characteristics: 39.1 EJ of crude oil and other feedstocks were taken in; 2.2 EJ of feedstock inputs were consumed for energy needs during refining; and 1.8 EJ of purchased outside energy was also consumed. Total energetic output in products was 35.2 EJ, whereas refined fuel products output (less asphalt and “miscellaneous” output) was 33.8 EJ (37).

Thus, in the aggregate, for every 1 MJ of crude oil input, 0.901 MJ of products were produced, and 0.864 MJ of refined fuels were produced. The resulting combustion CO₂ emissions amount to 7.7 gCO₂/MJ of total product output, or 8.0 g CO₂/MJ refined fuels. [This emissions estimate is calculated by applying fuel-specific emissions factors to all of the fuels consumed in refining, both those produced internally (such as coke and still gas and residual oils) and those purchased from external energy suppliers (such as purchased electricity, natural gas, or steam). In addition to these combustion emissions, non-combustion emissions from refining also exist.] The energy and carbon intensity of a specific refined fuel will differ from this average value. For example, reformulated gasoline has 1.15 to 1.3 times the energy intensity of the average refinery output

Table 5. Estimates of hydrogen requirements of shale oil upgrading, converted to emissions of CO₂

	Case	Reported requirements		Emissions
		Value	Unit	gCO ₂ /MJ crude shale oil
Speight (18)	Low	1400	scf H ₂ /bbl	4.93 ^a
	High	2060	scf H ₂ /bbl	7.25 ^b
Probstein and Hicks (32)	Low	2.1	kg H ₂ /100 kg shale oil	4.30 ^c
	High	40	m ³ H ₂ /100 kg shale oil	7.31 ^d
Johnson <i>et al.</i> (35)	–	126.6	MJ/bbl of shale oil	0.97 ^e

^a Value from Speight ((21), p. 1028) for hydrocracking of oil from Occidental MIS retort. Converted to CO₂ emissions using efficiency and CO₂ emissions from modern steam methane reformation, which equal 9.1 gCO₂/g H₂ produced, assuming efficiency (LHV basis) of 76% (36). ^b Value for hydrocracking of Paraho crude. CO₂ emissions calculated as in note a. ^c Minimum stoichiometric demand for hydrotreatment of Paraho crude. See text for explanation. CO₂ emissions calculated as in note a. ^d High estimate of actual demand for hydrotreatment of raw shale oil. CO₂ emissions calculated as in note a. ^e For upgrading 21 °API raw shale oil to 38 °API. CO₂ emissions calculated assuming natural gas is feedstock energy source for upgrading.

(38), and will therefore have higher emissions. For example, in the GREET model, a full fuel cycle emissions model from Argonne National Laboratory, total emissions from reformulated gasoline production are 12.4 gCO₂/MJ RFD, significantly higher than the average values calculated above.

The energy intensity and CO₂ emissions from refining upgraded shale oil will differ depending on the degree of upgrading. Minimal upgrading would likely result in refining emissions that are higher than these aggregate values for U.S. refineries, due to the lower quality of partially-upgraded shale oil. However, more extensive upgrading would result in lower refining emissions than for conventional crudes. This is because the degree of upgrading required to remove the nitrogen and arsenic compounds present in raw shale oil will also result in near-elimination of sulfur and a reduction in the undesirable high-molecular-weight fraction of the shale oil (21). [For example, Paraho crude upgraded by Sohio or LETC hydroprocessing had very low sulfur concentrations (0.02 - 0.05 wt%), and LETC hydroprocessing reduced the residuum fraction of shale oil (> 1000°F) from 12.7 wt% of the raw crude to 2.7 wt% of the upgraded crude.] This will lead to a higher proportion of liquid fuel product outputs from a given input of upgraded shale oil.

Given the uncertainties involved, we make simple and conservative assumptions for this chapter:

- That preliminary upgrading is moderate to high in intensity, and results in emissions of 5 gCO₂/MJ of refined fuel delivered;
- That the upgraded product delivered to refineries is of high quality so that the emissions from reformulated gasoline production equal to ¾ of those from

conventional feedstocks. This gives a result for emissions from refining of 9.3 gCO₂/MJ of refined fuel delivered.

Using these assumptions, total upgrading and refining emissions for production of reformulated gasoline from shale oil amount to 14.3 gCO₂/MJ RFD, whereas those for conventional petroleum from the GREET model total 12.4 gCO₂/MJ RFD.

Carbon Dioxide from Combustion of Shale-Derived Gasoline and Diesel

Carbon dioxide emissions from the combustion of shale-derived liquid fuels will be generally equal to those from fuels derived from conventional petroleum. This is because shale-derived fuels will be refined to the same standards as conventionally-derived fuels. The carbon intensity of the refined fuel assumed here (U.S. Federal standard reformulated gasoline) is 67.2 gCO₂/MJ (22).

Carbon Dioxide from Materials Inputs to Extraction

In addition to direct emissions from the three stages of the fuel cycle, comprehensive CO₂ accounting necessitates counting indirect or “embodied” emissions from the manufacture of capital and material inputs to oil shale extraction technologies (39).

For example, for the Shell ICP (6), indirect emissions were calculated for the following inputs: steel used in well casing, surface collection equipment, and facilities; cement used in well casing and facilities; and HDPE piping. Total embodied energy was calculated at 30–35 MJ/t shale processed, the majority of which is consumed for steel manufacture. This energy demand results in emissions of < 1gCO₂ eq/MJ of refined fuel delivered. (Often, embodied emissions are difficult to calculate because it is unclear which fuel is used in each manufacturing process. Here we assume the carbon intensity of consumed fuels is on average equal to diesel fuel.)

Except in the most capital intensive of operations, indirect emissions will tend to be very small when compared to direct emissions. This is true for both shale-derived fuels and conventional petroleum-based fuels. In fact, such values will generally be within the uncertainty range of emissions from any given shale retorting process.

Uncertainty in Magnitude of Carbon Emissions

The discussion above illustrates that there is significant uncertainty with regard to emissions from oil shale production depending on what process is used. This uncertainty is primarily present in the retorting process stage; emissions from refining and combustion of refined fuels are more easily defined. One aspect of these uncertainties is explored further below in an industry-scale model of one particular implementation of in situ shale oil production that uses electric power

as a heat source. This model explicitly includes distributions of shale properties (such as shale richness), and uses these distributions to calculate probabilistic emissions from an industry producing 3 Mbbbl/d of crude shale oil.

Probabilistic Model for CO₂ Generation from Production of Shale Oil

Boak (4) presented a simplified model developed for the output of CO₂ from retorting processes. Three sources of CO₂ are included – power plant emissions, mineral reactions, and kerogen – using data on the processes available in the public domain. The model runs in Lumina Decision Systems' *Analytica*[™], a visual tool for creating, analyzing, and communicating decision models. *Analytica*[™] performs multiple calculations using a Monte Carlo algorithm to provide a statistically-based distribution of results for calculations involving uncertain parameters, and is especially useful for probabilistic modeling where many variables are uncertain. It is relatively easy to evaluate the importance of uncertainties in the model result, and therefore determine what parts of the model most require refinement. In addition, the system supports linking of variables in a graphical manner, making the model relatively transparent, so that anyone can reasonably understand how the model calculates a result.

Currently, the model only includes emissions from the retorting portion of the fuel cycle (that is, it does not address CO₂ emissions from upgrading and refining, or CO₂ released by burning the resulting fuel). This approach captures most of the uncertainty with a relatively simple model. The model calculates the impacts of a large oil shale industry with 3 mbbbl/d output of crude shale oil.

The model is expected to capture the range of possible values, and to provide insights into the problems that may need to be addressed to define better the likely emissions of an oil shale industry. The model was refined for calculations supporting this chapter and a more detailed description of the model is underway.

Modeling Methods

The estimated release of CO₂ from natural gas fired power plants is based upon a value of 50.2 gCO₂/MJ (40), with an estimated uncertainty applied based on Boak (4). This value is in accord with the number for natural gas in Table 3, before adjustments to reflect the efficiency of the power plant. The calculations for this chapter assume an efficiency range from 40-55%, which allows for some understanding of the effect of power plant efficiency, including the potential for improvements in natural gas power plant efficiency. The quantity of electricity is very large, so electricity supply might be diversified, at least until production reaches levels justifying dedicated power plants. It would be valuable to develop a specific scenario that included both the energy efficiency and carbon output presuming some fraction of power comes from lower efficiency coal-fired power plants. No allocation was made of additional energy expended in maintaining the freeze wall to contain the local ground water. In this respect the model is non-

conservative. However, the model also did not consider the potential to preheat a block of rock using heat recovered from a previously heated block.

Boak (4) used the estimate of Burnham and McConaghy (41) for the amount of energy required to retort oil shale of (87-124 kWh/t) in the range from 300-400°C. This range is somewhat lower than in Table 2, in part, because it does not include energy to dry the shale. The values shown in this chapter were calculated from a baseline value for the mineral content (323.5 MJ/t) and adjusted for water content (27 MJ/t per weight percent water) and kerogen content (4.345MJ/t for each FA yield increase of 1 gallon/ton). Release of CO₂ from mineral reactions in the oil shale was estimated by presuming that any trace of nahcolite present in the rock would break down at temperatures below about 150°C (42) in accordance with reaction 8 from Table 1. Results from LLNL (30, 43) provide data on the amount of nahcolite present in the Mahogany zone of the Green River Formation. The average value is 0.8 wt %, in agreement with Figure 1. The range of values sampled is fairly large, so that the calculation may be somewhat representative of quantities of CO₂ released near heaters, where other carbonates may break down.

Additional CO₂ is released from the kerogen. Kerogen from the Mahogany zone of the Green River formation is estimated to contain 5.75 wt % oxygen on average, whereas shale oil contains 1.2 to 1.8 wt % (44). At the point at which the model was run, no information was available on the fraction of oxygen that might form CO₂ during in situ pyrolysis. So a mean value of 50% with a standard deviation of 15% was assigned. The value cited above of 4.1% of kerogen as CO₂ represents about 51% of the oxygen content of GRF kerogen.

Values for the amount of oil and gas produced were derived from results for Shell's in situ experiments, reported by Vinegar (45). Boak (4) assumed that an average of 78% of FA was removed from the rock as oil, and that gas was removed at an energy equivalent 30% of Fischer Assay oil. The average FA value for the entire industrial production was derived from average Fischer Assay values over the entire Green River Formation from 200 wells assembled by Y. Bartov at the Colorado School of Mines. All Fischer Assay data are tabulated by the U. S. Geological Survey. The Fischer Assay data were related to kerogen content based upon the relationship shown in Baughman (44), Figure 10. For the calculations shown here, the oil recovery was reduced, based upon personal communication with Shell personnel suggesting that, due to outward migration of a portion of the liquids, recovery is reduced to about 55-60% of FA yield. (These yields are likely lower than commercial yields due to the high surface-area-to-volume ratio in the small ICP tests.)

The model calculates oil and gas production from organic matter content and expected process efficiency. It calculates CO₂ both as tons/year and as SCF/day, which allows comparison to global CO₂ figures, but also allows comparison of the size of gas operations for production and separation.

Results

Results of the model are shown in Figures 3 through 8. The quantity of CO₂ generated annually varies by a factor of about eight from about 118 Mt (130 M

ton) to one simulation (of 1000 runs) above 363 Mt (400 M ton). See Figure 3, which shows this distribution (probability units are fraction of runs that achieve the plotted value). The modal, median and mean are all in the vicinity of 190 Mt (210 M tons). The cumulative distribution of values is shown in Figure 4, which indicates that the probability of exceeding 225 Mt is less than 10%.

Figure 5 shows the fraction of the CO₂ produced by the power plant, which is greater than 90% at the midpoint of the range. The values for CO₂ generated from breakdown of trace nahcolite and kerogen pyrolysis may include values that are higher than is likely for an entire operating industry. As a consequence, revision of the model to more accurately reflect these fractions may well shift the distribution toward higher fractions coming from the power plant. This change could reduce the total quantity of CO₂ produced by in situ conversion.

Figure 6 shows the result of a sensitivity analysis of the outcome for total CO₂ production. It illustrates the importance of the various input parameters to the uncertainty in the output. The most significant variable is the Shale Oil Production Efficiency, the fraction of the Fischer Assay value recovered by the process. Experimental refinement of this value will be essential to better understanding of the CO₂ emissions.

Figure 7 shows the relationship between Fischer Assay (which is linearly related to the kerogen content, but provides a more familiar measure of oil shale richness). It indicates that, although the emission rates are around 350 Mt for one or two simulations, the bulk of the values lie between 135 and 250 Mt per year. The mean value of FA in the sampling distribution is ~100 l/t (~24 gallons/ton), which better represents the grade of oil shale that the industry will produce from in the GRF for many years. The efficiency of the power plant generating the electricity for the downhole heaters is also important to the uncertainty of the emission estimate.

Nahcolite decomposition and kerogen pyrolysis, although a minor fraction of the total CO₂ produced, can affect the quality of the gas produced. Figure 8 shows the relationship of CO₂ fraction in produced gas to the quantity of nahcolite and to the fraction of the kerogen oxygen that combines with carbon to make CO₂. The figure also shows the mean value assumed for each of the underlying parameters. Very few simulation results that have gas fractions of CO₂ greater than 0.10 result from below average fractions of one or the other (or both) of these two parameters. Even for values below one weight percent nahcolite, the fraction of CO₂ can be remarkably high. One other parameter, the kerogen content, is important to this result. Higher kerogen content provides a larger oxygen content to be converted.

The low temperature breakdown of nahcolite could result in an early pulse of CO₂-rich gas, which is unlikely to be a significant problem, as heating of the rock is uneven, which would provide mixing of this pulse. Higher temperature reactions (such as decomposition of dolomite) could be a problem at remarkably low levels of reaction. This is because they form a much larger fraction of the mineral matter. These reactions may occur during in situ retorting, but only in the local environment near heater wells where temperatures could reach high levels. The production of other gases from mineral or organic matter is a possibility, which could dilute the CO₂ concentration in retort gas, which will affect the costs and prospects of capturing this CO₂ source for sequestration.

The quantities of CO₂ expected to be emitted by an oil shale industry are very large. A value of 190 Mt of CO₂ for an output of 3 Mbbl/d is equivalent to 0.17 tCO₂ per barrel of crude shale oil produced, or 1.09 gCO₂/l. Assuming that the oil from this industry has the energy density of the 36 °API raw crude oil produced in Shell's in situ retorting tests, this equals 28.6 gCO₂/MJ of raw shale oil. Low and high bounding estimates derived from the cumulative probability distribution in Figure 4 (10% and 90% probabilities) result in emissions of 24.7 – 34.1 gCO₂/MJ of raw shale oil produced.

Comparison of Full-Fuel-Cycle Carbon Dioxide Emissions Estimates

Estimates of CO₂ emissions from oil shale retorting processes have been presented in the literature and in reports produced by oil shale producers. Here we convert these estimates to common terms and compare them to estimates of CO₂ emissions from conventional petroleum production and bitumen extraction and upgrading from the Athabasca tar sands.

In order to compare the estimates accurately, each was adjusted to consistent system boundaries and output products. For all cycles, we assume the end product is reformulated gasoline (U.S. Federal standard), upgraded and refined as described above. For each estimate, if a given process stage is not included, we use the default values for conventional petroleum refined to reformulated gasoline from the GREET fuel cycle model (46). For example, most of these estimates do not include transport of the reformulated gasoline from the refinery to the end consumer, so we add the default value of 0.45 gCO₂eq/MJ from the GREET model.

For ex situ retorting processes, we include two estimates of emissions from shales retorted in the Alberta Taciuk Processor (ATP), as compiled for environmental impact assessments by the project operators Southern Pacific Petroleum (SPP) and Oil Shale Exploration Company (OSEC) (25, 26). For comparison to the ATP results, we provide an estimate from the literature for a generic hot recycled solids (HRS) retort, of which the ATP is a specific type (8). For in situ retorting, we include two estimates of emissions from a low temperature in situ retorting process (Shell's ICP technology) (6), and one estimate of emissions from a modified in situ (MIS) retort (8). Lastly, we present a range of emissions generated from Boak's cumulative probability distribution (Figure 4), with the base case being the mean case discussed above (emissions equal to 190 Mt/y), and the error bars representing the 10% - 90% confidence interval. Because Boak focused on upstream emissions, we add upgrading, refining, transport and combustion emissions equal to the average of Brandt's low and high ICP cases. These estimates are plotted below in Figure 9. Note that the range of emissions presented is significant, from just over 100 gCO₂/MJ RFD to as high as 160 gCO₂/MJ RFD.

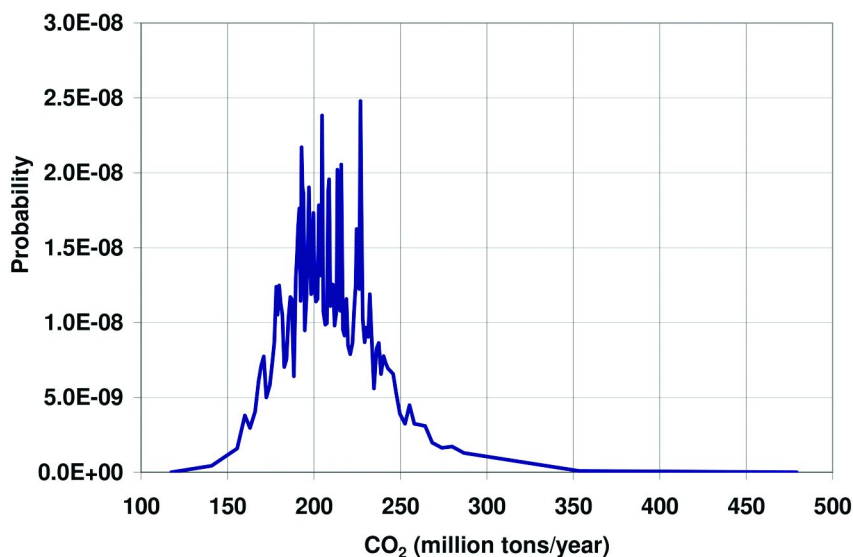


Figure 3. Annual CO_2 generation from oil shale production. To convert to Mt, multiply by 0.907.

It is instructive to compare these emissions to other estimates from the literature:

1. estimates of emissions from tar sands mining, upgrading, and refining, which range from 96 to 101 gCO_2/MJ RFD (also for reformulated gasoline) (47).
2. estimates of emissions from tar sands in situ production (SAGD), upgrading and refining, which range from 100 to 111 gCO_2/MJ RFD for reformulated gasoline (47).
3. an estimate of emissions from conventional petroleum extraction and refining, which is 86 gCO_2/MJ RFD for reformulated gasoline production (46).

Given the uncertainties involved and the large range shown in Figure 9, a reasonable estimate of the emissions range is between 1.25 to 1.75 times those from conventional oil. These emissions are generally equal to or greater than those from oil sands production. In a future of low conventional oil availability, it is likely that the marginal hydrocarbon resource will be tar sands. If for this reason tar sands emissions are used as the basis for comparison, then oil shale will have a comparatively smaller emissions penalty. However, there is a strong desire to replace conventional petroleum with fuels that are less GHG intensive, thus we use conventional petroleum as the basis for comparison.

Of importance is that the highest emissions (from MIS retorting) are approximately 1.9 times the full-fuel cycle emissions from conventional reformulated gasoline production. But these high-carbon retorting systems (e.g., MIS retorting) are unlikely to be adopted: they would be very difficult to justify under carbon regulation, and at this time, this technology does not appear to be under consideration anywhere in the world. Importantly, there are a number of ways of reducing this CO_2 emissions penalty by a factor of two or more by using a variety of methods described below.

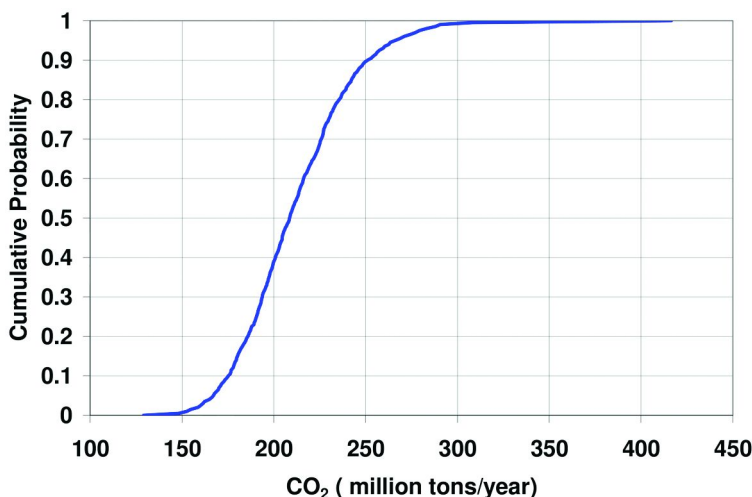


Figure 4. Cumulative probability plot for CO₂ release. To convert to Mt, multiply by 0.907.

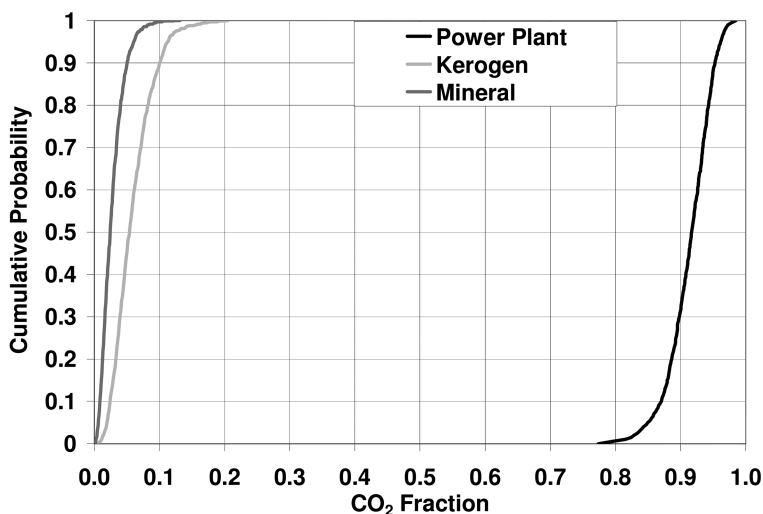


Figure 5. Fraction of CO₂ produced by the power plant, nahcolite mineral breakdown, and kerogen pyrolysis

Mitigation of Carbon Dioxide Emissions

Boak's (4) industry-scale model described above (using gas-fired electric power) provides a central estimate of 190 Mt of CO₂ emitted per year from a 3 Mbbl/d in situ oil shale industry. United Nations data on CO₂ emissions by country for 2004 (48) show roughly comparable values: emissions from Saudi Arabia are approximately 300 Mt, and emissions from Thailand and Turkey are on order 200 Mt. Thus, a large oil shale industry in western Colorado would be a

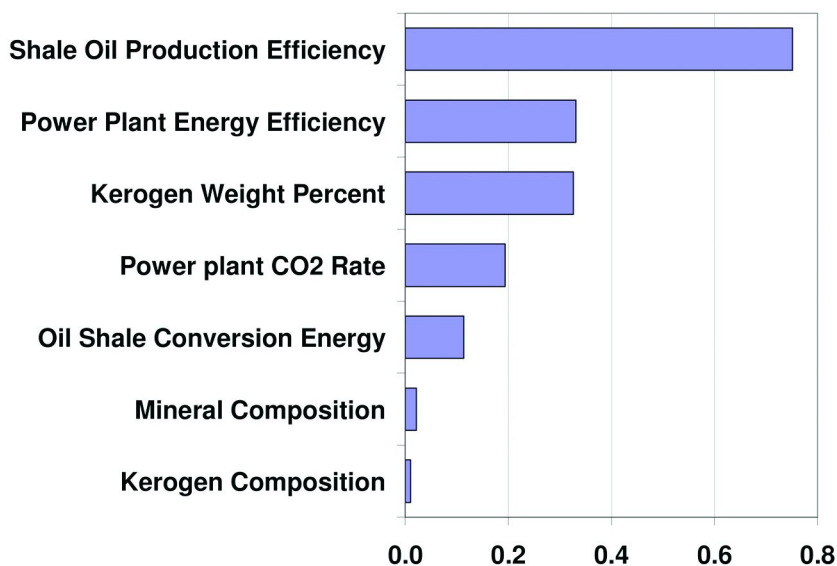


Figure 6. Importance of variables to CO_2 produced by oil shale

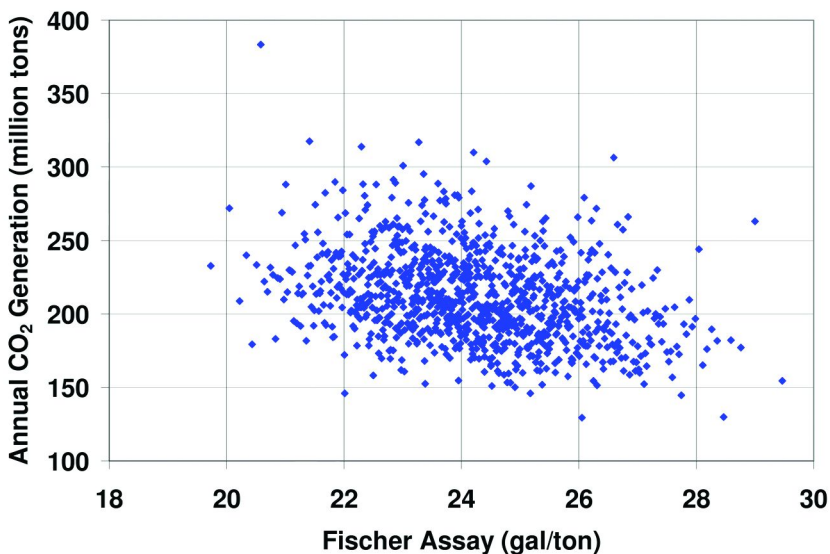


Figure 7. CO_2 produced as a function of average Fischer Assay of oil shale.
To convert to Mt, multiply by 0.907.

major global emitter. As another point of comparison, carbon dioxide emissions from flaring of stranded gas associated with oil production are reported to be approximately 400 million tons (49).

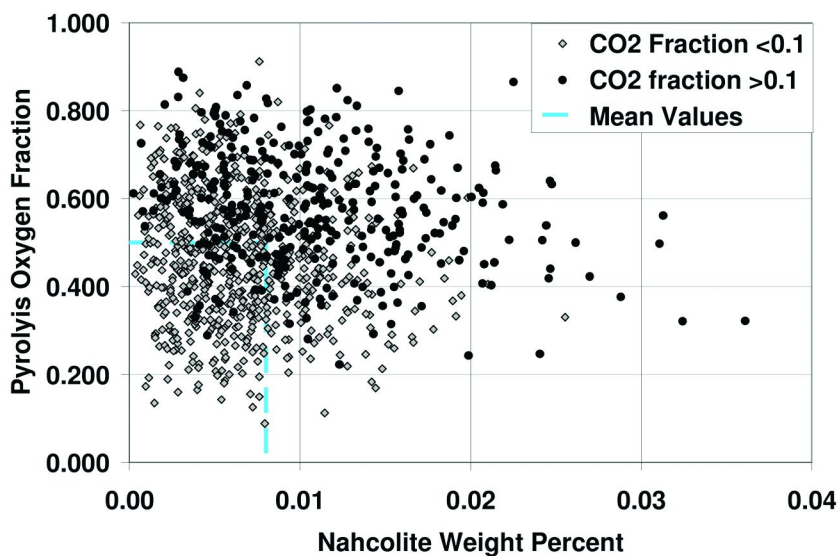


Figure 8. The fraction of oxygen removed from kerogen as CO₂ plotted against nahcolite weight fraction. Individual points reflect sampling of the range of uncertain parameters, and the symbols distinguish samples for which the resulting CO₂ fraction in the gas is less than or greater than 0.1.

Given the potential scale of emissions, it is clear that mitigation of CO₂ emissions from oil shale development will be needed to comply with any future CO₂ regulation.

Methods of Mitigating Emissions

A variety of methods exist to mitigate CO₂ emissions from oil shale extraction. These include substitution of low-carbon primary energy sources, heat recovery and efficiency improvements, low temperature retorting to avoid carbonate mineral decomposition, and capturing and sequestering carbon emissions from retorts

The primary opportunity for reducing CO₂ emissions from oil shale retorting lies in the substitution of low- or zero-carbon energy sources for high carbon sources. Using the carbon intensities from Table 3, this clearly means avoiding the use of coal and shale char for process heat and encouraging usage of natural gas or co-produced HC gases. Substitution of natural gas for coal or char will nearly halve the carbon burden of retorting. For example, in Boak's industry-scale model described above, if all power were generated from the newest high efficiency gas turbines, it could reduce the emissions from the values presented here, perhaps by 10-15 percent. Even more radical reductions could be achieved through the use of near-zero GHG sources such as off-peak wind power (50), nuclear power (51) or solar power (52, 53) for retorting heat requirements. Replacing the retorting heat source with a near-zero-carbon energy source would bring emissions from

oil shale-derived fuels quite near to those from conventional oil production, as the CO₂ generation from mineral and kerogen reactions is less than 10% of the total.

These low-carbon energy resources tend to be more costly than the approximately free (shale char) or inexpensive (coal) high carbon energy carriers. This cost differential is the reason that less attention has focused on these energy sources in the past. But the future imposition of carbon regulation could significantly change the economics of fuel switching by rendering traditional high-carbon energy sources more expensive.

Another improvement might be made by switching from an electricity-based process to a thermal process. Depending on the depth of the resource and the need to protect aquifers, generation of thermal energy on the surface and sending it down into the formation, e.g., as proposed by EGL (54) and Petroprobe (55) could improve thermal efficiency. Even better, downhole generation of heat, as proposed by both Shell and EGL (56), could reduce the CO₂ emissions from retorting by about a factor of two from the gas-fired electricity case examined in the probabilistic model.

Improving heat recovery or reducing process heat losses will also result in lower emissions. These strategies are already practiced in existing retorting processes, due to the simple fact that they reduce operating costs. For example, in the ATP retort, countercurrent flow of hot spent shale preheats the incoming shale, driving off moisture and raising the shale to $\approx 250^{\circ}\text{C}$ before it enters the retort zone (57). In the case of in situ retorting, it might be economically feasible to recycle heat from a spent region to another region undergoing retorting. This could significantly reduce the energy requirements of retorting.

Efficiency improvements often involve reducing the heat losses through the boundary of the retorting zone. In the ATP retort, early patents noted that heat losses through the retort shell amounted to 20% of the thermal energy input ((20), *column 19*), whereas in more modern incarnations of the ATP, heat losses through the shell have been reduced to 5-10% of the total demand (58). In the case of in situ retorting, increasing the size of the retorting region significantly reduces heat lost to over- and under-burden and the perimeter shale. Reducing these losses can significantly reduce the thermal demand and therefore the carbon emissions. The feasibility of this approach is limited by the economic risk involved with greatly increasing the scale of investment. (For example, an in situ operation spanning multiple km² would have negligible heat losses, saving large amounts of energy. However, the economic risk of such large investments would likely be prohibitive.) Other obvious efficiency improvements can result from reducing the waste associated with heat generation, as in switching from electricity to natural gas burned in down-hole burners for in situ processing. Such a change would eliminate the waste of $\approx 50\%$ of the energy content of the natural gas, which occurs in even the most efficient power generation system.

Another method of reducing carbon emissions is to reduce the temperature achieved by shales that contain significant amounts of carbonate minerals. This can be done by retorting the shale slowly (e.g., in a conductive in situ retorting scheme) or by avoiding shale char as an energy source. Using shale char as the energy source involves combusting spent shale at temperatures where significant carbonate decomposition can occur (see Table 1). Even using spent shale simply

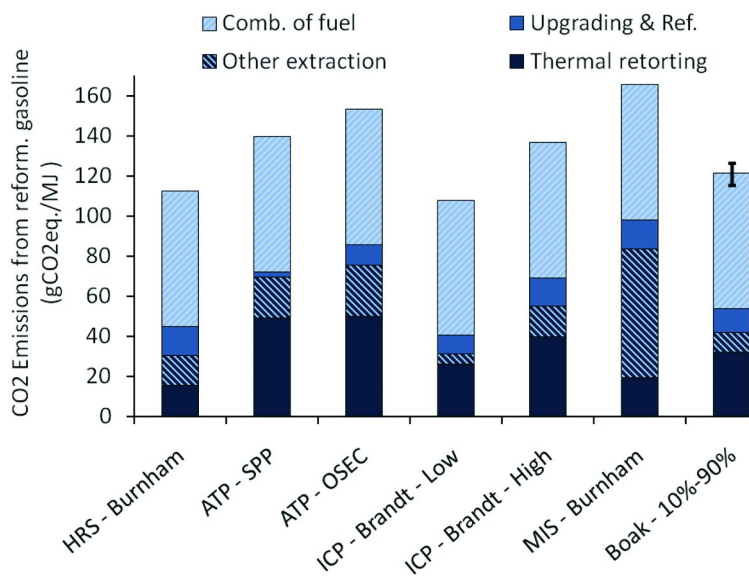


Figure 9. Estimates of CO₂ emissions from oil shale production processes. See text for sources.

as a heat carrier (e.g., heated with external combustion of natural gas) can result in the heating of carbonate minerals numerous times due to the recycling of spent shale through the retort zone.

Lastly, the CO₂ emissions from shale retorting could be captured and stored in geologic formations (36). This solution is generally capital and energy intensive, and will likely be considered after the other options addressed above. Capture is most effective and least costly when it is applied to a concentrated CO₂ stream. This reduces the cost of separating CO₂ from exhaust gases at diffuse concentrations (36).

A clear low-cost opportunity for capturing of concentrated CO₂ streams in oil shale retorting is from H₂ manufacture for upgrading. H₂ manufacture via steam methane reforming is readily adaptable to CO₂ capture, as the exhaust stream is already a CO₂-rich mixture (36). Concentrated CO₂ could also be captured at relatively low cost from pyrolysis gas, as the volume fraction of CO₂ can be quite high. A longer-term option for producing concentrated CO₂ streams is oxygen combustion, which removes the diluting N₂ before combustion rather than after combustion. The options for non-concentrated CO₂ capture include the emissions from power generation for oil shale retorting, such as from a natural gas combined cycle plant. This is a very large source, which will be critical to capture or eliminate. The more diffuse exhaust stream in power generation makes capture more difficult and costly. The cost of capturing CO₂ from a new hydrogen plant is estimated at 12 \$/tCO₂, which can be compared to 44 \$/tCO₂ for a new natural gas combined cycle plant ((36), Table 8.1). (These are 2002 dollars. These estimates are deemed representative values, with ranges of 2-39 \$/tCO₂ for the hydrogen plant and 33-57 \$/tCO₂ for the NGCC plant.)

Conclusions

The CO₂ emissions from oil shale production are dependent on properties of both the shale itself and the retorting process used. Important shale properties include the fraction organic matter, the mineral makeup of the shale, and the raw shale moisture content. The key retorting properties affecting CO₂ emissions are the retorting temperature and residence time, as well as the amount of heat recovery from spent shale.

The industry-scale model of CO₂ emissions described here is intended to highlight the value of transparent, mechanistic and probabilistic modeling tools to estimate the potential emissions and to define the most significant parameters. This will focus research efforts by allowing improvements to those model components that are most likely to affect the outcome. Further refinement of this model and consideration of more types of processes is necessary to more accurately reflect the expected CO₂ release from an in situ oil shale industry.

This simple model suggests that the dominant CO₂ source would most likely be power plant emissions for the particular in-situ process considered. It is important to better define sources of CO₂ from underground, both organic and mineral in nature, for a wider range of processing conditions.

Collected estimates from a variety of sources, based on both operating data and models of production processes, suggest that, without mitigation, full-fuel-cycle emissions from the production, refining, and consumption of refined fuels from oil shale (in this case reformulated gasoline) will result in CO₂ emissions that are approximately 1.25 to 1.75 times those from conventional petroleum production.

These baseline emissions can be lowered with a variety of mitigation options, including fuel switching, efficiency improvements, and carbon capture and sequestration. As many of these mitigation technologies are untried, there is still uncertainty about which option will be most cost effective. But, there is little doubt that CO₂ mitigation from oil shale production will be required if greenhouse gas regulations become binding.

References

1. Dyni, J. R. *Geology and Resources of Some World Oil-Shale Deposits*; 2005-5294; US Geological Survey: Reston, Virginia, 2006; p 42.
2. Boak, J. *Proceedings of the 26th Oil Shale Symposium*; Colorado Energy Research Institute Document 2007-3; Colorado School of Mines: Golden, CO, 2007.
3. Sundquist, E. T.; Miller, G. A. Oil shales and carbon dioxide. *Science* **1980**, *208* (4445), 740–741.
4. Boak, J. *CO₂ Release from In-Situ Production of Shale Oil from the Green River Formation in the Western United States*, 27th Oil Shale Symposium, Colorado Energy Research Institute Document 2008-1; Boak, J., Ed.; Colorado School of Mines: Golden, CO, 2008.

- Brandt, A. R. *Comparing the Alberta Taciuk Processor and the Shell In Situ Conversion Process - Energy Inputs and Greenhouse Gas Emissions*, 27th Oil Shale Symposium, Colorado Energy Research Institute Document 2008-1; Boak, J., Ed.; Colorado School of Mines: Golden CO, 2008.
- Brandt, A. R. Converting oil shale to liquid fuels: Energy inputs and greenhouse gas emissions of the shell in situ conversion process. *Environ. Sci. Technol.* **2008**, *42* (19), 7489–7495.
- Burnham, A. K.; Carroll, S. *CO₂ Sequestration in Spent Oil Shale Retorts*. 28th Oil Shale Symposium, Colorado Energy Research Institute Document 2009-2; Boak, J., Ed.; Colorado School of Mines, Golden CO, 2009.
- Burnham, A. K.; McConaghy, J. R. *Comparison of the Acceptability of Various Oil Shale Processes*; UCRL-CONF-226717; Lawrence Livermore National Laboratory: Livermore, CA, 2006.
- Friedmann, S. J. In *In-Situ Oil-Shale Recovery, Carbon Capture and Storage, and the Importance of Large Projects*, 26th Oil Shale Symposium, Colorado Energy Research Institute Document 2007-3; Colorado School of Mines, Golden CO, Boak, J., Ed. 2007.
- Hatfield, K. E.; Smoot, L. D.; Coates, R. L. *Near-Zero CO₂ Emissions from the Clean, Shale-Oil Surface (C-SOS) Process*, 28th Oil Shale Symposium, Colorado School of Mines, 2008.
- Hendrickson, T. A. *Synthetic Fuels Data Handbook*; Cameron Engineers, Inc.: 1975.
- Lee, S.; Speight, J. G.; Loyalka, S. *Handbook of Alternative Fuel Technologies*; CRC Press: Boca Raton, FL, 2008.
- Camp, D. W., *Oil Shale Heat Capacity Relations and Heats of Pyrolysis and Dehydration*, Twentieth Oil Shale Symposium, Gary, J. H., Ed.; Colorado School of Mines Press: Colorado School of Mines, 1987; pp 130–144.
- Burnham, A. K. *Chemical Kinetics and Oil Shale Process Design*; UCRL-JC-114129; Lawrence Livermore National Laboratory: Livermore, CA, July, 1993.
- Mraw, S. C.; Keweshan, C. F. Calorimetric determination of the heat of retorting oil shales to 773 K. *Fuel* **1986**, *65* (1), 54–57.
- Campbell, J. H. *The Kinetics of Decomposition of Colorado Oil Shale II: Carbonate Minerals*; Lawrence Livermore National Laboratory: Livermore, CA, March 13, 1978.
- Burnham, A. K.; Kirkman Bey, N.; Koskinas, G. J., Hydrogen Sulfide Evolution from Colorado Oil Shale. In *Oil Shale, Tar Sands, and Related Materials*; Stauffer, H. C., Ed.; American Chemical Society: 1980.
- Burnham, A. K.; Taylor, R. W. *Occurrence and Reactions of Oil Shale Sulfur*; UCRL-87052; Lawrence Livermore National Laboratory: Livermore, CA, 1982.
- Thorsness, C. B. *Modeling Study of Carbonate Decomposition in LLNL's 4TU Pilot Oil Shale Retort*; Lawrence Livermore National Laboratory: Livermore, CA, October 14, 1994.
- Taciuk, W.; Caple, R.; Goodwin, S.; Taciuk, G. Dry Thermal Processor. U.S. Patent 5217578, 1993.

21. Speight, J. G. *Fuel Science and Technology Handbook*; Marcel Dekker: New York, 1990.
22. *Carbon Emissions Factors - per Quadrillion (10¹⁵) BTU*; Energy Information Administration: Washington, DC, accessed March, 2009.
23. Huss, E. B.; Burnham, A. K. Gas evolution during pyrolysis of various Colorado oil shales. *Fuel* **1981**, *61*, 1188–1196; December.
24. *Electric Power Annual 2007*; Energy Information Administration: Washington, DC, 2009.
25. *Oil Shale Research, Development (OSEC), and Demonstration Project: White River Mine, Uintah County, Utah*; Oil Sands Exploration Company and U.S. Department of the Interior, Bureau of Land Management, Vernal field office: Vernal Utah, September 18, 2006.
26. *Stuart Oil Shale Project - Stage 2 Consolidated Report*; SPP, Queensland Government, Department of Infrastructure and Planning: November, 2003.
27. Stanfield, K. E. *Properties of Colorado Oil Shale*; U.S. Bureau of Mines: 1951.
28. Campbell, J. H.; Gallegos, G.; Gregg, G. Gas evolution during oil shale pyrolysis 2: Kinetic and stoichiometric analysis. *Fuel* **1980**, *59*, 727–732; October.
29. *Good Practice Guidance and Uncertainty Management in National Greenhouse Gas Inventories*; IPCC XVI/Doc. 10 (1.IV.2000); Intergovernmental Panel on Climate Change (IPCC): Montreal, May, 2000.
30. Singleton, M. F.; Koskinas, G. H.; Burnham, A. K.; Ralyey, J. H. *Assay Products from Green River Oil Shale*; UCRL-53272, Rev. 1; Lawrence Livermore National Laboratory: Livermore, CA, February 18, 1986.
31. Jukkola, E. E.; Denilauler, A. J.; Jensen, H. B.; Barnet, W. I.; Murphy, W. I. R. Thermal decomposition rates of carbonates in oil shale. *Ind. Eng. Chem.* **1953**, *45* (12), 2711–2714.
32. Probst, R. F.; Hicks, R. E. *Synthetic Fuels*; Dover Publications: Mineola, NY, 2006.
33. Speight, J. G. *Synthetic Fuels Handbook: Properties, Process, and Performance*; McGraw Hill: New York, 2008.
34. Berchenko, I.; Rouffignac, E. P.; Fowler, T. D.; Karanikas, J. M.; Ryan, R. C.; Shahin, G. T.; Stegemeier, G. L.; Vinegar, H. J.; Wellington, S. L.; Zhang, E. *In Situ Thermal Processing of an Oil Shale Formation Using a Pattern of Heat Sources*; 6991032 B2; Shell Oil Company: 2006.
35. Johnson, H. R.; Crawford, P. M.; Bunger, J. W. *Strategic Significance of America's Oil Shale Resource: Volume II - Oil Shale Resources, Technology and Economics*; AOC Petroleum Support Services, LLC: Washington, DC, March, 2004.
36. IPCC, *Special Report on Carbon Dioxide Capture and Storage*; Cambridge University Press: Cambridge, UK, 2005.
37. Wang, M. Q. *Estimation of Energy Efficiencies of U.S. Petroleum Refineries*; Center for Transportation Research, Argonne National Laboratory: Argonne, IL, March, 2008.
38. Wang, M.; Lee, H.; Molburg, J. Allocation of energy use in petroleum refineries to petroleum products - Implications for life-cycle energy use and

- emission inventory of petroleum transportation fuels. *Int. J. Life Cycle Assess.* **2004**, *9* (1), 34–44.
39. *ISO 14044: Environmental Management - Life Cycle Assessment - Requirements and Guidelines*; ISO: Geneva, 2006.
 40. *Natural Gas 1998 - Issues and Trends*; Energy Information Administration (EIA): Washington, DC, 1999.
 41. Burnham, A. K.; McConaghy, J. R. *Comparison of the Acceptability of Various Oil Shale Processes*, Colorado Energy Research Institute Document 2007-3; 26th Oil Shale Symposium, Golden CO, 2007, .
 42. Yamada, S.; Koga, N. Kinetics of the thermal decomposition of sodium hydrogencarbonate evaluated by controlled rate evolved gas analysis coupled with thermogravimetry. *Thermochim. Acta* **2005**, *431*, 38–43.
 43. Campbell, J. H. *Modified In Situ Retorting: Results from LLNL Pilot Retorting Experiments*; Lawrence Livermore National Laboratory: Livermore, CA, 1981.
 44. Baughman, G. L. *Synthetic Fuels Data Handbook* 2nd ed.; Cameron Engineers: Denver, CO, 1981.
 45. Vinegar, H., *Shell's In-situ Conversion Process*, 26th Oil Shale Symposium, Colorado Energy Research Institute Document 2007-3; Boak, J., Ed.; Colorado School of Mines: Golden CO, 2007.
 46. Wang, M. Q. *GREET Model 1.8b*; Argonne National Laboratory: 2008; available from <http://www.transportation.anl.gov/software/GREET/>.
 47. Charpentier, A. D.; Bergerson, J.; MacLean, H. L. Understanding the Canadian oil sands industry's greenhouse gas emissions. *Environ. Res. Lett.* **2009**, *4* (014005), 14.
 48. Wikipedia List of Countries by Carbon Dioxide Emissions. http://en.wikipedia.org/wiki/List_of_countries_by_carbon_dioxide_emissions.
 49. Elvidge, C. D.; Erwin, E. H.; Baugh, K. E.; Tuttle, B. T.; Howard, A. T.; Pack, D. W.; Milesi, C. Satellite data estimate worldwide flared gas volumes. *Oil Gas J.* **2007**, 50–58; November 12.
 50. Bridges, J. E. Wind power energy storage for in situ shale oil recovery with minimal CO₂ emissions. *IEEE Trans. Energy Conversions* **2007**, *22* (1), 103–109.
 51. Forsberg, C. Nuclear energy for a low-carbon-dioxide-emission transportation system with liquid fuels. *Nucl. Technol.* **2008**, *164*, 348–367; December.
 52. Berger, R.; Fletcher, E. A. Extracting oil from shale using solar energy. *Energy* **1988**, *13* (1), 13–23.
 53. Burnham, A. K. On solar thermal processing and retorting of oil shale. *Energy* **1989**, *14* (10), 667–674.
 54. Lerwick, P.; Vawter, G.; Day, R.; Harris, H. G. *The EGL Oil Shale Process*, 26th Oil Shale Symposium Colorado Energy Research Institute Document 2007-3; Boak, J., Ed.; Colorado School of Mines: Golden CO, 2007, .
 55. *Secure Fuels from Domestic Resources: The Continuing Evolution of America's Oil Shale and Tar Sands Industries*; U.S. Department of Energy (DOE), Office of Petroleum Reserves, Office of Naval Petroleum and Oil Shale Reserves: Washington, DC, June, 2007.

56. Day, R.; Lerwick, P.; Burnham, A. K.; Vawter, G.; Wallman, H.; Harris, G.; Hardy, M., *The EGL Oil Shale Project*, 27th Oil Shale Symposium, Colorado Energy Research Institute Document 2008-1; Boak, J., Ed.; Colorado School of Mines: Golden, CO, 2008.
57. Brandt, A. R. *Converting Green River Oil Shale to Synthetic Crude Oil with the ATP Retort: Energy Inputs and Greenhouse Gas Emissions*; Energy and Resources Group, University of California: Berkeley, CA, June 1, 2007.
58. Rojek, L. Personal communication with L. Rojek regarding ATP reactor; September, 2008.

Chapter 12

A Review of Activities To Address the Environmental Impacts of Oil Shale Development

David K. Olsen,^{*,1} Arthur Hartstein,² and David R. Alleman³

¹International Centre Heavy Hydrocarbons, Bartlesville, Oklahoma 74006

²Technical and Management Service, Arlington, Virginia 22209

³ALL Consulting, Tulsa, Oklahoma 74119

*dolsenoildrop@sbcglobal.net

The last two major increase in energy prices generated renewed interest in development of the huge United States (Colorado, Utah and Wyoming) Green River oil shale (kerogen) resource as a potential source of liquid transportation fuel. Today's oil shale environmental issues and needs facing developers nearly mirror those of the 1970's. Workshops to identify challenges were conducted in conjunction with the 26th (2006) and 27th (2007) Oil Shale Symposia at Colorado School of Mines. The workshops summaries and follow-on analysis point to the need for coordinated efforts such that problems are addressed in a timely manner and stakeholders benefit from best use of our abilities to predict future impact.

Introduction

Before a commercial oil shale industry is established in the United States (U.S.), technologies that are technically feasible, economically viable, and environmentally sound must be demonstrated to capture part of the estimated 2.5 trillion barrel resource. This chapter addresses the history and status of the environmental aspects of oil shale development. During the early 1970's at the inception of the last major interest in oil shale, The U.S. Department of Interior's (DOI) U.S. Geologic Survey (USGS) published a Programmatic Environmental Impact Statement (PEIS) (*I*). This PEIS permitted the USGS to

conduct a prototype lease sale that resulted in four leases being purchased, two in Colorado and two in Utah. The projects envisioned by the companies that won these leases as well those who chose to operate on private lands raised a series of environmental issues that were cited by local and state officials, as well as interested individuals as a reason to object to the commercialization of the oil shale resource.

In May of 1978 Governor Lamm of Colorado wrote to U.S. Department of Energy (DOE) Secretary Schlesinger requesting DOE assistance in the analysis of potential oil shale impacts. In his letter the Governor asked DOE “to assist Colorado by working with us in developing additional research and analyses of current and future efforts.” As a result, an environmental and health task force was created that planned for and managed an umbrella organization of oil shale researchers that included National Labs, Universities, and others. The DOE Oil Shale Task Force planned, implemented, and coordinated a comprehensive, integrated research program on the environmental and health impacts of oil shale production technologies. The program involved five major areas of activity: (1) source characterization, (2) health effects, (3) environmental fate and effects, (4) environmental control technology, and (5) integrated assessment. The Task Force included most of the organizations involved in the ongoing oil-shale related projects funded by DOE, cooperated with other research groups to minimize unnecessary duplication of R&D efforts, and worked closely with the private entities trying to develop a commercial industry. Results of the Task Force included the development of effective environmental control strategies and methods. With declining oil prices in the early 1980’s, companies started to close operations and abandon the nation’s commercial oil shale activity. In 1984 the Task Force was disbanded when the DOE funding for oil shale was drastically reduced.

Energy (oil) prices again rapidly increased in the first half of the 2000’s and once again the U.S. is on the brink of development of an oil shale industry and has restarted field R&D to test hypothesis and pilot recovery processes. As such, environmental issues are again being raised. The Energy Policy Act of 2005, Section 369, “Oil Shale, Tar Sands, and Other Strategic Unconventional Fuels” directed the DOI’s Bureau of Land Management (BLM) to lease government land in Colorado, Utah, and Wyoming for industry to conduct oil shale R&D, complete a PEIS for a commercial leasing program within 18 months, and then announce the commercial leasing program (2). As a consequence, BLM issued six R, D & D leases (five in Colorado and one in Utah). However, during the preparation of the PEIS (3) the BLM determined that it did not have, adequate information on the (a) magnitude of commercial development and pace of that development, (b) potential locations for commercial leases, (c) technologies that will be employed, (d) size or production level of individual commercial projects, and (e) development times for individual projects to support decisions about lease issuance. BLM noted that “Published information defining both oil shale and tar sands commercial development is dated (i.e., mostly dating back to the mid-1980s or earlier) and unlikely to accurately describe future commercial technologies.” Many times in the document BLM laments the lack of definitive information

about the environmental aspects of the technologies that will be employed in commercial operations.

Concurrently, the renewed interest in oil shale prompted the Colorado School of Mines (CSM) to resume the annual Oil Shale Symposium that had been suspended in 1992 at the conclusion of the 25th Symposium for lack of interest. This symposium remains the preeminent meeting of the oil shale community. In conjunction with the 26th (2006) and 27th (2007) Oil Shale Symposia the DOE, Colorado Energy Research Institute (CERI) and CSM hosted two one-day workshops addressing “Oil Shale Environmental Issues and Needs” following the Symposium. Summaries of these workshops are published on two different websites: 26th workshop at CSM (4) and 27th at DOE (5). The results of these workshops and follow-up discussions with attendees and the proceedings of previous Oil Shale Symposium (6) provide much of the basis for this chapter. As anticipated given the one-day duration of the workshops, topics, recommendations and priorities are general; require further refinement, prioritization and funding to address the environmental challenges voiced by participants.

With the exception of carbon dioxide (CO₂) emissions, the issues surrounding oil shale today mirror those of the 1970-80's during the last cycle, of what has historically been a very cyclic industry in the U.S. Many of the companies with an interest today in developing the resource are the same or are descendants of previous companies who operated in the 1970's. U.S. Government agencies with responsibility of management of the oil shale property have changed from DOE and DOI to DOI but DOE has an interest in that the resource is a national energy asset. DOE Office of Petroleum Reserves has published a brief history (7, 8), partial list (9) of players in oil shale and a series of publications on a roadmap for Federal agencies (10).

Oil Shale Environmental Issues and Needs

Many environmental topics of concern in the 1970's are the same today. However, today the world moves faster - communication is quicker, reaches a broader audience that responds quicker. Environmental science and supporting disciplines have made huge advances in detection limits and knowledge of system interaction. Regulations have become more stringent. The public is more active and environmentally contentious. Permitting has increased with more agencies, each with different regulations, standards, forms and reporting (no one-stop shop). Today's society is also more litigious, even after permits are issued. The population around the Green River oil shale deposit has dramatically increased and evolved since the 1970's from mostly ranching, farming, and energy extraction to include a significant segment that is retired or chooses living in the area because of its esthetics. Advances in technology, communication and transportation allow them earn a living in a rural area. An area that has been experiencing growth due to development of the regions other natural resources - natural gas and coal and the associated infrastructure to deliver these resources to meet the nations growing demand for energy.

Although the previous oil shale industry complied with the existing laws of the time, public perception and vocal adversaries often characterize the industry as non-compliant. Oil shale developers on private and government leases are required to satisfy National Environmental Policy Act (NEPA) requirements by developing environmental impact studies (EIS) or Environmental Assessments (EA) and then obtain appropriate permits for their project(s). EIS beyond their boundaries or impacts on basin wide or in combination with other developers, energy production, infrastructure development or development by other industries (recreation, tourism, housing, etc.) in the area or cumulative impacts are not required of the oil shale developer or of other industries beyond their site boundary. Therein lays the largest environmental issue and need – evaluation of the environmental issues and needs of the greater Green River Basin. This could be said of most areas of the U.S. where previous development has occurred without having done such analysis before industries located in an area.

The BLM recently conducted the first basin-wide PEIS in connection with oil shale and again the study indicated a need for answers to questions and relied on significant information from the 1970-80's with extrapolations to a large industry producing a million barrels of oil a day (BOPD) (3). Today's (2008), average annual oil production) for the entire U.S. petroleum industry is 4.955 million barrels oil per day (11).

Results of most of the environmental studies conducted during the 1970-80's are dispersed in regional libraries, government agency archives, company files and personal archives. Attempts are being made to collect, consolidate and electronically scan documents to help provide lasting copies and ready access. Most of the environmental findings of the 1970-80's remain sound. However, many of today's technologies envisioned for kerogen conversion and oil extraction are different; environmental rules and regulations are more stringent, and our understanding of environmental systems is more thorough.

Results of 2006 Environmental Issues and Needs Workshop (4)

The 57 workshop participants attending the 2006 workshop identified four environmental issues and needs areas: Water Quality and Quantity, Air Quality Impact, Surface and Ecosystem Impact, and Social and Economic Impact. Each breakout group identified a set of challenges facing industry, government, and communities in the affected areas. Groups attempted to classify those challenges as being near-term (needing to be addressed by 2010), mid-term (by 2015), or long term (beyond 2020). Groups were also charged with identifying whether issues were specific to an oil shale industry focused on surface retorting or on *in-situ* processing of the shale, or were issues common to both. Two break-out groups identified whether the critical actions were appropriately assigned to government, industry, or both, and one group assigned a priority to the required action (4). A brief summary is described below:

Water Quality and Quantity

Water or the perceived lack of water in the Colorado River Basin due to multiple uses and growing number of users downstream, for municipalities on the eastern slope of Colorado and the unknown impact of water consumed and water quality due to oil shale development is the highest concern for local residents and the broader population downstream. As the current oil shale projects are R&D projects, that will require a decade of investment and optimization in order to determine their water requirements, quantification of the impact but the impacts can be broad bracketed.

Air Quality Impact

During some periods of the year, some designated pollutants currently exceed established limits due to emissions from naturally occurring flora (sage brush, etc.), dust, emissions from vehicles along interstate highway I-70, agricultural burning, emissions from states west of the Green River Basin, and energy production within the Basin. Production of oil and gas from future oil shale development within the Green River Basin is energy intensive. Current emissions combined with unknown energy demand (from an oil shale industry that is at the R&D stage) and associated development of other entities including communities prompt establishment of baseline monitoring systems, and development of basin wide air models. Having compatible models that can yield usable information to local, state and federal regulators is very important.

The impact of legislation on CO₂ emissions and their cost to the end user are unknown. The potential for CO₂ geosequestration in oil reservoirs such as Rangely Field, Colorado, where a CO₂ enhanced oil recovery (EOR) project has been operating for the last 20 years is but one option. Saline reservoirs, depleted insitu oil shale strata and other oil fields are additional potential CO₂ sinks.

Studies by local and state entities on air quality and the impact of existing and potential future growth and energy needs have been and are being conducted. Monitoring of emissions provide a baseline that is always changing as emission sources grow both within the Basin and from areas upwind of the Basin.

Surface and Ecosystem Impact

The impact on roadways from greater traffic, larger communities, and higher energy use to support families in these communities are in addition to the surface impact required for in-situ or surface processing of oil shale.

Spent shale from mining operations is of concern. However, twenty years of studies on surface disposal embankments is available from processes used at the time. Potential for commercial use of the spent shale remains unknown but may provide opportunity for new industries.

Ecosystems are dynamic and changes in human population and animal populations are anticipated. Quantification of impact, like many other

environmental factors associated with oil shale development is illusive. Establishing base lines at the present time can be compared to the numerous studies of baselines developed during oil shale development of the 1970-80's.

Social and Economic Impact

Oil shale and other energy development within the Basin, and other developments impact local, state and national economies. Impact at the local level remains a high priority, as local infrastructure (housing, schools, water, sewer, streets, etc.) to support workers and their families which rely upon taxes to provide part of these services. Upfront funding is needed but the current oil shale projects are R&D projects, with no guarantee of success. Severance taxes on federal leases provide a major source of local government revenue. Area residents are concerned that there may be another oil shale boom and bust cycle that again leaves them without jobs, declining housing assets and communities without funding to provide for services or debt repayment.

Results of 2007 Environmental Issues and Needs Workshop (5)

In general, the 50 participants at the 2007 workshop affirmed the results of the 2006 workshop in terms of the need for R&D related to oil shale environmental issues. Many stakeholders were the same or from the same organizations as the previous year but usually at a higher management level within their organization. To better focus efforts in a limited time, discussions of the social and economic impacts were omitted, although they are equally important. Participants prioritized (1= highest priority) the issues and needs as shown in Table 1.

Combined Result from 2006 and 2007 Workshops and Follow-up Analysis

Follow-up to the 27th (2007) Oil Shale Symposium (5, 6) by a short study of who was doing what on oil shale issues and needs around within greater Green River Basin (including studies from other energy and infrastructure development – coal, gas, etc.); what had recently been completed; and what was scheduled to be undertaken by authors. The results indicated a coordinated effort – a clearinghouse - was needed to help researchers better use their limited resources and help them become aware of parallel and often complementary efforts by others.

Certain crosscutting issues are evident from the workshops. The water, air, and ecosystem groups identified needs in (a) data collection and (b) model refinement/development and validation as high priority for their areas. Thus, it appears that, for water, air, and ecosystem issues, the groups considered (either explicitly or implicitly) the following steps that need to be taken:

- Define data and model requirements, as well as end users (regulators, etc.) needs
- Review existing data and models

Table 1. R&D Needs Prioritization Results

<i>Area</i>	<i>R&D Need</i>	<i>Overall Priority</i>
AIR	Develop protocol for basin/regional emissions monitoring	
AIR	Develop accurate, predictive regional models for release, fate and transport of emissions	2
AIR	Conduct process, resource- specific emissions research and evaluate best available cleanup technology (BACT)	8
AIR	Identify gaps, and conduct R&D to develop innovative technologies for reducing or controlling (capture/separation) emissions	5 - 6
AIR	Integrate and coordinate with CO ₂ regional partnerships (CO ₂ sources and sinks/markets) for development of a CO ₂ Management Plan	7
AIR	Assess life-cycle emissions under various development scenarios, including full suite of infrastructure requirements (that have yet to be determined)	
AIR	Specific regional assessment of potential CO ₂ end uses.	
WATER	Develop integrated basin/regional baseline for surface and groundwater data (including quality and quantity). Incorporate GIS-based analytical tools	1
WATER	Conduct process-specific research to evaluate generated contaminants and water consumption; evaluate BACT	3
WATER	Conduct R&D to develop new, low water consumption processes; cost-effective water treatment and improved water recycle/reuse options	9
WATER	Conduct R&D to characterize and assess potential spent shale leachate. Develop solutions.	
WATER	Assess water requirements and potential effluents for multi-site oil shale development in conjunction with other regional water use planning efforts for the development of a Water Resource Management Plan	
WATER	Perform a basin/regional climate variability/climate change assessment for water supply	
LAND	Spent shale characterization and R&D for alternative by-products from spent shale	5 - 6
LAND	Conduct research and analysis to reduce process/development foot print	10

- Identify data and modeling gaps
- Plan and conduct data gathering and model development/refinement
- Evaluate likely impacts in the various areas iteratively to refine the requirements, data and models

Each group identified particular issues requiring data gathering and evaluation. The water and air groups explicitly identified crosscutting issues relating to data management, advisory boards and technical team management, as well as policy development. There appears to be a consensus that coordinated data management will be important, and that a formal structure similar to that put in place in the Task Force of the 1970's - 80's would be valuable in coordinating

and integrating research on and evaluation of the potential impacts of oil shale development.

Although the social and economic impact group did not identify a similar range of needs for their area, it seems likely that at least a subset of the tasks defined in the preceding paragraphs and from the workshops (4, 5) may need to be evaluated. Both the social and economic impact groups and the subgroups looking at surface and ecosystem impacts, identified education and outreach as a priority issue. In the other areas, there were indications that these outreach activities may span the full range of impact evaluations to some degree. Most groups recognized that stakeholder involvement in environmental monitoring and review of data and models are important parts of outreach.

The activity might involve two complimentary thrusts:

- The first would be thoughtful examination and amplification of the products of this workshop by small groups knowledgeable in the areas.
- The second would be the review, modification and validation of the efforts of these smaller groups in similar Oil Shale Environmental Issues and Needs workshops.

Conclusions and Next Steps

A central theme of the workshops was that the development of the Green River oil shale resource should be evaluated in concert with the ongoing and future development of all natural resources Basin-wide. Thus, strategies to manage the environmental aspects of air, water, solid, and carbon should be addressed on a regional as well as site specific basis.

A second general theme was the idea that all purposes would be better served if information and data is shared publicly as much as possible, and some type of ground-truth set of data concerning the environmental baseline for air, land and water could be agreed to by all stakeholders as a point of departure for modeling and forecasting and would be beneficial to all.

There continues to be an expression of general support from the oil shale community for a Federal government role in helping to accomplish four important things:

- Facilitating communication among industry; local, state and federal regulators; local and state planning bodies; and other stakeholders.
- Providing funding and direction for a data gathering and regional systems modeling effort that can be used to help determine the costs and benefits of various resource development scenarios in a manner that takes into account the entire spectrum of land use options and recognizes the potential for and impacts of cumulative impacts.
- Facilitating the collection of a data set that all stakeholders can rely on as being objective and finding a way to make this data available to the largest possible number of users without raising intellectual property issues for technology developers.

- Facilitating the location, collection and dissemination of historical data and other information from the oil shale development during the 1970 - 80s, that could be useful in the modeling and analytical activity carried out by any and all stakeholders.

One possible way to accomplish these objectives would be to re-establish the Oil Shale Environmental Task Force. The previous Oil Shale Environmental Task Force, active from 1978 to 1984, managed an umbrella organization of oil shale researchers that included National Labs, universities, and others. The Task Force planned, implemented, and coordinated a comprehensive, integrated research program on the environmental and health impacts of oil shale production technologies. The program involved five major areas of activity: (a) source characterization, (b) health effects, (c) environmental fate and effects, (d) environmental control technology, and (e) integrated assessment. The Task Force included most of the organizations involved in the ongoing oil-shale related projects funded by the DOE, it cooperated with other research groups to minimize duplication of efforts, and it also worked closely with the private companies trying to develop a commercial industry.

This approach could be beneficial in that it would:

- Provide a framework for organizations to contribute data and expertise in a transparent and collaborative manner.
- Act as an aggregator of data and a developer of “bigger picture” regional/basin level assessments, work that no individual technology or resource developer has any economic motivation to pursue.
- Provide a mechanism for strengthening the interaction among state and local governments, the public, various federal agencies, the industry, environmental groups, and others interested in ensuring that any oil shale industry is developed in an environmentally sound manner.
- Assist the Office of Fossil Energy in the planning and analysis of research funded by the DOE, or by other government agencies.

The purpose of the Environmental Task Force would be to help plan and coordinate a comprehensive, integrated research program that will provide the effected states (initially Colorado and Utah), DOE, and other interested organizations and individuals with as complete an understanding as possible of the environmental and health consequences of oil shale recovery processes and of the alternative strategies for eliminating or reducing any adverse impacts that may occur. This is obviously a very sweeping purpose and it is fully recognized that there are limitations on resources as well as the potential for duplication of effort. As a result, every effort would need to be made to coordinate activities with those of DOI, EPA, NIOSH, state regulatory agencies, and others.

More specifically, the results of the 2007 Workshop indicate that the top priorities of the group of workshop attendees which represent a good cross section of those involved in ongoing oil shale development investigations and activity, can be summarized as:

- Development of an integrated basin/regional baseline for surface and groundwater data (quality and quantity) and GIS-based analytical tools for analyzing and working with the data.

- Development of accurate, predictive regional models for release, fate and transport of air emissions from oil shale operations and other activities.
- Conducting process-specific research to evaluate generated contaminants and water consumption, and evaluation of Best Available Control Technology (BACT).
- Development of a regional energy/resource system model that will enable cost/benefit analysis of a large variety of resource development and land use alternatives in a comprehensive way.

While the participants provided thoughts and perspectives on a wide variety of issues and concerns, the above four elements continued to rise to the top of the list of Oil Shale Environmental Issues and Needs. These efforts can help address questions posed within but not answered within recent EIS and management plans for the Green River Basin issued by BLM (3, 12).

References

1. *An Assessment of Oil Shale Technologies, Volume II: A History of the Federal Prototype Oil Shale Leasing Program*; National Research Council, Office of Technology Assessment: Washington, DC, July 1980.
2. *Oil Shale, Tar Sands and Unconventional Fuels Act of 2005*; 2005 U.S. Energy Policy Act, Public Law 109-58, Section 369, August 2005.
3. *Proposed Oil Shale and Tar Sands Resource Management Plan Amendments to Address Land Use Allocations in Colorado, Utah, and Wyoming and Final Programmatic Environmental Impact Statement*; FES 08-32, September 2008, available at Oil Shale EIS Information Center, <http://ostseis.anl.gov/>.
4. Boak, J. *Report of the Workshop on Environmental Issues and Research Needs for Oil Shale Development*; Golden, CO, October 19, 2006, available at <http://ceri-mines.org/publications2.htm>.
5. *2007 Environmental Issues and Research Needs Workshop*; Golden, CO, October 18, 2007, available at <http://www.netl.doe.gov/technologies/oil-gas/publications/EP/2007-OilShaleEnvWorkshop.pdf>.
6. *Proceedings of 26th, 27th and 28th Oil Shale Symposia*; Colorado Energy Research Institute: Golden, CO, available at <http://www.ceri-mines.org/>.
7. Johnson, H. R.; P.M Crawford; J. W. Bungler *Strategic Significance of America's Oil Shale Resource, Volume I – Assessment of Strategic Issues*; DOE Office of Naval Petroleum and Oil Shale Reserves: March 2004, available at http://www.fossil.energy.gov/programs/reserves/keypublictions/npr_strategic_significancev1.pdf.
8. Johnson, H. R.; P.M Crawford; J. W. Bungler *Strategic Significance of America's Oil Shale Resource, Volume II – Oil Shale Resources, Technology, and Economics*; U.S. Department of Energy, Office of Naval Petroleum and Oil Shale Reserves: March 2004, available at http://www.fossil.energy.gov/programs/reserves/keypublictions/npr_strategic_significancev2.pdf.
9. *Secure Fuels from Domestic Resources, The Continuing Evolution of America's Oil Shale and Tar Sands Industries, Profiles of Companies*

Engaged in Domestic Oil Shale and Tar Sands Resource and Technology Development; U.S. Department of Energy, Office of Petroleum Reserves, Office of Naval Petroleum and Oil Shale Reserves, June 2007, available at http://www.fossil.energy.gov/programs/reserves/npr/Secure_Fuels_from_Domestic_Resources_-_P.pdf

10. Shages, J. W.; Dammer, A. R. *America's Oil Shale Resource, A Roadmap for Federal Decision Making*; , Office of Naval Petroleum and Oil Shale Reserves: December 2004, available at http://www.fossil.energy.gov/programs/reserves/npr/publications/oil_shale_roadmap.pdf.
11. *U.S. Crude Oil Supply and Disposition*; U.S. Department of Energy, Energy Information Administration; available at http://tonto.eia.doe.gov/dnav/pet/pet_sum_crdsnd_adc_mbbldpd_a.htm.
12. *Resource Management Plan Amendment and Environmental Impact Statement, Roan Plateau Planning Area, Including Former Naval Oil Shale Reserves Numbers 1 and 3, Glenwood Springs, CO*; DES04-04; U.S. Department of the Interior, U.S. Bureau of Land Management: November 2004, available at <http://ostseis.anl.gov/>.

Chapter 13

Economics of Oil Shale Development

Khosrow Biglarbigi,^{*1} James Killen,² Hitesh Mohan,¹ Marshall Carolus,¹ and Jeffrey Stone¹

¹INTEK Inc., Arlington, VA 22201

²U.S. Department of Energy, Washington, DC 20585

^{*}e-mail: kbiglari@inteki.com

With high attention being focused towards the development of unconventional fuels, the United States' domestic oil shale resource has been given significant consideration as a viable source for domestic fuel. The United States is home to the world's most concentrated oil shale resources. The development of an oil shale industry has the potential to provide significant economic benefits; however, major development hurdles must first be overcome. This chapter will discuss the current state of oil shale economics in regards to the market value of oil shale, development costs, project schedules, risks, and leasing regulations.

Introduction

Oil shale production is characterized by high capital investment, high operating costs, and long periods of time between expenditure of capital and the realization of production revenues and return on investment. For first-generation facilities there is substantial uncertainty about the magnitude of capital and operating costs because technologies are not yet proven at commercial scale. Revenues are uncertain because world crude oil prices are volatile and future market prices for shale oil and byproducts are unknown. These and other uncertainties pose investment risks that make oil shale investment less attractive than other potential uses of capital.

Technology uncertainty is the largest single risk factor associated with oil shale development. This uncertainty remains even after 50 years of government and industry research to develop a commercially viable retorting technology to

convert kerogen to shale oil. In other countries, namely Brazil, China and Estonia retorting of spent shale has been commercial for many decades. Despite the termination of commercialization efforts by the United States Federal government in the 1980s, the several technologies developed for surface and in-situ production of shale oil in that era still hold significant promise. Technology advances achieved since 1980, oil shale experience in other countries, and expectations for sustained higher oil prices all contribute to an improved outlook for oil shale development. Project development and expansions by private industry are expected to continue at a pace dictated by economics.

The development economics issue is short-term (years to decades). Once commercial operation is successfully demonstrated, capital and operating costs will fall as operations become more efficient and the industry matures and learns how best to economically develop the resource. If oil prices are maintained at only current levels, second and third generation technologies will continue to improve, profitability will increase, and the relative economics of oil shale development will become more attractive. Over the longer-term, improving economic operations will attract the additional investment capital needed to expand operations just as it has for oil sands development in Canada.

This chapter provides an overview of oil shale development economics. Specifically, it will discuss:

- Market value of shale oil
- Components of project development costs
- Project development schedule
- Leasing regulations
- Range of costs for representative technologies
- Minimum economic prices
- Cash flow of a generic project with surface mining and retort
- Cost variances due to market dynamics

Market Value of Shale Oil

Shale oil is analogous to petroleum except for its high nitrogen and metals content. These are removed by upgrading which makes shale oil a premium quality refinery feedstock. Upgraded shale oil has almost no heavy residuals and is best suited to the production of diesel and jet fuels. However, the waxy nature of the feedstock allows the refiner to crack as deeply as desired to make either distillate fuels or motor gasoline.

Shale oil, whether produced from retorted oil shale at the surface or in situ, will require upgrading to meet current pipeline specifications. Upgraded shale oil will then be refined to produce finished fuels and chemicals. Traditional upgrading typically involves catalytic hydrogenation to remove heteroatoms (nitrogen, arsenic, sulfur, metals, and others). Upgraded shale oil, like Canadian syncrude from oil sands, will be free of distillation residue and will contain low concentrations of nitrogen and sulfur. These characteristics coupled with high hydrogen content add market value to the product. Thus, the upgraded shale oil

will likely sell at a premium to West Texas Intermediate (WTI) crude (the industry benchmark).

Typical yield of products produced from shale oil are compared with Brent and West Texas Intermediate crudes in Figure 1. This comparison shows that shale oil is a highly desirable feedstock for diesel and jet fuel production, or for producing a range of fuels including gasoline.

Oil Shale Development Costs

Oil Shale Technologies Considered

Over the past sixty years, energy companies and petroleum researchers have developed, and in many cases tested a variety of technologies for recovering shale oil from oil shale and processing it to produce fuels and byproducts. Except for a few small scale projects abroad, none of these technologies have been demonstrated at a commercial scale in the United States. One of the greatest challenges to investment in commercial scale oil shale operation is the fact that these technologies are considered by the investment community to be “unproven” and not ready for commercial project financing. This also makes them deemed risky by the companies that can finance them internally. However, a number of technologies that were previously developed and tested at semi-work pilot scale, as well as some emerging technologies, are now thought to be ready for commercial demonstration.

Four technologies are considered for economic discussion in this chapter, and they are: 1) Surface mining and surface retorting, 2) Underground mining and surface retorting, 3) Modified In-Situ conversion process, and 4) True In-Situ conversion process. These technologies were selected based on their historic and current stage of development and availability of economic data. They are intended to provide examples across a broad range of options for both surface, near surface, and deeper oil shale deposits. A brief description of these technologies is provided below:

Surface Mining with Surface Retorting

Surface mining is applicable to those deposits that are near the surface or that are situated with an overburden-to-pay ratio of less than about 1:1. Once the shale has been mined, it is heated to temperatures between 400 and 500 degrees centigrade to convert – or retort – the kerogen to shale oil and combustible gases. The retort technology considered in this paper is the Gas Combustion Retort (GCR) Vertical retort (Figure 2-A). This technology was originally developed by the U.S. Bureau of Mines in the 1940’s and it is considered as one of the most successful retort technologies with high retorting and thermal efficiency. A variation of GCR is currently in use in Brazil producing 4,000 barrels (Bbl) of shale oil per day.

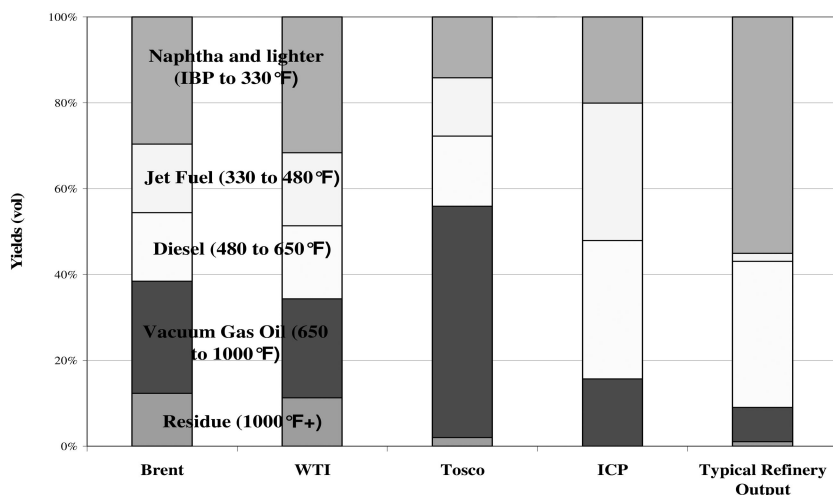


Figure 1. Typical Yields of Produced Shale Oil versus Crude Oil (1)

Underground Mining with Surface Retort

Room and pillar mining is applicable to resources that outcrop along steep erosions or via shafts. This method of mining was used successfully by government and by private industry to extract oil shale from along the southern boundary of the Piceance Creek Basin. The retort technology considered in this paper for this resource is the GCR vertical retort as described above (Figure 2-B). Variations of surface retorts using underground mines are currently operating in China and Estonia.

Modified In-Situ Conversion Process(MIS)

The Modified In-Situ technology involves mining some of the target shale before heating. Once the shale is mined, the virgin shale is rubblized to create a void space of 20 to 25 percent. Combustion is started on the top of the rubblized shale and moves down the column. In advance of the combustion front, oil shale is raised to retorting temperature that converts the kerogen to shale oil and to gases (Figure 2-C). Both products are captured and returned to the surface. MIS processes can improve performance by heating more of the shale, improving the flow of gases and liquids through the rock, and increasing the volume and quality of the oil produced. An example application of this process was the Occidental Oil Shale MIS Retort developed in the 1980s which demonstrated mining, rubblizing, ignition and simultaneous processing of oil shale (2).

True In-Situ Conversion Process(TIS)

The True In-Situ technology requires no mining and it is applicable to deeper oil shale deposits. The TIS technology considered in this paper is similar to Shell's In-Situ Conversion Process (ICP) as shown in Figure 2-D. The process uses electric heaters, placed in closely spaced vertical wells, to heat the shale for 2 to 4 years. The slow heating creates micro-fractures in the rock to facilitate fluid flow to production wells. Resulting oil and gases are moved to the surface by conventional recovery technologies. The ICP's slow heating is expected to improve product quality and recover shale oil at greater depths than other oil shale technologies. Additionally, the ICP process may reduce environmental impact. An innovative "freeze wall" technology is being tested to isolate the production area from groundwater intrusion until oil shale heating, production, and post production flushing has been completed.

Components of Oil Shale Development Costs

Project development costs vary according to the oil shale resource and the process selected. For mining and surface retorting, the costs are associated with mine development (surface or underground), retorting and upgrading facilities, and infrastructure including roads, pipelines, power, utilities, storage tanks, waste treatment, pollution control and handling of spent shale. For in-situ conversion processes, the costs include:

- Subsurface facilities: wells or shafts to access and heat the shale, recover liquids and gases, and isolate and protect subsurface environments.
- Surface facilities: production pumps and gathering systems, process controls, upgrading facilities and spent shale handling.
- Environmental monitoring/ environmental restoration.

These costs fall into two broad categories: capital costs and operating costs.

Capital Costs

Capital costs encompass the cost of extraction, retorting, and other equipment necessary for the production of oil from oil shale. The costs, and the specific technologies to which they are applied, are provided in Table I.

Operating Costs

Operating costs consist of normal daily expenses and maintenance of both surface and subsurface equipment. The components of the operating costs are different for each technology depending upon the mining, retorting, and upgrading

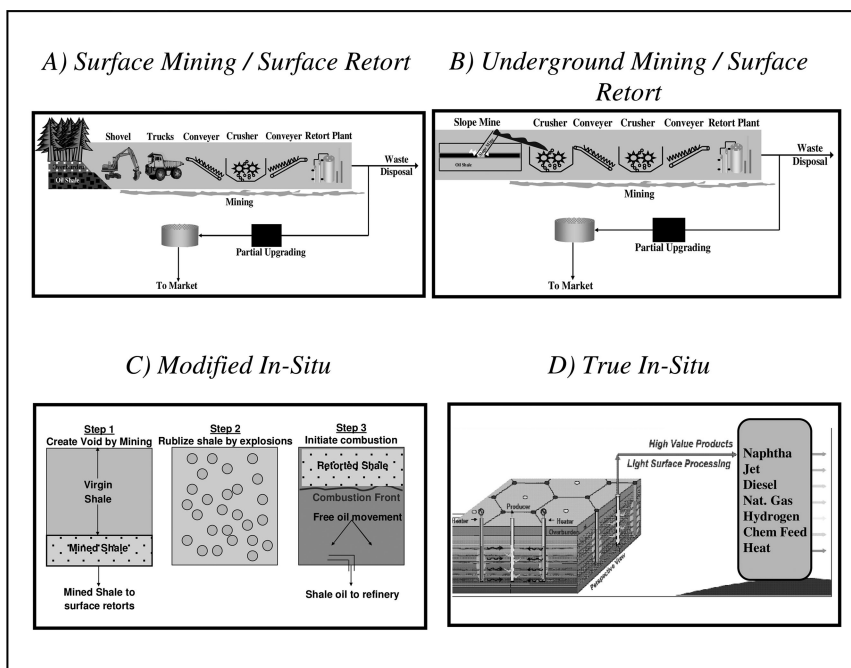


Figure 2. Representative Oil Shale Development Technologies (3)

Table I. Capital Costs for Selected Oil Shale Technologies (4)

Cost Category	Surface Mining	Underground Mining	Modified In-Situ	True In-Situ
Drilling and Equipment Costs for New Producers				☑
Lifting Costs				☑
Mining plus spent shale handling	☑	☑	☑	
Retorting	☑	☑	☑	
Oil Recovery	☑	☑	☑	☑
Oil Upgrading	☑	☑	☑	☑
Utilities	☑	☑	☑	☑
Facilities	☑	☑	☑	
Cost of Capital	☑	☑	☑	☑
Others including environmental	☑	☑	☑	

facilities requirements of the technology. The technologies and their component operating costs are provided in Table II.

Availability of Cost Data

Information is available for most of the steps in these processes. The technologies for mining, drilling, and upgrading are well established. This provides reliable economic data for several components necessary for economic analysis. Details are publicly available for these components of the oil shale development processes. In this section, the availability of the economic data will be discussed.

Mining Costs

While there is no commercial scale oil shale mining currently in the United States, the mining cost data is reliably available from other resources. The data can be obtained from coal mining in the United States as well as the mining of oil sands in Alberta, Canada. It has recently been estimated that the capital cost for a 5,000 tonne per day open pit mine is approximately \$1,600 per tonne of daily capacity while the operating costs is \$5.33 per tonne of mined rock (5).

Drilling Costs

Cost data is available for U.S. drilling activity. Figure 3 shows the annual average cost (2007 dollars) to drill a well in the states containing the Green River Basin (Utah, Colorado, and Wyoming) for two depth ranges. As the figure shows, the average cost for drilling an oil well less than 1,250 feet deep has increased from approximately \$260,000 to nearly \$540,000 between 2004 and 2007. During the same time period, the cost to drill an oil well between 1,250 and 2,500 feet deep has increased from nearly \$560,000 to \$1,200,000. In both cases, this is a price increase of more than 210%.

Retorting Costs

The cost of retorting is highly dependent upon the technology selected for the project. Except for the technologies experimented with during the 1970's and 80's, no cost data is publically available. The heating and/or retorting of oil shale is most likely to be dependent upon the availability of natural gas. Much of the gas required for the process can be produced during the pyrolysis of the oil shale. The balance of required natural gas will be acquired on the market.

Upgrading Costs

The technologies for upgrading have been proven and are currently being applied in Alberta, Canada. Currently more than 1.2 million barrels (MMBbl) of oil are being upgraded each day. The widespread application of the technology

Table II. Component of Operating Costs for Selected Oil Shale Technologies (4)

<i>Cost Category</i>	<i>Surface Mining</i>	<i>Underground Mining</i>	<i>Modified In-Situ</i>	<i>True In-Situ</i>
Mining	☑	☑	☑	
Subsurface				☑
Plant	☑	☑	☑	
Surface				☑
Maintenance	☑	☑	☑	☑
Finance & Administration	☑	☑		
Environmental, Health, & Safety	☑	☑		
Electricity	☑	☑		
Natural Gas	☑	☑		
Energy				☑
Chemicals	☑	☑		
Water & Nitrogen	☑	☑		
Contingency	☑	☑		☑
Overhead	☑	☑	☑	☑
G&A on Capital Investments	☑	☑	☑	☑
G&A on Operating Expenditures	☑	☑	☑	☑

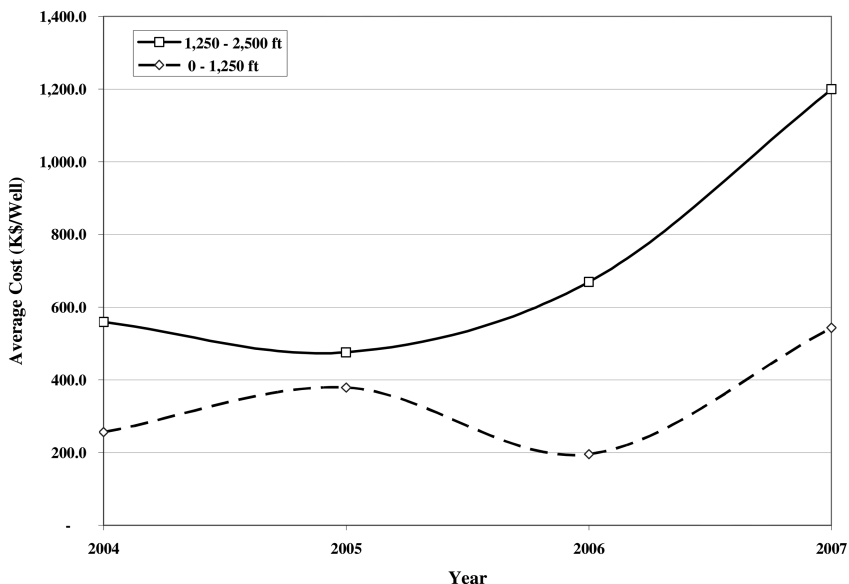


Figure 3. Average Drilling Costs in Green River Formation (2004-2007) (6)

provides a strong basis for economic data which can be used for oil shale analysis. Between 2004 and 2007, there has been a significant increase in the upgrading costs reported. As Table III displays, the capital costs (2007 U.S. Dollars) have increased more than 230% during this time period.

During the same time period, there was a similar cost increase in the operating costs associated with upgrading. The operating cost increased from \$3.74 to \$6.35 (2007 U.S. Dollars) between 2007 and 2008 (8, 10).

Later in this chapter, an aggregate range of operating and capital costs are discussed for the four oil shale technologies. The operating costs for surface mining, underground mining, and Modified In-Situ were developed based on information available from the Prototype Leasing Program in the early 80's as well as other sources. The operating cost categories for True In-Situ were developed using information obtained from industry sources.

Project Development Schedules

The size of the commercial scale oil shale projects would depend upon the recovery technology. Due to the capital intensity of the projects, the long lead time for permitting and development, and the goal of obtaining production as soon as possible, the projects will most likely be developed in modular stages. The size of each stage, approximately 25,000 barrels of daily capacity for mining with surface retorting, is limited by the capacity of the retorting vessels.

Before shale oil production from a surface mine with surface retorting, several development stages must be completed. These stages include the engineering and permitting of the project, the development of the mine, the construction and installation of the retorting equipment, and the construction and installation of the refining and upgrading facilities. The time span for the development stages for the first module is provided in Figure 4.

As the figure shows, the total project lead time before first production is realized is seven years. However, recent awardees of BLM leases (surface and in-situ) have experienced significantly longer permitting periods to obtain startup permits and complete baseline environmental studies required for the the federal, state, and local permits. Lessons learned during the development of the first stage would be applied to the construction of subsequent stages. This results in shorter development times required for the expansion of the mine and the construction and installation time required for additional retorting facilities.

The development of an oil shale project using a True In-Situ technology has similar stages before production is first realized. These stages include the engineering and permitting of the project, the drilling of heating and producing wells, and the heating of the formation. The total project lead time before production is first realized could be six years. The lengths of these stages are provided in Figure 5.

Table III. Capital Costs for Oil Sands Upgrading

<i>Year</i>	<i>Cost</i>
2004 (7)	\$24,617 per STB ^a
2006 (8)	\$45,638 per STB
2008 (9)	\$60,000 per STB

^a STB – Stream Day Barrel of Daily Capacity

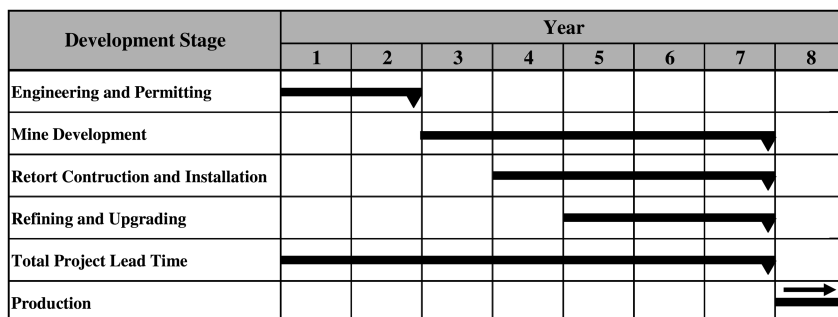


Figure 4. First Stage Development – Surface Mining with Surface Retort (11)

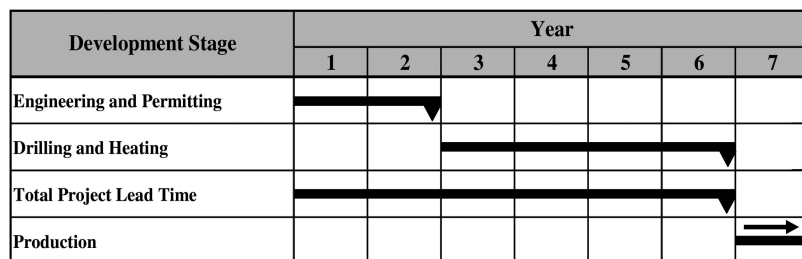


Figure 5. Development Schedule – True In-Situ (11)

Regulations for Lease Acquisition

Well over 70% of the Green River oil shale deposit in the U.S. is located on Federal lands. The balance of the resource is located on state lands as well as private lands. In November 2008, the U.S. Department of the Interior (DOI), Bureau of Land Management (BLM) issued final regulations for commercial development of oil shale (12). The provisions for the royalty structure, rent, and lease bonuses are shown in Table IV. Other significant provisions of the leasing regulations are:

Table IV. Provisions of Royalty Structure, Rent, and Lease Bonuses (12)

<i>Regulation</i>	<i>Provision</i>
Royalty Rate	The royalty rate will be 5% for the first 5 years of the lease, after which it will increase by 1% per year to a maximum of 12.5%. The point of determination for royalties will be when oil shale products are sold or transferred from the lease area (no value is assigned to raw shale). This regulation is open to father determination as the industry moves from R&D to commercial operations.
Rents	Rental rate is \$2 per acre until royalties can be collected; upon 10 th year, if lease is not producing, rent will be \$4 per acre.
Bonds	Minimum lease bond is \$25,000.
Bonus	Minimum bonus bid of \$1000 per acre. The amount is not reflective of fair market value (FMV), but intended to dissuade nuisance bids.

Exploration License

The maximum acreage for an exploration license is 25,000 acres. Exploration license is valid for 2 years. Prior to issuance of an exploration license, BLM will conduct an Environmental Impact Statement (EIS) analysis. Operator is required restore condition of disturbed land to pre-exploration quality or higher (12).

Leasing Process

As part of the process, the BLM will issue a request for interest through a competitive bidding process, with the highest bidder winning the lease. Minimum bid is determined at \$1000 per acre. The maximum lease size is 5,760 acres and the leasing period is for 20 years. BLM will conduct an EIS analysis prior to offering a tract for competitive lease. Winning bidder must repay BLM for EIS (12).

Leasing Requirements

Operators must meet a number of milestones. Within 2 years of lease, the operator is required to submit a plan of development. Final plan of development (approved by BLM) is due within 3 years. The operator must also apply for all permits/licenses within 5 years. Prior to the end of the 7th year, the operator must begin installation of permitted infrastructure, and by the end of 10th year, production must begin. In addition, the operator must meet certain reclamation criteria: 1) The operator must restore land to pre-mining condition or higher and 2) The operator is required to save topsoil for reclamation. If a milestone is not met, operator will be charged \$50 per acre per milestone missed (12).

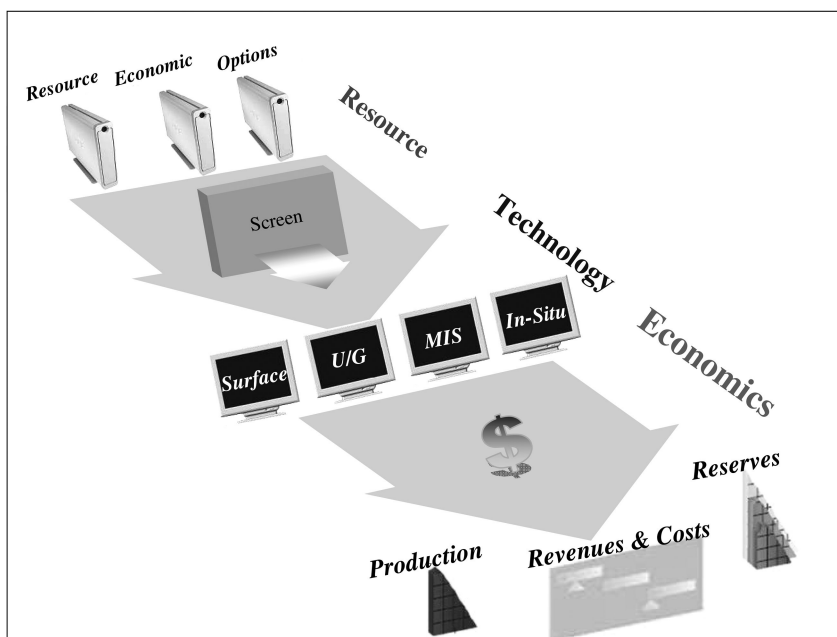


Figure 6. Logic Flow of National Oil Shale Model (14)

Land Exchange

BLM may exchange leases if it is determined that the exchange will facilitate the recovery of oil shale. There is no provision for logical mining units.

The Current State of Oil Shale Economics

Given the current status of the oil shale extraction technology and lack of any project at commercially viable scale, it is almost impossible to quantify the development economics of these projects. The only publicly available source of economic data dates back to the Oil Shale Prototype Leasing Program of 1970's and 80's (13). These data do not reflect the current market conditions nor do they reflect the current slate of technologies. They do, however, provide a solid starting point to identify the components of investments and operating cost elements. Using this approach and working with technology vendors, the U.S. Department of Energy (DOE), has developed a first set of approximations of these cost elements for the four technologies discussed earlier. These cost elements are incorporated into an analytical system for planning and evaluation. The information from this system is the basis for the economic discussion for the remainder of this chapter. The system has been peer reviewed by the U.S. DOE and the Industry. A brief description of the system is provided below.

Table V. First Generation Capital Requirements and Operating Costs (3)

<i>Item</i>	<i>Unit</i>	<i>Range</i>
Capital Costs ^a	K\$/SDB ^b	40 – 55
Operating Costs ^a	\$/Bbl	12 – 20

^a Inclusive of mining (or drilling), retorting, & upgrading ^b Stream Day Barrel of Daily Capacity

National Oil Shale Model

This analytical system was developed to evaluate potential U.S. oil shale development under different economic and public policy regimes. This system allows analysts to perform sensitivity analyses relative to price, tax, royalty and incentives, perform cash flow analyses under alternative leasing options and evaluate cost and benefits of various public policy options and incentives to stimulate oil shale project investment. Figure 6 provides the logic flow of the analytical system

The system consists of a detailed resource module, technology screening module, and a detailed economic module.

- *Resource Module*: Contains detailed petrophysical and geological characteristics for 25 development tracts in the states of Colorado, Utah, and Wyoming. These tracts collectively account for 70 billion barrels of resource in place. Characteristics of these 25 tracts were studied in detail as part of the 1972 Department of the Interior Prototype Oil Shale Leasing Program (13). Because of prior industry nomination, it is assumed that these tracts represent locations of commercial interests. These nominated tracts therefore provide a solid technical basis for the present analysis (14).
- *Screening Module*: Screening criteria for various technologies were developed based on the geological characteristics such as depth, dip angle, yield and thickness of the resource. The technologies considered are: 1) Surface mining with surface retorting, 2) Underground mining and surface retorting, 3) Modified In-Situ Conversion Process, and 4) True In-Situ Conversion Process. Each tract was screened for each of the above technology options. Each tract was then assigned the most appropriate technology and evaluated under the specific process. Specific development schedules were also assigned to each tract based on the type of technology applied (14).
- *Economic Module*: The production forecasts, predicted for each tract (based on its development schedule), are used in the economic module for cash flow analysis. The economic module estimates annual and cumulative cash flow before and after taxes, capital costs, operating cost, transfer payments (royalties), revenues, and profits. The tracts that meet the economic hurdles are then carried forward and results are aggregated to national total. The economic module has average capital and operating costs based on technology and development schedule over the life of the project. The components of

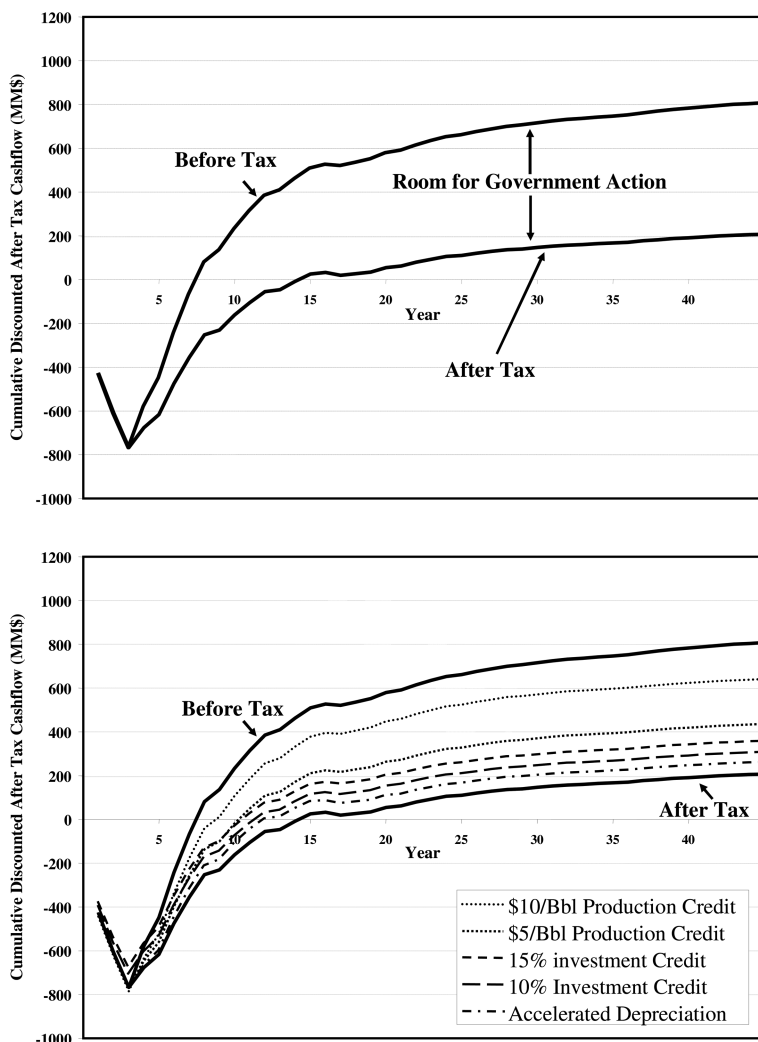


Figure 7. Cashflow of a Generic Oil Shale Project & Impact of Incentives (3)

the costs are different for various technologies used for mining, retorting, and upgrading (14).

The system also estimates a number of economic benefits at state and national levels. The benefits to local, state, and Federal treasuries are attributed to the implementation of economically feasible projects over the next 25 years. These benefits include: 1) Direct Federal Revenues; defined as the sum of business taxes as well as one-half of royalty payments on oil shale production from Federal lands, 2) Direct State Revenues; defined as the sum of business taxes, production taxes, as well as one-half of royalty payments on oil shale production from Federal lands, and 3) Direct Public Sector Revenues; defined as the sum of the Direct Federal and Direct State Revenues.

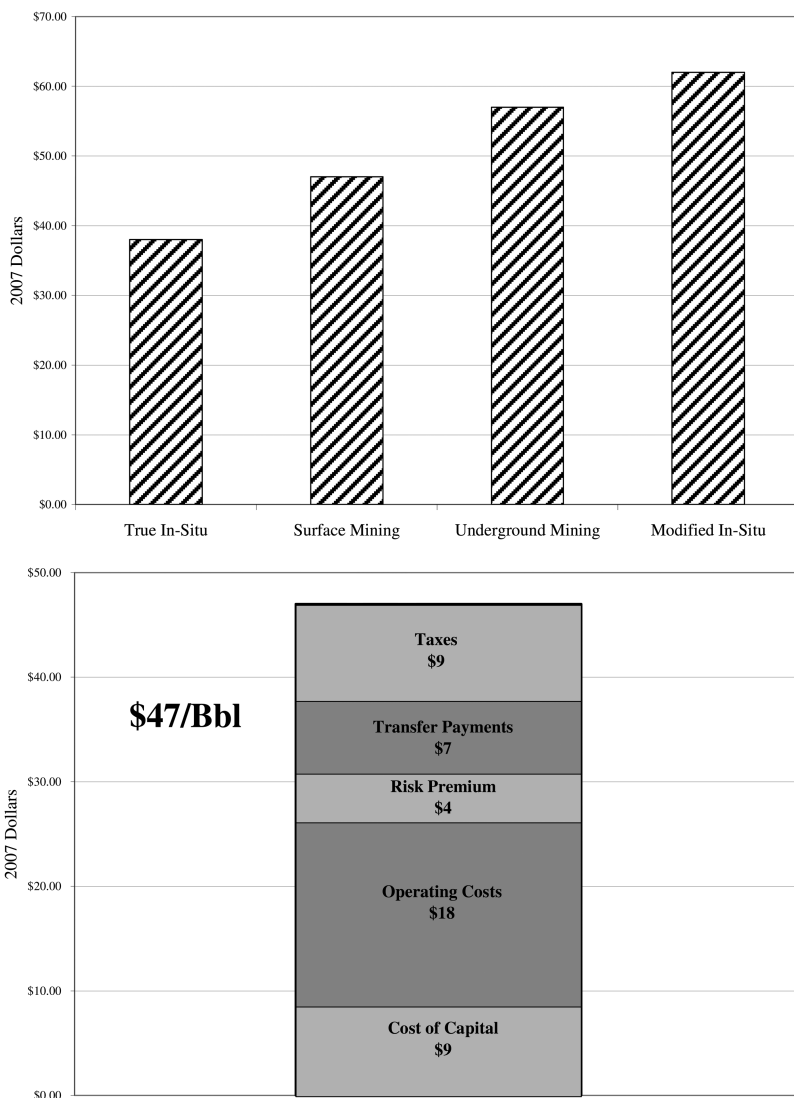


Figure 8. Minimum Economic Price for Oil Shale Technology & Breakdown of Price for Generic Surface Project with 15% Rate of Return (3, 15)

The nation as a whole also benefits from oil shale production. Each additional barrel of domestic production can replace a barrel of oil imports. Each dollar of increased Gross Domestic Product (GDP), which would otherwise pay for imports, could reduce the trade deficit by a dollar. To estimate the direct effects on the GDP (excluding the multiplier effect and potential negative impacts on other domestic export industries), the system uses the gross revenue from the potential oil shale production, inclusive of oil, natural gas, and ammonia. Similarly, the value of potential production is used to measure the impact on the trade deficit. The system

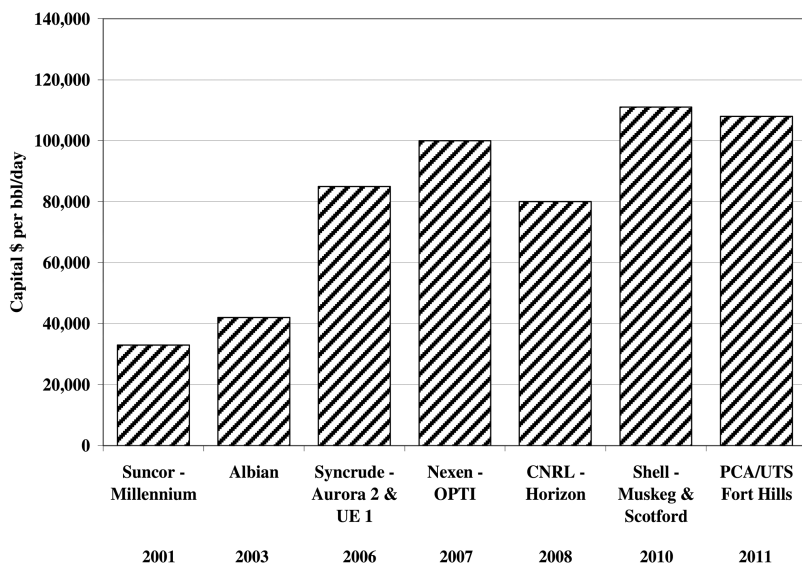


Figure 9. Canadian Oil Sands Capital Costs (17)

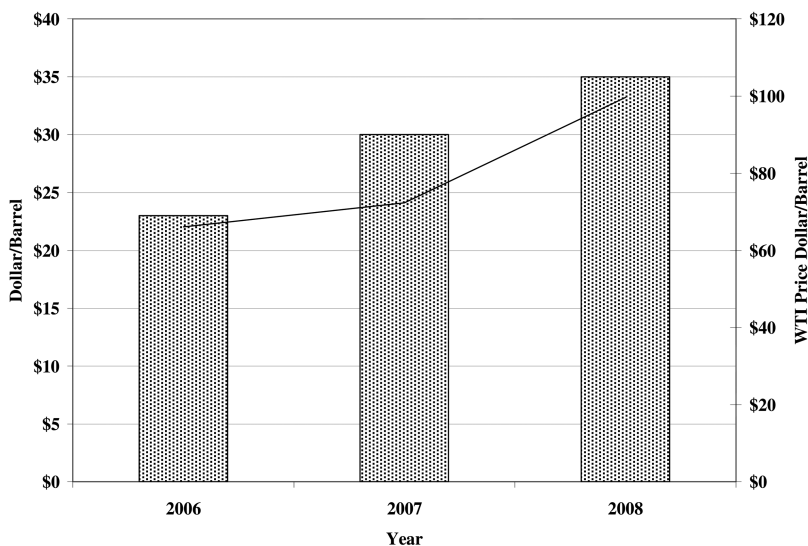


Figure 10. Canadian Oil Sands Operating Costs(18)

also estimates potential employment associated with the oil shale projects. Labor costs (wages and fringe benefits) are calculated by isolating the labor component of all major cost elements. Labor costs are then converted into estimated annual employment using average wages (including benefits) for comparable industries as reported by the U.S. Department of Labor.

Estimated Costs of “1st Generation” Oil Shale Projects

Commercial oil shale projects could range in size from 10,000 to 100,000 barrels per day (Bbl/d) for surface retort to as much as 300,000 Bbl/d for full scale in-situ projects. The costs, in terms of capital and operating costs, vary depending on the process technology and the quality of the resource. The model estimates the operating costs in the range of \$12 to \$20 per barrel (\$/Bbl) of shale oil produced (Table V). The capital costs are estimated in the range of \$40,000 to \$55,000 per barrel of daily (stream day) capacity. These costs are inclusive of mining (or drilling), retorting, and upgrading. It is important to note that these costs pertain to fully operational first generation projects and they are expected to change as technologies mature with time (3).

Cash Flow of Generic Surface Mine and Surface Retort Oil Shale Project

Figure 7 shows the cumulative discounted before and after tax cashflow for a generic oil shale project. The generic oil shale project used for this example is a four-stage, surface mine and retort project. The total production is 112 MBbl/d which was developed over twenty years with each stage assumed to be 28 MBbls of daily capacity. This cash flow was constructed using oil prices in the range of \$50 to \$65/Bbl over the next twenty five years. As the figure shows, the payout of the project, before taxes, is eight years. The payout period, once taxes are levied, is extended to fourteen years. The length of the project payout, especially in comparison with the payout period of conventional oil projects, is a significant factor in the development of oil shale projects.

Figure 7 also shows the impact of some example tax incentives that could be offered by the Federal government to make the project economically more feasible. As shown, the incentives, if designed properly, could improve the profitability while shortening the payout period significantly.

These incentives are presented to demonstrate the sensitivity of the generic oil shale project's profitability and project payout to different economic conditions. The authors do not intend this presentation to imply either the endorsement of, or the recommendation of any or all of these incentives.

Minimum Economic Price

The minimum economic price for oil shale projects also varies depending on technology and resource quality. The minimum economic price is defined as the world crude oil price needed to yield a 15% rate of return (ROR) on the project. The 15% ROR is to cover the cost of capital and the technical and financial risk on the project. Based on the assumptions utilized in this analysis, the model estimates that for a mature 100,000 Bbl/d capacity plant, the average minimum economic prices are \$38/Bbl for True In-Situ, \$47/Bbl for Surface Mining, \$57/Bbl for Underground Mining, and \$62/Bbl for Modified In-Situ (Figure 8) (3, 15).

While these estimates are highly sensitive to both technological and economic assumptions, discussions with industry have proven these estimates reasonable.

Figure 8 also provides a breakdown of the minimum economic price for a generic surface project. The largest components of the price are the cost of capital and the operating cost. They contribute \$9/Bbl and \$18/Bbl to the price respectively. The risk factor, which is the technical risk of the recovery process, accounts for \$4/Bbl. The transfer payments, which include royalty and severance taxes, account for an additional \$7/Bbl. Finally, the state and Federal business taxes contribute an additional \$9/Bbl. The taxes and transfer payments, defined as royalty and severance payments, collectively account for one third of the price requirement (3).

Cost Variance Due to Market Dynamics

Market Dynamics

As seen in the last few years before the start of the recession, the market has had a significant impact on the capital investments and operating costs for Alberta oil sands. Several factors contributed to this impact. The sustained high oil prices provided an incentive for companies to begin or expand oil sands projects. The high oil prices impacted the prices of commodities required for construction of mining, retorting, and upgrading equipment. This impact could be readily seen in the increased steel prices. Between 2004 and 2007, the price of tubular steel increased from \$863 per ton to \$1,335 per ton. Similarly, the price of hot rolled steel increased from \$550 to \$740 per ton between 2008 and 2008 (16). The growing prices of commodities and equipment contributed to growing capital investments. The higher energy prices also contributed to increased operating costs because of the dependence of the retorting and upgrading phases upon availability of natural gas.

At the same time, the increased number of projects increased the demand for skilled labor. The tightness of the labor market contributed to the rising costs.

Impact of Cost Variance on Capital and Operating Costs

The Canadian Association of Petroleum Producers (CAPP) has reported in April 2008 that capital investments for oil sand operations in Canada are expected to increase by more than 300%. As Figure 9 illustrates, the capital cost for a barrel of daily capacity has increased from approximately \$30,000 to more than \$110,000. For a 100,000 barrel per day project this corresponds to a cost increase from \$3 Billion to \$11 Billion (17).

There is a similar increase in the operating cost. As reported by Suncor, the operating cost has increased from \$23 per barrel to \$35 per barrel between 2006 and 2008 (18). As Figure 10 shows, this corresponds with a 50% percent increase in the average oil price for West Texas Intermediate Crude (shown on the right axis).

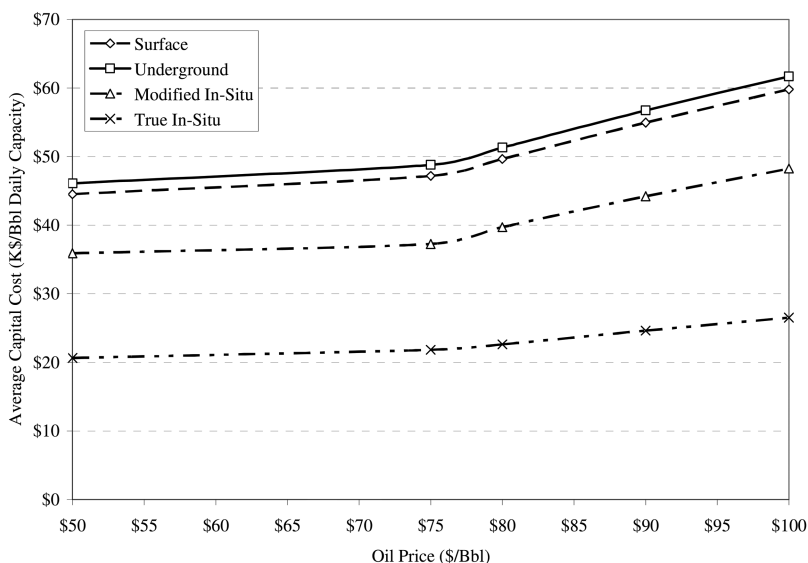


Figure 11. Oil Shale Capital Cost Variance (19)

To estimate the oil shale cost variance associated with market dynamics, the Department of Energy conducted an analysis of the cost data publicly available for the Alberta oil sands. The collected data was converted to 2007 U.S. dollars and normalized using average oil prices. The oil price was used as a surrogate for the changes in commodity and energy prices associated with changes in the market. The normalized data was used to develop a series of correlations which related the capital or operating cost and the price of oil. Cost correlations were developed for the following cost categories:

- Capital cost for mining
- Capital cost for upgrading
- Capital cost for tangible and intangible oil equipment
- Operating cost for mining and upgrading
- Operating cost for oil operations
- Energy

The impact of increased oil prices is calculated using the differential of the cost correlation. For example, the increase in the capital cost for mining associated with oil prices increasing from \$75/Bbl to \$85/Bbl is detailed in equation 1.

$$Var_{cap\ mine} = \frac{(Cost_{cap\ mine}(85) - Cost_{cap\ mine}(75))}{Cost_{cap\ mine}(75)} \quad (1)$$

In this example, a ten dollar oil price increase results in an 8% increase in capital costs for mining. The variance factors are applied to the appropriate capital and operating cost categories listed in Tables II and III.

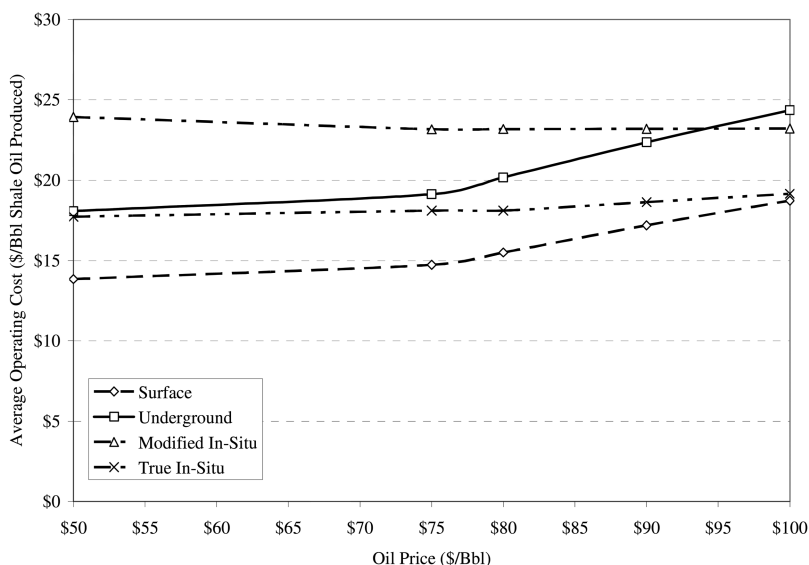


Figure 12. Oil Shale Operating Cost Variances (19)

The impacts of changing oil prices were calculated for the capital and operating costs using oil prices ranging between \$50 and \$100 per barrel. Figure 11 shows the potential variances in average capital costs for each of the four representative oil shale technologies. In this figure, the changes in oil price are used as a surrogate for changes in not only energy and commodity prices, but also the changes in the labor market. As the figure demonstrates, the capital prices increase substantially as the oil price increases. For example, the capital cost for surface mining with surface retorting increases from approximately \$45,000 to \$60,000 per barrel of daily capacity as oil prices increase from \$50/Bbl to \$100/Bbl.

The operating costs, illustrated in Figure 12, show a similar impact to increased energy prices and tightening labor markets. In the figure, the operating costs for underground mining with surface retorting increase from \$18 to nearly \$25 dollars per barrel of shale oil produced over the same ranges of oil price.

Conclusions

The production of oil shale is associated with high capital and operating costs as well as substantial technical and economic risks. As there are currently no large-scale oil shale projects operating, and the latest publicly available economic data is from the Prototype Leasing Program of the 1980's, there is deep uncertainty about the economics of oil shale development. This uncertainty will last until the first generation of oil shale projects reach commercial size.

However, economic analysis has been conducted on four technologies selected because of their historic and current state of development as well as the availability of economic data.

The capital costs for these technologies have been estimated, using analytical tools developed by the Department of Energy, to range between \$40,000 and \$55,000 per barrel of daily capacity. The operating costs have been estimated to be within a range of \$12 and \$20 per barrel of shale oil produced. These costs are both all inclusive and are dependent upon the technology and the quality of the resource. The same analysis concluded that the four technologies are economic under sustained oil prices ranging between \$40 and \$60 per barrel for the life of the project.

These economics are expected to change. They will be impacted by the market dynamics and the changing costs of energy and other required commodities. In addition, the economics will change as improvements in commercialized technologies bring capital and operating costs down.

Acknowledgements

Authors acknowledge funding for paper and previous projects from the U.S. Department of Energy, Office of Strategic Petroleum Reserves.

References

1. *Strategic Significance of America's Oil Shale Resource: Volume 2 – Oil Shale Resources Technology and Economics*; U.S. Department of Energy, Office of Petroleum Reserves, Office of Naval Petroleum and Oil Shale Reserves: Washington, DC, 2004.
2. *Proposed Oil Shale and Tar Sands Resource Management Plan Amendments to Address Land Use Allocations in Colorado, Utah, and Wyoming and Final Programmatic Environmental Impact Statement*; Department of the Interior, Bureau of Land Management: Washington, DC, 2008; p A-42.
3. Biglarbigi, K. Oil Shale Development Economics. Presented at the EFI Heavy Resources Conference, Edmonton, Canada, May 16, 2007.
4. *National Strategic Unconventional Resource Model: A Decision Support System*; U.S. Department of Energy, Office of Naval and Petroleum and Oil Shale Reserves: Washington, DC, 2006.
5. Cost Models of Theoretical Mining Operations. Western Mine Engineering, Inc., <http://costs.infomine.com/costdatacenter/miningcostmodel.aspx>.
6. *2007 Joint Association Survey on Drilling Costs*; American Petroleum Institute: Washington, DC, 2009.
7. *Overview of Canada's Oil Sands*; TD Securities: 2004.
8. *Will the Challenges Facing Oil Sands Projects Curtail Industry Growth?* Strategy West: 2006.

9. Dunbar, B. The Economic Implications of the Challenges Facing Canada's Oil Sands Industry, 2008 Global Petroleum Conference, 2008.
10. *Dialed In*; Flint Energy Services Ltd.: 2007.
11. *National Unconventional Resources Model: Peer Review*; U.S. Department of Energy, Office of Naval Petroleum and Oil Shale Reserves: Washington, DC, July 2006.
12. *Final Regulations, Oil Shale Management – General*; U.S. Department of the Interior, Bureau of Land Management: Washington, DC, 2008.
13. *Final Environmental Statement for the Prototype Oil Shale Leasing Program, Volume 1: Regional Impacts of Oil Shale Development*; U.S. Department of the Interior: 1973.
14. *National Oil Shale Model, A Decision Support System*; U.S. Department of Energy, Office of Naval Petroleum and Oil Shale Reserves: Washington, DC, 2005.
15. Biglarbigi, K. Potential Development of United States Oil Shale Resources. Presented at the 2007 EIA Energy Outlook Conference, Washington, DC, March 28, 2007.
16. United States Securities and Exchange Commission, Form 10-K; United States Steel Corporation, 2007.
17. Stringham, G. *Canada's Oil and Gas*; Canadian Association of Petroleum Producers (CAPP): Washington, DC, 2008.
18. *Delivering Shareholder Value, Investor Information*; Suncor Energy: 2008.
19. *National Strategic & Unconventional Resources Model: Status of Model Cost Updates*; U.S. Department of Energy, Office of Petroleum Reserves: Washington, DC, 2009.

Chapter 14

Resource Management Challenges in the Context of Potential Oil Shale Development

Kirsten Uchitel,* John Ruple, and Robert Keiter

The Wallace Stegner Center for Land, Resources and the Environment
& The Institute for Clean and Secure Energy, University of Utah,
Salt Lake City, Utah 84112
*uchitelk@law.utah.edu

Ongoing efforts to commercialize the oil shale resource face numerous environmental challenges due to the potential impacts of oil shale development on air, land, water and wildlife resources. Although many of these resource management challenges cannot be meaningfully addressed until proven oil shale technologies emerge, certain of these anticipated conflicts would benefit from attention and investigation by oil shale developers and policymakers in advance of detailed commercial oil shale leasing and development plans. This chapter discusses three such resource management challenges: the impacts of oil shale development on wildlife, aquatic and plant resources; issues associated with the development of oil shale and other co-located minerals; and water availability for oil shale development.

Introduction

The unrealized promise of domestic oil shale development has existed for over a century and a half, prompting the oft-cited observation that oil shale is the fuel of the future and it always will be (1–3). In the oil shale development activities of the late 1970s and early 1980s, oil shale's insurmountable challenges were primarily economic, using technologies that were predecessors to those currently being developed and that are no longer being considered (4, 5). The economics of oil shale development still inform and direct the debate over the

value and timing of commercialization of the oil shale resource, but in the oil shale era ushered in by the Energy Policy Act of 2005 (6) (and the attendant Research, Development and Demonstration leases issued by the Bureau of Land Management (BLM) in Colorado and Utah (7, 8)) significant environmental, land management and public opinion challenges also loom. Today's oil shale activities take place in a water constrained, environmentally regulated, and litigation prone world. Even the language of the Energy Policy Act, widely criticized by opponents as 'rushing' oil shale development, made clear that "research and commercial development [of the oil shale resource] should be conducted in an environmentally sound manner, using practices that minimize impacts . . . with an emphasis on sustainability" (9).

The environmental and regulatory challenges facing oil shale are far-reaching and significant, encompassing anticipated threats to air, climate, land, wildlife (including aquatic species and plant life), and water resources. Future development of some oil shale resources may be curtailed under federal law due to competing land uses, such as protections afforded by the Wilderness Act or critical habitat designated pursuant to the Endangered Species Act. Other potential areas of development that are not legally off-limits are nonetheless likely to provoke significant disagreement over whether oil shale development constitutes a sound use of public lands. Compounding this debate will be ownership and management authority questions as the oil shale resource is located across federal, state and tribal lands (10).

Research has been underway and continues apace on various in situ and modified in situ technologies. These technologies, it is hoped, will succeed in developing oil shale in an economically and environmentally sound manner. Emerging technologies offer the prospect of development while avoiding levels of environmental degradation that fail to meet regulatory standards or offend public sentiment such that development activities are delayed or blocked by policymakers or litigation. In addition, oil shale developers and land managers will need to address the acknowledged challenges of managing concurrent or consecutive development of oil shale along with other co-located energy resources. And they will need to ensure access to adequate water supplies for oil shale development while meeting agricultural, recreational, wildlife, municipal, and industrial demands for water in the prospective areas for oil shale development.

Until individual technologies are identified as commercially feasible, specific sites are selected for development, and detailed air, water and climate impacts of these technologies are reliably evaluated, any discussion of specific environmental impact scenarios is necessarily speculative. However, the prospect of oil shale development does present some fundamental resource management challenges that are amenable to advance analysis and planning by developers and policymakers. This chapter will discuss three such challenges: wildlife, aquatic life and plant management pursuant to the Endangered Species Act and equivalent state law protections; co-located mineral management; and water demand and management in prospective oil shale areas. While numerous other environmental and management challenges will be germane should commercial oil shale development come to fruition, these issues offer an opportunity for

developers and policymakers to engage in constructive advance planning, which will be critical to environmentally responsible oil shale development whichever oil shale technologies ultimately emerge.

Competing Land Uses and the Endangered Species Act

The areas that have been identified as most the geologically prospective for oil shale development include diverse habitats for a wide range of terrestrial, plant, and aquatic species. Oil shale development can be expected to impact habitat for several species, including some that enjoy special legal protections, leaving developers and land managers to find legally and politically acceptable solutions. In the context of oil shale leasing, the Endangered Species Act (ESA) (11) will require consultation at the leasing phase and is likely to require additional consultation at the development and reclamation stages of operations (12, 13). As discussed in greater detail in the following paragraphs, consultation will not merely require an assessment of the lease site, but also an overall evaluation of the indirect and cumulative effects of commercial development on listed species and their critical habitats (14).

Wildlife

The Colorado Division of Wildlife describes the Piceance Basin as “home to the largest migratory mule deer herd in North America, a large migratory elk population, one of only six sage-grouse populations in Colorado, conservation and core conservation populations of Colorado River cutthroat trout, and a host of other wildlife species” (15). Areas within Colorado that could be opened to commercial leasing under the Programmatic Environmental Impact Statement (PEIS) include 880 acres of important aquatic habitat, 7 acres of active bald eagle nests, 190,478 acres of elk production area, 6,506 acres of greater sage-grouse leks, 125,563 acres of greater sage-grouse production area, 78,093 acres of critical mule deer winter range, and 31,479 acres of mule deer migration corridors (15).

Wildlife habitat acreage within the Uinta Basin that overlies oil shale resources has not been quantified by the Utah Division of Wildlife Resources, but Utah’s conservation database indicates that the most geologically prospective area for oil shale development contains important habitat for a number of species of interest, including elk, mule deer, pronghorn antelope, and sage grouse (16). According to the BLM, the most geologically prospective oil shale area also includes crucial elk and mule deer winter range, as well as a lynx linkage zone (17).

Several species potentially affected by oil shale development may claim protection or be under consideration for protection under the ESA. The ESA directs the Secretary of the Interior to identify imperiled species and list them as threatened or endangered (18). Five factors weigh on the decision to list a species: habitat degradation; overuse of the species; disease or predation impacts; the

inadequacy of existing regulatory protections for the species; and other natural or human threats to the species' survival (19). The over-arching aim of the ESA is to provide "a means whereby the ecosystems upon which endangered species and threatened species depend may be conserved, to provide a program for the conservation of such endangered species and threatened species, and to take such steps as may be appropriate to achieve the purposes of [relevant] treaties and conventions" (20). In the hopes of avoiding species listings and the attendant regulatory restrictions, state officials and federal land managers often will employ proactive measures to safeguard dwindling species and their habitat, including, in some instances, imposing state law protections.

Section 9 of the ESA protects and aids in the recovery of imperiled species and their ecosystems (20) by prohibiting the "take" of listed (21) animals, except under federal permit (22). This prohibition against taking listed species applies regardless of land ownership (23, 24). To take means "to harass, harm, pursue, hunt, shoot, wound, kill, trap, capture, or collect or attempt to engage in any such conduct" (25). Regulations implementing the ESA further define "harm" as an act that "actually kills or injures wildlife" (26). Significant habitat modification or degradation may be considered a taking where it actually kills or injures wildlife by "significantly impairing essential behavioral patterns, including breeding, feeding, or sheltering" (26).

Section 7 of the ESA requires federal agencies to promote the conservation purposes of the ESA and to consult with the U.S. Fish & Wildlife Service (USFWS) as necessary to ensure that the effects of actions they authorize, fund, or carry out will not jeopardize the continued existence of listed species (27). Federal agencies are also required to avoid the "destruction" or "adverse modification" of designated critical habitat (28). During consultation, the action agency receives a "biological opinion" or concurrence letter from the USFWS addressing the proposed action (29). In the relatively few cases in which the USFWS makes a jeopardy determination, the agency offers "reasonable and prudent alternatives" about how the proposed action could be modified to avoid jeopardy (29).

The ESA also requires the designation of "critical habitat" for listed species when "prudent and determinable" (30). Critical habitat includes geographic areas containing either physical or biological features that are essential to the successful conservation of a listed species (31). Critical habitat may include areas that are not occupied by the species at the time of listing but which are identified as being critical to future conservation efforts (32). An area can be excluded from critical habitat designation if the economic benefits of excluding it outweigh the benefits of designation, unless failure to designate the area as critical habitat may lead to extinction of the listed species (33).

Section 10 of the ESA provides relief to non-federal landowners who want to develop property inhabited by listed species (34). Non-federal landowners can receive a permit to take listed species consequent to otherwise legal activities, provided they have developed an approved Habitat Conservation Plan (35). A Habitat Conservation Plan includes an assessment of the anticipated impacts on the species from the proposed action, the steps that the permit holder will take to minimize and mitigate those impacts, and an explanation of the funding available to carry out the mitigation (36).

Uintah County, which is the most likely to experience the direct impacts of oil shale development within Utah, offers an example of the scope of potential ESA and equivalent state law impacts on oil shale development. Within Uintah County, there are ten federally-listed or ESA candidate species, 19 species designated as a state species of concern, and 5 species receiving special management in order to avoid federal listing (37). Beyond the existing mix of species conservation efforts loom listing decisions for species such as the sage grouse. The sage grouse is a wide-ranging species, and listing and designation of habitat for the sage grouse would significantly impact oil shale (as well as oil and gas) development. Due to the variety of existing and pending species conservation efforts that must be coordinated and consistently applied by multiple land managers across federal, state and local boundaries, effective wildlife management practices are complex and require substantial advance planning. Efforts such as the Western Governors Association's Wildlife Council (38), which involves collaboration across federal, state and local boundaries, may be a useful model for cooperative and proactive management of these issues by developers and policymakers.

Aquatic Life

In order to protect listed aquatic species, the ESA may impose obligations on federal agencies (including their licensees and permittees) that can supersede state water rights. In such instances, water resources may be available physically but unavailable legally. In Colorado, the stream reach below Rio Blanco Lake is designated critical habitat for ESA-listed fish (39), and most of the White, Green, and Colorado rivers in Utah are critical habitat for ESA-listed fish (40). Accordingly, activities within the Yampa/White/Green river system will require consultation and be subject to the provisions of the ESA. In addition, much of the Yampa/White/Green river system is subject to in-stream flow requirements under Colorado and Utah state law.

Designation of critical habitat can have a major effect on the exercise of water rights because the designation essentially reallocates water for species protection (41). Utilization of state water rights is subject to the ESA's prohibition against the "take" of a listed species under Section 9 (42). Under these provisions, in-stream flow requirements for listed species can trump water rights, including water rights apportioned by interstate compact (43). Therefore, while water for listed species does not have a fixed priority date, it effectively supersedes all competing uses. Moreover, in-stream flow requirements for listed fish may require operation of reservoirs to maximize species protection, effectively subordinating state-created water rights and Federal Bureau of Reclamation water rights to species protection (43).

Plant Life

The most geologically prospective oil shale area is home to several plant species, already subject to federal protections, as well as several additional plant

species that are candidates for federal protection. ESA protections applicable to plants are different than those affecting fish and wildlife. While the section 9 prohibition against taking protected species does not apply to plants (44), the ESA does make it illegal to:

[R]emove and reduce to possession any [plant] species from areas under Federal jurisdiction; maliciously damage or destroy any such species on any such area; or remove, cut, dig up, or damage or destroy any such species on any other area in knowing violation of any law or regulation of any State or in the course of any violation of a State criminal trespass law (45).

Section 7 consultation requirements still apply, and all federal agencies must

[I]nsure that any action authorized, funded, or carried out by such agency . . . is not likely to jeopardize the continued existence of any endangered species or threatened species or result in the destruction or adverse modification of habitat of such species which is determined by the Secretary, after consultation as appropriate with affected States, to be critical (28).

Oil shale development poses a unique set of challenges with respect to rare plant species, as several endemic species are known to grow only on oil shale outcrops. Efforts to increase knowledge about these scarce and legally protected plant resources, inventorying known and potential habitat, and researching the feasibility of reintroducing populations into areas that are subject to less development pressure would benefit both developers and policymakers. Conducting such surveys and analysis prior to leasing also would help ensure that potential bidders have an accurate assessment of potential development constraints.

Competing Mineral Development

Another challenge for future oil shale development is competing, co-located resource development. The BLM has said that “[c]ommercial oil shale development . . . is largely incompatible with other mineral development activities and would likely preclude these other activities while oil shale development and production are ongoing” (46). Depending on the technologies used, extracting oil shale or the organic component of the oil shale prior to oil and gas development, or the reverse, may impact the later extraction of the other resource (47). For example, prior fluid mineral development that has resulted in significant geologic fracturing or drilling might compromise either groundwater management or the ability to efficiently locate wells for in-situ oil shale production. Conversely, fracturing for in-situ oil shale development has the potential to damage cap rock containing natural gas. Advance evaluation of

the scope of this potential conflict, as well as possible solutions, would benefit both developers and policymakers, and would add certainty to future oil shale development scenarios.

The potential for conflicts over co-located mineral management and development is significant as a large portion of the federal lands available for oil shale leasing are already the site of oil and gas exploration (47). According to the Utah Geological Survey:

A significant portion of the Uinta Basin's oil-shale resource, approximately 25% for each grade, is covered by conventional oil and gas fields. . . . In particular, the extensive Natural Buttes gas field covers a significant portion of land underlain by oil shale averaging 25 GPT [gallons per ton], ranging to 130 feet thick, and under roughly 1500 to 4000 feet of cover. Furthermore, this field is expected to expand in size and cover more oil-shale rich lands to the east. Of the 18.4 billion barrels contained in 25 GPT rock having thicknesses between 100 and 130 feet, 7.8 billion barrels, or 42%, are located under existing natural gas fields.

However, lands where the oil-shale deposits are under less than 1000 feet of cover currently do not contain significant oil and gas activity (except the Oil Springs gas field) as compared to lands with deeper oil-shale resources. The majority of planned oil-shale operations will be located on lands having less than 1000 feet of cover. This does not mean that oil-shale deposits located within oil and gas fields will be permanently off limits. In fact, most of the conventional oil and gas reservoirs are located far below the Mahogany zone. It simply demonstrates that regulators will need to recognize that resource conflicts exist and plan their lease stipulations accordingly (48).

Similarly, the Congressional Research Service estimates that within the most geologically prospective oil shale areas administered by the BLM, 94% of the land in Colorado is already leased for oil and gas, 83% of the land in Utah is already leased for oil and gas, and 71% of the land in Wyoming is already leased for oil and gas (3).

Where multiple minerals occur on private land, the mineral estate owner can treat them as he or she wishes, contractually prescribing conditions for third party development. But because the United States operates under an array of allocation systems for different types of minerals, development of multiple minerals on federal land can present difficult complications (49). While the Multiple Mineral Development Act (50) provides some guidance for conflicts between lessees and locators, it does not apply to conflicts arising between persons interested in different leasable minerals such as oil shale and oil or natural gas (51). Instead, potential oil shale lessees must rely on the BLM's regulatory provision, which states:

The granting of a permit or lease for the prospecting, development or production of deposits of any one mineral shall not preclude the issuance

of other permits or leases for the same lands for deposits of other minerals with suitable stipulations for simultaneous operation, nor the allowance of applicable entries, locations or selections of leased lands with a reservation of the mineral deposits to the United States (52).

The BLM's RD&D leasing program for oil shale confirms its policy of addressing multiple mineral conflicts at the leasing stage. Under an RD&D lease, the BLM reserves the "right to continue existing uses of the leased lands and the right to lease, sell, or otherwise dispose of the surface or other mineral deposits in the lands for uses that do not unreasonably interfere with operations of the Lessee under this lease" (53). Under the final commercial leasing rules, commercial leases will contain a similar provision, allowing multiple use development so long as it "does not unreasonably interfere with the exploration and mining operations of the lessee" (54). These lease provisions reiterate the BLM's intended policy of managing potential mineral development conflicts on a case-by-case basis at the leasing stage.

Some earlier federal oil and gas leases offer clearer protections for potential oil shale lessees. Between 1968 and 1989, federal oil and gas leases issued on oil shale-bearing lands in Colorado, Utah, and Wyoming contained stipulations protecting the interests of future oil shale developers, generally preventing oil and gas drilling that would result in undue waste of oil shale resources or otherwise interfere with development of the oil shale resource (46).

Leases issued on Utah School and Institutional Trust Lands reserve "the right to enter into mineral leases and agreements with third parties covering minerals other than the leased substances, under terms and conditions that will not unreasonably interfere with operations under this Lease in accordance with Lessor's regulations, if any, governing multiple mineral development" (55). These leases also reserve the right to designate Multiple Mineral Development Areas and impose additional terms and conditions deemed necessary to effectively integrate and coordinate the development of multiple minerals (56). Consequently, the management of multiple mineral development conflicts on Utah School and Institutional Trust Lands is largely committed to agency discretion, while affording some degree of protection to the first leaseholder to develop his or her rights.

Managing Competing Water Demands

Addressing water demand turns first and foremost on water availability. Thus any discussion of water availability for oil shale development must begin by considering the allocations and recognized shortages within the existing system of water rights. Although quantified water demands associated with oil shale extraction technologies may not yet be known, realistic evaluations of water in the system that is actually available for oil shale development would be of benefit to developers and policymakers alike.

Water rights associated with most of the geologically prospective oil shale areas are governed by the Colorado River Compact (57) and state law. The Colorado River Compact apportions water among the seven states that drain to the Colorado River: Arizona; California; Colorado; Nevada; New Mexico; Utah; and Wyoming (58). The Compact divides the watershed into Upper and Lower Basins based on whether lands drain to the Colorado River at points above or below Lee Ferry, Arizona (59). State law controls allocation of each state's Compact apportionment. The most important aspect of Colorado and Utah's state water rights system is their common reliance on the prior appropriations doctrine. In both states, the first in time is the first in right and during times of drought, senior water right holders are entitled to their entire right before junior water right holders receive any water from that source.

Under the Compact, both the Upper and Lower Basins are entitled to annual consumptive use of up to 7,500,000 acre-feet of water (60). The Lower Basin also has "the right to increase its beneficial consumptive use of such waters by one million acre-feet per annum," which can be exercised after all other obligations are met (61). Pursuant to treaty, Mexico is entitled to 1,500,000 acre-feet annually (62). Mexico's entitlement was intended to be provided out of surplus flows; however, where surplus flows are not available, the treaty obligation is satisfied by an equal reduction in each Basin's apportionment.

The Upper Basin's stated annual entitlement to 7,500,000 acre-feet is somewhat misleading as the Upper Basin assumed the risk that during times of shortage it would be forced to reduce its water consumption in order to satisfy the Compact rights of the Lower Basin (63, 64). There are rarely sufficient surpluses to accommodate obligations to Mexico so the Upper Basin normally satisfies its half of the obligation to Mexico, 750,000 acre-feet, by reducing allowable diversions. More importantly, the Upper Basin's original apportionment under the Compact was based on assumed levels of flow that rarely occur.

The data relied upon during Compacts negotiations supported the premise that the Colorado River flows averaged at least 17,400,000 acre-feet at Lee Ferry (65, 66). In actuality, the river flow from 1906 through 2005 ranged between 5,399,000 and 25,432,000 acre-feet, averaging 15,072,000 acre-feet (67, 68). More recent estimates of average annual streamflow are often even lower. Considering realistic estimates of river flows and the Upper Basin's obligations to the Lower Basin and Mexico, the Upper Basin states are left with an average annual allocation of at most 6,000,000 acre-feet or 80% of their original anticipated apportionment under the Compact.

The Upper Basin's share is further apportioned internally under the Upper Colorado River Compact (69). Arizona receives 50,000 acre-feet annually; Colorado, New Mexico, Utah, and Wyoming receive 51.75, 11.25, 23, and 14 percent of the remainder, respectively (70). Applying these percentages to the 6,000,000 acre-foot figure indicates that Colorado and Utah's right to divert from the Colorado River (and its tributaries) are respectively 3,079,000 and 1,369,000 million acre feet annually. Reasonable estimates are that, on an average year, Colorado has roughly 1,000,000 acre-feet of unused appropriations under the Compact (71). Utah has, during an average year, roughly 520,000 acre-feet of unused Colorado River apportionments (71).

Utah is one of the driest states in the West (72) and reliable water supplies are crucial to municipal, recreational, industrial and agricultural development. Although Colorado enjoys higher levels of precipitation, it too faces severe internal and external competition for water resources. Compounding these water management challenges, both Utah and Colorado have experienced, and continue to experience, rapid population growth. Consequently, oil shale developers and water resource planners must consider not just the water demand that is directly and indirectly due to oil shale development, but the demand that is likely to occur independent of oil shale development.

In Colorado, the populations of Moffat, Rio Blanco, and Routt counties (which make up the majority of the Yampa/White/Green river basin) are anticipated to grow by 56% between 2000 and 2030, from 39,300 to 61,400 (73). Gross water demand is anticipated to increase by 79% over the same period, from 29,400 to 52,600 acre-feet (73). Although Colorado believes that 900 acre-feet of water can be offset through conservation, 22,300 acre-feet of new depletions are anticipated within Colorado's portion of the most geologically prospective oil shale area without accounting for direct and indirect demand associated with oil shale development.

In Utah, the State Water Plan for the Uinta Basin places the basin's population at 39,596 in 1998, projecting an increase of 15,855 people or 29% by 2020, bringing total basin population to 54,706 (74). Basin employment is projected to increase from 17,823 jobs in 1995 to 28,025 in 2020 (75). Municipal and industrial diversions from public suppliers within the basin is anticipated to increase from 13,140 acre-feet in 2000 to 16,900 acre-feet in 2020 (76); industrial depletions from privately held water rights, which are generally around half the volume diverted, are projected to increase from 11,830 acre-feet in 1996 to 23,700 acre-feet in 2050 (77). As with the Colorado projections, these figures do not reflect potential water demands for commercial oil shale development. Non-agricultural irrigation is projected to increase diversions by 770 acre-feet over the same period while irrigation related diversions falls to 790,480 acre-feet from its 1995 level of 797,610 acre-feet (76). Clearly, oil shale developers will become subject to increasingly fierce competition for constrained water supplies as Colorado and Utah continue to grow.

Prospective oil shale developers have long recognized the value of senior rights to large quantities of water, having already obtained extensive rights in portions of the Piceance Basin as well as in the Uinta Basin. These rights fall into two general classifications: (1) conditional or unperfected water rights, often with priority dates in the 1950s and 1960s that are tied to storage, and (2) very senior agricultural water rights, often with priorities dating to the 1880s or earlier, that are currently being leased to agricultural users.

In Colorado, conditional water rights allow developers to secure rights to water prior to starting construction on capital intensive projects such as reservoirs. Provided that the developer exercises sufficient diligence in developing their project, the priority date reverts back to the date of the initial application. Utah achieves much the same result through the "relating back" doctrine. Therefore, while undeveloped, some large water rights could be senior to important existing diversionary rights. Development of these conditional rights would make less

water available to some existing junior water rights holders. Potentially affected interests include communities along Colorado's Front Range holding relatively junior rights to augment existing supplies as well as resort communities and recently developed towns on Colorado's western slopes. These communities could be severely impacted if oil shale development undermines the security of their planned water supplies (78, 79).

An almost certain consequence of increased interest in oil shale development is increasing scrutiny of conditional water rights. As water users increasingly see conditional right development as a threat to their water supplies, they will invariably grow more aggressive in challenging industry's diligence in pursuing development. Furthermore, many of the proposed reservoir sites are located high in the watershed. If located within inventoried roadless areas, management requirements may complicate, if not prohibit, reservoir construction (80). Development of these valid legal rights will almost certainly face fierce legal challenges.

Conversion of acquired agricultural water rights pose other planning challenges. These often very senior agricultural rights almost invariably allowed diversion of far more water than was actually consumed in exercising the rights, the excess being used to create water pressure and move water through the irrigation system. However, when these rights are converted to other uses such as oil shale development, only the amount of water actually consumed is made available for the new use (81). Another planning challenge of reallocating agricultural water use to oil shale development is the impacts of lost agricultural production. Traditionally, the most valuable water rights are held by the most well-established and productive farms in the area. These farms are generally dominant forces in the local communities; removing them from community life can significantly alter the fabric of these communities.

The direct and indirect water demands of a commercial oil shale industry are not well defined and, absent emergence of a viable technology, cannot be known. The BLM estimates that conventional mining with surface retorting will require from 2.6 to 4.0 barrels of water for each barrel of shale oil produced (82, 83). Estimating water needs for in-situ retorting is similarly imprecise. Although the BLM cites a 2005 Rand Corporation study (84) for the proposition that in-situ development would require one to three barrels of water for each barrel of oil produced (85), that same Rand study predicts that "[r]eliable estimates of water requirements will not be available until the technology reaches the scale-up and confirmation stage" (84). Dr. Laura Nelson, Chair of the Utah Mining Association's Oil Shale and Oil Sands Committee, recently testified that water use is falling rapidly as industry continues to innovate and currently sits at an average of 1.5 barrels of water for each barrel of shale oil produced, with some processes using almost no water (86).

The Utah Mining Association has also suggested that water re-use technologies have the potential to reduce water demand associated with oil shale development facilities:

Many of the oil shale and tar sands deposits in Utah are located near existing oil and gas activities where produced water is generally trucked

from the site or replaced through injection wells. With injection well siting providing its own set of challenges and water removal transport requiring additional roadway activity, the environmental benefits of utilizing local produced water extend beyond minimization of fresh water requirements. Solutions such as recycling of produced water from conventional oil and gas production could be utilized to help offset water requirements for oil shale production (87).

While water demand is currently uncertain, changing technologies bring with them the promise of greatly reduced water usage. However, even if direct demand for water is much less than BLM projections suggest, the impacts of competing uses and indirect demands for water (including increased demands resulting from population growth due to oil shale development) will remain significant, especially as competition for scarce resources increases. Moreover, re-using water generated during oil and gas development raises complicated legal issues that must be resolved before re-use can be treated as a potential source of supply.

Conclusion

Although the path to commercial oil shale development is fraught with uncertainties, some environmental and resource management challenges can be addressed even at this preliminary stage. Prior to selection of oil shale technologies, the decision to identify and plan potential oil shale development sites in a manner that conserves protected and threatened wildlife, as well as aquatic and plant resources, can be made even in the absence of a full commercial development plan. Similarly, developers and policymakers can begin now to determine how best to approach the various issues presented by the development of oil shale and other co-located minerals. Lastly, analysis of competing demands for water, and the impacts of shifting water resources from those demands to oil shale, can and should be addressed now, well in advance of any commercial scale oil shale leasing and development. Identifying and coordinating analysis of these fundamental resource management challenges will serve to benefit developers, policymakers and the public and can set a sound precedent for proactively working through the several environmental and resource management challenges that are sure to accompany future steps towards commercialization of the oil shale resource.

References

1. Youngquist, W. Shale Oil – The Elusive Energy. *Hubbert Center Newsletter*; M. King Hubbert Ctr. For Petroleum Studies: Golden, CO, October, 1998 at 5.
2. Branscomb, J. *Focus on Energy Policy: U.S. Oil Shale – From Resources to Reserves*, 6 Geo. J.L. & Pub. Pol’y 397, 2008; pp 398–405.

3. Andrews, A. *Developments in Oil Shale*; Congressional Research Service: November 17, 2008.
4. *Strategic Significance of America's Oil Shale Resource, Vol. I, Assessment of Strategic Issues*; Office of Deputy Assistant Secretary for Petroleum Reserves, Office of Naval Petroleum and Oil Shale Reserves: 2004.
5. *America's Oil Shale: a Roadmap for Federal Decision Making*; Deputy Assistant Secretary for Petroleum Reserves, Office of Naval Petroleum and Oil Shale Reserves: 2004.
6. *Energy Policy Act of 2005 § 369(c)*, codified at 42 U.S.C. § 15927(c).
7. *Interior Department Issues Oil Shale Research, Development and Demonstration Leases for Public Lands in Colorado*; News Release; U. S. Bureau of Land Management: December 15, 2006.
8. *Interior Department Issues Oil Shale Research, Development and Demonstration Lease for Public Lands in Utah*; News Release; U.S. Bureau of Land Management: June 28, 2007.
9. *Energy Policy Act of 2005 § 369(b)*, codified at 42 U.S.C. § 15927(b).
10. The BLM approximates that only 60% of the most geologically prospective oil shale resource is found on federal lands. *Proposed Oil Shale and Tar Sands Resource Management Plan Amendments to Address Land Use Allocations in Colorado, Utah, and Wyoming and Final Programmatic Environmental Impact Statement*; U.S. Department of Interior, Bureau of Land Management: September 2008; Final PEIS, at 2-13.
11. Within the most geologically prospective area for oil shale, the ESA is administered by the Department of Interior through the U.S. Fish & Wildlife Service. *16 U.S.C. §§ 1531-43*; 2008.
12. *Village of False Pass v. Clark*, 733 F.2d 605, 611-12, 9th Cir. 1984; holding additional Section 7 consultation is required where initial consultation identifies only conceptual measures and other statutes require additional information regarding development at later phases.
13. *Accord Pit River Tribe v. U.S. Forest Service*, 469 F.3d 768, 783-84, 9th Cir. 2006, holding supplemental NEPA required for development where leasing analysis does not consider impact of development.
14. *Connor v. Burford*, 848 P.2d 1441, 1453-54, 9th Cir. 1988.
15. *Comments of Colorado Governor Bill Ritter on BLM Oil Shale and Tar Sands Programmatic EIS*, March 20, 2008, reprinted in Final PEIS, September 2008; vol. 4, p 5313.
16. <http://atlas.utah.gov/wildlife/viewer.htm>.
17. *Proposed Resource Management Plan and Final Environmental Impact Statement*, Figure-46; U.S. Department of the Interior, Bureau of Land Management, Vernal Field Office: August 2008.
18. *16 U.S.C. § 1533(a)(1)*.
19. *16 U.S.C. § 1533(a)(1)*, (A) through (E).
20. *16 U.S.C. § 1531(b)*.
21. Under the ESA, species may be listed as either endangered or threatened: "endangered" species are in danger of extinction throughout all or a significant portion of their range, *16 U.S.C. § 1532(6)*; "threatened" species are likely to become endangered within the foreseeable future, *16 U.S.C. §*

1532(20). Section 4 of the ESA requires species to be listed based solely on their biological status and threats to their existence; economic impacts of a listing decision are not considered, 16 U.S.C. § 1533. The USFWS also maintains a list of “candidate” species which warrant listing, but whose listing is precluded by higher listing priorities.

22. 16 U.S.C. § 1538(a)(1)(B).
23. 16 U.S.C. § 1538(a)(1).
24. *Babbitt v. Sweet Home Chapter of Communities for a Great Oregon*; 515 U.S. 687, 703, 1995.
25. 16 U.S.C. § 1532(19).
26. 50 C.F.R. § 222.102.
27. 16 U.S.C. § 1536(a).
28. 16 U.S.C. § 1536(a)(2).
29. 16 U.S.C. § 1536(b)(3).
30. 16 U.S.C. § 1533(a)(3)(A).
31. 16 U.S.C. § 1532(5)(A)(i).
32. 16 U.S.C. § 1532(5)(A)(ii).
33. 16 U.S.C. § 1533(b)(2).
34. 16 U.S.C. § 1539.
35. 16 U.S.C. § 1539(a).
36. 16 U.S.C. § 1539(a)(2).
37. *Utah's State Listed Species by County*; Utah Division of Wildlife Resources: July 1, 2008).
38. <http://www.westgov.org/wga/initiatives/corridors/index.htm>.
39. *Statewide Water Supply Initiative*; Colorado Water Conservation Board: November 2004; p 3–83.
40. The four endangered fish are the Humpback Chub (*Gila cypha*), Bonytail Chub (*Gila elegans*), Colorado Pikeminnow (*Ptychocheilus lucius*), and the Razorback Sucker (*Xyrauchen texanus*). <http://criticalhabitat.fws.gov/>.
41. Tarlock, A. D. *Law of Water Rights and Resources*; § 9.29, 2008.
42. *United States v. Glenn-Colusa Irrigation Dist.*, 788 F.Supp 1126, 1134, E.D. Cal., 1992.
43. Tarlock, A. D. *Law of Water Rights and Resources*, § 9.31, 2008.
44. 16 U.S.C. §§ 1538(a)(2).
45. 16 U.S.C. § 1538(a)(2)(B).
46. *Final PEIS*, at 4-18.
47. Lundberg, C. K. *Shale We Dance? Oil Shale Development in North America: Capoeira or Funeral?*, 52 Rocky Mtn. Min. L. Inst. 13-1, 2006.
48. Vanden Berg, M. D. *Basin-Wide Evaluation of the Uppermost Green River Formation's Oil-Shale Resource, Uinta Basin, Utah and Colorado*: Utah Geological Survey, 10, 2008, internal references omitted.
49. Coggins, G. C. ; Glickman, R. L. *Public Natural Resources Law § 41:1*, 2nd ed., 2008; see generally.
50. 30 U.S.C. §§ 521-531.
51. 30 U.S.C. § 526(a).
52. 43 C.F.R. § 3000.7.

53. *Oil Shale Research, Development and Demonstration (RD&D) Lease*; United States Department of the Interior, Bureau of Land Management: 70 Fed. Reg. 33755, June 9, 2005.
54. 73 Fed. Reg. 69414, 69472, November 18, 2008, codified at 43 C.F.R. § 3900.40.
55. *Utah State Mineral Lease for Oil Shale § 2.2*, Oil Shale Lease Form 6/22/05.
56. *Utah State Mineral Lease for Oil Shale § 15*, Oil Shale Lease Form 6/22/05.
57. *Colorado River Compact*, 70 Cong. Rec. 324, 1928. Congress officially approved the Colorado River Compact in the Boulder Canyon Project Act, 43 U.S.C. § 617l, 2000.
58. *Colorado River Compact at Preamble*.
59. *Colorado River Compact at Art. II §§ (f) and (g)*.
60. *Colorado River Compact at Art. III § (a)*.
61. *Colorado River Compact at Art. III § (b)*.
62. *Treaty Between the United States of America and Mexico Respecting Utilization of Waters of the Colorado and Tijuana Rivers and of the Rio Grande*, Act of Feb. 3, 1944, U.S.–Mexico 59 Stat. 1219 at Art. 10.
63. *Colorado River Compact at Art. III § (d)*.
64. Adler, R. W. *Restoring Colorado River Ecosystems: A Troubled Sense of Immensity*; 22, 2007.
65. Hundley, N., Jr. *Water and the West: The Colorado River Compact and the Politics of Water in the American West*, 184, 1975.
66. Compact negotiators are reported as claiming that the Colorado River had a total supply of as much as 21.6 million acre feet; on file with authors. Kuhn, E. *The Colorado River: The Story of a Quest for Certainty on a Diminishing River*; 22 n. 63, Roundtable ed., May 8, 2007.
67. *Final Environmental Impact Statement, Colorado River Interim Guidelines for Lower Basin Shortages and Coordinated Operations for Lake Powell and Lake Mead*; U.S. Dept. of Interior, Bureau of Reclamation: 3-15, October 2007.
68. Other analysis, including studies extending the hydrologic record by analyzing tree ring data conclude that undeveloped flow at Lee Ferry is probably closer to 13.5 million acre feet annually. Kuhn, E. *Colorado River Water Supplies: Back to the Future*; Southwest Hydrology 20, March/April 2005.
69. *Pub. L. No. 81-37*, 63 Stat. 31; Upper Colorado River Compact: 1949.
70. *Upper Colorado River Compact at Art. III § (a)*.
71. Between 1998 and 2006, Colorado consumed an average of 2,060,000 acre-feet of Colorado River Basin water annually. Given a right to consume up to 3,079,00 acre-feet annually, Colorado has roughly 1,000,000 acre-feet remaining. Between 1998 and 2006, Utah consumed an average of 848,000 acre-feet of Colorado River Basin water annually. Given a right to consume up to 1,369,000 acre-feet annually, Utah has roughly 520,000 acre-feet remaining. *Provisional Upper Colorado River Basin Consumptive Use and Losses Reports*: U.S. Department of the Interior, Bureau of Reclamation: <http://www.usbr.gov/uc/library/envdocs/reports/crs/crsul.html>.

72. Clyde, S. E. *Marketplace Reallocation in the Colorado River Basin: Better Utilization of the West's Scarce Water Resources*, 28 J. Land Resources & Envtl. L. 49, 50, 2008.
73. *Statewide Water Supply Initiative Fact Sheet*; State of Colorado: February 2006.
74. *Utah State Water Plan: Uinta Basin*; Utah Department of Natural Resources, Division of Water Resources: December 1999; p 4-1.
75. *Utah State Water Plan: Uinta Basin*; Utah Department of Natural Resources, Division of Water Resources: December 1999; p 2-2.
76. *Utah State Water Plan: Uinta Basin*; Utah Department of Natural Resources, Division of Water Resources: December 1999; p 9-14.
77. *Utah State Water Plan: Uinta Basin*; Utah Department of Natural Resources, Division of Water Resources: December 1999; p 18-2.
78. *Water on the Rocks: Oil Shale Water Rights in Colorado* ; Western Resource Advocates: 2009; pp 33–35, discussing communities whose domestic water rights that may be impacted by development of conditional water rights for oil shale.
79. *Water on the Rocks: Oil Shale Water Rights in Colorado* ; Western Resource Advocates, 2009; Figures 3 and 5.
80. Harmon, G. Grand Junction, Ute Water Officials See Threat to Water Storage. *The Grand Junction Daily Sentinel*, March 21, 2009; Gov. Bill Ritter could back a proposal for prohibiting water storage in roadless areas of national forests in Colorado.
81. *Oil Shale Development in Northwestern Colorado: Water and Related Land Impacts*; University of Wisconsin-Madison: 1975; pp 198-200.
82. *Final PEIS*, at 4-4, 4-8.
83. *Final Environmental Impact Statement for the Prototype Oil Shale Leasing Program*; U.S. Department of Interior: 1973; Vol. 1, p III-34.
84. Bartis et al. *Oil Shale Development in the United States: Prospects and Policy Issues*; Rand Corporation: 2005; 50.
85. *Final PEIS* , at 4-11.
86. *Testimony before the Utah Legislature's Interim Committee on Natural Resources, Agriculture, and the Environment*; June 17, 2009; <http://le.utah.gov/asp/interim/Commit.asp?Year=2009&Com=INTNAE>.
87. Nelson, L. S.; Wall, T. J. *Development of Utah Oil Shale and Tar Sands Resources*; Utah Mining Association: October 2008; 9.

Subject Index

A

- Agricultural water rights, 295
- Air quality impact
 - environment, 252, 253
 - R&D needs prioritization, 255*t*
- Alaska
 - oil shale, 6
 - oil shale quality, 9*t*
- Alberta oil sands
 - capital costs for upgrading, 269, 271, 272
 - mining energy, 91
 - overall efficiency, 100
- Alberta Taciuk Process (ATP)
 - estimates of carbon dioxide emissions, 237, 243*f*
 - horizontal rotating kiln, 39–40, 44*f*
- Albert oil shale, Canada, 16
- Alum shale, Sweden, 17
- American Shale Oil, LLC (AMSO)
 - calculated temperature around vacuum insulated tubing vs. distance and time, 156, 157*f*
 - carbon dioxide generation, 158
 - cavity diameters formed during nahcolite recovery, 153*t*
 - CCR™ retort (conduction, convection and reflux)
 - concept, 150–154
 - convective vs. conductive heat transfer, 156, 158*f*
 - EGL technology, 46*t*, 56–57, 128
 - heat delivery capacity at
 - constant pressure drop, 154, 156, 157*f*
 - heating issues, 154, 156
 - horizontal heater and production wells in illite-rich oil shale at Green River Formation base, 152–153, 155*f*

- oil shale strategy and environment, 159
 - possible commercial implementation of CCR process, 154, 155*f*
 - propagation of
 - thermomechanical fracture wave at retort boundary, 151, 153*f*
 - strength and stress vs. temperature, 150, 152*f*
 - thermomechanical fragmentation, 152*f*
 - water, CO₂ and energy gain issues, 156–158
- AMSO. *See* American Shale Oil, LLC (AMSO)
- Anatolia, Turkey oil shale, 18
- Aquatic life, oil shale development, 289
- Attarat Um Ghudran deposit, Jordan, 12, 13*t*
- Australia
 - map of oil shale deposits, 14*f*
 - oil shale characteristics, 15*t*
 - oil shale deposits, 13–15
 - resource volume, 7*t*

B

- Backpressure
 - carbon number distribution vs. imposed, 164, 172*f*
 - chemical composition changes with, 164, 172*f*
 - hydrogen content of in-situ conversion process (ICP), 164, 171*f*
- Best Available Control Technology (BACT), evaluation, 258
- Bioturbation
 - Green River Formation, 75
 - method, 66

- Bitumen production, laboratory testing, 164, 170*f*
- Bituminous coal, methane and hydrogen evolution profiles from, 121, 124*f*
- Borehole microwave, Phoenix-Wyoming, 46*t*, 51
- Brazil
 map of oil shale resources, 10*f*
 oil shale characteristics, 11*t*
 oil shale deposits, 9–10
 Petrosix retort, 34
 resource volume, 7*t*
 surface technologies, 23
- Bureau of Land Management (BLM)
 Energy Policy Act of 2005, 250–251
 mineral development, 290–292
 Programmatic Environmental Impact Statement (PEIS), 252
 regulations for lease acquisition, 272–274
 water demands, 295
See also Environment
- C**
- Calcareous mudstones, Green River Formation, 70–72, 76*f*
- Calcined coke
 calcining temperature and coke resistivity, 190*f*
 oil shale-conductant sandwich construction, 190*f*
 photograph, 188, 189*f*
 resistivity, 188, 189*f*
- Calcite
 decomposition, 224*t*, 228
 fraction decomposed vs. time and temperature, 230*f*
- California, Union Oil Company, 34
- Canadian Association of Petroleum Producers (CAPP), capital and operating costs, 280–282
- Capital costs
 oil sands upgrading, 272*t*
 oil shale, variance, 281*f*, 282
 oil shale development, 267, 268*t*
See also Economics
- Carbon dioxide
 annual generation from oil shale production, 235–236, 238*f*
 carbonate decomposition models, 228, 230*f*
 comparing full-fuel-cycle, emissions estimates, 237–238, 243*f*
 cumulative probability plot for, release, 236, 239*f*
 emission by auxiliary energy use in retorting, 225–226
 emission from hydrocarbon generation in oil shale retorting, 221–228
 emission from oil shale, 226–228
 emissions from thermal requirements for retorting, 221–225
 enthalpy change with mineral reactions, 224*t*
 estimates of, emissions from oil shale production processes, 243*f*
 fraction produced by power plant, nahcolite breakdown, and kerogen pyrolysis, 236, 239*f*
 from combustion of shale-derived gasoline and diesel, 233
 from materials inputs to extraction, 233
 generation during oil shale recovery, 158
 generation rate during fluidized-bed isothermal pyrolysis of Colorado oil shale, 122–123, 125*f*
 importance of variables to, produced by oil shale, 236, 240*f*
 key sources, 220
 mineral reactions, 222, 224*t*

- mitigation of, emissions, 239–243
- modeling methods, 234–235
- oil shale and, 219–220
- oxygen removed from kerogen as, vs. nahcolite weight fraction, 236, 241*f*
- probabilistic model for, generation from shale oil production, 234–237
- production as function of average Fischer Assay of oil shale, 236, 240*f*
- uncertainty in magnitude of carbon emissions, 233–237
- yield vs. shale grade for Green River oil shale, 226, 229*f*
- Carbon footprint, estimate for oil production, 145
- Carbon intensity, thermal energy sources, 227*t*
- Carbon number distribution in Mahogany field experiment, 169, 174*f*
- distribution vs. backpressure, 172*f*, 174*f*
- range of ICP vs. surface retorted oil, 164, 167*f*
- CCR™ retort (conduction, convection and reflux). *See* American Shale Oil, LLC (AMSO)
- Characteristics, U.S. oil shale, 9*t*
- Chattanooga Process, fluidized bed combustion, 36–37, 42*f*
- Chemical log, Green River Formation well P4, 69*f*
- Chevron CRUSH process, hot gas injection, 46*t*, 52–54, 55*f*; 128, 129–130
- China oil shale characteristics, 17*t*
- oil shale deposits, 15–16
- resource volume, 7*t*
- surface technologies, 23
- Clastic mudstones, Green River Formation, 70, 72*f*
- Coal, carbon intensity, 227*t*
- Coke. *See* Calcined coke
- Coking concentration comparison, 143, 144*f*
- nature of oil, 123
- oil and yield losses, 125–126
- reactions affecting oil yield, 123
- Colorado gas generation during fluidized-bed isothermal pyrolysis of, oil shale, 122–123, 125*f*
- Green River Formation, 6, 8*f*, 64, 66*f*
- Long Ridge Project, 34
- methane and hydrogen evolution profiles from oil shale, 121, 124*f*
- Piceance Basin, 149–150, 162, 181
- true-in-situ retorting, 128
- water demands, 294–295
- See also* Green River Formation (GRF)
- Colorado Energy Research Institute (CERI), environmental workshops, 251
- Colorado River Compact, water rights, 293
- Colorado School of Mines (CSM), Oil Shale Symposium, 251
- Completion strategy basic initial value problem in superposition approach, 203, 205*f*
- calculated yields from kerogen chemical decomposition model, 204, 206*f*
- Electrofrac, 200–207
- geomechanical model, 200–202, 203*f*
- hydrocarbon generation through time, 207, 209*f*
- procedure for screening calculations, 204, 207*f*
- rock physical properties for Electrofrac screening calculations, 206, 208*t*

- stacking multiple layers of heating wells, 202, 204*f*
 temperature and kerogen conversion history for two layers of staggered Electrofracs, 206, 209*f*
 thermal conduction screening tools, 203–205
See also ExxonMobil Electrofrac™ Process
- Composition
 oil shale, 4
See also Shale oil composition
- Conductant identification
 calcining temperature and coke resistivity, 190*f*
 Electrofrac, 188, 189*f*, 190*f*
- Core sedimentology. *See* Green River Formation
- Cost variance
 impact of, on capital and operating costs, 280–282
 market dynamics, 280
 oil shale capital, 281*f*, 282
 oil shale operating, 282*f*
See also Economics
- Cracking
 kinetic models of oil, 123–125
 oil yield vs., of generated oil, 128*f*
 reactions affecting oil yield, 123
- CRUSH process, Chevron's hot gas injection, 46*t*, 52–54, 55*f*, 128, 129–130
- Curly Tuff, Green River Formation, 68, 74–75, 79*f*
- D**
- Dawsonite, Piceance Basin of Colorado, 207
- Deep heater test (DHT), Shell's Mahogany site, 178
- Degradation, kinetics of oil, 123–126
- Democratic Republic of the Congo, resource volume, 7*t*
- Demonstration pilot, Shell's in-situ conversion process (ICP), 180–181
- Department of Defense (DoD), shale oil JP-8 jet fuel, 174, 179*t*
- Department of Energy (DOE)
 Office of Petroleum Reserves, 251
 potential oil shale impacts, 250
See also Environment
- Department of Interior (DOI)
 Bureau of Land Management (BLM), 250–251
 regulations for lease acquisition, 272–274
 U.S. Geologic Survey (USGS), 249–250
See also Environment
- Deposition, oil shale, 3–4
- Development
 Shell's in-situ conversion process (ICP), 180–181
 uncertainty and economics, 263–264
See also Economics
- Devonian Kettle Point Formation, Canada, 16
- Dictyonema Shale, Estonia, 15
- Direct current, in-situ heating, 46*t*, 52, 53*f*
- Direct heating
 Fushun retort, 35, 37*f*
 Gas Combustion Retort (GCR), 32–33
 Kiviter technology, 35–36, 41*f*
 Paraho technology, 33–34, 35*f*
 Petrosix, 34
 Union B Retort, 34–35
- Distribution, oil shale, 4
- Dolomite
 enthalpy change, 224*t*
 fraction decomposed vs. time and temperature, 230*f*
- Dolomitic mudstones, Green River Formation, 72–73, 77*f*
- Dow Chemical, in-situ process, 45, 46*t*

Down hole heaters, Shell In-Situ
Conversion Process (ICP), 46*t*,
47–48, 49*f*
Drilling costs, Green River
Formation (GRF), 269, 270*f*

E

Earth Search Sciences, Inc., hot gas
injection, 46*t*, 54, 55*f*
Eastern oil shale, methane and
hydrogen evolution profiles
from, 121, 124*f*
Eastern Queensland, oil shale
deposits, 14–15
Eastern United States
oil shale, 8
oil shale characteristics, 9*t*
oil shale quality, 9*t*
oil yield vs. heating rate, 123,
126*f*

Economics

Canadian oil sands capital costs,
278*f*, 280
Canadian oil sands operating
costs, 278*f*, 280
capital costs, 267, 268*t*, 272*t*,
275*t*
cash flow of generic oil shale
project, 276*f*, 279
challenges in oil shale
development, 285–286
components of oil shale
development costs, 267–268
cost variance due to market
dynamics, 280–282
current state of oil shale, 274–
282
drilling costs, 269, 270*f*
environmental impact, 252, 254
estimated costs of "1st
generation" projects, 275*t*,
279
exploration license, 273
impact of incentives, 276*f*, 279
land exchange, 274
leasing process, 273

leasing requirements, 273
logic flow of national oil shale
model, 274*f*
market dynamics, 280
market value of shale oil, 264–
265
minimum economic price, 277*f*,
279–280
mining costs, 269
modified in-situ conversion
process (MIS), 266, 268*f*,
268*t*
national oil shale model, 275–
276
oil shale capital costs variance,
281*f*, 282
oil shale operating costs
variances, 282*f*
oil shale technologies, 265–266
operating costs, 267–268, 270*t*,
275*t*
project development schedules,
271, 272*f*
provisions for royalty structure,
rent and lease bonuses, 273*t*
regulations for lease acquisition,
272–274
retorting costs, 269
risk factors for oil shale
development, 263–264
surface mining with surface
retorting, 265, 268*f*, 268*t*,
272*f*
true in-situ conversion process
(TIS), 267, 268*f*, 268*t*, 272*f*
underground mining, 266, 268*f*,
268*t*
upgrading costs, 269, 271, 272*t*
yields of produced shale oil vs.
crude oil, 266*f*

EcoShale

detailed composition, 109*t*, 110*t*,
111*t*, 112*t*
In-Capsule™ Process, 30*t*, 31,
32*f*
Red Leaf Resources EcoShale™
technology, 98
See also Shale oil composition

- Ecosystem impact, environment, 252, 253–254
- Efficiency
 oil grade and overall, 98*f*, 99
 overall, 100–101
 self-sufficiency vs. imported energy, 99–100
 thermal, and global energy, 89–90
- EGL Oil Shale LLC
 novel heat distribution method, 150
See also American Shale Oil, LLC (AMSO)
- Electrical continuity
 construction of oil shale-conductant sandwiches, 188, 190*f*
 externally heated, experiment, 188–189, 192*f*
 internally heated, experiment, 189–191, 193*f*
- Electric heaters, use for heating oil shale, 165–166
- Electricity, carbon intensity, 227*t*
- Electrofrac™ Process
 direct current in-situ heating, 46*t*, 52, 53*f*
See also ExxonMobil Electrofrac™ Process
- Electrothermic method, Swedish history, 166
- El-Lajjun deposit, Jordan, 11, 13*t*
- Emissions
 mitigation of carbon dioxide, 239–243
See also Carbon dioxide
- Endangered Species Act (ESA), oil shale development, 287–289
- Energy
 balance in retort unit, 95–96
 carbon dioxide emission by auxiliary, in retorting, 225–226
 carbon intensity of thermal, sources, 227*t*
 combustion of in-situ shale oil, 158
 Energy Policy Act of 2005, 250
 enthalpy change in mineral reactions, 224*t*
 estimated heats of retorting, 226*t*
 gain/loss by heaters, 142*f*
 industry challenge, 162
 net gain/loss estimation, 144–145
 oil prices and oil shale industry, 250
- Energy Policy Act of 2005, 250–251
- EnShale, rotary kiln with sweep gas injection, 37
- Environment
 air quality impact, 253
 Best Available Control Technology (BACT), 258
 Bureau of Land Management (BLM), 250–251
 challenges, 286
 Colorado School of Mines (CSM) and Oil Shale Symposium, 251
 Department of Energy (DOE) Oil Shale Task Force, 250
 economic impact, 254
 ecosystem impact, 253–254
 Energy Policy Act of 2005, 250
 follow-up to 2007 Oil Shale Symposium, 254–256
 future steps, 256–258
 issues and needs workshop of 2006, 252–254
 issues and needs workshop of 2007, 254
 Oil Shale Environmental Task Force, 250, 257
 permitting, 251
 Programmatic Environmental Impact Statement (PEIS), 249–250
 public perception, 251–252
 R&D needs prioritization, 255*t*
 social impact, 254
 surface impact, 253–254
 U.S. Geologic Survey (USGS), 249–250

water quality and quantity, 253
 Equation of state (EOS), phase
 behavior model, 191, 194*f*
 Equations, heat balance, 94–95
 Equity Oil and Gas, in-situ process,
 45, 46*t*
 Estonia
 Galoter process, 38, 39, 44*f*
 Kiviter lump shale retorts, 35
 map of oil shale resources, 16*f*
 oil shale characteristics, 16*t*
 oil shale deposits, 15
 resource volume, 7*t*
 surface technologies, 24
 Evaporite, Green River Formation,
 74, 79*f*
 Evolution
 Lake Uinta, 78–82
 models by lake-basin type, 80–
 82
 oil shale technologies, 23, 25*f*
 ExxonMobil Electrofrac™ Process
 activation energy spectrum for
 kerogen decomposition, 204,
 205*f*
 application of screening tools to
 typical, case, 206–207
 aromatic ring compounds and
 effective stress, 198, 199*f*
 basic initial value problem in
 superposition approach, 203,
 205*f*
 block of oil shale starting
 material, 196*f*
 calcining temperature and coke
 resistivity, 188, 190*f*
 calculated yields from kerogen
 chemical decomposition
 model, 204, 206*f*
 chemical composition of
 generated oil, 192–200
 completion strategy, 200–207
 compositional experiments, 200
 conductant identification, 188,
 189*f*, 190*f*
 core-plug-scale laboratory
 experiments, 186–187
 critical technical issues, 186
 direct current in-situ heating,
 46*t*, 52, 53*f*, 128
 effective stress and argon
 pressure influence, 198, 202*f*
 effective stress and hydrostatic
 pressure influences, 195
 electrical continuity, 188–191,
 192*f*, 193*f*
 energy-efficient method, 185,
 214
 equation-of-state (EOS) phase
 behavior model, 187, 191,
 194*f*
 experimental protocol, 192–195
 experimental results, 195–199
 geomechanical modeling, 187,
 200–202, 203*f*
 geometry, 186, 187*f*
 hydrocarbon expulsion, 191,
 194*f*
 hydrostatic pressure changes,
 198, 201*f*
 longer *n*-alkanes and effective
 stress, 196, 197*f*
 methodology for normalizing
 whole oil chromatograms,
 196, 197*f*
 normalized whole oil
 chromatograms, 198, 199*f*
 numerical models, 186–187
 oil shale-conductant sandwich
 construction for electrical
 continuity, 188, 190*f*
 phase behavior modeling of
 kerogen products, 191, 195*f*
 photos of fracture proppant and
 calcined coke, 189*f*
 Piceance Basin of Colorado,
 187, 200–202, 203*f*
 procedure for oil shale screening
 calculations, 204, 207*f*
 profile of hydrocarbon
 generation through time, 207,
 209*f*
 recovery concept for shale oil
 and nahcolite, 212*f*, 213–214
 resistivity for calcined coke
 samples, 188, 189*f*

rock physical properties for,
screening calculations, 206,
208*t*
saturated rings and effective
stress, 198, 200*f*
schematic diagram, 187*f*
schematic for heating scenario
with two layers of stacked
fractures, 202, 204*f*
sodium minerals production,
207–214
thermal conduction screening
tools, 203–205
use of fractures, 186
See also Sodium minerals

F

Facies associations, Lake Uinta, 79,
80*f*, 81
Fischer-Assay-like apparatus,
measuring oil generation, 120,
122*f*
Fluidized bed combustion
Chattanooga Process, 36–37, 42*f*
fired hydrogen heater, 36–37
Formation, oil shale, 3–4
Fracture proppant, photograph of
20/40 mesh, 188, 189*f*
Freeze point, specifications, 176
Freeze-wall technology, Shell, 46*t*,
48, 49*f*
Fuel cycle
stages, 220
See also Carbon dioxide
Full-fuel-cycle, carbon dioxide
emissions, 237–238
Fushun deposit
China, 15–16, 17*t*
lump shale retort, 35, 37*f*
surface technologies, 23

G

Galoter retort, solid heat carrier, 39,
44*f*

Gamma log
Green River Formation, 75–77
method, 67
U059 well data in Uinta basin
(Utah), 139*t*, 140
Gas Combustion Retort (GCR),
U.S. Bureau of Mines, 32–33
Gas generation
first-order and nucleation-
growth reaction models, 118*f*
kinetics, 121–123
See also Kinetics
Geokinetics, Inc., in-situ process,
45, 46*t*
Geology, Green River Formation,
64–65
Geometry
Electrofrac process, 186, 187*f*
Shell in-situ conversion process
(IC) well, 139*f*, 140
Geophysical log, Green River
Formation well P4, 69*f*
Geothermic fuel cells (GFCs),
Independent Energy Partners
(IEP), 46*t*, 48–50
Global energy, thermal efficiency,
89–90
Global oil shale resources
Australia, 13–15
barrel estimate worldwide, 5
Brazil, 9–10, 11*t*
Canada, 16
China, 15–16, 17*t*
Estonia, 15, 16*f*
Israel, 17
Jordan, 11–12, 13*f*
map of world resources, 7*f*
Morocco, 11, 12*f*
Russia, 8
Sweden, 17
Syria, 17
Thailand, 17
top ten ranked countries by
volume, 7*t*
Turkey, 18
United States, 6–8, 18
U.S. oil shale characteristics, 9*t*
U.S. oil shale quality, 9*t*

- See also* Oil shale
- Global research, oil shale challenges, 24
- Grade, oil shale, 5
- Green River Formation (GRF)
- abundance of clastic vs. calcareous mudstones, 76–77
 - basin margin analysis, 81
 - bioturbation, 75
 - bioturbation and lake-basins, 81
 - calcareous mudstones, 70–72, 76*f*
 - clastic mudstones, 70, 72*f*
 - CO₂ yield vs. shale grade, 229*f*
 - core sedimentology, 67–75
 - Curly Tuff, 68, 74–75, 79*f*
 - deposition phases, 63
 - dolomitic mudstones, 72–73, 77*f*
 - drilling costs, 269, 270*f*
 - evaporite, 74, 79*f*
 - evolution of Lake Uinta, 78–82
 - facies associations, 79, 80*f*, 81
 - fuel cycle, 220
 - gamma log, 75–77
 - gamma signatures, 77
 - geophysical, chemical, ichnological, and lithological logs for well P4, 69*f*
 - horizontal heater and production wells in illite-rich oil shale, 155*f*
 - kerogen from Mahogany zone, 235
 - lithofacies, 67
 - local geology, 65, 68*f*
 - location, 64, 66*f*
 - location of well P4 (U059), 67*f*
 - mass balance, 93, 97*f*
 - methods, 66–67
 - models of overfilled, balanced-filled and under-filled lake basins, 80–81
 - nahcolite, 74, 79*f*
 - oil production, 90
 - oil shale, 69–70, 71*f*
 - oil shale deposition in Lake Uinta, 81
 - photo-micrographs of thin sections and core plugs, 212*f*, 213
 - regional geology, 64–65
 - sandstones, 67–68, 73–74, 78*f*
 - schematic lake-level evolution of Laramide basins, 80*f*, 81
 - stratigraphic nomenclature, 68*f*
 - study area, 65, 67*f*
 - terminal fan delta model, 80*f*, 82
 - tuff beds, 68, 74–75, 79*f*
 - Wavy Tuff, 68, 74–75, 79*f*
 - western U.S. oil shale deposit, 6, 8*f*
 - zeolite sands, 74–75, 79*f*
- Green River shale
- kinetic experiments, 119
 - pyrolysis experiments, 125
- Groundwater protection, classification and status, 46*t*
- ## H
- Hashemite Kingdom of Jordan, oil shale, 11–12, 13*f*
- Heat balance, properties and equations, 94–95
- Heat gas injection
- American Shale Oil, LLC (AMSO) EGL technology, 56–57
 - Chevron CRUSH process, 46*t*, 52–54, 55*f*, 128, 129–130
 - classification and status, 46*t*
 - in-situ vapor extraction (IVE), 57–58
 - PetroProbe process, 54, 55*f*
- Heating issues
- oil shale retorting, 154, 156
 - thermal requirements for retorting, 221–225
- Horizontal rotating kiln, Alberta Taciuk Process (ATP), 39–40, 44*f*
- Horse Bench sandstone, ripples, 68, 78

- Hot recycled solids retort, estimates of carbon dioxide emissions, 237, 243*f*
- Hydrocarbon expulsion
 equation-of-state (EOS) phase behavior model, 191, 194*f*
 in situ stress, 191
 phase behavior modeling of kerogen products, 191, 195*f*
 spring-loaded frame and sample preparation, 191, 194*f*
- Hydrocarbons
 methods for, generation, 219–220
 normalized profile of, generation through time, 207, 209*f*
 upgrading and refining oil-shale-derived, 230–233
- Hydrogen
 content of in-situ conversion process (ICP) oil vs. backpressure, 164, 171*f*
 estimates of, requirements of shale oil upgrading, 232*t*
 evolution profiles from oil shale and coal, 121, 124*f*
 generation rate during fluidized-bed isothermal pyrolysis of Colorado oil shale, 122–123, 125*f*
 kinetics of generation, 121–123
 oil coking product, 123
 schematic of high pressure and pyrolysis yields, 123, 127*f*
- Hydrogenation, reactions affecting oil yield, 123
- Hydrogen-donor solvent, Rendall process, 38, 43*f*
- I**
- Ichnological log, Green River Formation well P4, 69*f*
- Illite shale
- CCR (conduction, convection and reflux) retort concept, 150–154
 commercial application of CCR process, 154, 155*f*
See also American Shale Oil, LLC (AMSO)
- In-Capsule™ Process, EcoShale, 30*t*, 31, 32*f*
- Independent Energy Partners (IEP), geothermic fuel cells (GFCs), 46*t*, 48–50
- Indirect heating
 CRE Clean Shale Oil Surface Process (C-SOS), 30, 32*f*
 EcoShale, 30*t*, 31, 32*f*
 oil shale retorting, 29–31
- In-situ Conversion Process (ICP)
 bitumen and oil production, 164, 170*f*
 carbon number distribution vs. backpressure, 172*f*, 174*f*
 carbon number range of ICP vs. surface retorted oil, 164, 167*f*
 chemical composition changes with backpressure, 172*f*
 commercialization of oil shale using, 172–173
 deep heater test (MFE) (2001–present), 178
 estimates of carbon dioxide emissions, 237, 243*f*
 freeze wall test (2005–present), 180, 181*f*
 hydrogen content of ICP oil vs. backpressure, 164, 171*f*
 kerogen conversion, 164, 170*f*
 laboratory setup, 166*f*
 laboratory testing, 163–165
 Mahogany demonstration project (MDP) (1998–2005), 169–170, 175*f*
 Mahogany field experiment (1996–1998), 168–169, 173*f*
 Mahogany isolation test (MIT) (2002–2004), 178–179, 180*t*
 MDP (south) (2003–2005), 170–177

- MDP (south) heat pattern, 175*f*
MDP (south) shale oil JP-8 jet fuel, 174, 179*t*
oil and gas production rates at MDP (south), 171, 176*f*
oil API gravity and heating rate, 162, 163, 167*f*
oil properties of MFE and MDP (south), 177*t*
Red Pinnacle thermal conduction test (1981–1982), 167–168, 173*f*
research, development and demonstration pilots, 180–181
shale oil refining process flow scheme, 178*f*
Shell, 47–48, 49*f*, 127–128, 130*t*
Swedish history (1941–1960) of, 165–166
upgrading oil to transportation quality products, 174
well geometry of Shell's ICP, 139*f*, 140
See also Shell
- In-situ prototype model
carbon footprint estimates, 145
coke concentration comparison, 144*f*
cumulative oil and gas production, 141*f*
energy to reservoir and energy lost to under/over burden, 142*f*
geometry, 139*f*, 140
hydrogen to carbon ratios of Green River oil shale, 139–140
initial conditions, 140
kerogen, 138
kerogen concentration comparison, 143*f*
net energy gain/loss, 144–145
oil and gas production rates, 142*f*
oil saturation comparison, 144*f*
production strategy, 140
reaction mechanism, 138
temperature history comparison, 143*f*
- In-situ technologies
advantages and disadvantages, 40–42
American Shale Oil, LLC (AMSO) EGL technology, 56–57
Chevron CRUSH process, 46*t*, 52–54, 55*f*, 128, 129–130
classification and status of, oil shale retorting, 46*t*
combustion approaches, 42, 44
direct current in-situ heating, 52, 53*f*
down hole heaters, 47–48
early approaches and variations, 45
Earth Search Sciences, Inc., 54, 55*f*
ExxonMobil's Electrofrac™ Process, 52, 53*f*, 128
Independent Energy Partners (IEP) geothermal fuel cell, 48–50
in-situ hot gas injection, 52–58
microwave heating, 51
modified in-situ (MIS), 42, 44, 45*f*, 46*t*
Mountain West Energy (MWE), 57–58
PetroProbe process, 54, 55*f*
Phoenix-Wyoming, 51
radio-frequency (rf) heating, 51
recent processes, 127–130
Schlumberger and Raytheon-CF rf, 51
Shell In-situ Conversion Process (ICP), 47–48, 49*f*, 127–128, 130*f*
Shell's freezwall, 46*t*, 48, 49*f*, 127
thermally conductive conversion, 46–47
true in-situ (TIS), 42, 44*f*, 46*t*, 127–128
vapor extraction, 57–58

In-situ vapor extraction (IVE),
Mountain West Energy, 57–58
Irati Formation, Brazil's oil shale,
10, 11*t*
Israel, oil shale deposits, 17
Italy, resource volume, 7*t*

J

Jet fuel, Mahogany demonstration
project shale oil JP-8, 174, 179*t*
Jordan
map of oil shale resources, 13*f*
oil shale characteristics, 13*t*
oil shale deposits, 11–12
resource volume, 7*t*
Jurf Ed-Darawish deposit, Jordan,
12, 13*t*

K

Kentucky, oil shale deposits, 8
Kerogen
benzene and, 161
chemical structure, 161
CO₂ production with, pyrolysis,
236, 239*f*
composition of, in Green River
shale, 229*t*
composition of, in Mahogany
zone of Green River, 235
concentration comparison for
distances from heaters, 143*f*
conversion in laboratory testing,
164, 170*f*
days for 90% conversion of, by
temperature, 162–163, 165*f*
oil and gas generation, 117
percent by depth in U059 well,
139*t*, 140
phase behavior modeling of,
products, 191, 195*f*
pyrolysis, 103, 117, 138, 236,
241*f*
simple, structures, 119, 120*f*

temperature and, conversion
history, 206, 209*f*
well-preserved, with algal
bodies, 118–119
See also Shale oil

Kinetics

apparatus for measuring oil
shale pyrolysis, 121*f*
first-order model for oil and gas
generation from shale oil,
116*f*
gas generation, 121–123
gas generation during fluidized-
bed isothermal pyrolysis of,
oil shale, 122–123, 125*f*
hypothetical kerogen structures,
119, 120*f*
methane and hydrogen evolution
profiles, 121, 124*f*
nucleation-growth reaction
models, 118–119
oil degradation, 123–126
oil evolution by Fischer-Assay-
like apparatus vs.
micropyrolysis, 120, 122*f*
oil generation, 117–120
See also Retorting oil shale
Kingdom of Morocco, oil shale, 11,
12*t*
Kiviter technology, vertical retort,
35–36, 41*f*
Kukersite, Estonia oil shale, 15
Kukersite deposit, Russia, 8

L

Laboratory testing
setup, 166*f*
Shell's soluble salt test, 163–165
Lake Uinta
evolution, 78–82
facies associations, 79, 80*f*, 81
oil-shale deposition, 81
schematic core litholog of well
P4, 80*f*
See also Green River Formation
(GRF)

Land, R&D needs prioritization, 255*t*

Lawrence Livermore National Laboratory (LLNL)

- apparatus for measuring oil shale pyrolysis kinetics, 121*f*
- carbonate decomposition models, 228, 230*f*
- first-order and nucleation-growth reaction models, 118*f*
- oil coking, 123
- oil shale pyrolysis experiments on Green River Shale, 125
- oil yield vs. heating rate, 123, 126*f*
- petroleum generation kinetic models, 120
- pyrolysis model work, 117
- qualitative mechanism for oil generation and degradation, 123, 126*f*

See also Kinetics

Lease acquisition

- mineral development, 292
- regulations for, 272–274

Li deposit, Thailand, 17

Liquids upgrading, retort technology, 99

Lithofacies

- calcareous mudstones, 70–72, 76*f*
- clastic mudstones, 70, 72*f*
- dolomitic mudstones, 72–73, 77*f*
- evaporite, 74, 79*f*
- Green River Formation, 67
- nahcolite, 74, 79*f*
- oil shale, 69–70, 71*f*
- sandstones, 73–74, 78*f*
- tuff beds, 74–75, 79*f*
- zeolite sands, 74–75, 79*f*

See also Green River Formation (GRF)

Lithological log, Green River Formation well P4, 69*f*

Lithology, oil shale, 4

Ljungström method, Swedish history, 166

Long Ridge Project, Union B retort, 34

Lurgi process, solid heat carrier, 39, 43*f*

M

Mae Sot deposit, Thailand, 17

Mahogany demonstration project (MDP)

- cumulative MDP (south) and model results, 171, 177*f*
- deep heater test, 178
- heated pattern of MDP (south), 171, 175*f*
- MDP (south) (2003–2005), 170–177
- MDP and Mahogany field experiment oil properties, 171, 177*t*
- oil and gas production rates at MDP (south), 171, 176*f*
- original MDP (1998–2005), 169–170, 175*f*
- shale oil refining process flow scheme, 172–173, 178*f*

Mahogany field experiment (MFE)

- carbon number distribution, 169, 174*f*
- deep heater test, 178
- in-situ conversion process (ICP), 168–169, 173*f*
- oil properties, 177*t*

Mahogany isolation test (MIT), commercialization of oil shale using ICP technology, 178–179, 180*f*

Mahogany Zone

- gamma log, 75–77
- horizontal heater and production wells in illite-rich oil shale at Green River Formation base, 155*f*
- oil-shale zone in Green River Formation, 65, 81

Manitoba, oil shale, 16

- Maoming deposit, China, 15, 16, 17*t*
- Maps
- Australian oil shale, 14*f*
 - Brazil oil shale resources, 10*f*
 - Estonia oil shale, 16*f*
 - Jordanian oil shale resources, 13*f*
 - Moroccan resources, 12*f*
 - U.S. oil shale resources, 8*f*
- Market value
- shale oil, 264–265
 - See also* Economics
- Mass balance, Green River
- Formation oil shale, 93, 97*f*
- Methane
- cumulative production, 141*f*
 - evolution profiles from oil shale and coal, 121, 124*f*
 - generation rate during fluidized-bed isothermal pyrolysis of Colorado oil shale, 122–123, 125*f*
 - kinetics of generation, 121–123
 - oil coking product, 123
 - production rates, 142*f*
- Microwave heating, Phoenix-Wyoming, 46*t*, 51
- Mineral development
- competing with oil shale development, 290–292
 - See also* Sodium minerals
- Mining costs, oil shale
- technologies, 269, 270*t*
- Mining energy, oil shale, 91–92
- Mining technologies
- modified in-situ approaches, 27
 - oil shale, 25–27
 - surface, 26, 27*f*
 - underground, 26–27
- Models
- carbonate decomposition, 228, 230*f*
 - first-order kinetic, for oil and gas generation, 116*f*
 - Lake Uinta by lake-basin type, 80–82
 - logic flow for national oil shale, 274*f*
 - national oil shale model, 275–278
 - nucleation-growth reaction, 118–119
 - See also* Carbon dioxide; National oil shale model
- Modified in-situ (MIS) process
- capital costs, 268*t*
 - combustion approach, 42, 44
 - conversion of oil shale to products, 45*f*
 - development costs, 266, 268*f*
 - estimates of carbon dioxide emissions, 237–238, 243*f*
 - minimum economic price, 277*f*, 279–280
 - operating costs, 270*t*
- Molecular composition. *See* Shale oil composition
- Morocco
- map of resources, 12*f*
 - oil shale characteristics, 12*t*
 - oil shale deposits, 11
 - resource volume, 7*t*
- Mountain West Energy (MWE), in-situ vapor extraction, 46*t*, 57–58
- Mudstones
- calcareous, facies, 70–72, 76*f*
 - clastic, facies, 70, 72*f*
 - dolomitic, facies, 72–73, 77*f*
 - See also* Green River Formation (GRF)

N

- Nahcolite
- cavity diameters formed during recovery of, 151, 153*t*
 - CO₂ production with, decomposition, 236, 239*f*
 - coproduction of oil shale and, with Electrofrac, 208–210
 - decomposition, 236, 241*f*
 - Green River Formation, 74, 79*f*

- low temperature breakdown, 236
- phase diagram, 210*f*
- Piceance Basin of Colorado, 207–208
- See also* Sodium minerals
- National Environmental Policy Act (NEPA)
- requirements, 252
- See also* Environment
- National oil shale model
- benefits of oil shale production, 276–278
- economic module, 275–276
- logic flow, 274*f*
- resource module, 275
- screening module, 275
- Natrite
- phase diagram, 210*f*
- properties, 211
- reaction, 210
- See also* Sodium minerals
- Natural gas, carbon intensity, 227*t*
- New Brunswick Albert Formation, Canada, 16
- New South Wales, oil shale resources, 14, 15*t*
- Nomenclature, Green River Formation, 68*f*
- Nucleation-growth reaction models, oil and gas generation, 118–119
- O**
- Occidental Modified In-situ Retort, in-situ process, 45, 46*t*
- Oil degradation
- calculated and measured oil yields and gas composition, 129*f*
- kinetics, 123–126
- oil yield vs. heating rate, 123, 126*f*
- qualitative mechanism for, 123, 126*f*
- Oil generation
- carbon footprint estimate, 145
- chemical composition by in situ conversion process, 192–200
- cumulative oil and gas production, 141*f*
- effective stress and hydrostatic pressure influencing, 195–199
- experimental protocol, 192–195
- first-order and nucleation-growth reaction models, 118*f*
- hydrous pyrolysis, 119
- kerogen pyrolysis, 117, 138
- kinetics, 117–120
- production rates, 142*f*
- qualitative mechanism for, 123, 126*f*
- See also* ExxonMobil Electrofrac™ Process; Kinetics
- Oil production, laboratory testing, 164, 170*f*
- Oil sands
- capital costs of Canadian, 278*f*, 280
- capital costs of upgrading, 269, 271, 272*t*
- operating costs of Canadian, 278*f*, 280
- Oil saturation, comparing by distance from heaters, 141–142, 144*f*
- Oil shale
- carbon dioxide and, 219–220
- carbon dioxide emitted from, 226–228
- classification scheme for processes, 116*t*
- composition, 4
- conversion to products, 25*f*
- deposition, 3–4
- description, 3, 21–22
- distribution, 4
- evolution of major technologies, 25*f*
- first-order kinetic model for oil and gas generation, 116*f*
- formation, 3–4

- grade, 5
 - Green River Formation, 69–70, 71*f*
 - heat equations, 94–95
 - lithology, 4
 - oil production from, 89
 - pyrolysis, 21–22, 130–131
 - quality factors, 4–5
 - recoverability, 5
 - richness, 5
 - technology choice, 22–23
 - technology maturation, 23–24
 - See also* Carbon dioxide; Global oil shale resources; In-situ technologies; Oil shale technologies; Thermodynamics of shale oil production
 - Oil shale development
 - competing water demands, 292–296
 - risk factors, 263–264
 - See also* Economics
 - Oil Shale Environmental Task Force
 - Department of Energy (DOE), 250
 - re-establishing, 257
 - See also* Environment
 - Oil Shale Symposium
 - Colorado School of Mines (CSM), 251
 - follow-up to 2007, 254–256
 - See also* Environment
 - Oil shale technologies
 - Alberta Taciuk Process (ATP), 39–40, 44*f*
 - Chattanooga Process, 36–37, 42*f*
 - conversion of oil shale to products, 25*f*, 29*f*
 - CRE Energy, Inc., 30, 32*f*
 - CRI Clean Shale Oil Surface Process (C-SOS), 30, 32*f*
 - direct heating methods, 30*t*, 31–36
 - EcoShale In-Capsule™ Process, 30*t*, 31, 32*f*
 - evolution of major oil shale, 25*f*
 - fluidized bed combustion, 36–37
 - Fushun retort, 35, 37*f*
 - Galoter process, 38, 39, 44*f*
 - Gas Combustion Retort (GCR) by Bureau of Mines, 32–33
 - indirect heating methods, 29–31
 - Kiviter vertical retort, 35–36, 41*f*
 - Lurgi approach, 38, 39, 43*f*
 - maturation, 23–24
 - mining for modified in-situ approaches, 27
 - mining techniques, 25–27
 - new challenges, 24
 - Paraho Development Corporation, 33–34, 35*f*
 - Petrosix retort, 34
 - Rendall Process, 38, 43*f*
 - retorting and pyrolysis, 27–38
 - rotary kiln with sweep gas injection from integrated gasifier, 37–38
 - solid heat carrier technologies, 38–40
 - surface mining, 26, 27*f*
 - surface retorting, 27–29, 30*t*
 - TOSCO II retort, 38
 - underground mining, 26–27
 - Union B Retort, 34–35
 - See also* In-situ technologies; Retorting oil shale; Sodium minerals
 - Operating costs
 - oil shale, variance, 282
 - oil shale development, 267–268, 270*t*
 - See also* Economics
- ## P
- Paraho Development Corporation
 - direct heating process, 33–34, 35*f*
 - gas combustion retort, 98
 - Paraíba Valley deposit, Brazil's oil shale, 9, 11*t*

Permitting, environmental regulation, 251–252

Petrobras
Brazil, 9
Petrosix retort, 34

PetroProbe process, hot gas injection, 46*t*, 54, 55*f*

Petrosix
retort, 34
surface technologies, 23

Phoenix-Wyoming, microwave heating, 46*t*, 51

Piceance Basin
Colorado, 149–150, 162, 181
Colorado Division of Wildlife, 287
Green River oil shale and sodium minerals, 207–208

Plant life, oil shale development, 289–290

Power plant, carbon dioxide production, 236, 239*f*

Programmatic Environmental Impact Statement (PEIS), U.S. Geologic Survey (USGS), 249–250

Project development schedules, oil shale, 271, 272*f*

Pyrite, enthalpy change, 224*t*

Pyrolysis experiments
Green River Shale, 125
kerogen, 103, 117, 138
oil shale, 21–22, 130–131
schematic of high pressure hydrogen and yields, 123, 127*f*

Pyromat™, measuring oil generation, 120, 122*f*

Q

Quality
oil shale factors, 4–5
upgrading oil to transportation, 174
U.S. oil shale, 9*t*

Queensland, oil shale resources, 14, 15*t*

R

Radio-frequency heating
energy balance, 99
in-situ technology, 46*t*, 51

Raytheon and CF Technology, radio-frequency heating, 51

Reconciliation, thermal balance, 97–98

Recoverability, oil shale, 5

Red Leaf Resources EcoShale™, technology, 98

Red Pinnacle, thermal conduction test (1981–1982), 167–168, 173*f*

Regional geology, Green River Formation, 64–65

Regulations
challenges, 286
exploration license, 273
land exchange, 274
lease acquisition, 272–274
leasing process, 273
leasing requirements, 273

Rendall process, hydrogen-donor solvent, 38, 43*f*

Research, Shell's in-situ conversion process (ICP), 180–181

Research community, oil shale challenges, 24

Resistivity
calcined coke, 188, 189*f*
calcining temperature and coke, 190*f*

Resource management
aquatic life, 289
challenges, 286–287
competing mineral development, 290–292
Endangered Species Act (ESA), 287–289
managing competing water demands, 292–296
plant life, 289–290
U.S. Fish & Wildlife Service (USFWS), 288
wildlife, 287–289

Retorting oil shale

- apparatus for measuring oil shale pyrolysis kinetics, 121*f*
 carbon dioxide emission by auxiliary energy use in, 225–226
 carbon dioxide emissions from thermal requirements for, 221–225
 classification scheme, 116*t*
 costs, 269
 estimated heats, 226*t*
 first-order kinetic model with oil and gas separation, 116*f*
 illite-shale CCR retort concept, 150–154
 kinetics of gas generation, 121–123
 kinetics of oil generation, 117–120
 power requirements, 93
 propagation of thermomechanical wave through retort, 151, 153*f*
 refluxing oil distributing heat through fractured, retorted oil shale formation, 151*f*
 retort operation, 98–99
 technology, 27–38
 thermal cycle, 92–93
See also American Shale Oil, LLC (AMSO); Oil shale technologies
 Richness, oil shale, 5
 Rock-Eval™ apparatus, measuring oil generation, 120
 Rocky Mountain Oilfield Testing Center (RMOTC), in-situ vapor extraction (IVE), 57–58
 Rotary kiln, sweep gas injection, 37–38
 Russia, resource volume, 7*t*
- S**
- Saline minerals
 enthalpy change, 224*t*
 reactions, 227
- Sandstones
 Green River Formation, 67–68, 73–74
 photographs, 78*f*
 Saskatchewan, oil shale, 16
 Schlumberger, radio-frequency heating, 51
 Sedimentology
 core, of well P4, 67–75
 method, 66
See also Green River Formation (GRF)
 Shale. *See* Oil shale
 Shale char, carbon intensity, 227*t*
 Shale oil
 market value of, 264–265
 purposes, 103–104
 Swedish history for recovery of, 165–166
 value, 104
 Shale oil composition
 analysis by Z-BaSIC™ (Z-Based Structural Index Correlation method), 104–105
 bulk properties, 105, 106*t*
 capability of Z-BaSIC, 110–111
 detailed molecular, of EcoShale 32, 107–108, 109*t*, 110*t*, 111*t*, 112*t*
 empirical formula, 104
 high temperature simulated distillation (HTSD) for EcoShale 32, 105, 107*t*
 insight into conversion chemistry, 111–112
 summary of molecular, 106–107, 108*t*
 Shale oil production. *See* Thermodynamics of shale oil production
 Shell
 freezwall technology, 46*t*, 48, 49*f*, 127
 freeze wall test, 180, 181*f*
 ICP (In-situ Conversion Process), 47–48, 49*f*, 127–128, 130*t*

- ICP energy balance, 99
soluble salt process, 162–163
well geometry of Shell ICP, 139*f*, 140
See also In-situ Conversion Process (ICP)
- Sinclair Oil and Gas, in-situ process, 45, 46*t*
- Smoke point, specifications, 176
- Social impact, environment, 252, 254
- Sodium minerals
core plugs and thin section
photo-micrographs of Green River oil shale, 212*f*, 213
ExxonMobil's concept for oil shale and nahcolite recovery, 212*f*, 213–214
nahcolite, 208–210
phase diagram for sodium carbonate, 210*f*, 211
production, 207–214
trona and natrite, 210–211
X-ray diffraction of nahcolite-oil shale mixture, 211*f*
See also Mineral development
- Solid heat carrier technology
Alberta Taciuk Process (ATP), 39–40, 44*f*
Galoter retort design, 38, 39, 44*f*
Lurgi process, 38, 39, 43*f*
TOSCO II retort, 38
- Steam Assisted Gravity Draining (SAG-D), 56
- Stratigraphic nomenclature, Green River Formation, 68*f*
- Sultani deposit, Jordan, 11–12, 13*t*
- Surface Impact, environment, 252, 253–254
- Surface mining
capital costs, 268*t*
cash flow of generic, 276*f*, 279
development costs, 265, 268*f*
first stage development, 271, 272*f*
impact of incentives, 276*f*, 279
minimum economic price, 277*f*, 279–280
oil shale, 26, 27*f*
operating costs, 270*t*
- Surface retorting
approaches, 28–29
classification and status, 30*t*
description, 27–28
- Sweden, oil shale deposits, 17
- Swedish history, in-situ conversion process (ICP), 165–166
- Syntec, rotary kiln with sweep gas injection, 37
- Syria, oil shale deposits, 17
- ## T
- Tarfaya deposit, Morocco, 11, 12*t*
- Technology
uncertainty and economics, 263–264
See also Oil shale technologies
- Texas, oil shale, 6
- Thailand, oil shale deposits, 17
- Thermal balance, reconciliation, 97–98
- Thermal conduction test, Red Pinnacle, 167–168, 173*f*
- Thermal cycle, retorting oil shale, 92–93
- Thermal efficiency
global energy trends, 89–90
resource characteristics, 90, 91*f*, 92*f*
- Thermally conductive conversion, in-situ retorting, 46–47
- Thermodynamics of shale oil production
average grade and efficiency, 98*f*, 99
corehole histogram, 91*f*
energy balance, 95–96
first law retort efficiency vs. grade, 98*f*, 99
global energy trends, 89–90
heat balance properties and equations, 94–95
liquids upgrading, 99
mass balance, 93, 97*f*

mining energy, 91–92
mining optimization of grade
and intercept, 92*f*
Modified Fischer Assay (MFA),
93
overall efficiencies, 100–101
resource characteristics
important to thermal
efficiency, 90, 91*f*, 92*f*
retort operation, 98–99
retort power requirements, 93
self-sufficiency vs. imported
energy, 99–100
thermal balance reconciliation,
97–98
thermal cycle in retorting oil
shale, 92–93
thermal efficiency, 89–90
Timahdit deposit, Morocco, 11, 12*t*
Toolebuc Formation, Australia, 14,
15*t*
Torbanite deposit, Queensland, 14,
15*t*
TOSCO II retort technology, solid
heat carrier, 38
Transportation, upgrading oil
quality to, 174
Trona
phase diagram, 210*f*
properties, 211
reaction, 210
See also Sodium minerals
True in-situ (TIS) process
capital costs, 268*t*
combustion approach, 42, 44,
127–128
conversion of oil shale to
products, 44*f*
development costs, 267, 268*f*
development schedule, 271, 272*f*
minimum economic price, 277*f*,
279–280
operating costs, 270*t*
Tuff beds, Green River Formation,
68, 74–75, 79*f*
Turkey, oil shale deposits, 18

U

Uinta Basin, Utah
location map of study area, 66*f*
location of well P4 (U059), 65,
67*f*
State Water Plan, 294
U059 well survey data, 139*t*,
140
See also Green River Formation
(GRF)
Underground mining
capital costs, 268*t*
development costs, 266, 268*f*
efficiency, 91–92
minimum economic price, 277*f*,
279–280
oil shale, 26–27
operating costs, 270*t*
Union B Retort, Union Oil
Company, 34–35
United States
eastern shale, 8
map of oil shale resources, 8*f*
oil shale characteristics by
region, 9*t*
oil shale quality by region, 9*t*
oil shale resource
characterization, 9*f*
resource volume, 7*t*
western shale, 6–7
University of Utah, rotary kiln with
sweep gas injection, 37–38
Upgrading costs, technologies, 269,
271, 272*t*
U.S. Bureau of Mines, Gas
Combustion Retort (GCR), 32–
33
U.S. Department of Energy (DOE)
potential oil shale impacts, 250
See also Environment
U.S. Department of Interior (DOI)
Bureau of Land Management
(BLM), 250–251
regulations for lease acquisition,
272–274
U.S. Geologic Survey (USGS),
249–250

- See also* Environment
- U.S. Fish & Wildlife Service (USFWS), 288
- U.S. Geologic Survey (USGS), Programmatic Environmental Impact Statement (PEIS), 249–250
- Utah
- Green River Formation, 6, 8*f*, 64, 66*f*
 - water demands, 294
 - See also* Green River Formation (GRF)
- Utah Geological Survey
- mineral development, 291
 - U059 well data, 139*t*, 140
- Utah Mining Association, water demand, 295–296
- V**
- Vapor extraction, in-situ (IVE), Mountain West Energy (MWE), 57–58
- Vertical retort, Kiviter technology, 35–36, 41*f*
- W**
- Wadi Maghar deposit, Jordan, 12, 13*t*
- Wadi Yarmouk Basin, Syria, 17
- Water, oil shale industry, 156–158
- Water demands
- availability, 292
 - Colorado, 294–295
 - Colorado River Compact, 293
 - direct and indirect, 295
 - Utah, 294
 - Utah Mining Association, 295–296
- Water quality and quantity environment, 252, 253
- R&D needs prioritization, 255*t*
- Wavy Tuff, Green River Formation, 68, 74–75, 79*f*
- Western Energy Partners, rotary kiln with sweep gas injection, 37
- Western United States
- oil shale, 6–7
 - oil shale characteristics, 9*t*
 - oil shale quality, 9*t*
 - oil yield vs. heating rate, 123, 126*f*
 - See also* Green River Formation (GRF)
- Wildlife, oil shale development, 287–289
- Workshops. *See* Environment
- World map, oil shale resources, 7*f*
- Wyoming
- Green River Formation, 6, 8*f*, 64, 66*f*
 - See also* Green River Formation (GRF)
- Y**
- Yarmouk deposit, Syria, 17
- Z**
- Z-BaSIC™
- capability, 110–111
- Z-Based Structural Index
- Correlation method, 104–105
 - See also* Shale oil composition
- Zeolite sands, Green River Formation, 74–75, 79*f*